

*CRANFIELD UNIVERSITY*

Bonini Francesca

**MOLECULARLY IMPRINTED POLYMERS  
FOR PROTEOME ANALYSIS**

CRANFIELD HEALTH

**PhD Thesis**



*UNIVERSITA' DEGLI STUDI DI VERONA*  
&  
*CRANFIELD UNIVERSITY*

CRANFIELD HEALTH

PhD Thesis

Academic Year 2005-2008

Bonini Francesca

**MOLECULARLY IMPRINTED POLYMERS  
FOR PROTEOME ANALYSIS**

Supervisors: Dr Alessandra Bossi  
Prof. Sergey Piletsky

January 2008

This thesis is submitted in partial fulfilment of the requirements for the degree of Doctor of Philosophy co-tutela between the University of Verona and Cranfield University.

© Cranfield University 2008. All rights reserved. No part of this publication may be reproduced without the written permission of the copyright owner.



*Alla mia mitica famiglia*

*“Τα πάντα ρει”, έλεγε ο Ηράκλειτος*



## **ACKNOWLEDGEMENTS**

I would like to acknowledge Dr. Alessandra Bossi for giving me the opportunity to work. For being my mentor and my inspiration throughout my PhD studies.

Also, I would like to acknowledge Prof. Sergey Piletsky for his valuable help and for being there in times of need and for his availability.

Also, I would like to thank all my family, Paolo, my friends and Italian laboratory. They deserve special acknowledgements in Italian language!

Un grazie speciale a mio papà, alla mia mamma e alla mia sorellina per avermi aiutato, sopportato e incoraggiato a portare a termine questa esperienza. Grazie soprattutto perché ci siete sempre.

Grazie a Paolo, che nonostante tutto è sempre presente, mi ha sempre aiutata, ascoltata e consigliata e sopportata nei piccoli momenti di isteria. Grazie per i bei momenti che mi regali.

## Acknowledgments

---

Grazie ai miei amici: Veronica, Chicca, Sara, Federica la prof. di mate, Said, per i bei momenti passati insieme per le tante avventure che abbiamo condiviso.

Grazie al laboratorio di Verona: Daniela, Rita, Alberto, Miki, Elena, Giacomo, Annalisa e il piccolo Fede per la bella esperienza condivisa.

Many thanks to my English school “Speak your Mind” to help me in this thesis defence!

Grazie a Mattia, Betta, Ivan, Ilenia, Luchino, alla mitica Squadra 10 della Croce Verde e a tutti quelli che non ho nominato ma che sono sempre nel mio cuore.



**ABSTRACT**

Fast and efficient methods for the detection of insurgence and progression of diseases are at the basis of modern diagnostics and medicine. In this concern, biomarkers represent a powerful diagnostic tool, as their expression profiles well correlate with the pathology progression. Thus, the pathological state could be diagnosed by measuring the altered presence of a biomarker.

In this direction, conspicuous help has been given by proteomics, intended as the study of the protein pattern of a sample and most frequently performed by two-dimensional electrophoresis. Although the proteome approach is a powerful analytical method, its application to biological samples for the detection and quantification of putative biomarkers is hampered by technical problems, in fact, the wide diversity in concentrations exhibited by the proteins present in the biological samples, with a concentration range spanning over

nine orders of magnitude, and the relative abundance of each protein, are responsible of masking the less abundant species and of their loss in traceability.

The aim of my PhD project is to apply Molecularly Imprinted Technology to the specific removal of a high abundance protein (Human Serum Albumin, HSA) frequently affecting proteomic analysis, in order to increase the detection of potential biomarkers.

This technology allows the creation of artificial recognition sites in synthetic polymers for a specific protein. These sites are tailor-made *in situ* by co-polymerisation of functional monomers and cross-linkers around the template molecules.

Two different approaches have been assayed in order to remove HSA:

- Immobilisation of protein template on a rigid silica support (bead) and creation of polymer around beads.
- Polymerisation in bulk of a polymer with protein template and application of this polymer to multicompartiment electrolyser.

In both of the cases, the chemical and structural features of the polymers have been analysed, after that they have been applied to complex proteome pre-treatment, obtaining encouraging results.



## **AIM AND OBJECTIVES OF THE THESIS**

The research work carried out in the last three years and presented in this thesis, has been conducted in the Laboratory of Biochemical Methodologies of the Scientific and Technologic Department of the University of Verona, in collaboration with Cranfield Health of the University of Cranfield (UK).

One of the main problems in proteome analysis is the presence of different ranges of proteins expression. There are the high abundance proteins in concentrations around mg/ml. These derived from house-keeping or structural genes and they mask the signal of low abundance ones, generally present at low concentrations, about ng/ml or pg/ml. The low ones are often very important because they are potential biomarkers to study and to detect specific diseases.

In literature different approaches for the removal of high abundance proteins are described, among which electrophoretic and chromatographic pre-fractionation techniques and antibody-mediated depletion of specific proteins from biological fluids (i.e., human serum, cerebrospinal fluid).

**The aim of my PhD thesis** has been using Molecularly Imprinted Polymers (MIPs) to manufacture a polymeric synthetic receptor

capable of recognising and removing the Human Serum Albumin (60% of the total serum proteins) from human serum.

Molecular imprinting can be defined as the process of template-induced formation of specific recognition sites (binding or catalytic) in a material, where the template drives the positioning and orientation of the material's structural components by a self-assembling mechanism. The polymer are very easy to prepare and to use, finally cheaper than some methods usually applied.

Such MIP would then be used to remove albumin from serum samples, in order to improve and to help the analysis of the "hidden" proteome for diagnostic field.

The objectives of my PhD project can be grouped in two different sections, briefly here summarised, according to which the present thesis is structured:

*Section I:* Development of a new methodology for imprinting silica beads for the recognition of Human Serum Albumin.

*Section II:* Creation of new imprinted polymers made of polyacrylamide gel capable of removing Human Serum Albumin from human serum, thus increasing the signal of low abundance proteins in two-dimensional maps.

In the *Section I* a new methodology for manufacturing imprinted beads for the recognition of human serum albumin was developed.

I adapted a specific protocol described in literature for the preparation of imprinted beads with human serum albumin made of with 3-aminophenylboronic acid. The beads are characterised as complete as possible and after experiments with solutions composed with only one protein, the beads were applied to biological complex sample in order to remove HSA with encouraging results. The ease of the derivatisation protocol, the short incubation time and the effectiveness of the removal approach make the MIP beads worth of further analysis and envisage forthcoming applications in proteomic and applied biotechnology.

In the *Section II* of the work of my PhD course, I have applied the templating approach for introducing structural modifications into polyacrylamide (PAA), with the aim of altering its functional properties. The templating approach was exploited for creating nanometer-sized recognition cavities and channels in PAA gels.

In a first set of experiments, the electrophoretic transport was performed on gel slabs made of PAA at different percentages. With these experiments it was possible to demonstrate a preferential migration of the template protein in MIP gels with respect to control gels, and that the migration rate correlates with both the PAA percentage and the template concentration. The method turns out to be labour intensive, nevertheless it allowed for setting the conditions for next experiments.

In a second set of experiments, the free flow electrophoretic migration was evaluated in a multi-compartment electrolyser, such a format allowing for fast and highly reproducible results. In this case the templated gels were polymerised as thin membranes on a glass fibre support. The migration properties of proteins across MIP and control membranes were tested, by estimating the transit time of a fixed quantity of protein across the membrane. From different kind of experiments, it became evident that there exists a correlation between the amount of template used for the polymerisation and the transport kinetics, most likely as a result of a more or less pronounced modification of the gel porosity induced by the template. Due to the encouraging results obtained with model protein mixtures, HSA templated membranes were then used for the treatment of human serum, in order to pre-fractionate the sample prior to proteome analysis.

The efficiency of the PAA-templated method for albumin removal was evaluated by two-dimensional gels and densitometric analysis of the protein spots. The results indicate that PAA-templated membranes are promising material for the pre-treatment and pre-fractionation of complex biological samples prior to proteome analysis.



## **TABLE OF CONTENTS**

<b>Acknowledgments</b> .....	<b>I</b>
<b>Abstract</b> .....	<b>III</b>
<b>Aim and Objectives of the Thesis</b> .....	<b>VII</b>
<b>Table of Contents</b> .....	<b>XI</b>
<b>List of Figures</b> .....	<b>XVII</b>
<b>List of Tables</b> .....	<b>XXVII</b>
<b>List of Abbreviations</b> .....	<b>XXIX</b>

### **CHAPTER I**

#### **PROTEOME AND PROTEOMICS**

<b>1.1. General introduction</b> .....	<b>1</b>
<b>1.2. Proteome analysis</b> .....	<b>3</b>
1.2.1. Sample preparation .....	<b>4</b>
1.2.2. Iso-electrofocusing .....	<b>6</b>
1.2.3. The Second dimension:SDS-PAGE run and staining	<b>7</b>
1.2.4. Results analysis .....	<b>9</b>

1.2.5. Mass spectrometry ..... 10

1.2.6. Limitations to be overcome 2D analysis ..... 13

## **CHAPTER II**

### **PREFRACTIONATION TECHNIQUE IN PROTEOME ANALYSIS**

**2.1. General introduction ..... 15**

**2.2. Fractional centrifugation ..... 16**

**2.3. Chromatographic approach ..... 17**

**2.4. Electrophoretic approach ..... 20**

    2.4.1. The Rotofor ..... 20

    2.4.2. The equaliser beads ..... 22

    2.4.3. The Multicompartement Electrolyser (MCE) ..... 23

    2.4.4. Other sample treatments method ..... 27

**2.5. Conclusions ..... 28**

## **CHAPTER III**

**MOLECULARLY IMPRINTED TECHNOLOGY**

**3.1. General introduction ..... 29**

**3.2. Recognition through the placement of few constrains  
on the polymer ..... 32**

**3.3. Shape recognition with polyacrylamide gels ..... 35**

**3.4. Epitope approach: exploiting a small structural element  
of the protein for its recognition ..... 40**

**3.5. Molecularly imprinted polymer grafted onto surface ..... 42**

**3.6. Immobilising template onto surface ..... 48**

**3.7. Conclusions ..... 51**

**CHAPTER IV**

**CREATION OF MOLECULARLY IMPRINTED POLYMER BEADS**

**FOR RECOGNITION HUMAN SERUM ALBUMIN**

**4.1. General introduction ..... 53**

**4.2. Material and Methods ..... 54**

4.2.1. Preparation imprinted silica using immobilised templates .....	54
4.2.2. Evaluation of percentage of derivatisation.....	56
4.2.3. Protein content determination .....	56
4.2.4. Calculation of the binding capacity.....	56
4.2.5. Binding kinetics .....	57
4.2.6. Protocol for protein elution from the beads .....	57
4.2.7. Binding experiment with human serum .....	58
4.2.8. SDS-PAGE and 2D PAGE .....	58
<b>4.3. Results and discussion .....</b>	<b>60</b>
4.3.1. Beads derivatisation protocol .....	60
4.3.2. Washing protocol .....	65
4.3.3. Qualitative characterisation of beads .....	67
4.3.4. Evaluation of the material binding capacity .....	68
4.3.5. Kinetics of binding .....	68
4.3.6. Recovery of bound protein .....	74
4.3.7. Competitive absorption .....	77
4.3.8. Applications of beads of biological sample .....	80
<b>4.4. Conclusions and future work .....</b>	<b>83</b>

---

**CHAPTER V****GATE-EFFECT IN TEMPLATE POLYACRYLAMIDE MEMBRANES****INFLUENCES THE ELECTRO-TRANSPORT OF PROTEINS AND****FINDS APPLICATIONS IN PROTEOME ANALYSIS**

<b>5.1. General introduction.....</b>	<b>87</b>
<b>5.2. Material and Methods .....</b>	<b>90</b>
5.2.1. Electrophoresis on imprinted gel slabs .....	<b>90</b>
5.2.2. Protein transport through imprinted PAA- membranes in a free flow electrophoresis system .....	<b>92</b>
5.2.3. Evaluation of retention capacity of PAA membranes ..	<b>94</b>
5.2.4. Removal of Human Serum Albumin from human serum through PAA-imprinted membranes .....	<b>95</b>
5.2.5. SDS-PAGE.....	<b>96</b>
5.2.6. Two-dimensional electrophoresis .....	<b>96</b>
5.2.7. Protein content determination .....	<b>97</b>
<b>5.3. Results and discussion .....</b>	<b>97</b>
5.3.1. Electrophoresis in gel slabs .....	<b>97</b>
5.3.2. Preparation of gel slabs for BSA recognition .....	<b>99</b>
5.3.3. Polyacrylamide membranes .....	<b>103</b>
5.3.4. Evaluation of electrophoresis permeability of PAA membranes .....	<b>105</b>

5.3.5. Evaluation of retention of the membranes .....	<b>114</b>
5.3.6. Applications of membranes to proteome analysis .....	<b>117</b>
5.3.6.1. Analysis through SDS-PAGE .....	<b>119</b>
5.3.6.2. Analysis through 2D analysis.....	<b>121</b>
5.3.6.3. 2D analysis pI [4.0-7.0] and Mr [250-65 kDa] ...	<b>124</b>
5.3.6.4. 2D analysis pI [5.0-8.0] and Mr [50-25 kDa].....	<b>125</b>
5.3.6.5. 2D analysis with strips 7 cm [4.0-7.0], gel 10 20% T and [5.0-8.0], gel 10-20%T .....	<b>127</b>
<b>5.4. Conclusions and future perspectives .....</b>	<b>132</b>

## **CHAPTER VI**

### **GENERAL CONCLUSIONS**

<b>6.1. Final Conclusions .....</b>	<b>139</b>
<b>References .....</b>	<b>145</b>
<b>Appendix: Publications .....</b>	<b>175</b>

**LIST OF FIGURES**

<i>Figure 1_ Schematic representation of first dimension (IEF)</i> <i>coupled to SDS-PAGE .....</i>	<b>7</b>
<i>Figure 2_ Schematic representations of ProteinChip Arrays with</i> <i>chemical functions responsible for protein capture.....</i>	<b>12</b>
<i>Figure 3_ Schematic representation of cells fractionation using</i> <i>differential centrifugation .....</i>	<b>16</b>
<i>Figure 4_ The Micro-Rotofor instrument from Biorad .....</i>	<b>20</b>
<i>Figure 5_ Functioning of the equaliser beads in overloading (A)</i> <i>or not overloading (B) conditions .....</i>	<b>23</b>

*Figure 6\_* Historical excursus of MCE instrument from the early version (a) to the present one (d), trough the prototypes tested in our labs ..... **26**

*Figure 7\_* Schematic representation of molecular imprinting ..... **30**

*Figure 8\_* Schematic representation of the metal-chelate approach ..... **34**

*Figure 9\_* Schematic representation of the epitope approach ..... **41**

*Figure 10\_* Schematic representation of protein immobilisation ... **50**

*Figure 11\_* Structure formula of APTMS ..... **61**

*Figure 12\_* 3-aminophenylboronic acid monomer and polymer .... **63**



---

<i>Figure 13_ Possible interactions between APBA monomer and chain groups of amino acids .....</i>	<b>64</b>
<i>Figure 14_ SDS-PAGE staining in Blue Coomassie.....</i>	<b>65</b>
<i>Figure 15_ Beads MIP washed one time with 1 M oxalic acid o/n and six times with 10 mM phosphate buffer pH 8.0 .....</i>	<b>66</b>
<i>Figure 16_ Evaluation of the binding capacity for control and MIP beads.....</i>	<b>69</b>
<i>Figure 17_ Binding kinetics. The amount in micrograms of HSA bound is plotted as a function of the time, under saturating conditions (a) and non-saturating conditions (b) .....</i>	<b>72</b>

*Figure 18\_* The IF calculated as micrograms of HSA bound by MIP/micrograms of HSA bound by the control, plotted as function of the time, both for saturating conditions and non-saturating conditions ..... **73**

*Figure 19\_* SDS-PAGE. Gel showing HSA recovered from the beads in conditions “b” after precipitation with acetone. C-control, M – MIP ..... **76**

*Figure 20\_* Competitive adsorption of HSA in presence of a non-specific protein, Carbonic Anhydrase ..... **78**

*Figure 21\_* Schematic representation of serum composition. Some proteins are related depending on concentration ..... **80**

---

*Figure 22\_* 2D-maps of human serum, a) untreated serum sample, b) serum treated with imprinted beads, for the depletion of HSA .....**82**

*Figure 23\_* Polyacrylamide gel polymerisation .....**98**

*Figure 24\_* The electrophoretic migration of BSA in standard running conditions (100 V, 3 hours) on control (a) and template (b) PAA gel slabs (6 %T 4% C) and control (c) or template (d) PAA gel slabs (10 % T 4% C) stained in Coomassie Blue R-250 ....**101**

*Figure 25\_* The free flow electrophoresis system. The instrument was equipped with four chambers, separated by three PAA membranes. Chamber I, anodic and chamber IV, cathodic, were separate by isoelectric membranes at pI 3.0 and 9.0

respectively, which created pI-selective barriers, preventing protein loss at the extremes. .... **104**

*Figure 26\_* Time course of the electric transport of proteins through control and templated with BSA PAA membranes. a) Catalase, b) BSA, c) myoglobin ..... **106**

*Figure 27\_* Protein molar transport plotted versus time (PAA templated membranes) ..... **110**

*Figure 28\_* The hypothesised mechanism for the electric transport of template and non-template small proteins, that has resemblances with the elution mechanism of size-exclusion chromatographic processes ..... **113**

---

*Figure 29\_* HSA recovered from Ch-III after 12 minutes are plotted as a function of the HSA amount (micrograms) loaded at the beginning in Ch-II ..... **115**

*Figure 30\_* HSA bound by the membrane after 12 minutes are plotted as a function of the HSA amount (micrograms) loaded at the beginning in Ch-II. The quantities were calculated according to equation [a] ..... **116**

*Figure 31\_* SDS-PAGE stained in Coomassie ..... **119**

*Figure 32\_* The effectiveness of the templated-PAA for removal of the high abundant protein human serum albumin from serum samples was demonstrated by the two-dimensional electrophoresis of serum subjected to electro-depletion of

albumin, Ch-II, (B) and control serum (A). Data are normalised  
in function of optical density of whole map ..... **122**

*Figure 33\_* Two specific regions are analysed, green ring pI [4.0-  
7.0] and Mr [250-65 kDa] and yellow ring pI [5.0-8.0] and Mr  
[65-50 kDa] ..... **123**

*Figure 34\_* shows a specific area with pI [4.0-7.0] and Mr [250-  
65 kDa] in control gel (A) and treated gel (B). Yellow crosses are  
the spots detected through pDQuest software ..... **124**

*Figure 35\_* Figure shows a specific area with pI [5.0-8.0] and Mr  
[50-25 kDa] in control gel (A) and treated gel (B). Yellow crosses  
are the spots detected through pDQuest software ..... **126**

- 
- Figure 36\_* Figure shows a specific area with pI [4.0-7.0] and Mr [250-5 kDa] in control gel (A) and treated gel (B) ..... **128**
- Figure 37\_* Figure shows a specific area with pI [5-8] and Mr [250-10 kDa] in control gel (A) and treated gel (B) ..... **129**
- Figure 38\_* Figure shows master map obtained from match between control and treated samples for two different ranges [4-7] (A) and [5-8] (B). Green circle represent common proteins in both samples, while red circle represent the new spot in sample treated with PAA membranes ..... **131**
- Figure 39\_* Two bar-graphs show the gain in total spot number after sample treatment (human serum) with PAA membranes. The experiments were performed in triplicate. White columns:

List of Figures

---

untreated samples; striped columns: samples treated with PAA-  
membranes ..... **134**



**LIST OF TABLES**

<i>Table 1_</i> The quantity of HSA eluted from the beads measured by densitometry of the spots of HSA in Figure 19. ....	<b>76</b>
<i>Table 2_</i> Summary of quantities of protein bound in the competitive experiment. ....	<b>79</b>
<i>Table 3_</i> Summary of the values of imprinting factor for each condition applied on gel slab. ....	<b>102</b>
<i>Table 4_</i> Comparison of protein transport times in templated- and control- PAA membranes. ....	<b>108</b>
<i>Table 5_</i> Molecular mass and charge characteristics of the protein tested. ....	<b>108</b>

*Table 6\_* Table indicates HSA spot quantification of gel showed in Figure 31. First column reported the name of lanes of Figure 31, second lane the name of sample, the third data related to intensity of HSA present in sample loaded on gel, the forth columns reported data related to whole sample..... **120**

**LIST OF ABBREVIATIONS**

1 DE	One Dimensional Electrophoresis
2-DE	Two Dimensional Electrophoresis
APBA	3- Aminophenylboronic Acid
APS	Ammonium persulfate
APTMS	3-Aminopropyl-trimethoxysilane
BSA	Bovine Serum Albumin
CA	Carbonic Anhydrase
CHAPS	3-[(3-Cholamidopropyl)dimethylammonio]-1- propanesulfonate
CRP	C-reactive protein
Da	Dalton
DTT	Dithiothreitol
EGDMA	Ethylene glycol dimethacrylate
ESI	Electro Spray Ionisation

## List of Abbreviations

---

FT-IR	Fourier Transform Infrared Spectroscopy
H	Hour
Hb	Haemoglobin
HPLC	High Performance Liquid Chromatography
HSA	Human Serum Albumin
IF	Imprinting Factor
IEF	Isoelectric Focusing
Im	Imidazole group
IPG	Immobilised pH Gradient
MAA	Methacrylic Acid
MALDI	Matrix Assisted Laser Desorption Ionisation
MCE	Multicompartment Electrolysers
MES	2-N-morpholine ethanesulfonic acid
MIP	Molecularly Imprinted Polymer
MOPS	3-(N-morpholino)propanesulfonic acid
Mr	Relative Mass

OD	Optical Density
o/n	Over Night
PAA	Polyacrylamide
PAGE	Polyacrylamide Gel Electrophoresis
PBS	Phosphate Buffer Saline
pI	Isoelectric Point
PTM	Post-Translational Modification
QCM	Quartz Crystal Microbalance
SDS	Sodium Dodecyl Sulphate
SELDI	Surface-Enhanced Laser Desorption Ionisation
TBP	Tributylphosphine
TCA	Trichloroacetic acid
TEGDMA	Tetraethylene Glycol Di-Methacrylate
TEMED	<i>N,N,N',N'</i> -tetramethylethylenediamine
TOF	Time of Flight
TRIS	Trishydroxymethylaminomethane

## List of Abbreviations

---

Vh            Volt x hour

## **CHAPTER I**

### **PROTEOME AND PROTEOMICS**

#### **1.1 GENERAL INTRODUCTION**

The terms of “Proteome” or “Proteomics” were introduced for the first time in the 1995 (Wilkins, 1995) to indicate, respectively, the protein equivalent of an organism genome and the scientific discipline deputed to its study. Because proteins are key structural and functional molecules, the molecular characterisation of proteome is necessary for a complete understanding of biological systems. Particularly, the proteomic is characterised by the identification and quantification of proteins in cells, tissues and biological fluids; by the analysis of changes in protein expression in normal *vs* pathologic cells; by the characterisation of post-translational modifications (PTMs), by the studies of protein-protein interactions, and structure-function relationships, localisation of proteins in sub-cellular tissues, and their expression range.

Today, proteomic represents one of the most important areas of research in the “post-genomic era”. In fact, the genomic is only the first step in understanding the complex biological functions performed by simple or complex living organisms. It is well known that the number of proteins present in an organism is higher than the number of genes (Southan, 2004). Especially, in higher organisms, post-

translational modifications (PTMs) including phosphorylation, glycosylation, acetylation, deamination, farnesylation, myristoylation, palmitoylation, proteolysis (Kreider, 2001; Miklos & Maletka, 2001) and differential splicing (Graveley, 2001) can significantly blur the information gained at DNA level. For all these reasons, it is not possible to predict the number of proteins from the gene number and genomic is not able to fully explain a complex biological system.

The proteome, reveals as a dynamic entity, in continuous development and able to overcome the genomic limits. Thus, maybe, the original definition showed at the beginning, can be replaced with a new and more recent definition, suggested from de Hoog and Mann, who stated that proteome is the protein complement of a given cell at a given time, including the set of all protein isoforms and their modifications (De Hogg & Mann, 2004).

Technically, proteomic can be classified into three categories (Lau *et al.*, 2003):

- Expression proteomic. It is the comparative analysis of protein expression patterns in normal and pathological cells or tissues. It is thus possible to identify proteins that are involved in specific diseases. This approach permits to identify new potential biomarkers for a specific disease.
- Structural proteomic. It identifies different protein complexes or the proteins present in a sub-cellular localisation or organelle, such as mitochondria, nuclei, lysosomes or chloroplasts.



- Functional proteomic. It investigates the biological functions of unknown proteins and it explains cellular mechanisms and interactions at a molecular level. This approach could identify particular sets of proteins; such as those that are pathway driven or that are involved in cell signalling.

## **1.2. PROTEOME ANALYSIS**

Although the comprehension of proteins relevance in a specific biological system was evident for more than 30 years ago (O'Farrel, 1975, Andersson *et al.*, 2001), only in the mid-1980s this area was emphasised (Righetti, 1983). At the beginning, one-dimensional electrophoresis (1-DE) was the best method chosen for the analysis of the proteins pattern of a specific sample. 1-DE can separate proteins on the basis of molecular mass, and it is highly reproducible and easy to manipulate. However, 1-DE method has the limitations. It can be used to separate proteins only in certain applications, and it does not distinguish protein with a similar molecular mass. For these reasons, 1-DE was later substituted by two-dimensional electrophoresis (2-DE).

Today, as described extensively in literature (Righetti & Boschetti 2007; Wittmann-Liebold *et al.*, 2006), the proteomic analysis makes use of 2-DE, often coupled with mass spectrometry, in order to identify the proteins expressed from a specific biological system. Particularly, 2-DE resolves complex samples, exploiting two

independent chemical-physical features, usually electric charge (isoelectric focusing, IEF) and molecular mass (sodium dodecyl sulphate electrophoresis, SDS-PAGE).

Nowadays, the 2-DE analysis represents a powerful tool for resolving proteome. It consists of five independent parts.

- the sample preparation
- the first dimension (IEF)
- the second dimension (SDS-PAGE)
- the results analysis through specific software
- the mass analysis.

### **1.2.1. SAMPLE PREPARATION**

This is the important step in a 2-DE analysis, because of the 2-D maps quality depends on this phase and because this step reduces complexity of protein mixture. Sample preparation can be subdivided into four fundamental steps: cell disruption, protein solubilisation, removal of interfering substances and, eventually, protein pre-fractionation (see the next chapter).

In the first phase the sample (blood, cells, matrix or tissue) has to be disrupted through different methods: osmotic lysis, sonication, high pressure (e.g. French press) or homogenisation.

The sample is solubilised in specific denaturing buffer containing protease inhibitors, chaotropes (usually urea and thiourea, to create unfolded proteins and to break the hydrogen bonds), detergents (e.g.

Triton X-100 or detergent sulphobetaines to solubilise hydrophobic cores of proteins) and reducing agents (tributylphosphine, TBP, to allow a complete reduction of disulphide bonds at low concentrations without interfering with thiourea), (Rabillaud, 1998). Thus, the original solubilisation buffer was proposed by O'Farrel (O'Farrel, 1975) in 1975 and it was constituted by 9 M urea, 4% 3-[(3-Cholamidopropyl)dimethylammonio]-1-propanesulfonate (CHAPS), 1% dithiothreitol (DTT) and 2% carriers ampholites (CA). Today, this buffer has been improved. Its composition is: 7 M urea, 2 M thiourea, 2-4% CHAPS, 40 mM Trishydroxymethylaminomethane (Tris), 5 mM tributylphosphine (TBP) and 1% CA (Rabillaud, 1998).

After solubilisation, it is necessary to remove from sample the interfering substances such as: lipids, salt ions, polysaccharides, polyphenols and nucleic acids, (Görg *et al.*, 2004).

Different methods were described in literature for removing interfering substances. For example for high salt ions concentration it is possible to exploit dialysis. For decreasing lipids concentration that interacts with membrane proteins organic solvent, acetone methanol or a mixture of these can be used (Mastro & Hall, 1999).

For removal polysaccharides and nucleic acids (that cause horizontal streaks in 2D-gel), precipitation with trichloroacetic acid (TCA) or organic solvents is a useful practice.

It is clear that a single method for sample pre-treatment does not exist, and for each time, the kind of sample and its composition

should be evaluated and, only after that, the best method for the preparation can be chosen.

### **1.2.2. ISO-ELECTROFOCUSING**

When the sample is ready, it can be processed at the first proteins separation: the isoelectro-focusing.

The first dimension (IEF) is performed using pH gradient gel strips with narrow or broad pH ranges, with a linear or not linear gradient.

The IPG gel were developed and described in the early-1980 from Bjellqvist and co-workers (Bjellqvist *et al.*, 1982). The IPGs strips are based on the chemistry of Immobilines, which are modified acrylamide molecules with the general structure  $\text{CH}_2=\text{CH}-\text{CO}-\text{NH}-\text{R}$ , where  $-\text{R}$  contains either carboxyl or amino groups buffering at different pH values, thus generating immobilised pH gradients chemically grafted to the polyacrylamide matrix. Once the sample is loaded, the electric field is applied, the protein migrate at the point in the gradient equal to its pI. At the completion of the IEF, the gel strips are immediately equilibrated in a buffer containing sodium dodecyl sulfate (SDS), transferred and separated using sodium dodecyl sulfate polyacrylamide gel electrophoresis (SDS-PAGE).

Equilibration buffer usually contains 2% SDS, 6 M urea and 20% glycerol (to minimise the interaction between surface charges of gel and proteins and to improve protein transfer from the first to the

second dimension) and Tris-HCl pH 8.8 for matching the typical conditions of SDS-PAGE.

### 1.2.3. THE SECOND DIMENSION: SDS-PAGE RUN AND STAINING

The 2<sup>nd</sup>-D run is carried out perpendicular to the 1<sup>st</sup>-D migration on SDS gel slabs, as showed in Figure 1. The SDS binds to the protein in a ratio of approximately 1.4 g SDS per 1.0 g protein, giving an approximately uniform mass: charge ratio for most proteins, so that the distance of migration through the gel can be assumed to be directly related to only the size of the protein. The 2-D map, displayed at the end of these steps, is the stained SDS-PAGE slab, where polypeptides are seen, after staining, as round spots, each characterised by an individual set of Isoelectric Point/ relative mass (pI/Mr) coordinates.

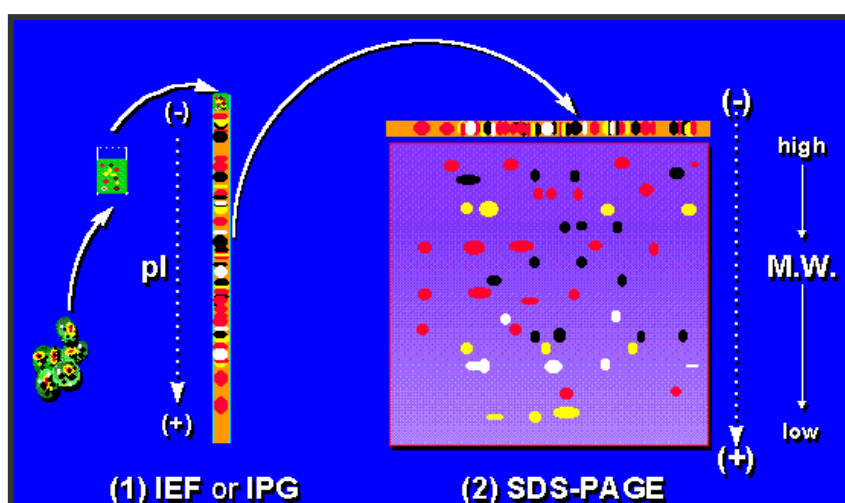


Figure 1\_ Schematic representation of first dimension (IEF) coupled to SDS-PAGE. The protein are separated at the beginning based on pI

and finally on molecular mass.

After SDS-PAGE gels are stained in order to detect proteins spots. The staining does not have to interfere with following mass-spectrometry analysis and it has to be quantitative method. These features cannot be ignored for comparative analysis.

The methods, which have both features, are staining with Coomassie blue colloid solution and Sypro Ruby, extensively described in literature. The Coomassie dye binds to proteins arginine and aromatic amino acid. It provides a good sensibility: about 10 ng/spot (Neuhoff *et al.*, 1988).

Sypro Ruby is an organo-metallic ruthenium chelate stain designed for proteomics applications. Sypro Ruby does not covalently bind to proteins. It associates with primary amines in proteins at acidic pH. Strongest interaction is with Lys, Arg, and His residues and less strong with Tyr and Trp residues. It provides an optimum sensitivity, about 1-2 ng/spot (Steinberg *et al.*, 2000).

There are the other methods, but they are not quantitative, for example photochemical methods of staining with silver (Nesterenko *et al.*, 1994; Shevcenko *et al.*, 1996). Moreover, it is not applicable in the case of mass spectrometry methods of peptide identification due to irreversible modification of lysine and arginine residues that make impossible trypsin digestion (Shevcenko *et al.*, 1996).

#### **1.2.4. RESULTS ANALYSIS**

The main objective of expression proteomics is the simultaneous analysis of as many proteins as possible from a complex proteome. The analyses have to be qualitative and quantitative for gaining an exhaustive view of the sample proteome. Once 2-D maps have been stained, image analysis is usually performed with the help of specific software after image digitisation. Some of the softwares available are: ImageMaster™ (Amersham Biosciences), Melanie 3 (GeneBio), Progenesis™ (Nonlinear Dynamics), PDQuest™ 2-D Analysis Software (Bio-Rad Laboratories), ProteinMine™ (Scimagix), and the Z3 2D-Gel Analysis System (Compugen Limited). Softwares allow creating master maps (that are virtual maps of the digitalised gels including all the spots having statistical significance). These maps are used to detect all the spots, to compare different samples (healthy *vs* pathological) and to quantify by densitometry spots detected. Particularly, they render the analysis as fast as possible and they reduce the intervention of operator.

After identifying the protein differentially expressed (statistically when the proteins expression level is increased by 2 folds or more), it is possible to cut the spots from gel and to analyse them through mass spectrometry, in order to identify their identity and their function.

### **1.2.5. MASS SPECTROMETRY**

Mass spectrometry is an analytical technique used to measure the mass-to-charge ratio of ions. It is most generally used to find the composition of a physical sample by generating a mass spectrum representing the masses of sample components.

Briefly, mass spectrometers are based on a combination of three essential components: ion source, which produces ions from the sample protein mixture; mass analyser, which resolves ionised analytes on the basis of their mass-to-charge ( $m/z$ ) ratio; and detector, which detects the ions resolved by the mass analyser, (Aebersold & Mann, 2003). Two types of MS are used for most proteomic studies: matrix-assisted laser-desorption ionisation (MALDI) and electrospray ionisation (ESI) MS instruments.

They are very different instruments. MALDI is usually coupled to time of-flight (TOF) analysers that measure the mass of whole proteins or peptides, whereas ESI has been mainly coupled to different MS instruments, such as ion traps or triple quadrupole instruments, to generate fragment ion (collision induced) spectra of selected precursor ions. MALDI-TOF is still widely used to study large proteins by what is known as 'peptide-mass mapping'.

With both instruments, the outputs obtained are analysed by comparison with online database in order to identify, which proteins match more correctly with the results.



Usually, a list of candidate proteins that most closely match the input data is generated by the search, and the candidate proteins are ranked using various scoring algorithms. An excellent annotated database is the SWISSPROT database that is maintained by the Swiss Institute of Bioinformatics and European Bioinformatics Institute, it has low redundancy and a high degree of annotation. (Bairoch *et al.*, 2004).

Other example is the SEQUEST program that is used for database searching against un-interpreted product-ion spectra. A number of search engines can also be accessed free-of-charge over the Internet, for example the PeptIdent and MultiIdent programs at the ExPASy Molecular Biology server, MS-fit and MS-Tag at the Protein Prospector server, or MASCOT at the Matrix Science server. These websites also provide additional proteomics software tools, technical information, and links to other resources.

Nowadays, one of the latest technology platforms that have been developed for proteomics includes chip-based arrays. Such arrays have been elaborated for separating proteins based on surface chemistries (*e.g.*, ion exchange, metal chelate, mix-mode, and the like) or known protein ligands (*e.g.*, antibodies), with subsequent analysis by MS. The principle of separating proteins is very similar mechanisms used in column chromatography, Figure 2.

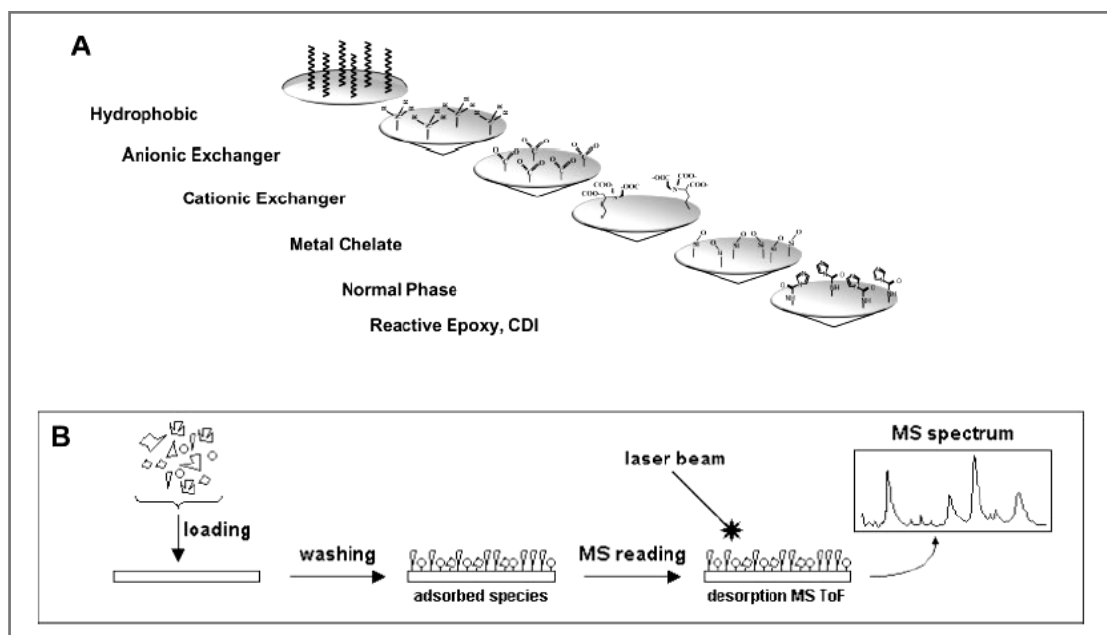


Figure 2\_ (A) Schematic representation of ProteinChip Arrays with chemical functions responsible for protein capture. (B) Mechanism of adsorption-desorption and ionisation of proteins prior entering a mass spectrometer analyser.

The difference here is that the sorbent is a flat surface and the desorption-detection is generated by a laser desorption/ionisation, concomitant to the use of an energy adsorption molecule in order to have proteins vaporised and ionised to enter a time of flight (TOF) MS tube. The main difference between this kind of structural analysis and MALDI-TOF desorption ionisation is that, in the latter case, the sample has to be manually transferred to a microwell plate, admixed with a special matrix (like sinapinic acid) and then desorbed/ionised via pulse laser shots. Conversely, in the protein chips, a stick

containing 8 (or multiples of) such affinity surfaces, which act as chromatography columns, with the captured protein, is directly inserted in the MS instrument and desorbed by surface-enhanced laser desorption/ionisation (SELDI), in the absence of added matrix (the surface of such arrays being, in fact, already coated with absorbing polymers).

Such instrumentation has been rapidly adopted in many clinical laboratories around the world and might soon become part of the standard instrumentation of such laboratories. A lot of papers have been recently published on the field of arrays exploiting SELDI technology (Kohli *et al.*, 2006; Smith *et al.*, 2007; Linke *et al.*, 2006).

#### **1.2.6. LIMITATIONS TO BE OVERCOME IN 2-DE**

Although the Proteomic is a powerful tool for analysis in details of the whole proteome of a specific tissue, it has several limitations, described below.

Firstly, existing 2-DE technology is limited in its ability to separate high molecular mass proteins due to gel pore sizes matrices (Candiano *et al.*, 2002).

Secondly, the hydrophobic proteins are biologically designed to be insoluble in solution, therefore they are nearly impossible to solubilised for electrophoretic purposes and they are not identified in 2-D maps.

Thirdly, the basic proteins remain a technical challenge to separate, while those at extremely alkaline pH ( $pI > 9.0$ ) are rarely separated using 2-DE. In recent times, novel IPGs have become available for separating basic proteins within the pH ranges 6–11, 7–10, 8–11 and 9–12, but often they are not detected during the focusing (Bae *et al.*, 2003).

Other limitation of 2-DE is the so-called “spot overlapping” (Campostrini *et al.*, 2005), which is caused by the use of too wide IPGs with much too complex protein mixtures.

Finally, many low abundance proteins are present on 2-D gels, but they cannot be visualised due to the overwhelming presence of abundant ‘housekeeping’ proteins (e.g. albumin, actin). Often, low abundance proteins are out-and-out potential biomarkers for specific diseases. Therefore, they are present in very small quantity and high abundance proteins mask their signal. For these reasons, it is necessary in proteomic analysis to remove the most of more significantly represented proteins.

## **CHAPTER II**

### **PREFRACTIONATION TECHNIQUE IN**

### **PROTEOME ANALYSIS**

#### **2.1. GENERAL INTRODUCTION**

Considering what described in Chapter 1, it is generally accepted that a major problem in proteome analysis is that a few proteins dominate the landscape and often obliterate the signal of the rare ones. For example, there is an enormous dynamic range, encompassing some 10 orders of magnitude between the least abundant (e.g. cytokines, at concentrations of <1 ng/ml) and the most abundant proteins (e.g. albumin, 50 mg/ml) (Righetti & Boschetti, 2007). The removal of Human Serum Albumin (HSA), for example, together with immunoglobulin G (IgG) (Anderson & Anderson, 2002), which represents the 60-80% of the total serum content, would increase the sample loading capacity and hereby improve the detection sensitivity of low abundant proteins. Potential novel disease markers are often present at low concentration and a pre-fractionation method prior to proteomic analysis can thereby assist in the biomarker discovery process.

This chapter propose to give a brief overview of some methods used for sample pre-fractionation.

## 2.2. FRACTIONAL CENTRIFUGATION

One of the oldest methods used in cell proteome analysis is the separation of cell substructures by the centrifugal cell-fractionation scheme. This method is described the first time by de Duve's groups (de Duve *et al.*, 1955). By this procedure, *via* a series of runs at different centrifugal forces, one can isolate, in a reasonably pure form, sub-cellular organelles, such as nuclei, mitochondria, lysosomes, peroxisomes, synaptosomes, microbodies.

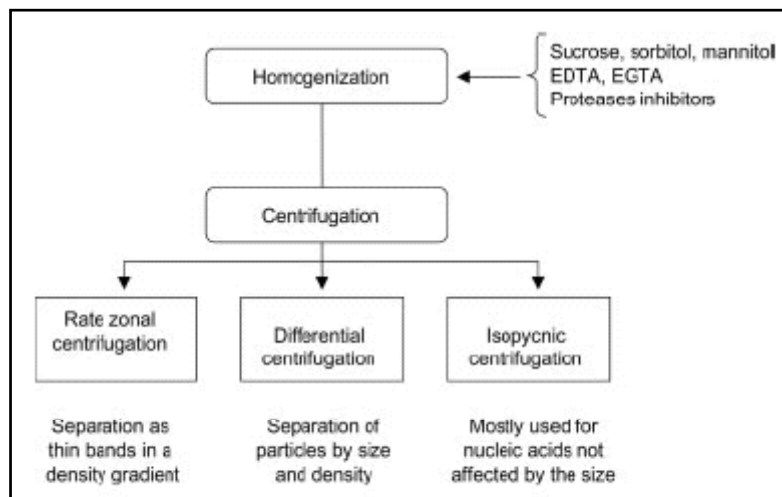


Figure 3\_ Schematic representation of cells fractionation using differential centrifugation (from Righetti *et al.*, 2005).

Clearly, this is the most direct and proficient method for enrichment of the desired protein fractions as they are part of specific substructures of the cells, if the proteome of such organelles has to be investigated. Such methods are still now used for proteome

analysis of mitochondria (Lopez, 2000) and nuclei (Turck *et al.*, 2004) with good results.

### **2.3. CHROMATOGRAPHIC APPROACH**

The solid-phase chromatographic techniques are tools that are of considerable interest in proteome analysis as they are based on a very large choice of solid-phase adsorbents. Low, as well as very high selectivity, can be implemented just by selecting appropriate sorbents and conditions of adsorption-elution. They can be used as a single operating unit or as a combination under the so-called two- or multidimensional liquid chromatography. Different applications are described in literature. First experiments were performed by Fountolaki's group, which enriched the proteome of gram-negative bacteria (*Haemophilus influenzae*) applying affinity chromatography on heparin gel (Fountolakis *et al.*, 1997) followed by chromatofocusing on polybuffer exchange (Fountolakis *et al.*, 1998) and hydrophobic interaction chromatography on phenyl column (Fountolakis *et al.*, 1999). The total number of new proteins identified with these three techniques was, at the end, 350.

In another work a high enrichment of *Escherichia coli* low-abundance proteins was reported by using column with immobilised reactive dye (Birch *et al.*, 2003). The authors demonstrated proteome changes when the strain was cultured at different pH and introduced the dye

chromatography as method for analysing the protein expression in prokaryotic cells.

Other methodologies of pre-fractionation were described recently for increasing the spot number detected and for analysis of a complex samples. Often the chromatographic approach is coupled to mass spectrometry (Martosella *et al.*, 2005; Govorukhina *et al.*, 2006). For example, human serum was depleted of the six most abundant proteins, using an immunoaffinity LC method. The proteins were further separated under a variety of reversed-phase (RP) conditions using macro porous silica C18 adsorbent. The fractions were collected for 2D-LC-MS/MS analysis. The combination of sample simplification by immuno-affinity depletion combined with a robust and high recovery RP-HPLC fractionation allowed high quality protein identifications.

In literature different other methods are described basing on chromatographic approach. For example albumin can be removed by using an immobilised dye: Cibacron Blue F3GA. For the purification of plasma components, Cibacron Blue was first recommended for simple group separation; conditions were used that ensured complete binding of albumin, while the unbound proteins were collected in a single fraction. The Cibacron Blue F3GA has been study extensively in detail at the beginning of its discovery, (Travis & Pannel, 1973; Leatherbarrow & Dean, 1980; Gianazza & Arnaud, 1982).



Other technique developed for removal of high abundance proteins is the use of immunoaffinity column. In this last case, for example, Steel and co-workers reported an investigation of the efficacy of an immunoaffinity resin for improving the specificity and efficiency of removing albumin from human serum samples (Steel *et al.*, 2003). The use of immunoaffinity resins for the selective removal or purification of proteins from solution is well established. However, their application to the problem of albumin removal is not entirely straightforward, primarily due to the enormous load of this single protein species in serum. It was showed that by using high affinity antibodies heavily loaded on beaded resin support, albumin and a large number of albumin fragments could be essentially quantitatively removed from human serum samples.

For both methodologies, it is important to note that generally all these methods described, have a main disadvantage. They may even be problematic for the discovery of peptides of interest that are associated to the removed proteins. In fact, if the protein is a carrier (as albumin), the probability that the other proteins are removed with it is high. In fact, this was recently reported by Mehta (Mehta *et al.*, 2003), where it appeared that the removal of high abundance species was in fact a way to misconsider a source of biomarker of disease significance.

## 2.4. ELECTROPHORETIC APPROACH

The electrophoretic approaches for sample pre-fractionation are described widely in the literature (Righetti *et al.*, 2005; Tam, 2006).

### 2.4.1. THE ROTOFOR

A convenient instrument for sample pre-fractionation is the Rotofor, recently commercialised by Biorad in its miniaturised version (Micro-Rotofor) USA (Hjerten, 1967). The operation principle of this device is based on electrophoresis in free flow (see Figure 4).



Figure 4\_ The Micro-Rotofor instrument from Biorad, USA.

The Rotofor system fractionates complex protein samples in free solution using preparative isoelectric focusing. The system is used for the initial clean up of crude samples and in purification schemes for the elimination of specific contaminants from proteins of interest that might be difficult to remove by other means. Slow rotation of the chamber (1 rpm) stabilises against convective and gravitational

disturbances. Purification using isoelectric focusing is especially advantageous when protein activity must be maintained. Bioactivity is maintained because the proteins remain in solution in their native conformation. The Rotofor has been successfully applied for sample preparation in proteome analysis (Thorsell *et al.*, 2007).

However, in recent times, this methodology has taken another, unexpected turn: the Rotofor is used directly as the first dimension of a peculiar 2-DE methodology, in which each fraction is further analysed by hydrophobic interaction chromatography, using non-porous reversed-phase HPLC (Zhu *et al.*, 2003). Each peak collected from the HPLC column is then digested with trypsin, subjected to MALDI-TOF MS analysis and MSFit database searching. By this approach, Wall and co-workers, (Wall *et al.*, 2000) have been able to resolve a total of ca. 700 bands from a human erythroleukemia cell line. It should be stated, though, that the pI accuracy of this methodology (which is still based on conventional carrier ampholyte-isoelectric focusing, CA-IEF, is quite poor: it ranges from  $\pm 0.65$  to  $\pm 1.73$  pI units, a large error, indeed). On a similar line of thinking, Davidsson (Davidsson *et al.*, 2001) have sub-fractionated human cerebrospinal fluid and brain tissue, whereas Wang (Wang *et al.*, 2002) have mapped the proteome of ovarian carcinoma cells.

### **2.4.2. THE EQUALISER BEADS**

Equaliser beads are a new technology developed by Ciperghen in attempt to improve the pre-fractionation technology and removing impurity traces (Fortis *et al.*, 2005, a-b). This approach is based on the use of combinatorial hexapeptide ligands immobilised on polymethacrylate beads (one ligand structure per bead). In order to produce a sufficient diversity of affinity ligands, a library of 6 millions of hexapeptides (made by combining the 20 natural amino acids in all the possible ways) was synthesised on polymethacrylate beads by Peptides International (Louisville, Kentucky). Each bead, with an average diameter of 65  $\mu\text{m}$ , carries about 50 pmoles of the same hexa-peptide distributed throughout its core. The purpose of this approach consists in the possibility of producing a sufficiently ample spectrum of different affinity ligands.

Equaliser beads reduce the dynamic range of proteome from complex biological samples using a large bead-based library of combinatorial peptide ligands by simultaneously diluting high abundance proteins and concentrating low abundance proteins. When a complex biological sample is incubated with this library, high abundance proteins saturate their high affinity ligand and excess protein is washed away. In contrast, low abundance proteins are “concentrated” on their specific affinity ligand(s), thereby increasing the abundance of trace proteins relative to high abundance proteins. The functioning mechanism of such a technology operated either in overloading or not

overloading conditions (the latter being the one required for achieving a highly purified protein in the flow through experiment is depicted in Figure 5).

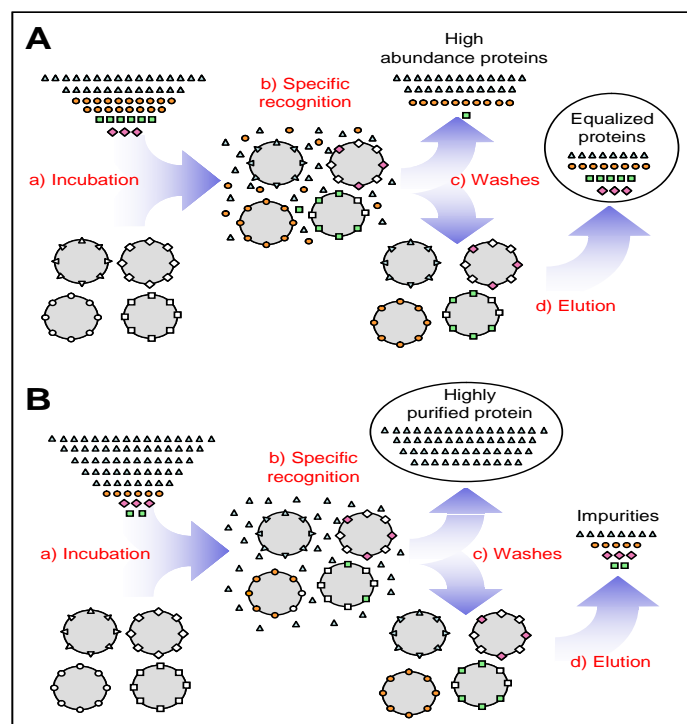


Figure 5\_ Functioning of the equaliser beads in overloading (A) or not overloading (B) conditions. Samples are first incubated with the Equaliser Bead library (a), and specific recognition takes place (b). Protein fraction (unbound proteins) is washed away (c) and the equalized sample (or the protein impurities) is recovered from the beads. Finally, beads are applied on biological fluid with good results (Castagna *et al.*, 2005; Guerrier *et al.*, 2006).

### 2.4.3. THE MULTICOMPARTMENT ELECTROLYSER (MCE)

MCE is another form of free flow Isoelectric Focusing (IEF) developed in the '80 (Righetti, 1983; Faupel *et al.*, 1987). MCE is equipped with

isoelectric membranes and was introduced for purifying proteins in an electric field. The technology employed for casting the membranes is an extension of the isoelectric focusing in immobilised pH gradient technique for which specific acrylamide monomers, known with the trade name of Immobiline, have been developed. They represent amphoteric-species, derivative from bi-functional acrylamide. The membranes are made of Immobilines and they act like barriers, entrapping only proteins with specific pI.

The only condition required is:

$$pI_{\text{cathodic membranes}} > pI_{\text{protein}} > pI_{\text{anodic membranes}}$$

Separation is possible by coupling an orthogonal sample flow to an electric field across the membranes.

MCE has some advantage respect to 2D separation. It is immediately compatible with MS or SELDI MS without any treatment, it is possible to create specific membranes to trap the most abundant species and mainly it allows high sample loading allowing the detection of low abundant proteins.

The MCE device for proteome analysis is quite different from the earlier instruments. In summary, the early MCE devices and the commercial instrument that stemmed from them, the IsoPrime (Amersham Biosciences), use sample recirculation, where the contents (10-100 ml) of each chamber are continuously recycled between the separation chamber in the electric field and an external reservoir. These instruments were designed for protein purification

for crystallography and other techniques where purity is crucial, and as a consequence, the heart of the system, the membranes, were not commercially available because each user requires a specialised set of membranes tailored to the pH value of the protein to be purified. In contrast, the latest MCE miniaturised version, is a small volume (2.5-5 ml/chamber) instrument with no sample recirculation: instead each chamber is stirred using magnetic stirrer bars driven by rotating magnets embedded in the peltier cooling plate. In the absence of recirculation the chamber contents speeds up the fractionation by continuously exposing the whole sample to the electric field. In addition the instrument (Proteome Systems) uses commercially available membranes which are matched to the pH endpoints of commonly used IPGs. It also has an integrated power supply and peltier cooling to ensure that run conditions are reproducible.

The MCE implementation followed a series of prototype version to the final commercially available one, Figure 6. The MCE in proteome analysis was used for instance for the removal of albumin from serum samples (Righetti *et al.*, 2001). In this work, for the first time, MCE has been applied to enrich the sample. The albumin is trapped in a chamber with pI 5.6-6.1. Thus higher sample loads can be applied and 230 spots were analysed by MALDI-TOF MS allowing identification of 130 polypeptides. Notwithstanding MCE is a powerful tool to remove specific proteins (for example albumin) from biological fluid and thus to enrich specific sample.

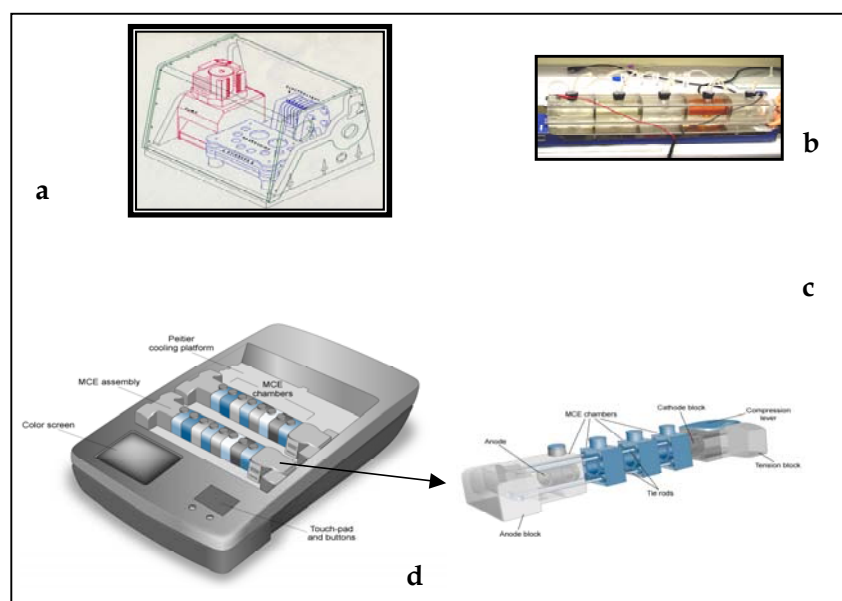


Figure 6\_ Historical excursus of MCE instrument: from the early version (a) to the present one (d), through the prototypes tested in our labs (b, c).

Proteome pre-fractionation in MCE is proposed from Fortis and co-workers (Fortis *et al.*, 2005, a), with substantial modifications as compared to the standard technique. Firstly, the classical isoelectric buffering membranes, delimiting each compartment and acting, in pairs, as isoelectric traps, have been replaced by isoelectric buffering beads. These membranes operate on the same principle, but allow unhindered migration of proteins (lack of sieving properties, contrary to typical continuous membrane barriers). Secondly, the isoelectric beads are composed of a hard, ceramic core, coated with an amphoteric buffering polymer. This minimises mass transfer resistance of proteins that are transiently adsorbed onto the beads.



As a result, significantly reduced separation times, of the order of ca. 3 h, instead the traditional method (overnight and much longer) in conventional MCE operating with isoelectric membranes. Examples of separation of standard marker proteins, as well as entire *Escherichia coli* lysates and human serum proteins, are given with good results.

#### **2.4.4. OTHER SAMPLE TREATMENTS METHODS**

Although not largely described in the literature, immunoprecipitation is other method that deserves a specific place among pre-fractionation methods prior protein analysis using 2-DE analysis. The principle is based on the use of antibodies that are selective for one or more groups of proteins sharing a similar epitope. This is the case for instance of phosphorylated proteins or protein isoforms. In practice the selected antibody is mixed with the protein extract and incubated the time necessary to form an immunocomplex. Then the immunocomplex is separated using a Protein A column. In this respect, a very convincing paper has been published by Watts (Watts *et al.*, 1997), where the separation of isoforms of tumour necrosis factor, were selectively separated and then analysed by 2-DE. An Immunoprecipitation approach used alone or in association with other separation methods, was extensively described as probes for elucidating some aspects of signal transduction (Sheffield & Gavinski, 2003) as well as for the analysis of phosphotyrosyl proteins in cerebrospinal fluid (Yuan & Desiderio, 2003). The

immunoprecipitation principle is also interesting for investigating the formation of protein-protein complexes (Schulze & Mann, 2004) and therefore contributing to the elucidation of some pathways. Although in literature more efficient protocols are described, immunoprecipitation remains an easy and cheap method for removal of high abundance proteins from a complex sample.

### **2.5. CONCLUSIONS**

As described briefly in this chapter, the proteome landscape changed dramatically during the last 20 years. Up to the early seventies, scientists could only separate a handful of proteins when attempting various electrophoretic or chromatographic approaches. Afterward, with the explosion of informatics technologies, the building of genome and proteome database, and other new methodologies (MCE and equaliser beads), the study of proteome has become much more comprehensive. We believe that the future will bring new methods and further improvements in proteins separation and analysis.

Finally, many more examples are present in literature, but it is outside of scope of this chapter to give their comprehensive description. The aim of this section was to give an overview of the methods present and extensively used in literature.

## **CHAPTER III**

### **MOLECULARLY IMPRINTED TECHNOLOGY**

#### **3.1. GENERAL INTRODUCTION**

*Molecular imprinting* can be defined as the process of template-induced formation of specific recognition sites (binding or catalytic) in a material, where the template drives the positioning and orientation of the material's structural components by a self-assembling mechanism, as shown in Figure 7. The material itself could be oligomeric (a typical example is the DNA replication process), polymeric (organic MIPs and inorganic imprinted silica gels) or two-dimensional surface assemblies (grafted mono-layer). Molecularly Imprinted Polymers (MIPs) have a range of advantages with respect to natural bio-molecules.

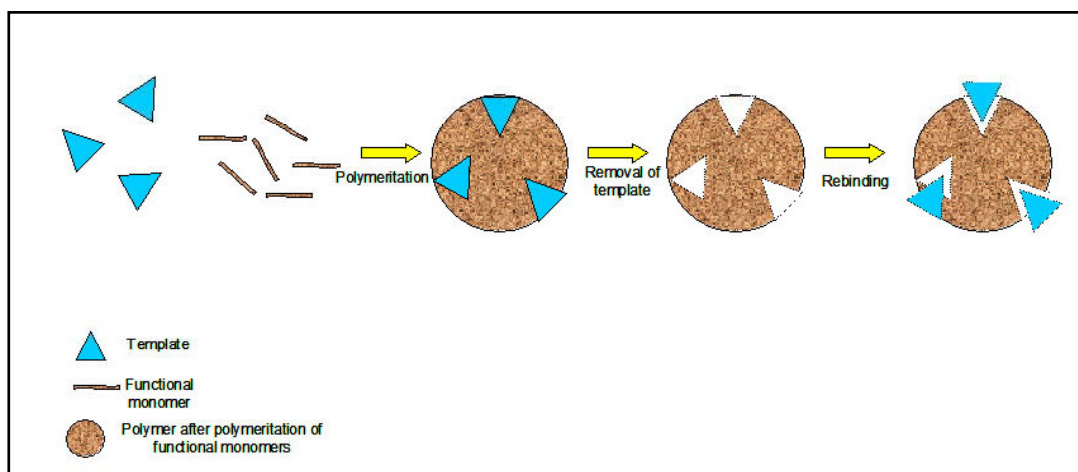


Figure 7\_ Schematic representation of molecular imprinting.

MIPs are potentially applicable to the areas of clinical analysis, medical diagnostics, environmental monitoring and drug delivery. Molecular imprinting technology allows for the creation of synthetic receptors with binding constants comparable to natural receptors, but capable of withstanding much harsher conditions, such as high temperature, pressure, extreme pH, and organic solvents as compared to proteins and nucleic acids. These materials are also less expensive to synthesise and can be manufactured in large quantities with good reproducibility. Moreover, they have a unique stability, which is superior to that of natural biomolecules.

Nevertheless molecular imprinting technology still needs to overcome some problems, such as template leakage, poor accessibility to the binding sites, low binding capacity and non-specific binding.

Molecularly imprinted technology, moreover, can be applied to specific sensors, but in this case some further specific limitations occur: absence of a general procedure for MIP preparation; difficulties in integrating them with transducers; difficulties in transforming the binding event into an electric signal; generally poor performance of MIPs in aqueous solution.

In the last years significant progress has been made in resolving part of these problems. Several promising protocols for MIPs creation were developed, including combinatorial (Lanza & Sellergren, 1999) and computational methods (Chianella *et al.*, 2003). These two approaches permit the creation of MIPs with affinity and selectivity comparable to those of antibodies (Chianella *et al.*, 2003).

Starting from the first 90s, MIP technology has been extensively exploited to create recognition sites for a range of different templates. Some examples are: polypeptides (Kempe & Mosbach, 1995; Andersson *et al.* 1995; Minoura & Rachkov, 2000), bacteria (Dickert *et al.*, 2003; Dickert *et al.*, 2006; Bolysai *et al.*, 2006), low molecular mass compounds (Katz & Davis, 2000; Pampi & Kofinas, 2004; Yilmaz *et al.*, 2000; Breton *et al.*, 2007), toxins, contaminants food or pesticides (Baggiani *et al.*, 2007; Turner *et al.*, 2004; Breton *et al.*, 2007) and proteins (Burow & Minoura, 1996; Bossi *et al.*, 2001; Guo *et al.*, 2004; Lin *et al.*, 2007).

Of all the examples listed above, imprinting of proteins represents one of the most challenging tasks. The reason for this lies in several

factors related to the properties of these templates. First of all proteins are usually soluble in water, a compound frequently incompatible with mainstream MIP technology, which relies on using organic solvents for the polymer preparation. Secondly, proteins have a flexible structure and conformation, which can be easily affected by changes in the environment such as e.g. temperature. From thermodynamic and practical standpoints, it is difficult to develop successful imprints for such molecules. Thirdly, proteins have a large number of functional groups available for the interaction with functional monomers. There is always a trade-off involved in the selection of imprinting protocols, which in some cases relies on using strong binding monomers, while in others involves weak binding monomers for the template recognition. The present chapter furnishes a comparative analysis of the different approaches developed, underling the advantages and disadvantages, highlighting the trends and hypothesising future developments.

### **3.2. RECOGNITION THROUGH THE PLACEMENT OF FEW CONSTRAINS ON THE POLYMER**

In general, approaches to protein imprinting can be divided into two major groups: either the imprinted polymer is targeted to recognise the sequence of the protein (or of a part of it), or to recognise the shape of a protein.

The first attempt to imprint protein by using a sequence-recognition approach was proposed in 1995 by Kempe and co-workers. The authors built a MIP capable of partially discriminate the spatial orientation of the protein, as shown in Figure 8 (Kempe & Mosbach, 1995; Kempe *et al.*, 1995). In this work, the interactions were based on metal co-ordination, as suggested previously by Mallik and co-workers in 1994, (Mallik *et al.*, 1994, a, b). Silica surfaces were derivatised with 3-(trimethoxysilyl)propylmethacrylate, thus introducing double bonds, which were then used as anchorage points for the imprinted polymer. The template protein, ribonuclease A, was mixed with metal ions and with the functional monomer N-(4-vinyl-benzyl) iminodiacetic acid (VBIDA). Imidazole groups (Im) of the histidines exposed on the surface of the protein formed complexes with the metal chelating functional monomers, creating complementary cavities with 'anchoring points' for the recognition of the protein. The imprinted silica particles were packed into chromatography columns, and tested for their separation selectivity. Binding capacity was evaluated by using the capacity factor  $k' = (t - t_0)/t_0$ , where  $t$  is the elution volume of the protein and  $t_0$  the void volume. Results indicated that the stationary phase imprinted with ribonuclease A (RNase) in the presence of metal ions, had a capacity factor ( $k'$ ) of 5.79 versus 2.46 measured for a competitor protein, lysozyme. Furthermore, the silica particles were compared with reference particles, prepared in the presence of bovine serum

albumin (BSA).

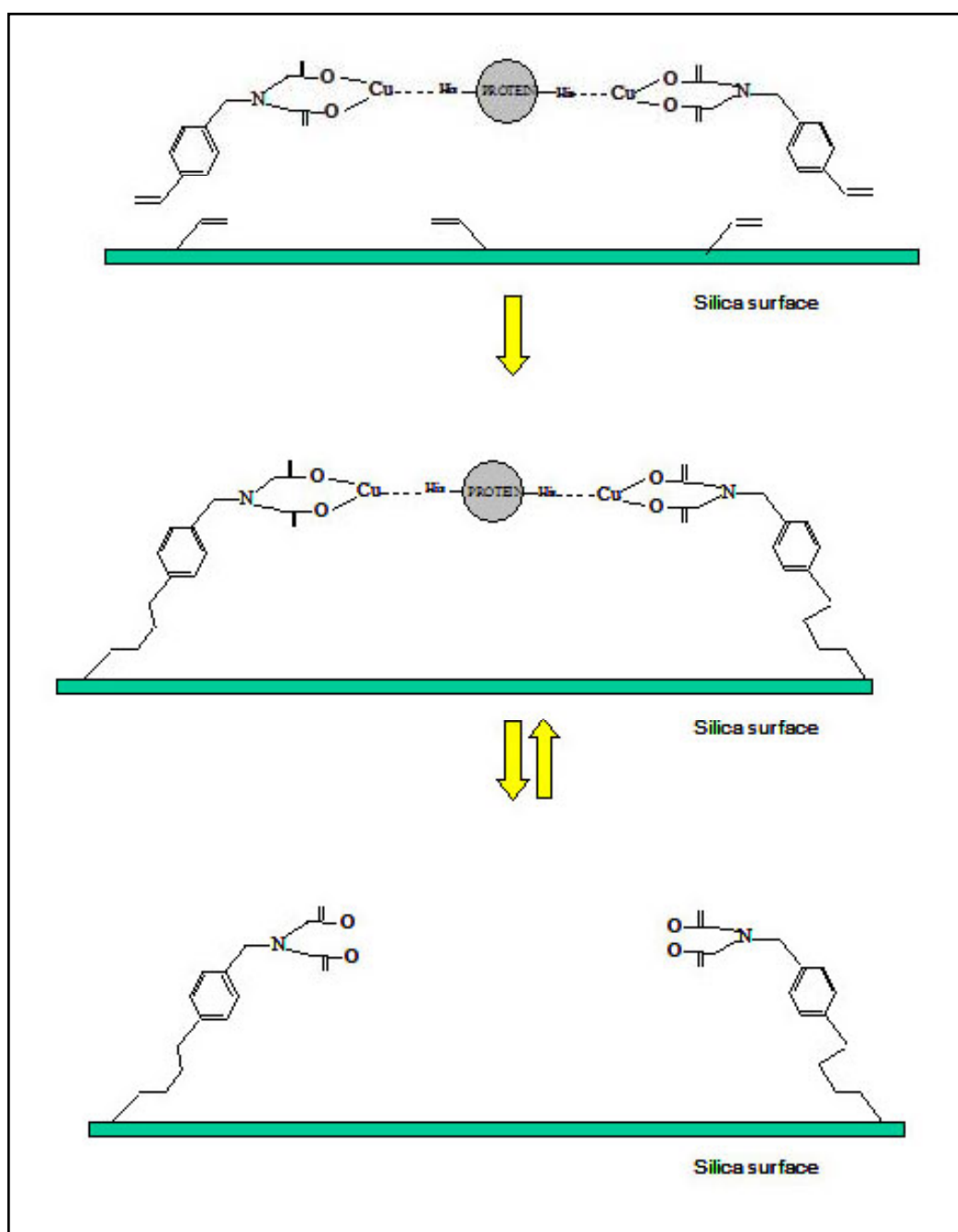


Figure 8\_ Schematic representation of the metal-chelate approach (modified from Kempe *et al.*, 1995).



In this case,  $k'$  was 2.68 for RNase and 1.63 for lysozyme, indicating that the imprinting strategy was effective in producing a surface selective for the template molecule. The RNase/lysozyme separation factor ( $\alpha$ ) achieved was 2.35 for imprinted adsorbent versus 1.64 for reference adsorbent. Despite the positive results, the metal chelating approach was not further exploited. The main reason for this might have been the applicability of such an approach solely to protein targets that expose histidine residues on their surface. Additionally, metal chelating groups provide strong anchoring points for non-specific interactions, which in real samples might seriously impede specific recognition. There are no recent publications concerning this method, as it has been replaced by more innovative approaches.

### **3.3. SHAPE RECOGNITION WITH POLYACRYLAMIDE GELS**

In the same period of Kempe's experiments, in the mid 90s, Hjertèn and co-workers were engaged in the development of a different approach to create molecularly imprinted polymers for the recognition of proteins. They chose to use a "soft" polyacrylamide (PAA) gel as matrix (Hjerten *et al.*, 1997; Liao *et al.*, 1997). This choice was motivated by the inert nature of PAA, its biocompatibility and its neutrality, thus non-specific interactions with proteins were expected to be minimised (Hjerten, 1962; Hjerten & Mosbach, 1962). The PAA gels, made of acrylamide and N-N'-methylene bisacrylamide, mixed at different ratios, were imprinted with the

following proteins: ribonuclease, haemoglobin, lysozyme, myoglobin and the Human Growth Factor (HGF) peptide. PAA imprinted gels were then pressed through a 100-mesh net to produce granules, which were packed into chromatographic columns. Each imprinted PAA polymer was tested for its binding affinity. The results showed that polymers had high recognition abilities (evaluated by measuring the differences in protein retention times on imprinted and non-imprinted columns). For example, the column prepared with RNase as template, was able to adsorb only RNase and not other competitor proteins. Of particular interest was the demonstration of the ability of the PAA-imprinted polymers to discriminate between two homologous proteins that differ only in 20 residues out of a total sequence of 153 residues. In this case, a column prepared using myoglobin from horse as template was proven to recognise (i.e., to adsorb) this template but not myoglobin from whale.

The PAA-soft-gel imprinting approach demonstrated a higher specificity and a broader applicability as compared with the metal-chelate approach. Moreover, the PAA-templating approach has been recently modified by the incorporation of chargeable functional monomers in the polymeric backbone. The use of methacrylic acid and of 2-(dimethylamino) ethyl methacrylate was described in the preparation of a material for the recognition of lysozyme (Ou *et al.*, 2004). The imprinting factor, calculated as a binding ratio between MIP and blank polymers, for lysozyme was 1.83. It was

demonstrated that binding was dependent on ionic strength, cross-linking degree and the amount of removed template. The lysozyme-template polymer was also tested for the binding of cytochrome c, which has molecular weight and isoelectric point (pI) similar to those of lysozyme, and for the binding of albumin, which presents highly different molecular size and pI. In contrast to the results obtained by Hjerten, in the case of modified and chargeable gels, the results indicated that the imprinted polymer could not discriminate efficiently between different proteins.

The main problem of PAA gels, however, lies in the softness and in the scarce mechanical strength of such material. Recently, Guo and co-workers proposed a strategy to overcome this problem. They developed a new method for derivatising beads made of PAA gel. In order to improve the mechanical strength of PAA gel, macro-porous chitosan beads were used, as matrix, chitosan is a natural polysaccharide, a biopolymer comprising d-glucosamine and d-acetylglucosamine, which is non-toxic and bio-absorbable. The soft polyacrylamide gel is entrapped in the chitosan beads, which confer to the polymer beads higher mechanical strength and chemical stability, as well as good hydrophilicity (Guo *et al.*, 2004, Liu *et al.* 2006). The selectivity test for chitosan-PAA MIPs was carried out using Bovine Serum Albumin (BSA) as reference protein and haemoglobin (Hb) as template, evaluating the amount of each protein adsorbed to the MIP under equilibrium conditions. The distribution

coefficient  $K_D$  is defined as  $K_D = 4 \cdot C_p / C$  (where  $C_p$  is the concentration of protein in the MIP beads (mg/g) and  $C$  is the concentration of protein in solution (mg/ml)). Generally, beads show a high specificity degree for the template molecule with respect to the reference protein ( $K_D$  for Hb is averagely 40, while for BSA it is only 1.7). Thus, the chitosan-PAA MIPs represent a fine and relatively easy strategy for reinforcing PAA porous gels, while maintaining a good degree of selectivity. It was demonstrated that selectivity is strongly related to the shape of the protein template. Hb and BSA are both globular proteins, but Hb is a tetrameric protein composed of pairs of two different polypeptide chains and has a biconcave shape. BSA consists of one polypeptide and has an ellipsoidal shape. Results showed that the cavities formed in the MIP recognised preferentially Hb, indicating that cavities matched the size of Hb better than BSA. Recently, after about 20 years, a new work on protein imprinting with polyacrylamide gel as been published (Takatsy *et al.*, 2006), thus suggesting that this approach, although presenting some limitations, is still used in MIP technology.

Artificial antibodies in the form of gel granules were prepared by the molecular imprinting technique from the monomers acrylamide and N,N-methylene-bis-acrylamide.

Gel granules, freed from the selectively adsorbed protein (the antigen), are neutral and, accordingly, do not migrate in an electrical field. However, upon selective interaction with the antigen at a pH

different from its pI, the granules become charged. The selectivity of the gel antibodies was studied by free zone electrophoresis in a tube with the inner diameter larger than the granule size. Such electrophoretic analyses showed that gel antibodies against iron-free transferrin had a high selectivity for this protein, although some cross-reactions took place with iron-saturated transferrin, indicating that these artificial antibodies can easily distinguish the minute differences in the 3-D structure of the transferrins. Analogously, gel antibodies against iron-saturated transferrin were highly selective for this protein, although presenting some cross-reactivity with iron-free transferrin. This can be explained if we consider that the mobilities of iron-free and iron-saturated transferrin are very similar, thus capillary free zone electrophoresis cannot distinguish between these structurally related proteins.

However the significant differences in the mobility of the selective gel granules can be observed depending on their interaction with iron-free or iron-saturated transferrin, therefore the artificial gel antibodies may become powerful analytical tools.

In fact, they are simpler to produce and more stable; experimental animals are not required for the synthesis; they could probably be more selective, since gel antibodies have a larger contact area with the antigen (protein antibodies clasp only a limited portion).

The potential applications are numerous: they can be valuable tools in both human and veterinary medicine, for instance for detection of biomarkers for clinical diagnosis, or for detection of HIV infections.

### **3.4. EPITOPE APPROACH: EXPLOITING A SMALL STRUCTURAL ELEMENT OF THE PROTEIN FOR ITS RECOGNITION**

In nature, antibody-antigen interactions depend on the recognition between the antibody and an antigenic site of the protein, the epitope.

The epitope is a short amino-acid sequence complementary to the binding site of antibody. In the field of Molecular Imprinting, Rachkov and co-workers used this observation to develop a new concept for the synthesis of protein recognition polymers (Rachkov & Minoura, 2000; Rachkov & Minoura, 2001). Instead of the whole proteins, a short peptide sequence exposed on the protein surface was used as a template for MIP preparation. Once the matrix has been polymerised the resultant imprinted material should be able to recognize and bind the whole protein. The concept was proven by using as a template a short sequence (3-4 residues) of a bioactive peptide, as shown in Figure 9. In their studies, Rachkov and co-workers created an imprinted polymer specific for the nonapeptide oxytocin, a neurohypophyseal hormone (Cys-Tyr-Ile-Gln-Asn-Cys-Pro-Leu-Gly-NH<sub>2</sub>). A small oxytocin sequence of three amino acids

proved to be enough for the recognition of the whole peptide sequence by the MIP.

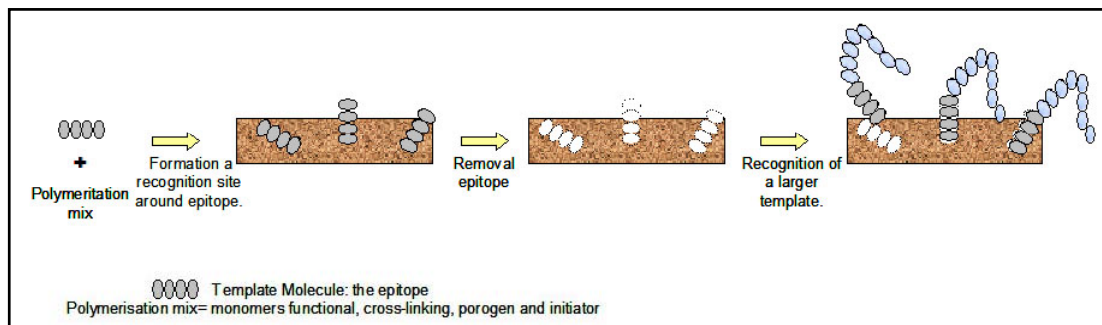


Figure 9\_ Schematic representation of the epitope approach (modified from Rachkov & Minoura, 2001).

The polymer was made of methacrylic acid (MAA) and ethylene glycol methacrylate (EGDMA). HPLC columns packed with epitope-imprinted polymers were used to define the optimal pH and ionic strength conditions for the oxytocin-MIP recognition. Ionic strength was varied in the range 0.5 - 20 mM, showing that as salt concentration increases the template retention time decreases. This experiment demonstrated that ionic interactions gave an essential contribution to the recognition and binding process. The optimal pH for proper recognition was carefully chosen, since the mobile phase pH played a crucial role in the binding. Another factor affecting the recognition process was the template to functional monomer ratio. The optimum template-peptide/MAA ratio was found to be between 1:10 and 1:20. An accurate tuning of all these parameters allowed

the optimal binding conditions for the polymers to be found. In order to evaluate the MIP selectivity, a polymer made of template-peptide/MAA (1:10) was tested for its binding capacity toward the template itself and oxytocin-related peptides. The mobile phase consisted of 10% water/90% acetonitrile, with different concentrations of acetic acid. The values of the separation factor  $\alpha$  (ratio between  $k'$  for tetrapeptide and  $k'$  for oxytocin) depended on the concentration of acetic acid and pH. The best value (i.e., 3.64) was obtained at pH 6.0 (2.5 mM acetic acid), while at pH 5.0 the value of  $\alpha$  dropped to 1.68.

Subsequently, the epitope-approach was applied for the recognition of the octa-peptide hormone angiotensin II (Rachkov *et al.*, 2004). Moreover, the epitope approach was extended to silica-based materials using double-strand DNA as a template (Slinchenko *et al.*, 2004). It is not the purpose of this chapter to describe systems using templates different from proteins. Moreover, it is difficult to evaluate the real efficiency of the epitope approach, since no experiments have been reported on polymers imprinted with a small peptide and used to recognise large protein molecules.

### **3.5. MOLECULARLY IMPRINTED POLYMERS GRAFTED ONTO SURFACES**

All the approaches described so far make use of polymeric networks extended in 3D-space. It is believed, however, that two-dimensional



imprints could have improved binding kinetics by reducing the time needed to attain diffusion-controlled equilibrium in the core of three-dimensional polymeric matrixes (Mirsky *et al.*, 1999). Earlier, Piletsky and co-workers had described a technique for coating polystyrene microplates with a thin polymer made of 3-aminophenylboronic acid (ABPA). This technique was applied for small molecules, such as atrazine or epinephrine (Piletsky *et al.*, 2001) and for proteins (Piletsky *et al.*, 2000; Bossi *et al.*, 2001). In the case of protein imprinting, after optimisation of washing and re-binding conditions, MIP-plates were tested for their binding selectivity. The authors used lactoperoxidase, haemoglobin, horseradish peroxidase, cytochrome c and microperoxidase as templates, which differed in size and isoelectric points. Rebinding experiments demonstrated that size and charge affected the binding capacity. The results indicate that small proteins have dissociation constants,  $K_d$ , in the  $\mu\text{M}$  range, while large proteins, such as lactoperoxidase, haemoglobin or horseradish peroxidase, have  $K_d$ s a thousand times smaller. The potency of the surface imprinting approach was demonstrated by the ability of the polymer to discriminate between haemoglobin (Hb) and its glycosylated isoforms (Hb-A1), with  $K_d$  values differing by more than 3 fold.

Subsequently, this approach was exploited for the development of a protein sensor, based on QCM (Quartz Crystal Microbalance). It is a simple, cost effective, high-resolution mass-sensing technique, based on the piezoelectric effect. As a methodology, the QCM evolved into a

valuable solution for mass measurements in analytical chemistry due to its large solution-surface interface and measurement capability. The technique possesses a wide detection range. Rick and co-workers describe a in literature recent example, where the QCM is applied to MIP technologies. Poly-APBA was deposited onto a quartz microbalance crystal (QCM) using lysozyme or cytochrome C as templates. The authors demonstrated a good selectivity for the template proteins, both for lysozyme-templated polymer and for polymer templated with cytochrome c. Negligible rebinding was observed for other protein competitors such as albumin or myoglobin. A remarkable achievement of the experiment was the demonstration of the ability of imprinted polymer to distinguish two proteins, lysozyme and cytochrome c, when used simultaneously as templates (Rick & Chou, 2005).

A second, more recent example is the positive results reported by Baltus and co-workers, who developed a ligand for a genetically engineered hormone-binding domain of the alpha-estrogen receptor, which were immobilised onto a piezoelectric quartz crystal (Baltus *et al.*, 2007). Two different approaches were used to attach the genetically altered receptor to the gold electrode on the quartz surface: (1) the mutant receptor containing a single solvent-exposed cysteine was directly attached to the crystal via a sulphur to gold covalent bond, forming a self-assembled protein monolayer, and (2) the N-terminal histidine-tagged end was utilised to attach the

receptor via a 3,3-dithiobis-[N-(5-amino-5-carboxypentyl)propionamide-N',N'-diacetic acid] linker complexed with nickel. These results illustrate that the immobilisation strategy used to bind the receptor to the sensor platform is fundamental for eliciting an appropriate response in this biosensor. This study has important implications for the development of QCM-based sensors using protein receptors.

QCM is currently widely used, and many papers are available in literature on this topic (Marx, 2003).

More recently a new application using QCM gave good results in the protein imprinting field (Turner *et al.*, 2007).

They employ APBA as a protein imprint matrix for discriminating between native and thermal- or solvent-induced protein conformations of the model protein, bovine  $\alpha$ -lactoglobulin. Circular dichroism is used here to confirm protein conformation changes. Protein (re)binding to imprinted and control poly(APBA) thin films is monitored using the quartz crystal microbalance. The surface properties of poly(APBA) at various stages of polymerisation are further characterized using atomic force microscopy and sessile water drop contact angle analysis.

Results indicate that using QCM to monitor protein adsorption, the greatest affinity was observed for rebinding of the isoforms to their own imprints, demonstrating the importance of steric contributions to the creation of protein-imprinted cavities. They however

demonstrate the validity of the molecular imprinting technique for the detection of distinct conformations of the same protein. This is a step forward from recognition between different proteins and, despite the modest selectivity, demonstrates the flexibility of the molecular imprinting technique. Therefore, as they self-highlighting these are preliminary and modest results respect to described in literature and reported in this chapter.

Thus, as the QCM method has already demonstrated extensively its effectiveness as an alternative screening and analysis method, the purpose of this chapter is not to describe all of its possible applications, but just to give some examples.

Recently a new approach was developed, called the micro-contact imprinting. The micro-contact imprinting approach is a chemical structuring method that involves the conformal stamping of self-assembling mono-layers in a specific pattern on a surface, so that it is possible to form recognition sites for the template. Chou and co-workers developed this method, (Chou *et al.*, 2005). At the beginning, they used a micro-contact imprinting approach to glass surface. They prepared a single layer on the surface of a microscope cover glass, together with the functional monomer (O-(4-nitrophenylphosphoryl) choline, 4-NPPC), the cross-linker (polyethylene glycol 400 dimethacrylate, PEG400MAA) and the template, which was C-reactive protein (CRP), a protein composed of five identical non-glycosylated sub-units of 206 amino acids each,

associated into a pentameric structure. Binding experiments demonstrated a good binding capacity for the polymer imprinted with the template protein, equal to 1  $\mu\text{g}/\text{cm}^2$  of CRP bound versus approximately 0.3  $\mu\text{g}/\text{cm}^2$  and 0.1  $\mu\text{g}/\text{cm}^2$  of human serum albumin and lysozyme, respectively. Under competitive binding conditions, it was demonstrated that the polymer imprinted with CRP is able to bind 3.78  $\text{ng}/\text{cm}^2$  of CRP protein versus 0.08  $\text{ng}/\text{cm}^2$  of the competitor protein (in this case human serum albumin).

Recently micro contact approach was further investigated. Authors suggested different mixtures for creating polymers capable of recognising specific proteins (myoglobin or lysozyme). They underlined the importance of monomer and cross-linker choice (Lin *et al.*, 2006). In fact the choice of the functional monomer(s) plays a key role in the selectivity of final MIPs.

The same authors have fabricated a new thin polymer film in order to recognise myoglobin and to increase the recognition capacity of previous polymers (Lin *et al.*, 2007). Different polymers with different properties were tested for creating specific supports for myoglobin. For example, tetraethylene glycol dimethacrylate (TEGDMA) exhibited the lowest affinity for the template species. The methacrylate (MMA) has been chosen as the functional monomer, since when it was used in conjunction with tetraethylene glycol dimethacrylate (TEGDMA), it exhibited maximum selectivity for the template compared to the polymers made with other functional

monomers. Rebinding in natural biological matrices, i.e. human serum or urine, showed that the imprinted films had significantly greater affinity than non-imprinted films. Re-binding in undiluted urine was found to be a facile process, with the imprinting factor, i.e. the ratio of MIP to not MIP binding, being determined as 37.4. Afterwards the binding and competitive experiments demonstrated the efficiency of such a technology and the possibility of further applications (Lin *et al.*, 2007).

Summarising, these results indicate that the micro-contact imprinting approach is able to generate MIPs having both good binding capacity and selectivity for the template molecule.

### **3.6. IMMOBILISING TEMPLATE ONTO A SURFACE**

Another imprinting method is based on the oriented immobilisation of the template molecule onto solid sacrificial supports. The growing MIP is polymerised in close contact with the template-carrying surface. After polymerisation, the support is dissolved by harsh chemical treatment. There are a number of advantages in using a molecule bound onto the surface as a template. For example, a template insoluble in the polymerisation mix can be easily used. Moreover, template immobilisation minimises protein aggregation and the resulting binding surface is more homogenous.

In a paper by Shi (Shi *et al.*, 1999), template was deposited onto a support surface such as mica, which is hydrophilic and negatively

charged. This is important to prevent the denaturing of the adsorbed proteins. The protein template was deposited onto mica, after that the protein-surface was coated with a disaccharide layer, and next with a thin film (10-30 nm) of hexa-fluoropropylene. The resulting film was fixed onto a glass cover by using epoxy resin, which was finally cured in an oven. Harsh washes were used to detach the mica support from the imprinted film, leaving cavities complementary to the template free for a new binding. The selectivity of such a MIP for its template protein was confirmed by competitive binding experiments, estimating the amount of competitor required to cause a 50% reduction in the maximum adsorption ( $R_{50}$ ). To investigate the shape specificity, two proteins very similar in physical chemical properties and isoelectric point were used, namely lysozyme and ribonuclease A (RNAase). In the case of RNAase adsorption from a mixture of lysozyme and RNAase, there was a 20 fold higher selectivity for RNAase in the related MIP. This demonstrates the high specificity of template recognition achieved.

A recent paper, published in 2005 (Shiomi *et al.*, 2005), exploits another approach to immobilise a protein template around silica beads, and represents an evolution of some pioneering attempts in the same direction published earlier (Glad *et al.*, 1985; Venton & Gudipati, 1995 a,b), where silica monomers were incorporated onto silica beads in the presence of the template protein, as shown in Figure 10.

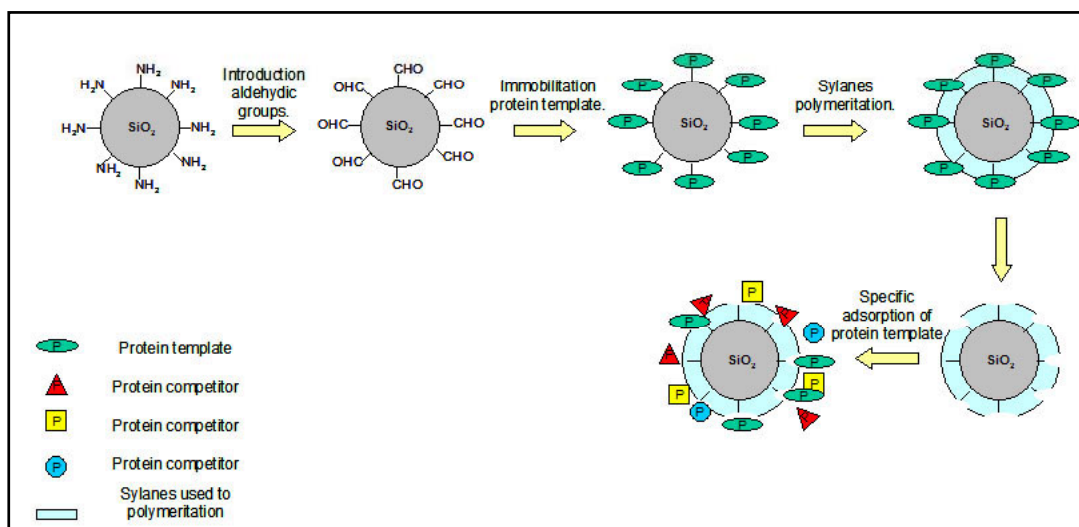


Figure 10\_ Schematic representation of protein immobilisation (from Shiomi *et al.*, 2005).

In this recent study, the protein (haemoglobin) is first covalently immobilised onto a derivatised silica surface, instead of being free in solution during the polymerisation. A comparison between such imprinted materials and imprinted silica beads obtained with conventional non-immobilised haemoglobin is then made. Materials imprinted with immobilised template showed a slightly higher binding capacity for the template, but a far better performance in competitive binding experiments: MIPs were able to bind the template specifically, while other proteins such as transferrin and chymotrypsinogen A were practically not absorbed. This suggests the formation of quite homogeneous binding cavities on the beads. However, proteins with charge similar to the template protein, such as myoglobin, with a pI almost identical as that of haemoglobin,



appeared to be slowly sequestered by MIPs from solution after long incubation times. In general, imprinting using immobilised template can be considered as a very promising way to create biomaterials for separation and sensing. In addition, nano-imprinting with immobilised template could be used for repetitive recreation of imprinted layers for sensor fabrication (Shiomi *et al.*, 2005).

These examples demonstrated that the recognition capability of a specific protein increases if the template is immobilised on a surface.

### **3.7. CONCLUSIONS**

Molecular imprinting technology has gained considerable momentum in its development since 1990. Important results have been achieved and discussed elsewhere with imprinting experiments using small molecules, such as peptides or amino acids. As regards proteins, MIP development has been considerably slower, because it is quite difficult to create polymer cavities specific for complex molecules such as proteins. The problems associated with imprinting of relatively unstable three-dimensional conformations, with possible rearrangement processes and with poor solubility of the template are usually the main reasons why the imprinting of proteins remains difficult. Different approaches have been developed to overcome these problems, the most important of which have been briefly discussed in this review. It is clear that further research is needed in order to make protein imprinting a truly practical

approach for molecular recognition in diagnostics, separations, drug delivery and other applications demanding accurate discrimination of critical components in living systems.

**CHAPTER IV**

**CREATION OF MOLECULARLY IMPRINTED**

**BEADS FOR RECOGNITION OF HUMAN SERUM**

**ALBUMIN**

**4.1. GENERAL INTRODUCTION**

Molecular imprinting is a technique for synthesising polymers with template specific binding sites, whereby monomers are polymerised in the presence of a template molecules. Different approaches are used in order to create specific polymers able to recognise a specific molecule target. In this section of my PhD thesis, I studied a new method for creating imprinted polymers targeted for the recognition of a protein: human serum albumin, HSA. These polymers were synthesised in aqueous media, using a strategy based on the exploitation of multiple weak interactions such as hydrogen bonds or Van der Waals forces contributing to specific recognition.

The derivatised beads were characterised by different methods in order to have a better understanding about binding process and also about applicability of these new materials for the recognition of proteins.

## **4.2. MATERIAL AND METHODS**

Acetic Acid, Aminopropyl silica (particle size 15-40  $\mu\text{m}$ , mean pore size 60  $\text{\AA}$ ), 3-aminopropyl-trimethoxysilane (APTMS), Ammonium persulfate (APS), Bradford Assay, [3-cholamidopropyl dimethylammonio]-1-propanesulfonate (CHAPS), Carbonic Anhydrase (AC) Ethanol, Glycine, Glutaraldehyde, Human Serum Albumin (HSA) (Mr 66 kDa), Methyl Acid, 2 N-morpholinethanesulfonic Acid (MES), Oxalic Acid, Propyl Triethoxy Silane, Sodium Chloride (NaCl), SDS, Sypro Ruby, Thiourea, Trizma, Urea, were obtained from Sigma Aldrich Chemie GmbH (Steinheim, Germany). Acrylamide, N,N-methylenebisacrylamide, *N,N,N',N'*-tetramethylethylenediamine (TEMED), dithiothreitol (DTT), linear Immobiline dry strips pH gradient 3-10 (7 cm) were obtained from Bio-Rad (Hercules, CA, USA).

### **4.2.1. PREPARATION OF IMPRINTED SILICA USING IMMOBILISED TEMPLATES**

Silica beads (1 g) were derivatised with 10% (w/v) APTMS in methanol in order to introduce  $\text{NH}_2$  functional groups. The beads were washed three times with ethanol and three times with deionised water and then dried at  $50^\circ\text{C}$  for 24 hours. They were then incubated with 10 mM 2-N-morpholinoethanesulfonic Acid (MES) buffer, pH 5.5 containing 1% glutaraldehyde for 12 hours at room temperature, in order to introduce aldehyde groups. The product was washed

repeatedly with deionised water. Finally, 1 ml of a 10 mM 3-N-3-(N-morpholino)propanesulfonic acid (MOPS) solution (pH 7.0) containing 2.0 mg/ml of protein solution (Human Serum Albumin (HSA), or Carbonic Anhydrase, AC) and 0.1 M NaCl was added and mixture stirred for 3 h at 4°C, in order to covalently bind the protein to the aldehyde groups. The beads were then incubated with 1 M Tris for 30 minutes in order to block the non-reacted aldehyde groups. Washes with deionised water followed and finally 1.5 ml of 50 mM ABPA water solution was added to the beads. After 45 min incubation, 1.5 ml of 25 mM ammonium persulfate (APS) water solution was added in order to start the polymerisation reaction. The polymerisation was carried out at room temperature for 1 h, after which the beads were washed again with ten volumes of deionised water ten times. Finally, 1 ml of 1 M oxalic acid was added in order to remove the template. This step was carried out at room temperature for 12 h.

The derivatisation protocol was checked at each step by FT-IR spectroscopy with a Magna FT-IR 760 Spectrophotometer (Nicolet, Offenbach Germany), samples were prepared mixing 2 mg of beads with 200 mg KBr, sample reading was 32x. The beads were finally conditioned with 10 mM phosphate buffer, pH 8.0, in order to increase the pH and remove the free protein in solution produced by the treatment with 1 M oxalic acid.

#### **4.2.2. EVALUATION OF THE PERCENTAGE OF DERIVATISATION**

In order to evaluate the percentage of silica beads derivatised, 1 g of beads were derivatised with APTMS, glutaraldehyde, APBA, as previously described. After each step, the beads were dried overnight at 87°C and they were weighed.

#### **4.2.3. PROTEIN CONTENT DETERMINATION**

Protein concentration was determined by Bradford Assay, by Sigma Aldrich Chemie GmbH (Steinheim, Germany). The quantification is performed in the microplate as recommended from the producer. The reference concentrations, ranging approximately is in the interval 0.1-3.0 mg/ml. The reference was the buffer used for experiment preparation, while the calibration curve was obtained by diluting a 3 mg/ml concentrated protein standard solution. Measurements were done by reading the absorbance at 595 nm.

In each experiments, calibration curves were performed using buffers used that don't interfere with the assay, as reported by producer.

#### **4.2.4. CALCULATION OF THE BINDING CAPACITY**

In order to evaluate the binding capacity, 0.500 g of beads were conditioned with 10 mM phosphate buffer, pH 8.0 and incubated with 300 ul of protein solution at different concentrations (0.036, 0.058, 0.073, 0.18, 0.3, 1.0, 2.6, 2.74 and 4.08 ug/ul) for different times (3, 5, 20, 60 minutes). The beads were centrifuged at 4000x g

for 3 minutes at room temperature, then the supernatant was transferred into new tubes and quantified with Bradford Assay at 595 nm, as previously described. The protein bound was expressed as the difference between the total micrograms of protein loaded and micrograms of protein in solution after the binding.

#### **4.2.5. BINDING KINETICS**

In order to evaluate the binding kinetics, a 0.500 g of control or MIP beads, conditioned with 10 mM phosphate buffer pH 8.0, were incubated with 300 ul of protein solution at different concentrations (0.036 ug/ul, 0.058 ug/ul, 0.073 ug/ul, 0.18 ug/ul, 0.3 ug/ul, 1.0 ug/ul, 2.6 ug/ul, 2.74 ug/ul and 4.08 ug/ul) for different times (3, 5, 20, 60 minutes). The quantity of bound protein was evaluated as described in the previous paragraph by Bradford Assay, at 595 nm.

#### **4.2.6. PROTOCOL FOR PROTEIN ELUTION FROM BEADS**

In order to evaluate the quantity of protein bound to beads, a 15 mg of control or MIP beads, conditioned with 10 mM phosphate buffer pH 8.0, were incubated with 300 ul of 0.1 ug/ul protein solution for 5 minutes. The beads were washed once with 10 mM phosphate buffer pH 8.0. The supernatant was discarded and the beads were incubated with a solution of 7% acetic acid and 0.1% Tween-20, selected after testing different solutions (7 M Urea, 2.2 M Thiourea, 3% CHAPS, 40 mM Tris, pH 8.0 (TUC buffer), pH 8.0, or TUC buffer,

followed by 9 M urea and 5% acetic acid pH 3.0, or 7% acetic acid, 0.1% Tween 20, or 0.1 M glycine, pH 3.0, 0.5 M NaCl, or 1 M NaCl, as discussed in 4.3.6. After 10 minutes the beads were centrifuged and the supernatant was recovered. The proteins were precipitated with 8 volumes of cold acetone and a short aliquot was analysed through SDS-PAGE.

### **4.2.7. BINDING EXPERIMENTS WITH HUMAN SERUM**

In order to evaluate the binding of HSA from a real complex sample, 0.300 g of MIP beads, conditioned with 10 mM phosphate buffer pH 8.0, were incubated with 300  $\mu$ l of 2.0  $\mu$ g/ $\mu$ l human serum solution for 5 minutes. The beads were washed as previously described. The supernatant was recovered and the proteins were precipitated and analysed through 2D-PAGE.

### **4.2.8. SDS-PAGE AND 2D-PAGE**

Electrophoresis of proteins was performed using regular SDS PAGE with 12% polyacrylamide gel, with a Tris-Glycine cathode buffer (192 mM glycine, 0.1% SDS and 40 mM Tris to pH 8.3). The run was performed by applying 15 mA/gel for 20 min followed by 25 mA/gel until the dye front reached the bottom of the gel.

For 2D-maps, the desired volume of each sample was subjected to protein precipitation in a cold mixture of acetone and methanol (v/v ratio 8:1) for 2 hours at -20°C, in order to remove lipids and salts and



to regulate the concentration of protein. The solution was then centrifuged at 10,000 *g* for 20 minutes. The pellet was solubilised in the 2-D sample buffer (7 M urea, 2 M thiourea, 3% 3-[(3-cholamidopropyl) dimethylammonio]-1-propanesulfonate, 40 mM Tris, 5 mM tributylphosphine and 10 mM acrylamide) and alkylated at room temperature for 90 minutes. DTT (10 mM) was used to block the alkylation reaction, and then the trace amounts of 0.5% ampholine and bromophenol blue were added to the solution. An aliquot (150  $\mu$ l) of protein solution was subsequently used for rehydrating 7 cm long non-linear immobilised pH gradient (IPG) strips (Bio-Rad), pH 3.0 to 10.0, for 4 hours. Isoelectric focusing (IEF) was performed with a Protean IEF Cell (Bio-Rad) at low initial voltage, followed by a voltage gradient up to 5000 V; the total product time voltage applied was 25000 voltage hour for each strip. For the second dimension, the IPGs strips were equilibrated for 26 minutes in a solution containing 6 mM urea, 2% SDS, 20% glycerol, and 375 mM Tris-HCl, pH 8.8, under gentle shaking. The IPG strips were then laid on an 8% to 18% T-gradient SDS-gel slab and cemented *in situ* with 0.5% agarose in the cathode buffer (192 mM glycine, 0.1% SDS, and Tris to pH 8.3). The electrophoretic run was performed by setting a current of 5 mA/gel for 1 hour, followed by 10 mA/gel for 1 hour and 20 mA/gel until run completion.

Finally, for SDS-PAGE and 2D-maps, gels were incubated in a fixing solution containing 40% ethanol and 10% acetic acid for 1 h, followed by overnight staining in a ready-to-use Sypro Ruby solution. Destaining was performed in 10% methanol and 7% acetic acid, followed by a rinse of at least 3 h in pure water. The gels were scanned with a Versa Doc Imaging System (Bio-Rad, Hercules, CA) and analysed with the software PDQuest Version 7.1 (Bio-Rad, Hercules, CA). A match set was created from the protein patterns of three replicate gels for each independent sample. A standard gel was generated out of the image with the highest spot number. Spot quantities of all gels were normalised to remove non expression-related variations in spot intensity. The results were evaluated in terms of spot OD (optical density).

### **4.3. RESULTS AND DISCUSSION**

#### **4.3.1. BEADS DERIVATISATION PROTOCOL**

More homogeneous binding sites are created when the template is immobilised to the support, instead of polymerising it in bulk solution (Shi *et al.*, 1999; Shiomi *et al.*, 2005). Moreover with covalent immobilisation of the template less leaching is expected. In order to covalently attach the substrate to the silica beads  $\text{NH}_2$  groups were introduced onto the silica surface, thus exploiting the same chemistry proposed by Shiomi. For this reason 10% of 3-aminopropyl-

trimethoxysilane (APTMS) was used for derivatising silica beads and introducing of amino groups on a surface, as showed in Figure 11.

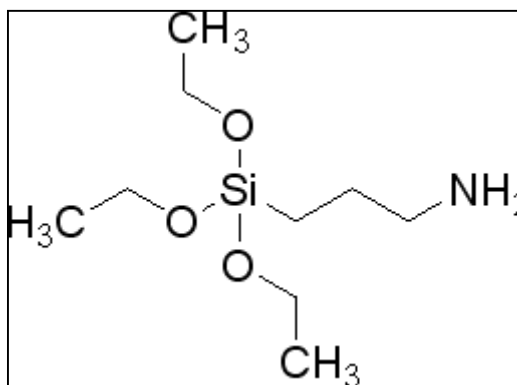


Figure 11\_ Structure formula of APTMS.

Next, a treatment with 1% glutaraldehyde was performed to introduce aldehydic groups. Aldehyde creates imine bound with amino groups (C=N), previously deposited on silica beads and exhibits aldehydic group (CHO) onto the surface. The functional groups exposed are able to bind with exposed lysines of the protein.

The immobilisation of the protein onto the surface of the silica beads happens through a covalent bond between  $\epsilon$  amino groups of lysines of the template and aldehyde groups onto the silica beads.

Human Serum Albumin (HSA) has been chosen as the main protein for the immobilisation and main characterisation experiments reported here. HSA (accession number in [www.expasy.org](http://www.expasy.org), UniProt: P02768) has 609 amino acids, a molecular weight of 69 kDa and an isoelectric point of 5.85. By analysis of amino-acidic sequence, the

lysines are about the 10% of all sequence. 64 lysines potentially can be involved in the bound with aldehydic groups, really only exposed residues can be able to create covalent bound.

HSA is the most abundant protein in human blood plasma. The amino acid sequence and crystal structure of human albumin have been determined (Sugio *et al.*, 1999). HSA is a protein with no carbohydrate content. It is a single polypeptide chain with one free sulfhydryl group on residue 34 and 17 intra-chain disulfide bonds.

It is produced in the liver. The main biological function of albumin is to regulate the colloidal osmotic pressure of blood. It is very abundant in blood serum: about 3.0 to 5.0 g/dl, (Anderson & Anderson, 1977; Jacobs *et al.*, 2005). It has a serum half-life of approximately 20 days.

In a second set of the experiments, the protein immobilised is Carbonic Anhydrase (CA). Carbonic anhydrase is a smaller protein (31 kDa) than HSA and it has 18 lysines that allow the binding with beads surface. The polymerisation conditions are the same as the HSA and the CA imprinted beads (after a brief characterisation, data no showed) are used only for competitive experiments, described next.

After coupling HSA (or CA) to the beads surface, the monomer was deposited onto the surface. We have selected for this role 3-amino-

phenylboronic acid (ABPA,  $\text{H}_2\text{NC}_6\text{H}_4\text{B}(\text{OH})_2 \cdot \text{H}_2\text{O}$ ), with the structure shown in Figure 12.

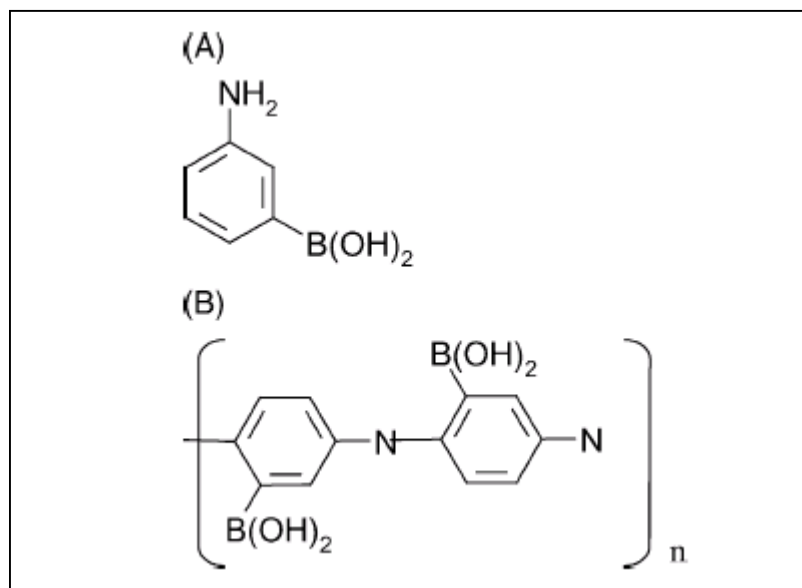


Figure 12\_ 3-aminophenylboronic acid monomer (A) and polymer (B).

Previous studies on the polymerisation of monomers of the same family of ABPA (e.g. aniline) showed that the polymer in solution forms relatively short chains (Mattoso *et al.*, 1995), flocculating in aggregates, while on the supporting surface, it deposits in a reasonably thin and ordered film. Moreover, during polymerisation offers a high number of favourable interactions with amino acids on the protein, as showed in Figure 13.

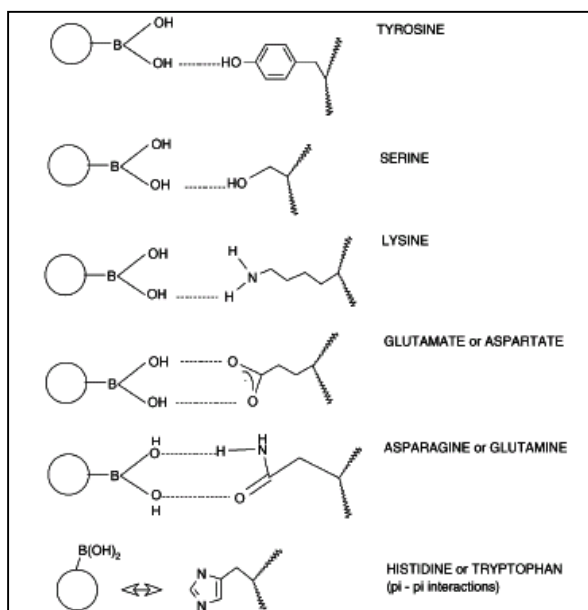


Figure 13\_ Possible interactions between APBA monomer and chain groups of amino acids.

The polymerisation procedure is straightforward: a 1:1 (v/v) ratio of the ammonium persulfate (25 mM) and APBA (50 mM) solution in water were allowed to react together in the presence of the protein-derivatised beads for 1 h under gentle stirring at room temperature (Bossi *et al.*, 2001; Bossi *et al.*, 2004).

After APBA polymerisation, it was necessary to remove the protein immobilised at the surface of the beads to get free binding cavities. The imine bond, between  $\epsilon$  amino groups of the amino acids of the template and aldehyde groups of the glutaraldehyde is covalent and therefore stable. Strong conditions have to be used to break this covalent bond.

For this concerns the beads templated with CA, data for characterisation are not showed, but the results are very similar as HSA characterisation. In the next sections, the HSA results are showed. The role of AC will be clearer in the competitive experiments.

#### 4.3.2. WASHING PROTOCOL

In order to cleave the protein immobilised onto the surface and free the cavities in the polymer for next binding, 1 M oxalic acid for 12 hours was adopted as removing procedure, as described in literature (Shiomi *et al.*, 2005), followed by a number of washing steps with 10 mM phosphate buffer pH 8.0.

After each washing step, the pH of solution was measured and the quantity of protein removed was recovered by acetone precipitation and analysed by SDS-PAGE (Figure 14), followed by a quantification of the HSA released through densitometry analysis.

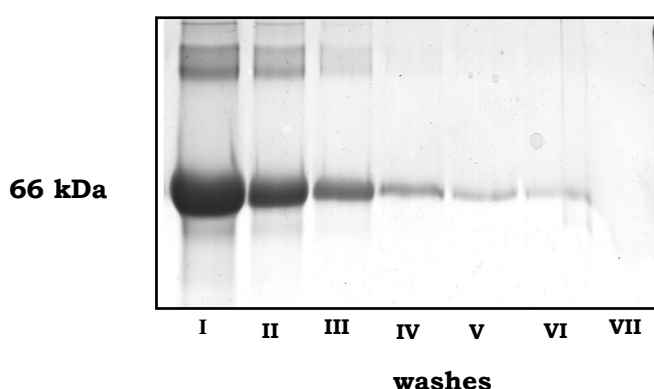


Figure 14\_ SDS-PAGE staining in Blue Coomassie. Proteins recovered after washes were precipitated by acetone and quantified by densitometry analysis.

The data were plotted as a function of the number of washing steps, as shown in Figure 15.

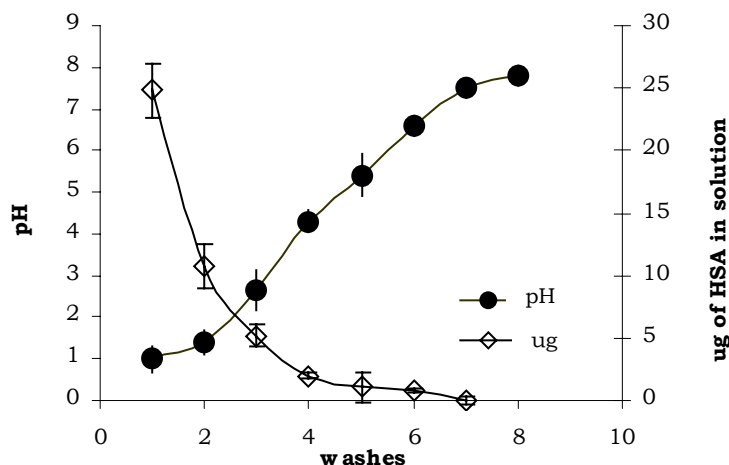


Figure 15\_ Beads MIP washed one time with 1 M oxalic acid o/n and six times with 10 mM phosphate buffer pH 8.0.

As indicated in Figures 14, 15, no template was detected in solution after seven washing steps. Moreover, after seven washes, the pH of the solution increases from 2.0 to 8.0, which is the chosen pH for binding experiments.

It is probable that a small part of HSA bound to the beads gets embedded in the polymer matrix. The contribution of such remaining template might be negative: occupying the binding sites thus preventing the re-binding of template. Nevertheless there are reports documenting a positive effect of the presence of the embedded template in the MIPs: as reported by Hjerten and co-workers; the residual template improves the mechanical stability of the polymer



architecture and conferring rigidity to the binding sites (Hjerten *et al.*, 1997).

#### **4.3.3. QUALITATIVE CHARACTERISATION OF BEADS**

Beads were characterised in two sets of different experiments.

Firstly, the quantity of the polymer deposited on the beads was evaluated. Starting from a known quantity of beads, the weight of the beads batch was monitored after each derivatisation step and following drying at elevated temperature.

The quantity of the polymer deposited onto the beads was evaluated too. Starting from a known quantity of beads, the weight of the batch of beads was monitored after the derivatisation step following drying step. The quantity of ABPA deposited around the silica beads was calculated as  $16.5 \pm 0.5$  mg of polymer/gram of beads. Respect to the quantity of ABPA used at the beginning of the experiments ( $23.2 \pm 0.3$ mg) the milligrams detected at the end of the derivatisation (after treatment with 1 M oxalic acid) is decreased. Probably washing acid step removes a few superficial layers of APBA MIP-polymer too. A qualitative evaluation of the persistence of the dark brown colour of the APBA-beads suggests that, in any case, part of the ABPA layers are resistant to the strong acidic treatment.

Secondly, Fourier Transform Infrared Spectroscopy (FT-IR) has been used to measure the efficiency of the derivatisation process. The spectra were obtained for beads derivatised with protein (HSA-AC)

and with phenyl boronic acid. Moreover, in order to exclude the possibility that the oxalic treatment removes ABPA polymer, beads treated with 1 M oxalic acid, were analysed too.

The protein content was analysed from the comparison of signals typical of peptide bonds ( $1650\text{ cm}^{-1}$ ) and carboxy groups ( $1300\text{-}1400\text{ cm}^{-1}$ ). The further polymerisation of APBA was confirmed by the vibration of phenyl-boronic groups (region  $1100\text{-}1200\text{ cm}^{-1}$ ; a shoulder at  $1250\text{ cm}^{-1}$ ; boronate contribution around  $3200\text{-}3400\text{ cm}^{-1}$ ). In fact, these preliminary data suggest that the derivatisation steps were successfully completed. Moreover, the treatment with 1 M oxalic does not remove the polymer; in fact no remarkable changes were detected in vibration spectra following hydrolysis apart of slight decrease of absorbance.

The characterisation results are the same with HSA and AC and this demonstrate the repeatability of the derivatisation experiments for different kinds of the proteins template.

#### **4.3.4. EVALUATION OF THE MATERIAL BINDING CAPACITY**

Binding experiments were performed in order to evaluate the binding capacity of both control and imprinted APBA beads for HSA. Control and MIP beads (0.500 g), conditioned with 10 mM phosphate buffer pH 8.0, were incubated with increasing quantities of HSA. The quantity of bound protein was evaluated by measuring the residual free protein in the supernatant using protein assay, as described in

section 4.2.2. In each experiments, it is important to note that reference buffer was used to perform the calibration curve in order to avoid quantification errors. The buffers used are compatible with the assay, as declared by producer. In this case the micrograms bound were plotted as a function of the quantity of protein used (see Figure 16).

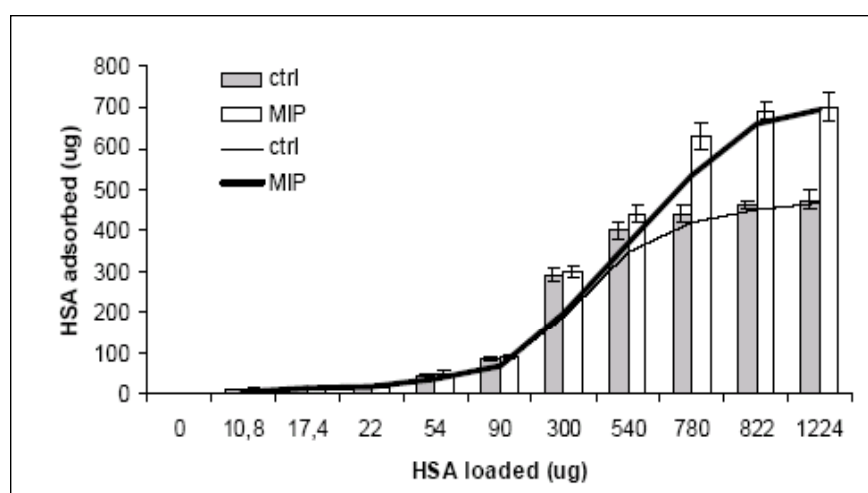


Figure 16\_ Evaluation of the binding capacity for control (solid) and MIP beads (open). Amount in micrograms absorbed to beads is plotted against amount in micrograms loaded.

No difference in the uptake of protein was observed between control and MIP beads when the quantity of protein loaded was below 780 ug, while a difference was observed –in favour of MIP beads- when the quantity of protein loaded was saturating (>780 ug) as show in Figure 16.

These results indicate that the indirect binding capacity for HSA for MIP beads is higher respect control beads (1.4 mg/g for MIP and 0.9 mg/g for control), being the MIP binding favoured by a factor 1.55. Such behaviour reflect probably a morphological characteristic of MIP beads, indicating MIPs possess a higher surface roughness in comparison with control, as pointed out often in literature (Sergeyeva *et al.*, 2006; Turner *et al.*, 2007).

It should be noted that the particular shape of the binding isotherm here presented does not match with the preferential binding concept in general associated and demonstrated with the selective cavities provided by a MIP material (Lin *et al.*, 2007; Nishino *et al.* 2006).

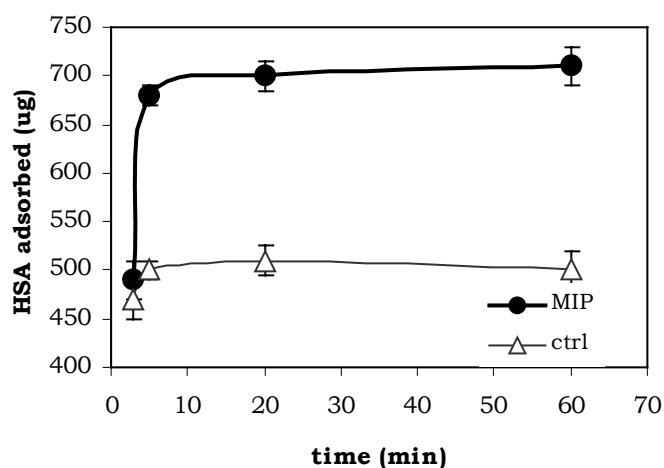
An explanation to the apparent contrasting phenomenon here observed could be found in the format chosen for the present experiment. The measure of the bound protein is here conducted indirectly, being the binding related to the quantity of protein left in the supernatant, thus there is no mean to assess and discriminate between specific and unspecific binding in Figure 16. As little could be said on the specificity of the MIPs versus control beads binding sites, in a next stage of the research, experiments were planned to clarify the issue of specific/unspecific binding.

Few considerations are pertinent for a better understanding of the Figure 16. First, the nature of the template is complex and multifunctional, thus it is expected that such a template is able to form several different weak interactions with the material surface. On

the other side, the nature of the polymeric material chosen and its homogeneous distribution of boronic functional groups on the beads surfaces, again is highly likely to induce and promote the formation of non-specific binding sites with exposed residues of amino-acids on the proteins surface, thus a fairly high and quite efficient non-specific binding is expected. Nevertheless, the MIP beads are supposed to bear cavities complementary with the template proteins, thus assays aimed at quantifying the binding of proteins to the MIP and control beads in a direct form (direct recovery and quantification of the protein bound to the beads) would be used to assess the specific binding and to demonstrate the hypothesis of having obtained imprinted beads.

#### 4.3.5. KINETICS OF BINDING

The kinetic experiments were performed to evaluate the optimum binding time (within the range 0.5 min - 60 min). The binding kinetic was evaluated for concentrations of HSA ranging from 0.073 ug/ul to 4.1 ug/ul.



a)

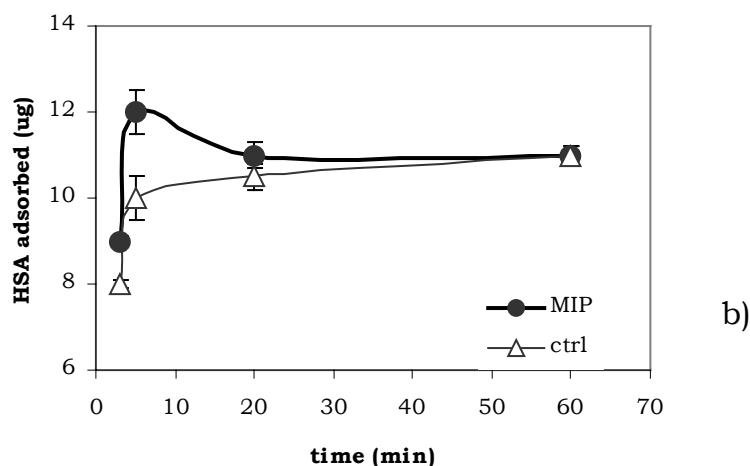


Figure 17\_ Binding kinetics. The amount in micrograms of protein bound is plotted as a function of the time (min), under saturating conditions (a) and no-saturating conditions (b).

As shown in Figure 17, the best incubation time was 5 minutes, irrespective of the protein concentration used.

Two different representative graphs are reported: under saturating conditions (a) and non-saturating conditions (b). For each graph a difference between control and MIP beads are detected in 3-5 minutes. Therefore, if the condition is non-saturating, the difference fails, if the condition is saturating the difference remains until 60 minutes. This result is confirmed further on, by the profile of the time course of the imprinting factor, calculated as ug bound by MIP / ug bound by control, and plotted in Figure 18. Graph shows a maximum IF of  $1.6 \pm 0.08$  for high HSA concentration at 5 minutes and a maximum IF of  $1.2 \pm 0.05$  for low, non-saturating, concentrations. The binding profile (Figure 17b and 18) for no-saturating HSA

concentrations indicates that for short incubation times (<5 minutes) the HSA molecules approach the surface and sticks randomly to it (IF is only slightly in favour of MIPs). When the incubation time rises to 5 minutes, the binding to specific cavities is appreciable and maximised (IF reaches its maximum).

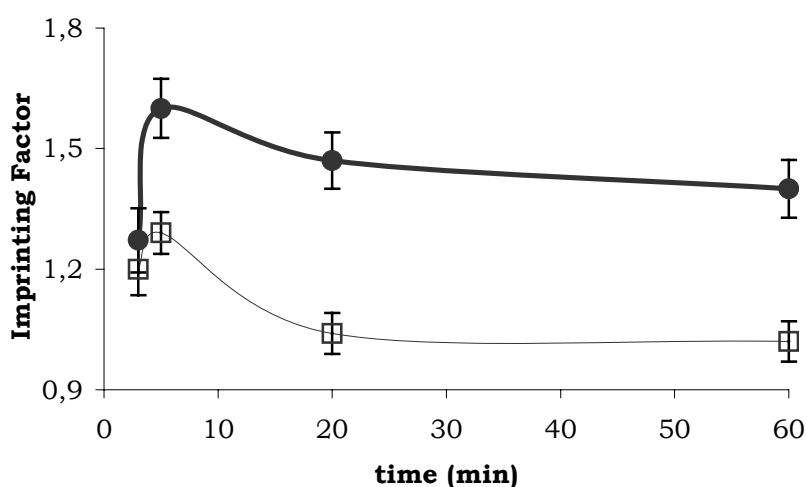


Figure 18\_ The IF calculated as (micrograms of HSA bound by MIP/ micrograms of HSA bound by the control), plotted as function of the time, both for saturating conditions and non-saturating conditions.

Since the total quantity of protein bound did not change significantly with respect to 3 minutes incubation, this suggests a thermodynamically driven rearrangement of the bound proteins and proteins on the MIP moving to the specific cavities. Finally, for longer incubation times (20-60 min), the specific binding sites were saturated and proteins became bound non-specifically. The same did not apply to the high concentration of HSA (4.1 ug/ul), accounting for

enough protein to get a fast saturation of non-specific binding sites. In this case, once the maximum IF was reached at 5 minutes, it remained almost constant over the time course.

#### **4.3.6. RECOVERY OF BOUND PROTEIN**

Thus far, results were evaluated for indirect binding. In fact, the values were calculated from the difference between the protein loaded at the beginning of experiments and the protein remained in the supernatant after binding. In order to calculate the quantity of HSA effectively bound to the beads it was necessary to set a protocol for the elution of protein from beads. The recovery of the bound protein allows evaluating the specificity of the recognition sites of MIP-beads as compared with the control ones.

Five protocols were tested:

*Solution 1:* 7 M Urea, 2.2 M Thiourea, 3% CHAPS, 40 mM Tris, pH 8.0 (TUC buffer), pH 8.0, buffer strongly denaturant. It is usually applied to treat sample before 2D-gel electrophoresis (Righetti, *et al.*, 2004).

*Solution 2:* 7 M Urea, 2.2 M Thiourea, 3% CHAPS, 40 mM Tris, pH 8.0 (TUC buffer), followed by 9 M Urea and 5% Acetic acid pH 3.0. It is usually applied for elution from beads, as described by Fortis and co-workers (Fortis *et al.*, 2005 a-b).

*Solution 3:* 7% Acetic Acid, 0.1% Tween 20. Solution reported for washing APBA-MIPs polymers, (Bossi *et al.*, 2001).



*Solution 4:* 0.1 M glycine, pH 3.0, 0.5 M NaCl. It is an acidic buffer supplemented with salt to increase the ionic strength.

*Solution 5:* 1 M NaCl. High ionic strength solution.

For each protocol, three conditions were tested:

- a. After the binding, the beads are centrifuged and treated with each of 5 different washing protocols for 5 minutes.
- b. After the binding the beads are centrifuged, washed once with 10 mM phosphate buffer pH 8.0 for 5 minutes and treated with each type of washing solutions for 5 minutes.
- c. After the binding the beads are centrifuged, washed once with 10 mM phosphate buffer pH 8.0 for 15 minutes and treated with each type of washing solutions for 5 minutes.

The condition “a” allows the recovery of all the protein bound or adsorbed to the beads, thus it did not give information on the specificity of the MIP binding. The condition “b” presents a first step; a brief washing that allows removal of the protein adsorbed to the beads. Finally, the condition “c”, allows quantifying the amount of protein bound to the MIP with high specificity. The quantity of the recovered protein was quantified through SDS-PAGE and densitometry as described in Material and Methods.

Condition b was chosen for all the following experiments.

Figure 19 and Table 1 indicate that the quantity of HSA eluted from beads, quantified by SDS-PAGE depends on the washing protocols applied and on the pH of the washing solution. Moreover, the presence of detergent seems to play a crucial role in the elution process.

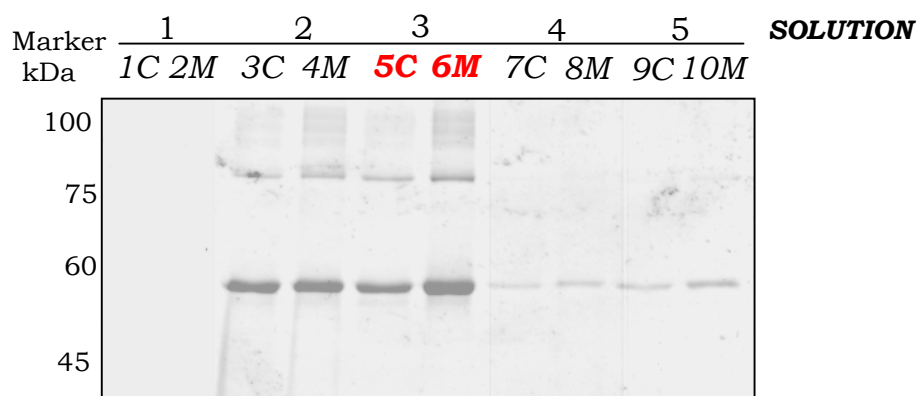


Figure 19\_ SDS-PAGE. Gel showing HSA recovered from the beads in conditions “b” after precipitation with acetone. *C*- control, *M* - MIP.

Table 1\_ The quantity of HSA eluted from the beads measured by densitometry of the spots of HSA in Figure 19.

	<b>CTRL ug</b>	<b>MIP ug</b>
<b>Solution 1</b>	0	0
<b>Solution 2</b>	5.5±1.7%	6.0±1.6%
<b>Solution 3</b>	4.4±1.7%	9.6±1.9%
<b>Solution 4</b>	0.4±2.0%	0.24±1.8%
<b>Solution 5</b>	0.57±1.9%	0.85±2.0%

It has been shown that in condition “b” no protein was eluted from the beads with solubilisation buffer (solution 1) (Figure 19, lanes 1-2); probably the basic pH is not able to remove the HSA from the beads. Solution 4 and 5 allowed to remove a little part of HSA bound to the beads (Figure 19, lanes 7-8-9-10), while with solution 2 and 3 the most of HSA was eluted (Figure 19, lanes 3-4-5-6).

Solution 2, particularly, allowed a fairly good recovery of bound protein, although the urea present in the solution tends to precipitate together with the protein during the acetone-precipitation step and it impedes quantification. Finally, the best results were obtained with solution containing 3, 7% acetic acid and 0.1% Tween-20, as demonstrated in lanes 5-6 of Figure 19. About 9.6 ug are eluted from MIP beads in these conditions, twice as much as these from the control beads. Probably the high elution rate is a result of effective solubilisation of the HSA. The effective elution of the proteins from poly-ABPA polymer in acidic solution is in agreement with previously published results (Bossi *et al.*, 2001). For this reason solution 3 was chosen for the next experiments.

#### **4.3.7. COMPETITIVE ADSORPTION**

Beads templated with HSA or AC are tested in order to evaluate the binding specificity. Before using AC templated beads, they have already been tested (data not showed) to make sure that the derivatisation process has been performed successfully. A competitive

experiment was performed (Figure 20). The beads were assayed for the rebinding with a mixture made of a fixed concentration of the template and an increasing concentration of a competing protein. The quantity of the protein bound to the beads was evaluated after elution using SDS-PAGE. The chosen competitor was CA, which has approximately the same isoelectric point as HSA but a smaller molecular mass (31 kDa), (Righetti & Caravaggio, 1976).

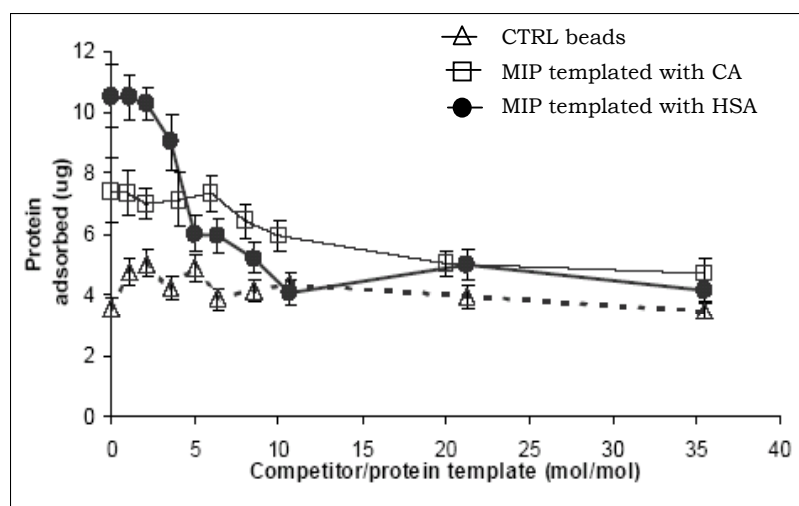


Figure 20\_ Competitive experiments. Open triangles indicate the HSA adsorbed onto control beads upon addition of increasing amount of the competitor protein. Filled circles indicate the amount of HSA adsorbed onto MIP-HSA beads when challenged with CA competitor. Open squares indicate the amount of CA adsorbed onto MIP-CA beads when challenged with HSA competitor.

Table 2\_ Summary of quantities of protein bound in the competitive experiment.

<b>Beads</b>	<b>Protein template used</b>	<b>Maximum protein template bound</b>	<b>Competitor/protein template (mol/mol) required to displace half of protein template</b>
CTRL	CA	$3.5 \pm 0.5$ ug	-
MIP	CA	$8.0 \pm 0.5$ ug	<i>HSA/CA 20/1</i>
CTRL	HSA	$3.5 \pm 0.5$ ug	-
MIP	HSA	$10.0 \pm 0.5$ ug	<i>CA/HSA: 4.5/1</i>

The shape effect on the binding was evaluated, as shown in Table 2 and Figure 20. The HSA binding to control beads (approximately  $3.5 \pm 0.5$  ug) was not perturbed by the addition of CA, accounting for the non-specificity of the binding. In the MIP, no displacement was observed for a CA/HSA molar ratio lower than 3.5/1, while the addition of the 4.5 fold excess of CA competitor displaced half of the HSA bound. The addition of 8-fold excess of CA led to substantial displacement of the bound HSA, which decreased from 10.3 ug to 3.5 ug.

These results indicate that the bound HSA is displaced only for relative high concentrations of competitor. In a second set of experiments CA was used as template and HSA as competitor. As shown in Figure 20 the displacement of CA by HSA is limited also to 20-fold excess of competitor (CA decreased from ca. 8 ug to 5.8 ug). Possible explanations of the phenomenon include the consideration that HSA is far bigger than CA, thus it results in a scarce competition effect. In practice the problem of competition for the imprinted

binding sites might be not important, because in biological fluid the HSA protein is very abundant, constituting about 60% of the total proteins. In this case most likely competition will not take place.

#### 4.3.8. APPLICATIONS OF BEADS OF BIOLOGICAL SAMPLE

The following experiments describe testing of biological samples.

Human plasma mainly composed of water, blood proteins, and inorganic electrolytes. It serves as transport medium for glucose, lipids, amino acids, hormones, metabolic end products, carbon dioxide and oxygen. Serum refers to blood plasma in which clotting factors (such as fibrin) have been removed naturally by allowing the blood to clot prior to isolating the liquid component. Serum contains different proteins as showed schematically in Figure 21.

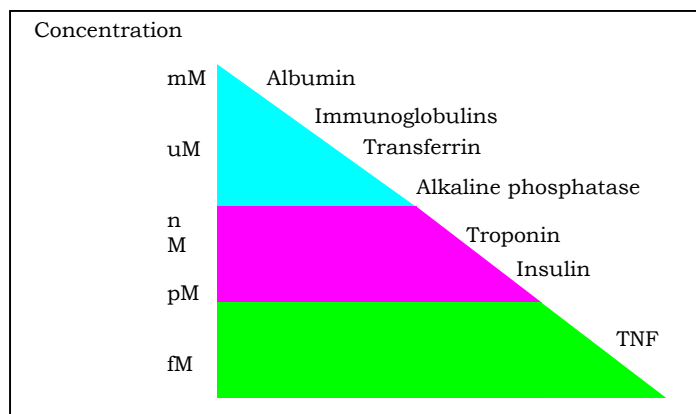


Figure 21\_ Schematic representation of serum composition. Some proteins are related depending on concentration.

As it was showed, approximately 60-80% of total protein of serum is albumin, the signal of high abundance proteins mask the signal of low ones.

For these reasons, the last part of our work was devoted to the evaluation of the binding performance of imprinted beads on real biological fluid human serum.

Serum samples are composed of thousands of proteins and peptides, released from various organs and travelling through the body through the vasculature, accounting for the high complexity of such fluid. Despite the fact that albumin and immunoglobulins constitute the vast majority of the protein fraction of serum (ca. 90%), interest is focused on proteins that form the minor fractions, as their presence or their quantitative variations are often correlated to pathological states. Therefore, methods for efficient removal of HSA are highly welcomed, as they permit tracing and analysis of low abundance proteins, usually masked by serum HSA.

The imprinted beads for albumin removal were incubated with serum as described in Material and Methods for 5 minutes. After binding beads were centrifuged and the supernatants recovered. Proteins were precipitated with TCA, quantified with protein assay, as described in section 4.2.2., and subjected to bi-dimensional (2D) electrophoresis analysis. In this case, different sets of maps were performed. Serum not treated was compared with serum depleted

and analysed through software PDquest (Biorad, Hercules, CA) (see Figure 22).

A following analysis was performed with whole 2D map to count the spot number. In this case pDQuest software was used.

Figure 22 shows a short segment of whole 2D map, for underling the decrease of HSA spot. The total number of protein spots counted for serum was 124 and 116 for MIP-treated serum, indicating again that the imprinted beads targeted HSA do not randomly remove other serum components.

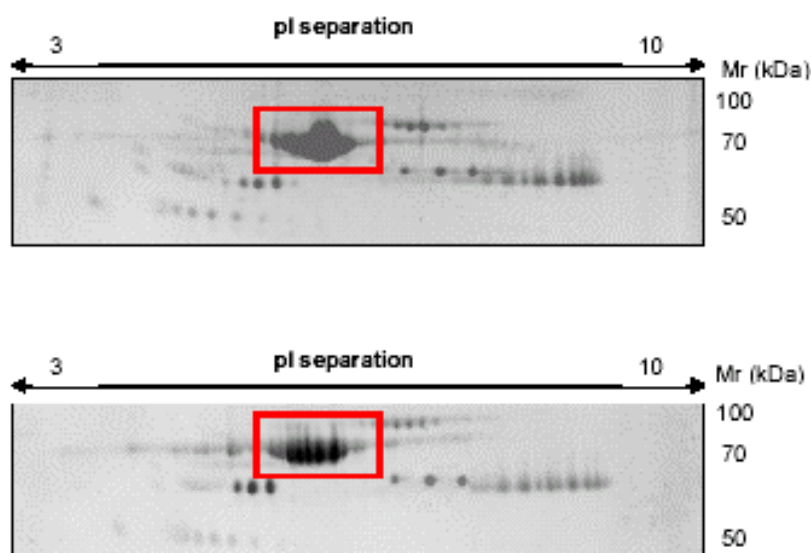


Figure 22\_ 2D-maps of human serum a) untreated serum sample, b) serum treated with imprinted beads, for the depletion of HSA. The map is obtained with 7 cm strip and stained with Sypro Ruby.



By analysing the optical density of the albumin spot, a decrease was reported for serum depleted with imprinted beads, in fact the spot intensity decreased by a factor  $1.7 \pm 0.3$  upon treatment indicating that 58% of HSA was removed.

The quantity of albumin removed from the beads was 183 ug, starting from original amount of 311 ug of HSA. It can be concluded that the imprinted beads also removed the protein target in a complex fluid, leaving the other proteins nearly unchanged.

The removal process was easy and straightforward with an optimal incubation time of 5 minutes. Naturally, the preliminary experiments with a complex fluid require further investigation where the quantity of imprinted beads would be optimised to obtain an almost complete depletion of HSA from serum.

#### **4.4. CONCLUSIONS AND FUTURE WORK**

Currently there are two main strategies for protein imprinting: the one based on imprinting of template immobilisation and the other one on imprinting of free template. The polymerisation can proceed with template in bulk or grafted on surface.

In this study we demonstrated the efficiency of the immobilisation approach for generating a polymer surface capable of recognising a specific protein target in simple or complex samples. Comparing to polymerisation with free template, our approach should not alter the shape of imprinting cavity. Moreover, in this case the polymerisation

takes place in aqueous conditions that are fully compatible with the three-dimensional structure of proteins and allow for a better protein solubilisation.

The polymer is 3-aminophenylboronic acid (APBA) is an attractive matrix for protein imprinting, providing a mild aqueous environment during polymerisation while offering a high number of favourable interactions with amino acids on the protein, and it was used many times in different applications.

Recently, Turner and co-workers demonstrated the efficiency of recognition of QCM imprinted with  $\beta$ -lactoglobulin and covered with a thin film of ABPA, (Turner *et al.*, 2007). QCM was able to recognise different isoforms of protein template. Therefore, the results presented are modest in terms of the magnitude of their effect, when compared to the recognition obtained by certain recent advances in protein imprinting. They however demonstrate the validity of the molecular imprinting technique for the detection of distinct conformations of the same protein but the recognition is made in a solution with three proteins at the most.

No other applications with this QCM system and ABPA polymer were described in literature with a more complex sample, excluding biological sample from experiments and limiting the applications field.

Moreover, in an unpublished work described in a PhD thesis (Sylvester, 2004), ABPA matrices were used for developing surface

plasmon resonance (SPR) sensors for monitoring of anticoagulation therapy. The surface of a Biacore-3000 chip was coated with APBA film imprinted with prothrombin. The resulting material possessed selectivity for prothrombin and was able to discriminate it from thrombin, when present in the same concentration range. Unfortunately when authors applied sensor to biological fluid, no adequate performance of the sensor in blood plasma are detected. We believe that the improvement achieved in our work has originated from the use of immobilised template.

Our polymer beads after preliminary characterisation by means of different assays that provided data on binding kinetics, binding capacity, elution and recovery conditions, demonstrated a good applicability in a complex sample. In fact the ability of the APBA imprinted polymer to specifically recognise HSA, and the ability of the APBA beads to remove HSA from a real biological fluid like human serum was tested. The efficient removal of high abundance proteins from biological fluids is highly necessary for clinical and diagnostic purposes, including proteomic analysis, thus any method capable of selectively capturing HSA is of great interest for clinical and biomedical research. Method to clinical and diagnostic applications has to have some important characteristic, such as: easy to prepare, good recognition capacity and cheap cost.

For this concern our results, in comparison with the article where the immobilised protein on silica surface was described for the first time

(Shiomi *et al.*, 2005), we have achieved some important improvements. In fact, our imprinted beads were applied successfully not only to a simple mixture of two or three proteins obtaining good imprinting factor, but also to a complex biological fluid, obtaining a decrease of 58% of abundant HSA without removing, apparently, any other proteins. Other investigators have not demonstrated this success, applying MIP technology to whole biological sample. Although such results are encouraging, they are not conclusive; in fact the proteome analysis needs probably further investigations: qualitative and quantitative.

Concluding, although further studies are necessary in order to improve the matrix specificity and affinity, we have demonstrated that the approach based on covalent immobilisation of the template is usable for creating specific surfaces capable of recognising target proteins in extremely complex samples such as biological fluids.

In the future, therefore, it will be important to evaluate if it is convenient to proceed with further testing because this process, although has had good results, is too laborious and long. These aspects don't fit with speed and simplicity required for diagnostic tools.

## **CHAPTER V**

### **GATE-EFFECT IN IMPRINTED**

### **POLYACRYLAMIDE MEMBRANES**

#### **5.1. INTRODUCTION**

Manipulation at a molecular level of the structure of a material is an effective way for altering its mechanical, optical and functional properties (Assender *et al.* 2002; Chailapakul & Crooks 1993; Kumar *et al.* 1994). Polymer design is of particular interest in bio-analytical separations and sensing. In particular, the hydrophilic polyacrylamide (PAA) is a typical constructing block that has a notable impact on bio-analysis. Variations in the PAA structure such as introducing large pores were applied for the separation of large biological entities or DNA fragments (Sahaya, 1976). However, the use of low cross-linking level led to the creation of mechanically very weak or soft gels, which changed easily their degree of swelling. Instead, PAA recipes based on high level of cross-linking produced highly porous materials with high mechanical stability (Righetti *et al.*, 1981). These gels showed a sponge type structure with large cavities, as indicated by SEM analysis (Righetti *et al.*, 1992).

By exploiting the principles of micro-segregation and partitioning typically observed for polymer blends (Krause, 1972), meso-

structured PAA gels were synthesised. Upon addition of polyethylene glycol (PEG) the dynamic of the gelation process was drastically influenced, inducing a lateral chain aggregation and the formation of thicker bundles of PAA, as confirmed by measures of low angle static light scattering (Asnaghi *et al.*, 1995).

The spatial distribution and the three dimensional organisation of polymeric chains could be controlled through a imprinting approach, in which the presence of the template, with a defined molecular mass and geometry in the polymerisation mixture causes modification of the growing polymer networks (Buter *et al.*, 1972; Spvbek & Schneider 1987; Hulvatt & Stupp, 2003). Mesoscale PAA-architectures were reported upon the polymerisation of AAs in the presence of lyotropic surfactants, which could assemble in ordered hexagonal, or bi-continuous cubic, or lamellar fashion (Pieransky *et al.*, 1986; Hyde *et al.*, 1987). The surfactant assemblies formed voids, as they displaced the polymer growth. Nanometer to micron sized pores, separated by highly cross-linked polymer regions, that provide mechanical stability, were reported (Antonietti *et al.*, 1999). Channels or spheroidal pores were embedded in PAAs by Rill and colleagues (Rill *et al.*, 1996), demonstrating a geometry-transfer in the imprinting process: semi-rigid rod-like polyelectrolytes (short fragments of DNA or xanthan) or spherical micelles of sodium dodecyl sulfate (SDS) were used as templates, inducing the distinct formation

of channels and pores respectively, which were used for the electrophoretic separation of biological macromolecules.

The high degree of transferred-spatial order achievable through a template approach was fully demonstrated in the work of Hjerten (Hjerten *et al.*, 1997), as described in Chapter 3. In this case, PAA-gels were synthesised in presence of a protein template, following a non-covalent molecular imprinting method (Mosbach, 1994). The imprinted cavities were selective for the template protein (horse myoglobin) but not for its homologous form (whale myoglobin), accounting for a significant conservation of the template geometry in the formed pores and representing an important achievement in the area of recognition materials (Vlatakis *et al.*, 1993; Haupt & Mosbach 1998).

Here we imprint hydrophilic PAA membranes with proteins for inducing template selection. The structural properties and recognition abilities of the formed materials were evaluated by studying the electrically driven transport of various proteins through such PAAs membranes. It was anticipated that the PAA pore size and distribution would correlate with the quantity and type of template used for the polymerisation, which would be reflected in varying electric transport properties.

A very interesting application for such membranes, explored here for the first time would be their use in proteome research for removal of a specific protein from a complex sample (Righetti *et al.*, 2003;

Chertov *et al.*, 2005; Steel *et al.*, 2003). It would be particularly important in a two-dimensional analysis of biological fluids where the predominant presence of certain proteins, e.g. albumin, that masks the resolution of a vast population of low-expressed proteins. The membranes imprinted with human serum albumin were employed in this work for a selective removal of albumin from serum.

## **5.2. MATERIAL AND METHODS**

Tris-hydroxyaminomethane, acetic acid, glutamic acid, bovine serum albumin (BSA) purification grade >99.0%, human serum albumin (HSA) purification grade >99.9%, whale skeletal myoglobin, catalase were purchased from Sigma (St. Louis, MO, USA). Ammonium persulphate, *N,N,N',N'*-tetramethylethylene diamine (TEMED), acrylamide, *N,N'*-methylene-bisacrylamide were purchased from BioRad (Hercules, CA, USA). Immobiline chemicals were from Pharmacia Amersham (UK). All other reagents, purchased from commercial sources, were of analytical grade. Support for membranes were Whatmann GF/D glass fibre membranes, 2.5 cm diameter (Whatmann).

### **5.2.1. ELECTROPHORESIS ON IMPRINTED GEL SLABS**

The polyacrylamide stock solution was prepared with 28.8 g acrylamide and 1.2 g bis-acrylamide to a final volume of 100 ml in water. It was defined as 30% T, according to its 30% content in total



monomer and cross-linker, and 4% C, where cross-linker constitutes 4% of the total monomers content (1.2 g of bis-acrylamide cross-linker / 30 g total monomers).

Thin gels, of 0.5 mm thickness, polymerised onto a Gel-Bond-PAG supporting film (Pharmacia-GE, Sweden), were prepared diluting the stock solution to 6%, 10%T and 15%T, keeping 4%C of the bis-acrylamide. The solutions were degassed in order to remove the oxygen bubbles that can interfere with homogeneous polymerisation. The polymerisation was with 1 ul/ml ammonium persulphate 40% (w/w), and 0.5 ul/ml TEMED for 2 hours at ambient temperature. To obtain imprinted-PAA, the template, bovine serum albumin (BSA), was added at concentrations of 0.5, 1, and 10 mg/ml to the monomer mixture. The template removal was achieved through water washing steps (3 x 1 hour) under mild agitation, followed by 2000 V\*h electroelution. Gels were next dehydrated. Prior of to using, gels were rehydrated for 2 hours with the running buffer solution Tris-HCl 298 mM, pH 8.8.

After protein loading, gels were run for 3 hours at 150 V and then stained with Coomassie Blue R-250. The relative electrophoretic migration ( $R_e$ ) was measured as migration distance of the protein respect the migration of the front, i.e. of a small dye not interacting with the pores. The imprinting factor (IF) for each pair template/control was calculated as ratio between  $R_e$  imprinted-PAA versus  $R_e$  control-PAA.

### **5.2.2. PROTEIN TRANSPORT THROUGH IMPRINTED PAA-MEMBRANES IN A FREE-FLOW ELECTROPHORESIS SYSTEM**

The set-up used for analysis of electrophoretic properties of PAA membranes was from Talent S.r.l. (Trieste, Italy) (Righetti *et al.*, 1989; Righetti *et al.*, 1996). It was assembled with four chambers of 5 ml volume: at the extremes an anodic and a cathodic chamber, in the middle a loading (Ch-II) and a collecting chamber (Ch-III). Chambers were delimited by three membranes (10%T, 4%C): anodic (pI 3.0), PAA imprinted or PAA control and cathodic (pI 9.0). The anodic chamber contained 100 mM acetic acid, whereas the cathodic reservoir was filled with 1 M Tris. Ch-II and Ch-III were filled with 20 mM glutamic acid. Anodic and cathodic compartments were introduced to avoid direct contact between electrodes and proteins, thus preventing electro-oxidation of the protein.

PAA membranes are templated with solution to 6%, 10%T and 15%T, keeping 4%C of the bis-acrylamide on a specific fibre support Whatmann GF/D, 2.5 cm diameter (Whatmann). The solutions were degassed in order to remove the oxygen bubbles that can interfere with homogeneous polymerisation. The polymerisation was with 1 ul/ml ammonium persulphate 40% (w/w), and 0.5 ul/ml TEMED for 2 hours at ambient temperature. To obtain imprinted-PAA, the template, bovine serum albumin (BSA), was added at concentrations of 0.5, 1, and 10 mg/ml to the monomer mixture. After the system set up the protein used, as template, is 1 mg/ml of Human Serum

Albumin. The template removal was achieved through water washing steps (3 x 1 hour). Before starting the experiments, the instrument was subjected to a 2 hours process of electrical conditioning at 4 mA, in order to remove non-reacted monomers and to swell the membranes in the solution with chosen pH. When the electrolyser was equipped with imprinted-membranes, the electrical conditioning served also for the removal of the template protein from the membrane pores. During such process, the solutions of Ch-II and Ch-III were repeatedly exchanged. To monitor the removal process the solutions of Ch-II and Ch-III were checked for their protein content with a Bradford assay in the correct buffer, as reported in Material and Method. After 1 hour the process of removal was completed, but the electrical conditioning was protracted up to 2 hours.

The proteins (4 mg per each protein, or an equal quantity in moles) were loaded in the Ch-II, delimited by the imprinted or by the control membrane, and collected in Ch-III. The electro-migration condition chosen were: 75V, 4 mA for 120 minutes. The transport progress was monitored by Bradford protein reagent assay (Sigma, St.Louis MO) from aliquots harvested in the loading and in the collecting chambers. Quantification of protein content was obtained by comparing absorbance units obtained from Bradford assay to a calibration curve made for each protein in the right buffer.

Quantification of the protein transport was also made by analysing withdrawn fractions of Ch-II and Ch-III (10  $\mu$ L sample mixed with

10  $\mu$ L loading buffer and boiled for 5 min) in electrophoresis using regular SDS PAGE with 14% T polyacrylamide gel, with a Tris-Glycine cathode buffer (192 mM glycine, 0.1% SDS and 40 mM Tris to pH 8.3). The run was performed by applying 15 mA/gel for 20 min followed by 25 mA/gel until the dye front reached the bottom of the gel. Gels were stained with Coomassie Blue (0.5 g in 10% acetic acid, 30% methanol) followed by an over night destaining in 10% acetic acid, 30% methanol. The gels were scanned with a Versa Doc Imaging System (Bio-Rad, Hercules, CA) and analysed with the software GQuest Version 7.1 (Bio-Rad, Hercules, CA). Protein quantification was evaluated in terms of optical density (OD) and compared to densitometric calibration curves.

### **5.2.3. EVALUATION OF RETENTION CAPACITY OF PAA MEMBRANES**

PAA membranes templated with HSA, are polymerised as described previously in 5.2.2.

The experiments were performed with different quantities of HSA for 12 min.

After 12 minutes sample in Ch-II and Ch-III was recovered and replaced with 20 mM glutamic acid. 75 V, 4 mA, were applied in order to remove the protein entrapped in the matrix of PAA membranes during binding experiment. This process, namely electroelution, was performed for 1 h. All the samples present in the loading

and collecting chambers before and after electro-elution were measured, by protein assay (Bradford Assay, Sigma).

Data obtained, were analysed and revised through Excel software.

These following equation were used for data calculation:

$[A] \text{ ug HSA bound by membrane} = \text{total loaded ug} - (\text{ug in Ch-II} + \text{ug in Ch-III})_{\text{after 12 min.}}$

#### **5.2.4. REMOVAL OF HUMAN SERUM ALBUMIN FROM HUMAN SERUM THROUGH PAA-IMPRINTED MEMBRANES**

Aliquots of ca. 800  $\mu\text{g}$  of human serum (stock solution 70 mg/ml) were diluted to a 0.2 mg/ml concentration and a final volume of 5 ml in 20 mM glutamic acid. The proteins content after dilution was quantified by Bradford assay, with reference plot, as suggested by producer. The serum solution was loaded in Ch-II and electrophoresis run at 75 V, 4 mA. The running time was 12 min, and then the contents of Ch-II and Ch-III were recovered and quantified by Bradford assay.

The effectiveness of the albumin removal was evaluated by mapping the proteome with a two-dimensional analysis of treated and untreated human serum, loading 500  $\mu\text{g}$  of total proteins on each 2D map.

### **5.2.5. SDS-PAGE**

Electrophoresis of proteins was performed using regular SDS-PAGE with 10% polyacrylamide gel, with a Tris-Glycine cathode buffer (192 mM glycine, 0.1% SDS and 40 mM Tris to pH 8.3). The run was performed by applying 15 mA/gel for 20 min followed by 25 mA/gel until the dye front reached the bottom of the gel. Gels are stained with Coomassie G-250 and destained with 5% acetic acid solution in water. The analysis was performed by densitometer and software Quantity One (Bio-Rad, Hercules, CA).

### **5.2.6. TWO-DIMENSIONAL ELECTROPHORESIS**

Samples (Ch-II and Ch-III contents) for two-dimensional (2D) electrophoresis were precipitated with 15% TCA. The pellet was washed 3 times with cold acetone, then solubilised, reduced and alkylated in the sample solution for the isoelectric focusing (IEF) containing 7 M urea, 2 M thiourea, 3% CHAPS, 5 mM TBP, 10 mM acrylamide, 10 mM DTT, 40 mM Tris and 1% carrier ampholytes.

Two dimensional polyacrylamide electrophoresis (2D-PAGE) was performed using a Protean IEF-Cell on commercial 7 cm IPG strips (Bio-Rad, Hercules, CA) pH 3-10 NL, pH 4-7 and pH 5-8. The run was stopped at 25000 V x hours. The second dimension was performed with an 8 –18% Tris-glycine, 0.1% SDS gels. The SDS-PAGE was run at 5 mA/gel current for 1 hour, followed by 10 mA/gel for 1 hour and 20 mA/gel until run completion. Gels were stained in Coomassie blue

G 250 and destained with 5% acetic acid. The images of the gels were digitalised with a Versa Doc Imaging System (Bio-Rad, Hercules, CA) and analysed with the software PDQuest Version 7.1 (Bio-Rad, Hercules, CA). A match set was created of the protein patterns of three replicate gels for each independent sample. The results were evaluated in terms of spot OD (optical density) and spot number.

### **5.2.7. PROTEIN CONTENT DETERMINATION**

Protein concentration was determined by Bradford Assay, by Sigma Aldrich Chemie GmbH (Steinheim, Germany). The quantification is performed in the microplate as recommended from the producer. The reference concentrations, ranging approximately is in the interval 0.1-3.0 mg/ml. The reference was the buffer used for experiment preparation, while the calibration curve was obtained by diluting a 3 mg/ml concentrated protein standard solution. Measurements were done by reading the absorbance at 595 nm.

All buffers used during quantification experiments don't interfere with the assay, as reported by producer.

## **5.3. RESULTS AND DISCUSSION**

### **5.3.1. ELECTROPHORESIS IN GEL SLAB**

As described in the literature the sieving properties of a polymer correlate with the fraction of gel-volume accessible to particles of

different dimensions (Ogston & Sherman, 1958). In other terms, for a certain molecule, the fraction of gel-volume accessible depends on the mean radius of the pores and on the pore-size distribution around the mean pore-size. PAAs have been demonstrated to have a wide variety of pore distribution depending on their composition: a characteristic that makes them highly versatile supports in the separation techniques.

Polyacrylamide gels are formed by copolymerisation of acrylamide and N,N'-methylene-bisacrylamide. The reaction is a vinyl addition polymerisation initiated by a free radical-generating system. Polymerisation is initiated by ammonium persulfate and tetra-methylethylene-diamine (TEMED). TEMED accelerates the rate of formation of free radicals from persulfate ammonium and these in turn catalyse polymerisation, as shows in Figure 23.

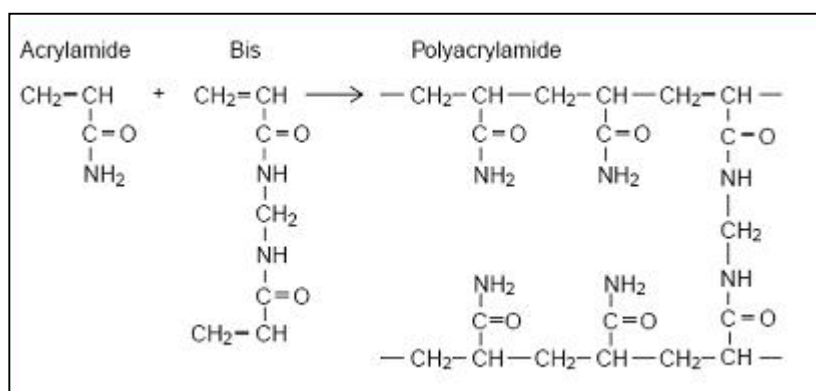


Figure 23\_ Polyacrylamide gel polymerisation.

In the first part of this work related to PAA gel, we focus the attention on the study of the alterations of the PAA functional electro-transport



properties induced by a protein imprinting process, relating these changes to modifications occurring in the PAA structure.

### **5.3.2 PREPARATION OF GEL SLAB FOR BSA RECOGNITION**

Imprinted PAA gel slabs were prepared with a bulk imprinting strategy, in which the template, bovine serum albumin (BSA), and the monomers were solvated together in an aqueous solution. Different concentrations of monomers and constant concentrations of cross-linkers, with consequently different sieving properties were tried, in order to identify the best composition of polymer.

Particularly, different concentration of monomer were used: 6% T (scarce sieving effect), 10% T (medium sieving effect), and 15% T (high sieving effect) but only one concentration of cross-linker was used (4% C). BSA was used at different concentration too: 1 mg/ml, 3 mg/ml, and 10 mg/ml.

After polymerisation, gel was washed to remove the protein template. The main problem in this case is the choice of washing protocol, in order to remove the protein polymerised and get free the cavities. As described from Hawkins and co-workers (Hawkins *et al.*, 2005), choice of conditions for template removal is very important for sieving effect. In fact, if the cavities are not free, the polymer is not able to explicate its sieving properties. Often, due to inadequate washing protocols, no difference between control and MIP gel slab were

detected. The protein template that remains entrapped in matrix gel, probably, decreases gel permeability.

In order to remove the protein the washing was in 100 mM Tris-acetate solution pH 8.0 with 2 mg/ml of trypsin and a step of electro-conditioning (2000V\*h). This ensures effective removal of the template.

In a first set of the experiments, control and template PAA gels slabs were analysed in order to test the migration rate of a specific protein. Bovine Serum Albumin (BSA) was used. BSA (accession number in [www.expasy.org](http://www.expasy.org), Uniprot P02769) is a protein of 607 amino acids, of 69 kDa with isoelectric point 5.82. It is soluble in aqueous solvents, very cheap and it has similar characteristics of Human Serum Albumin, (HSA), used in next experiments (as described in chapter 4). BSA was loaded at the top of gel slab (as showed in Figure 24) and after, the electric field was applied. From results obtained, it was observed that BSA runs differently in control or MIP gel. As it emerges from the analysis of gels composition, the difference between the samples analysed is caused by percentage of polyacrylamide and the concentration of template. Probably, the different run of the protein depends on gel porosity and composition too, as it can be seen in Figure 24.

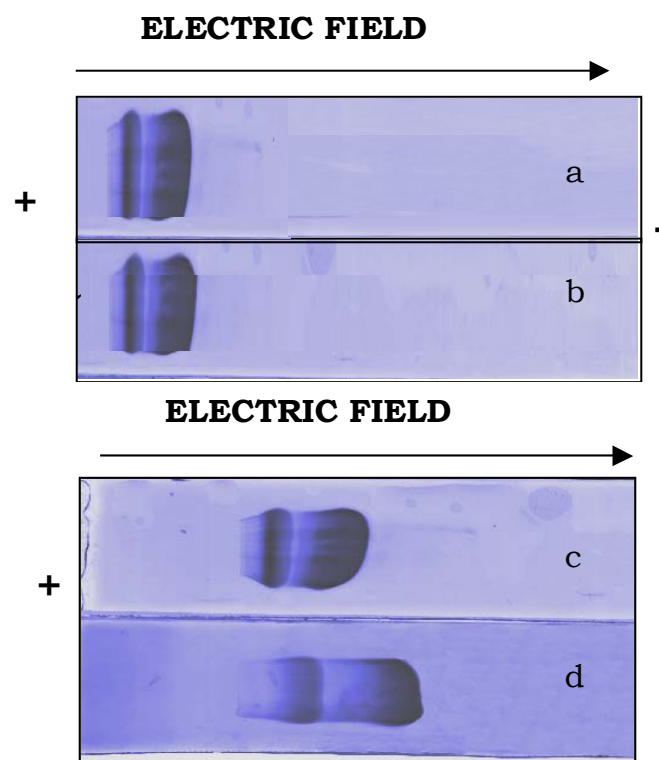


Figure 24\_ The electrophoretic migration of BSA in standard running conditions (100 V, 3 hours) on control (a) and templated (b) PAA gel slabs (6 %T 4% C) and control (c) or templated (d) PAA gel slabs (10 % T 4% C) stained in Coomassie Blue R250.

Figure 24 shows the electrophoresis run with gel at different concentrations of monomer 6%T 4%C (Figure 24 a, b) and 10%T 4%C (Figure 24 c, d). In order to evaluate the differences, slab gels were stained with Coomassie blue and electrophoretic migration ( $R_e$ ) was calculated as relative, as shown in Figure 24. The imprinted factor (IF) was calculated as ratio between  $R_{MIP}/R_{CTRL}$ . In Figure 24, 15% T 4%C gel is not showed, because it has a fragile structure and has

been broken during the dehydration procedure. Data can be summarised in Table 3.

Table 3\_ Summary of the values of imprinting factor for each condition applied to gel slabs.

<i>Concentration of protein template (mg/ml)</i>				
<i>Concentration of monomer (%T), constant cross-linker (4%C)</i>		<b>0.5 mg/ml</b>	<b>1 mg/ml</b>	<b>10 mg/ml</b>
	<b>6% T</b>	1.0±0.05	1.06±0.05	-
	<b>10% T</b>	1.0±0.05	1.35±0.05	-
	<b>15% T</b>	Gel cracking	Gel cracking	Gel cracking

In Table 3, the IF is related to the quantity of protein template used and to the monomer quantity. As it can be noted, in polymer 6% T no differences are detected irrespectively to the quantity of protein used as template. Probably, the 6%T gel matrix is too soft and unable to retain the structure.

Gel 15 % T is broken during the dehydration step.

Interesting results were obtained, instead, with 10% T gel. Particularly the effect of the template quantity on the gel structure was identified. By varying the BSA concentration in the pre-polymerisation mixture and by monitoring the electro-migration of BSA, the IF changes. The use of 0.5 mg/ml BSA did not results in an appreciable variation of the migration in the template gels as

compared with the control. A 1 mg/ml concentration of BSA affected the  $R_e$  of BSA significantly. The use of 10 mg/ml BSA implies in practice great protein consumption and washings steps prolonged for days, thus it was considered of scarce interests for further practical developments. In general, the migration trends observed for protein-template PAAs gel slabs were in agreement with the results described for other imprinting processes (Rill *et al.*, 1997). From these preliminary experiments, encouraging results were obtained.

### **5.3.3. POLYACRYLAMIDE MEMBRANES**

As the gel slab format proved to be excessively labour intensive, experiments towards a more detailed analysis of the imprinting effect on PAA, by the investigation of the permeation properties, were performed in the free flow electrophoresis system equipped with PAA membranes (imprinted or control). The PAA was deposited on fibreglass supports: as described in Material and Methods. The membranes were applied in multi-compartment electrolyser. The free electrophoresis format permitted to overcome gel slab limitations, allowing a fast and highly reproducible collection of results.

The scheme of the electrolyser herein used (Righetti *et al.*, 1989) is reported schematically in Figure 25 and previously in Figure 6. The electrolyser instrument is composed by 4 identical units (or chambers). Each unit is in a plastic material and it can adhere to the

followed units (as described in Figure 6). It was assembled with 4 chambers of 5 ml volume: at the extremes an anodic and a cathodic chamber, in the middle a loading (Ch-II) and a collecting chamber (Ch-III). Chambers were delimited by three membranes: anodic (pI 3.0) separates anodic chambers from Ch-II, PAA imprinted or PAA control separate Ch-II from Ch-III and cathodic (pI 9.0) separates Ch-III from cathodic chamber. The anodic and a cathodic chamber were introduced in the set-up, to preserve the protein from electrode contact, which cause protein oxidation and breaking (Righetti *et al.*, 1996). Proteins were loaded in chamber II (Ch-II) and collected in chamber III (Ch-III), the electro-migration process was monitored by quantifying the protein content in the two chambers over a time course of 60 min.

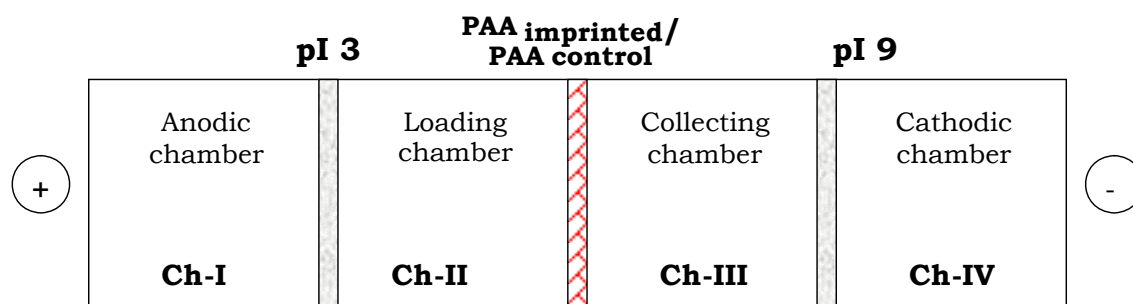


Figure 25\_ The free flow electrophoresis system. The instrument was equipped with four chambers, separated by three PAA membranes. Chamber I, anodic and chamber IV, cathodic, were separate by isoelectric membranes at pI 3.0 and 9.0 respectively, which created

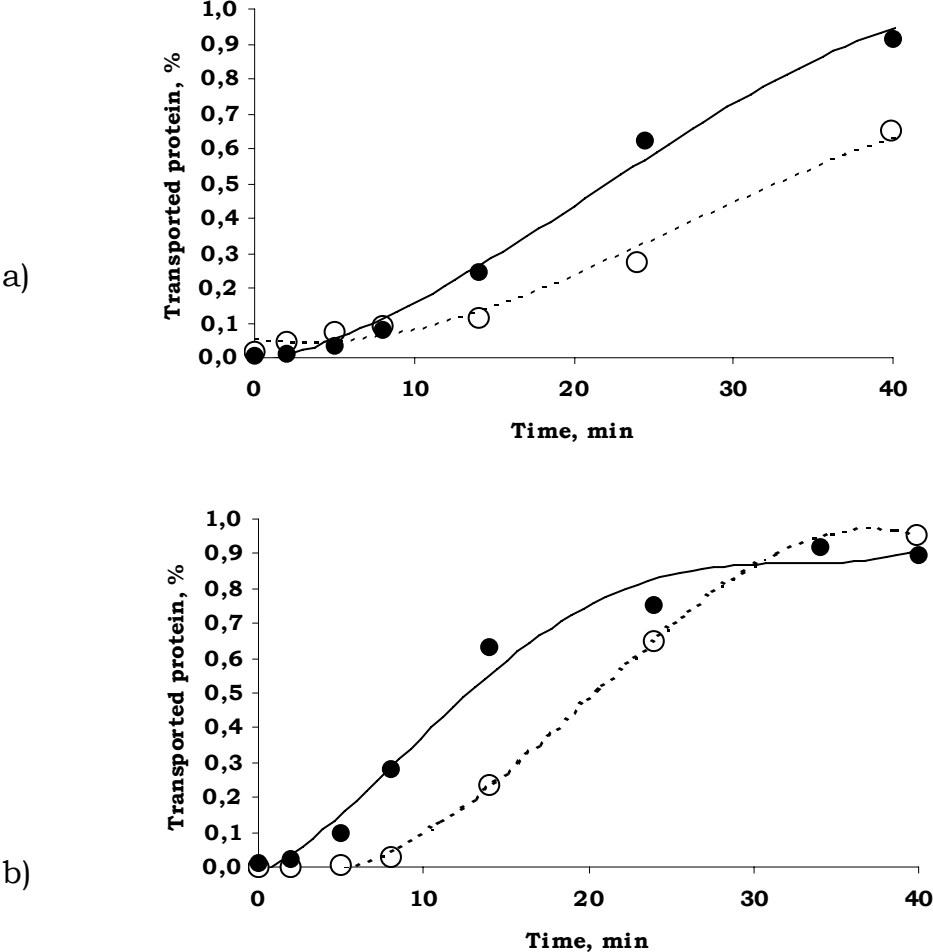
pI-selective barriers, preventing protein loss at the extremes. Chamber I was filled with acetic acid solution 0.1 M, chamber II and III were filled with glutamic acid 20 mM, chamber IV, cathodic, was filled with 1 M Tris base. The concentration of the solutions was adjusted in order to minimise the differences in conductivity between the chambers. The imprinted or control membranes were placed between chamber II and III. Proteins were loaded in Chamber II and collected in chamber III, the electro-migration process was monitored by quantifying the protein content in these two chambers over a time course of 60 min.

#### **5.3.4. EVALUATION OF ELECTROPHORESIS PERMEABILITY OF PAA MEMBRANES**

The first step, in order to characterise the system, was to evaluate electrophoretic permeability of membranes (imprinted with BSA or control) for three different proteins: Bovine Serum Albumin (BSA), Myoglobin, and Catalase, whose characteristics are described in the Table 4. For the same reasons described previously, to set up the system the membranes are templated with BSA, after then the protein used, as template, will be HSA.

Proteins were loaded in Ch-II and collected in Ch-III, the electro-migration process was monitored by quantifying the protein content in the two chambers over a time course of 60 min. Comparison of the

migration curves through control and BSA-imprinted membranes of three proteins are reported in Figure 26.





c)

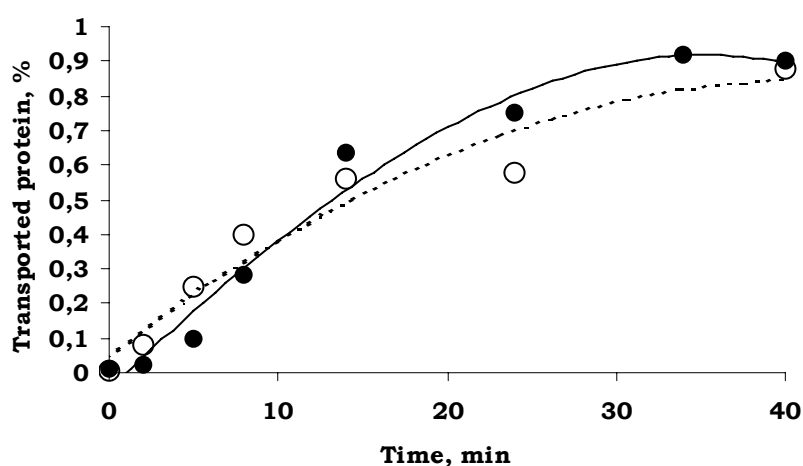


Figure 26\_ Time course of the electric transport of proteins through control (dotted line) and imprinted with BSA (solid line) PAA membranes. a) Catalase, b) BSA, c) myoglobin.

An overall reduction in the migration times characterised the transport through imprinted membranes. A hyperbolic saturation course is evident for the smallest protein tested, myoglobin, while the profiles becoming sigmoid upon increase in protein dimensions, accounting for a sieving effect of PAA for large molecules. As shown by data reported in Table 4, the imprinting process had no impact on the transport of myoglobin, the smallest protein tested, while significantly faster transports were evident in imprinted PAA for proteins of higher dimensions, i.e.  $Tr_{50\%}$  was 39% faster for BSA and 32% faster for catalase.

Table 4\_ Comparison of protein transport times in imprinted- and control- PAA membranes.

<b>Protein</b>	<b>Molecular mass (kDa)</b>	<b>pI</b>	<b>Imprinted-PAA Tr<sub>50%</sub>, min</b>	<b>Ctrl-PAA Tr<sub>50%</sub>, min</b>
BSA	66.4	6.8	12.7	20.7
Myoglobin	17.0	6.8	11.2	12.5
Catalase	220.0	5.4	21.5	32.0

The electric transport through the imprinted PAA was tested for a variety of proteins, differing in molecular masses and pIs (Table 5).

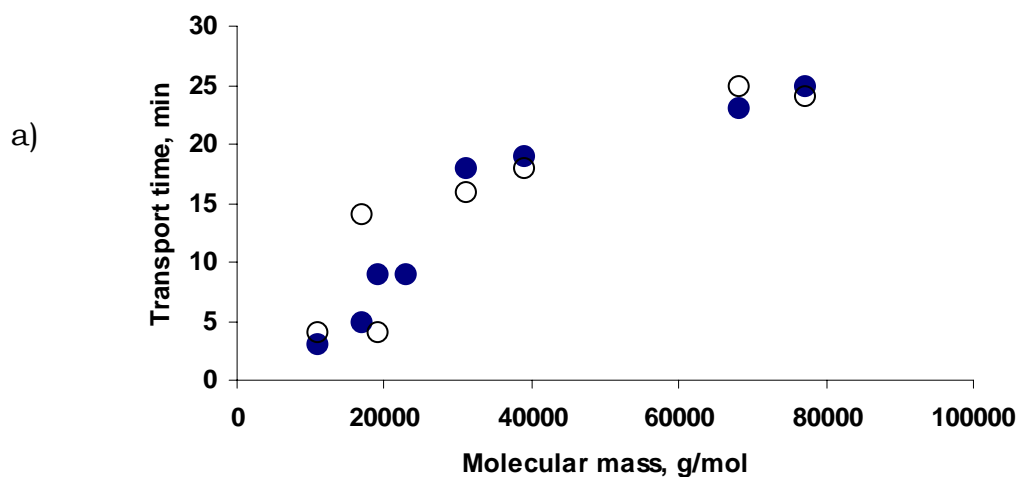
Table 5\_ Molecular mass and charge characteristics of the protein tested.

<b>Protein</b>	<b>M<sub>r</sub>, kDa</b>	<b>pI*</b>
BSA	66.4	6.2
Human serum albumin	65.6	5.9
Haemoglobin	tetramer, 64.0	7.1
Myoglobin	17.0	7.4
Horseradish peroxidase	39.0	Isoforms, 4.7 - 9.13
Trypsin	23.9	4.9
Conalbumin	75.8	6.7
Glucose oxidase	dimer, 160	4.2
β Lactoglobulin b	dimer, 36.4	4.8
Cytochrome c	11.0	10.2
Carbonic anhydrase	29.0	6.4

\*Isoelectric points and molecular weights of proteins according to [35] and Swiss-prot, ExPASy (Expert Protein Analysis System).

In order to standardise the measurement conditions by fully protonating the proteins tested, the acidic pH 3.2 was chosen. The molar transport ( $1.5 \cdot 10^{-2} \mu\text{mol}$ ) was plotted as function of time (Figure 27).

The transport of proteins through imprinted PAA membranes appeared to be significantly dependent on the applied imprinting conditions. Experiments show that the transport times of proteins 11-77 kDa across the membrane imprinted with 0.5 mg/ml BSA (Figure 27a, solid circles) and a control PAA membrane (Figure 27a, open circles) were super-imposable. The transport times were distributed in the range 3-25 min. A linear dependence of the log of molecular masses versus transit times was calculated ( $R^2 = 0.94$ ), in accordance with the permeation theory in PAAs (Casassa, 1976).



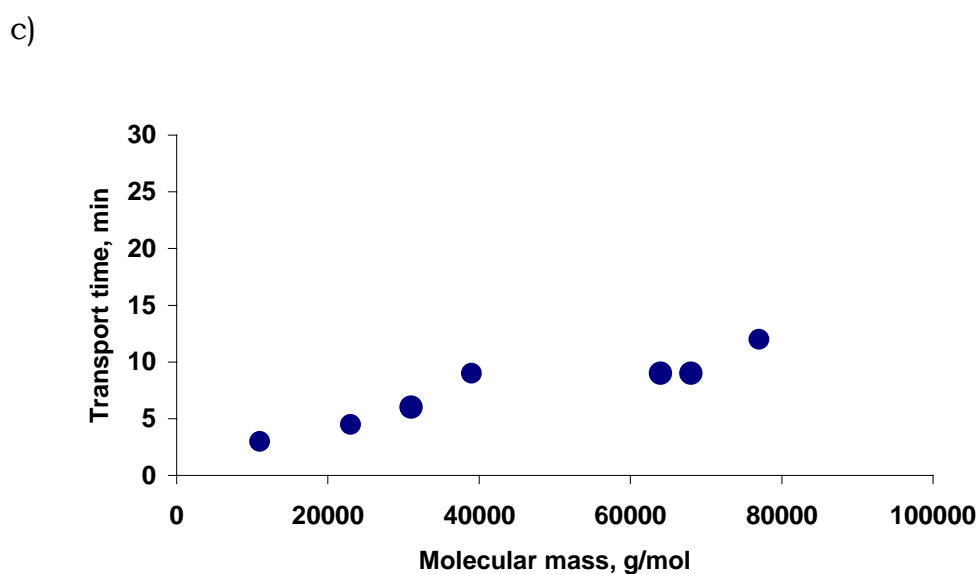
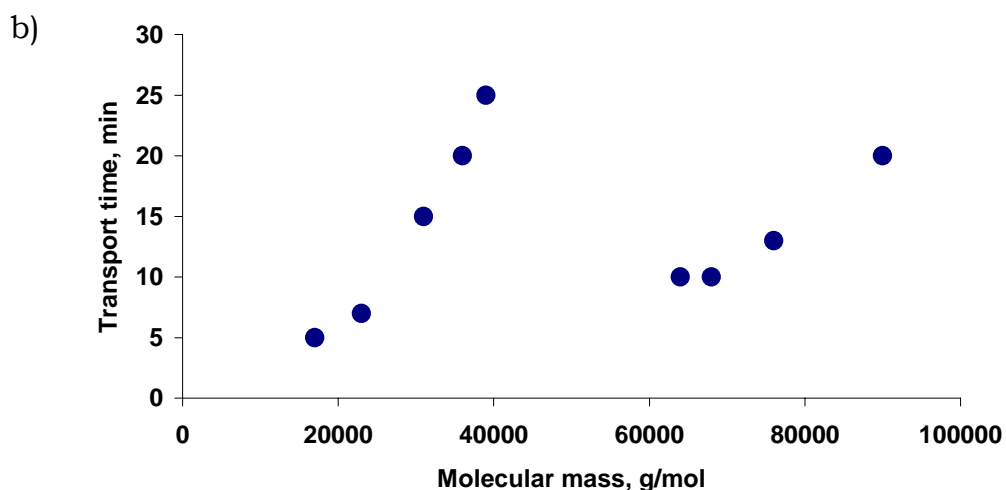


Figure 27\_ Protein transport time (min) is plotted versus Molecular mass (g/mol) (PAA imprinted membranes with BSA). a) The transport across the membrane imprinted with 0.5 mg/ml (solid circles) of BSA shows a sieving course comparable with a non imprinted PAA (open circles). b) PAA imprinted with 1 mg/ml of BSA showed two different electro-transport behaviours, depending on the size of proteins. A fast transport of the template and similar dimension proteins is evident. c) The transport across a 10 mg/ml of BSA imprinted PAA membrane

is characterised by quite fast transport times for all the proteins tested, thus accounting for a scarce sieving effect.

As 0.5 mg/ml imprinted membranes display the sieving properties expected for non-imprinted PAA (Figure 27a, open circles), it could be concluded that 0.5 mg/ml is too low template concentration for inducing the significant number of template-monomer interactions able to alter the polymerisation rate and to finally induce extended pore-size modifications (Piletsky *et al.*, 1997). Whereas, in case of PAAs imprinted with 10 mg/ml (Figure 27c) all the proteins tested, in the range of masses between 11 and 77 kDa, migrated through the membrane barrier within an 8 min range (11 kDa in 4 min and 77 kDa in 12 min). A scarce sieving effect was evident, but a significant alteration in the permeability.

The most interesting results were observed for the transport through the 1.0 mg/ml imprinted PAA (Figure 27b), in which the membrane shows a double sieving behaviour, seemingly molecular mass dependent. In this case, proteins with size up to 45 kDa had migration time distributed between 5-25 min. The transport follows a 'slow' exponential kinetic behaviour, with equation  $y = 28.96x - 311.25$ ;  $R^2 = 0.91$  plotted on a semilog scale. The template and similar mass-range proteins (64-67 kDa) migrate faster (10-12 min) than what expected from the above calculated equation (transport

time for template being comparable to a 27 kDa protein in the slow kinetic).

Proteins with molecular masses above 67 kDa followed a 'fast' exponential kinetics, with migration times varying from 11 to 20 min, described through semi-log plot by the equation  $y = 22.83x - 219.53$ ;  $R^2 = 0.91$ .

Apparently, it could be hypothesised that there are different structural modulus in the 1 mg/ml imprinted membranes that can be roughly classified into:

- Sieving pores that are able to fit proteins < 45 kDa,
- Sieving pores of template dimension,
- Sieving pores of higher dimensions.

The generation of different pore classes during the polymerisation is a phenomenon expected from the conventional 'bulk' MIP technology, in which there is a simultaneous generation of randomly oriented imprinted sites together with the formation of the polymer matrix, including its own pore structures (Ulbrich, 2004). As a consequence, there is a random distribution of uneven sieving pores in the volume of the PAA imprinted membrane together with the specialised imprinted pores. The imprinting process resulted in a significant modification of the sieving properties of PAA. Imprinting, rather than forming a specific barrier, resulted in both the preferential template selection together with the transfer of several different proteins. Figure 27b shows that the migration time for the template protein

coincides with the migration time of proteins below 26 kDa. There is however a marked preferential electro-transport of the template that had striking resemblance to the 'gate-effect', a phenomenon reported for the electro-transport of the substrate molecule through substrate-selective membranes, defined broadly as alteration of the permeability/conductivity of the material upon template binding/interaction (Piletsky *et al.*, 1994).

The preferential transport of template is attributed to the effect of the imprinting process, which leads to the formation of template size-specific homogeneous pores, regularly distributed in the 3D-space, moreover an adaptation of the imprinted structures when interacting with the template is supposed. As a consequence, the template protein and molecules of about 65 kDa find preferential electro-migration ways, fitting perfectly within the channels (Figure 28B).

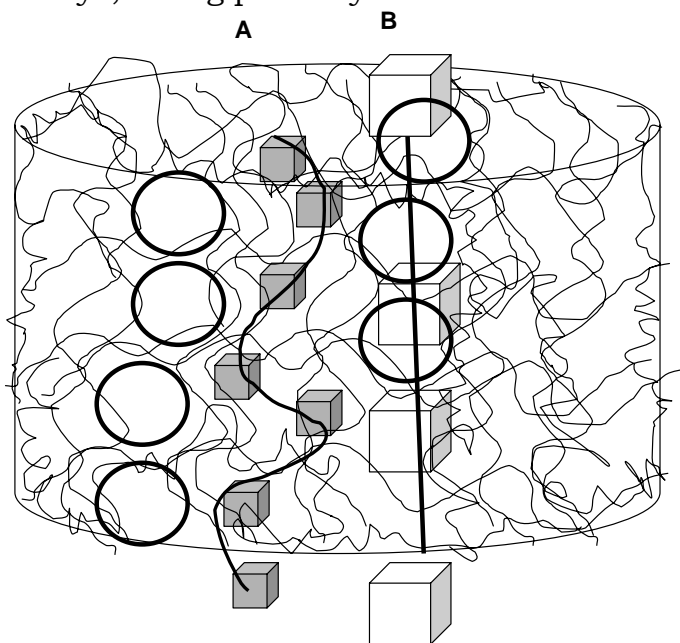


Figure 28\_ The hypothesized mechanism for the electric transport of template (fast kinetic, B) and non-template small proteins (slow

kinetic, A), that has resemblances with the elution mechanism of size-exclusion chromatographic processes.

A minority of the pores population has the typical dimensions of non-imprinted PAAs, with a range of distribution up to  $9 \pm 2$  nm: small proteins could distribute during the electro-migration process both in imprinted channels and in randomly distributed pores, thus migrating through a twisty path, with the consequence of an increase in transport times (Figure 28B). The mechanism hypothesised resembles a size-exclusion chromatography process, where large proteins have a shorter path to go to reach the column's end, respect small molecules, fully explaining the observed preferential electro-migration of template.

The method was set up with BSA a protein less expensive than HSA. In the next experiments, as described in material and methods, the protein used as template is HSA, the real target of my project. The membranes are, in fact, applied to a biological sample contained HSA.

### **5.3.5. EVALUATION OF RETENTION OF THE MEMBRANES**

As demonstrated, the PAA membranes are able to retain preferentially the protein used as template; this ability depends not only on the percentage of monomers used during the membrane polymerisation, but also on the template concentration.



Now, Human Serum Albumin (HSA) was used as template. It was chosen with a purified grade  $\geq 99.9\%$  in order to avoid contaminations and interferences. PAA membranes were polymerised as described in 5.2.2. and the run was performed for 12-minutes. After, the HSA amount present in the loading (Ch-II) and collecting chambers (Ch-III) was measured, by protein assay as declared by producer.

Data obtained, were analysed through the equation [a] of 5.2.3.

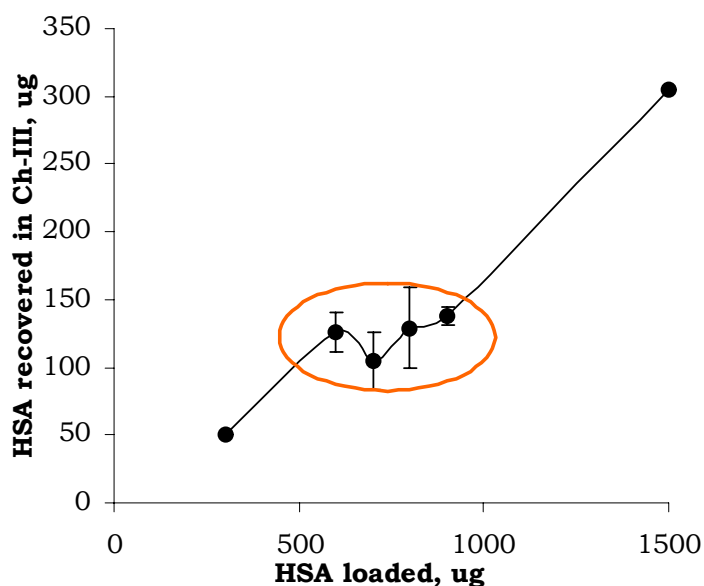


Figure 29\_ HSA recovered from Ch-III after 12 minutes are plotted as a function of the HSA amount (micrograms) loaded at the beginning in Ch-II. Red circle indicates the saturation region, next showed more clearly in Figure 30.

The graph in Figure 29 indicates that the quantity of HSA recovered in Ch-III after 12 minutes is not proportional to the total protein

loaded at the beginning in Ch-II. Particularly, there is a window between 700 and 900 ug where the protein recovered from Ch-III is quite constant (red circle).

When the protein amount bound by the membrane, calculated according to [a], is plotted against the starting protein amount, a saturation curve can be observed, as showed in Figure 30.

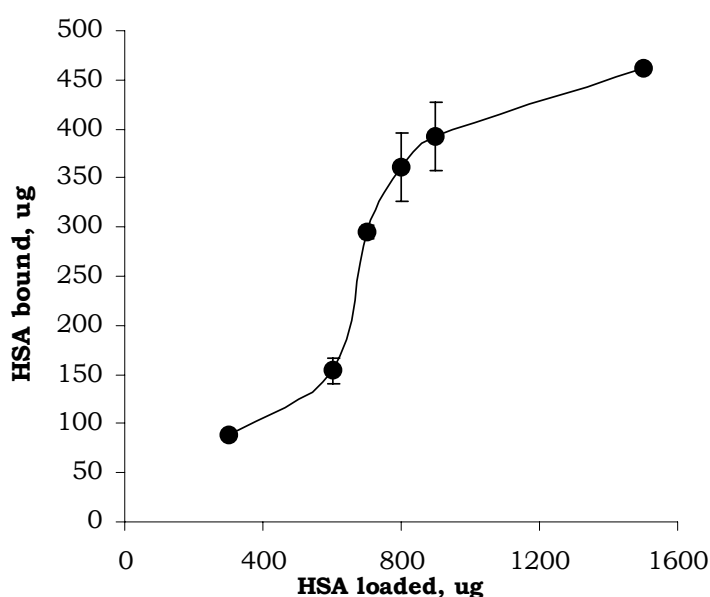


Figure 30\_ HSA bound by the membrane after 12 minutes are plotted as a function of the HSA amount (micrograms) loaded at the beginning in Ch-II. The quantities were calculated according to equation [a].

In the same range as previously indicated (700 ug – 900 ug), the curve is constant, thus indicating that the membrane binds the same amount of protein irrespective of the amount of HSA loaded.

It possible to introduce a new parameter to characterise PAA membranes: the *retention* of polyacrylamide imprinted membranes. *Retention* can be here defined as the maximum template amount (in micrograms, or in %) that a PAA membrane is able to retain. This parameter is very important to fix the efficiency and potency of PAA membranes. We considered as a good retention a value higher than 30%. Graph in Figure 30 demonstrate that the *retention* of the PAA membrane reaches its maximum for  $430\mu\text{g}\pm 30$  for 900  $\mu\text{g}$  loaded, *id est*  $44\%\pm 8\%$  of protein respect to the amount loaded at the beginning. The value can be considered satisfactory in order to continue with next experiments, with more complex samples.

Moreover, considering that membrane area is about  $4.8\text{ cm}^2$ , the retention capacity compared to the surface area of membrane should be approximately  $\sim 0,10\text{ mg}$  of HSA bound/ $\text{cm}^2$ .

### **5.3.6. APPLICATIONS OF MEMBRANES TO PROTEOME ANALYSIS**

Membranes with novel selective abilities are required especially in the area of bio-separation (van Reis & Zydney, 2001) where many very specialised fractionations are needed, often as key step for complex and multi-step analytical tasks, like in genomic and proteome analysis (Ulbrich, 2004). The sieving properties of the PAA imprinted membranes match the needs of proteomic analysis performed with 2D-electrophoresis, as the analysis focuses mainly on a protein

population of >25 kDa. In our case, the permeation properties of the PAA imprinted membranes have been further exploited for the selective removal (pre-fractionation) of a predominant protein from a complex biological fluid – which is an important task in proteome analysis.

PAAs imprinted with human serum albumin have been used for the treatment of human serum, in order to pre-fractionate the sample and remove albumin, whose high abundance (50-70% of the total proteins in serum) poses serious problems in the detection of low expressed proteins (Chertov *et al.*, 2005). The removal of albumin prior to proteome analysis of serum is essential for increasing the resolution of the proteome analysis (Steel *et al.*, 2003). In our experiments 800  $\mu$ g of serum have been loaded in Ch-II and the albumin-electro-depletion was performed for 12 min. After, the solutions were removed from Ch-II and Ch-III and 5 ml of 20 mM glutamic acid was added in each chamber. Field electric (5 mA) was applied in order to remove proteins entrapped in the gel matrix. After 12 min sample was recovered, quantified by Bradford Assay and performed for 2D analysis. Proteins entrapped in polyacrylamide membrane were electro-eluted and analysed as described previously.

About  $160 \pm 10$   $\mu$ g protein were detected in Ch-III after the process, and  $470 \pm 10$   $\mu$ g protein were measured in Ch-II. After electro-removal about  $100 \pm 12$   $\mu$ g were recovered by Ch-III. In order to evaluate the

efficiency of the removal, aliquots of non-treated and electro-depleted serum were analysed firstly through mono-dimensional electrophoresis and after by 2D-electrophoresis.

### 5.3.6.1. ANALYSIS THROUGH SDS-PAGE

In order to quantify the spot density and to have more accurate spot quantification, SDS-PAGE was performed with 30 ul of each sample collecting in Ch-II and Ch-III before and after the binding experiments and the electro-elution process. Gel stained was analysed through densitometry analysis and the HSA spots were quantified through regression plot. The spot density was calculated for 30 ul of sample and for the whole sample. Gel is showed in Figure 31 and respective quantification is reported in Table 6.

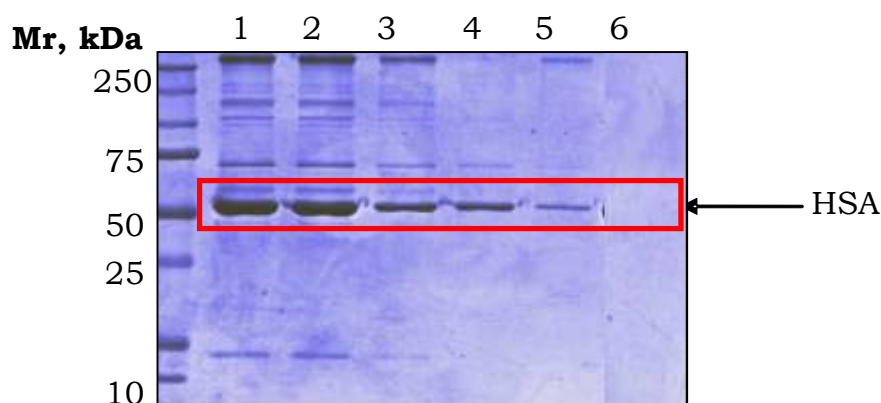


Figure 31\_ SDS-PAGE stained in Coomassie. Lane 1-2: sample not treated, Lane 3: sample recovered in Ch-II after 12 minutes, Lane 4: sample recovered in Ch-III after 12 minutes, Lane 5: sample recovered in Ch-III after electro-elution, Lane 6: sample recovered in Ch-II after electro-elution.

From quantification, it is particularly evident, that after 12 minutes there is a decrease of quantity of HSA loaded in Ch-II. This calculated decrease about 55%. After 12 minutes only  $110 \pm 8$  ug were recovered in Ch-III. Apparently 260 ug are entrapped in the matrix of membrane, value similar respect to previous experiment. In order to remove the protein entrapped in the matrix of PAA membrane an electro-elution process was performed. This step performed by electric field, 75 V, 4 mA for 1 h, allows removing the HSA entrapped in the pores of MIP membrane.

Table 6\_ Table indicates HSA spot quantification of gel showed in Figure 31. First column reported the name of lanes of Figure 31, second lane the name of sample, the third data related to intensity of HSA present in sample loaded on gel, the forth columns reported data related to whole sample.

<b>Lane</b>	<b>Sample</b>	<b>ug of HSA recovered in 30 ul</b>	<b>ug of HSA recovered in whole sample</b>
1	Sample not treated	$5,47 \pm 3$	$810 \pm 3$
2	Sample not treated	$5.49 \pm 5$	$811 \pm 5$
3	Sample recovered from Ch-II after 12 min	$2,97 \pm 7$	$440 \pm 7$
4	Sample recovered from Ch-III after 12 min	$1,08 \pm 8$	$110 \pm 8$
5	Sample recovered from Ch-III after electro-elution	$0,68 \pm 4$	$100 \pm 4$
6	Sample recovered from Ch-II after electro-elution	0	0

After 1 h only  $100 \pm 4$  ug were recovered, less than the quantity expected. It could be hypothesized that part of the protein remains entrapped into the membranes, due to self-aggregation and formation of large macro-proteinaceous complexes (Vetri *et al.*, 2007).

Mono-dimensional analysis permits to analyse only some spots but not whole sample. It does not allow the evaluation of the number of spots decreased after the treatment with MIP membrane, therefore, it does not give information on the specificity of membrane for HSA. While, bi-dimensional analysis will allow a more complete analysis: membrane specificity and number of proteins trapped or sieved by the membrane.

#### **5.3.6.2. ANALYSIS THROUGH 2D ANALYSIS**

Human serum treated and not treated, analysed in first dimension, are analysed through bi-dimensional analysis. 2D-gels obtained were compared using software PDquest (Biorad, Hercules, CA), as shown in Figure 32. The efficiency of the PAA-imprinted method for albumin removal was evaluated densitometrically. Comparing gel A *vs* gel B, it has been found a reduction of 60% of intensity HSA. For analysis, all the different HSA isoforms are considered (red circle). This is an interesting and encourages result that demonstrates a recognition capacity of membranes towards protein used as template. Moreover, spot analysis revealed an in significant decrease of the overall spot

intensity, an indication of proteins is present in the same quantity, and in the control and treated sample.

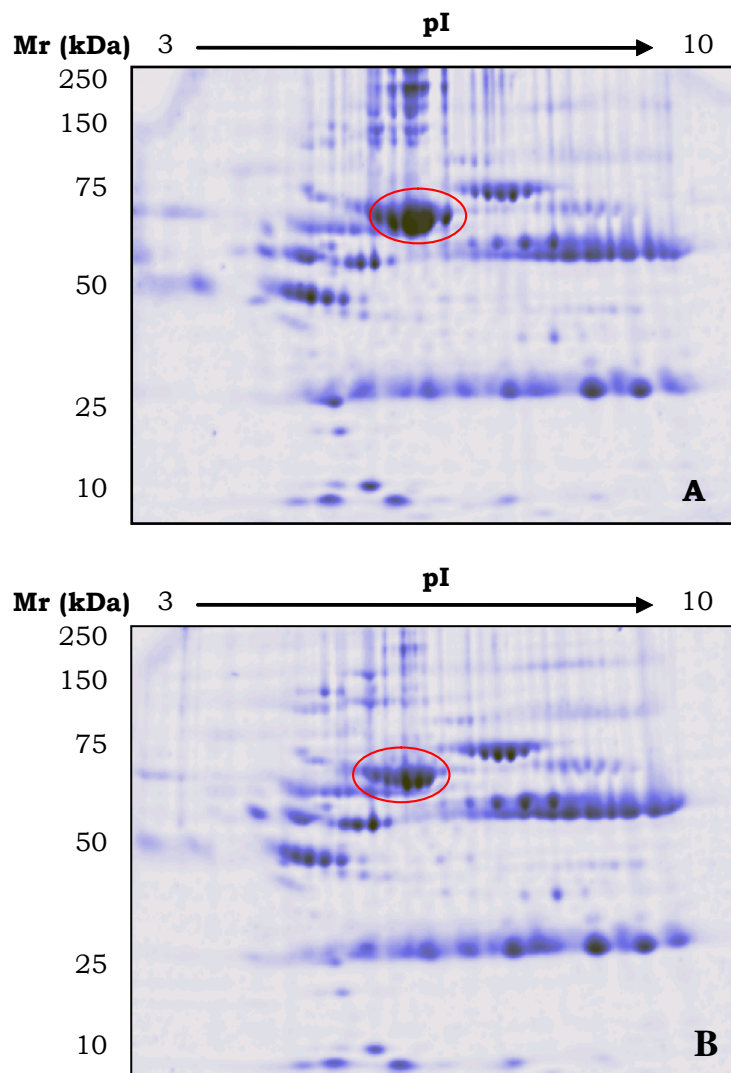


Figure 32\_ The effectiveness of the imprinted-PAA for removal of the high abundant protein human serum albumin from serum samples was demonstrated by the two-dimensional electrophoresis of serum subjected to electro-depletion of albumin, Ch-II, (B) and control serum (A). Data are normalised in function of optical density of whole map.



Spot computation indicates a significant advantage of Ch-II with  $287 \pm 10$  spots *vs*  $211 \pm 10$  versus not treated sample, with 76 more spots detected for treated sample.

The increase of spots number induced a question: in which region is there the change of the spots number? Is increase of spots number random or it depends on treatment with PAA membranes?

The answer is obtained through analysis by pDQuest software. We give attention to two specific regions as reported in Figure 33 in yellow or green ring.

- pI [4.0-7.0] and Mr [250-65 kDa] (Green ring in Figure 33 A)
- pI [5.0-8.0] and Mr [65-50 kDa] (Yellow ring in Figure 33 A)

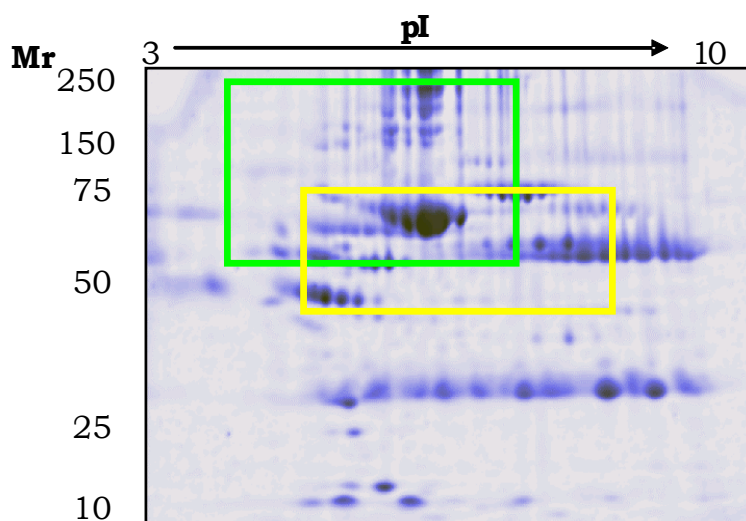


Figure 33\_ Two specific regions are analysed, green ring pI [4.0-7.0] and Mr [250-65 kDa] and yellow ring pI [5.0-8.0] and Mr [65-50 kDa].

### 5.3.6.3. 2D analysis pI [4.0-7.0] and Mr [250-65 kDa]

In order to deepen the analysis, the specific region of 2D maps is analysed using specific software in order to count the spots. As showed in Figure 34, the region including areas with pI [4.0-7.0] and Mr [250-65 kDa] is different in control gel as compared with treated gel, and the difference is more appreciable than the one seen in Figure 33. The region in gel B is well defined while in gel A is not. In fact, in B it is possible to identify 6 isoforms of HSA while in A only 4.

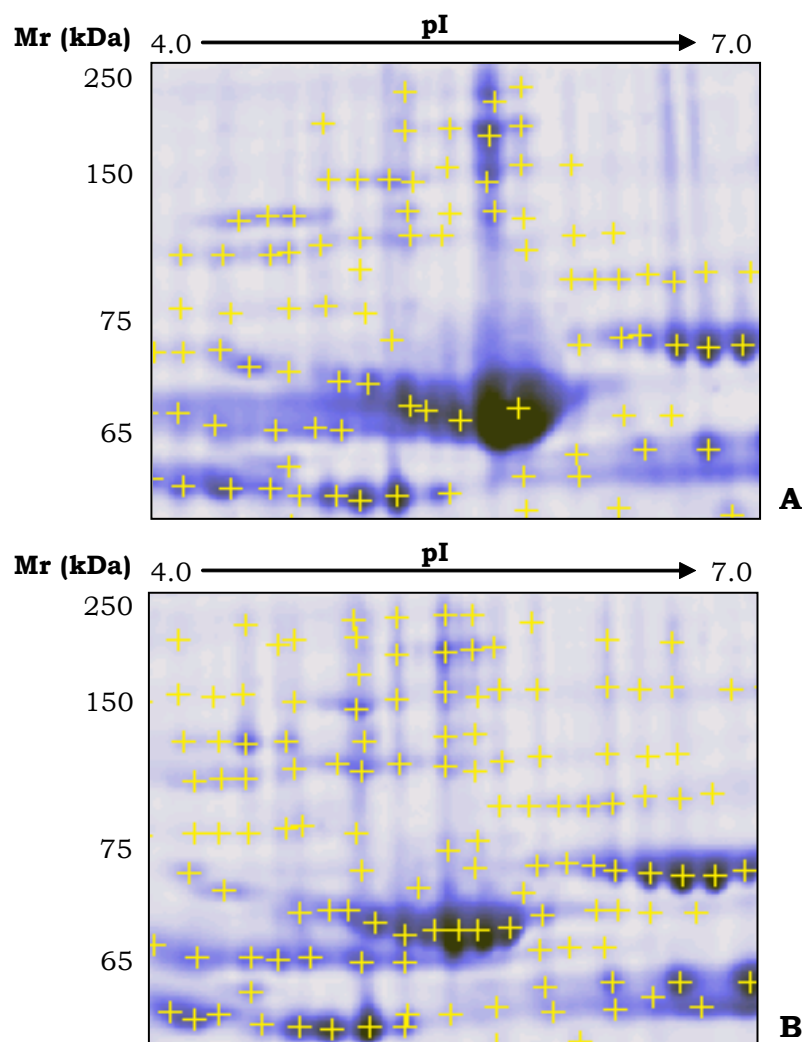


Figure 34\_ Figure shows a specific area with pI [4.0-7.0] and Mr [250-

65 kDa] in control gel (A) and treated gel (B). Yellow crosses are the spots detected through pDQuest software.

In this last case spots are stretched out and not well separated in first dimension, probably due to excessive quantity of HSA. After the treatment with PAA membranes, a removal of 60% of HSA was noticeable as well as an increase of resolution in gel B. The spots with high molecular mass, for example, are not stretched in gel B, but well defined.

Moreover encouraging results are obtained analysing the spots number in this specific region (yellow ring):  $77 \pm 5$  spots in gel A as compared with  $105 \pm 5$  spots in gel B, with an increase of  $28 \pm 5$  new spots. The same strategy is applied to the second region.

#### **5.3.6.4. 2D analysis pI [5.0-8.0] and Mr [50-25 kDa]**

As described in previous paragraph and showed in Figure 33, an other region choose in order to deep the analysis of 2D map is pI [5.0-8.0] and Mr [50-25 kDa]. In this case, as in 5.3.8.3., PDQuest software allowed analysing the spots number in a specific region. The more alkaline region close to albumin and ferritin chains, often, is difficult to analyse because the spots are very faint. After treatment with MIP membranes, more spots are detected. Particularly, through pDQuest analysis  $80 \pm 5$  are counted in control gel and  $114 \pm 5$  in

treated gel. In treated gel  $34 \pm 5$  new spots are detected, after treatment with PAA membranes.

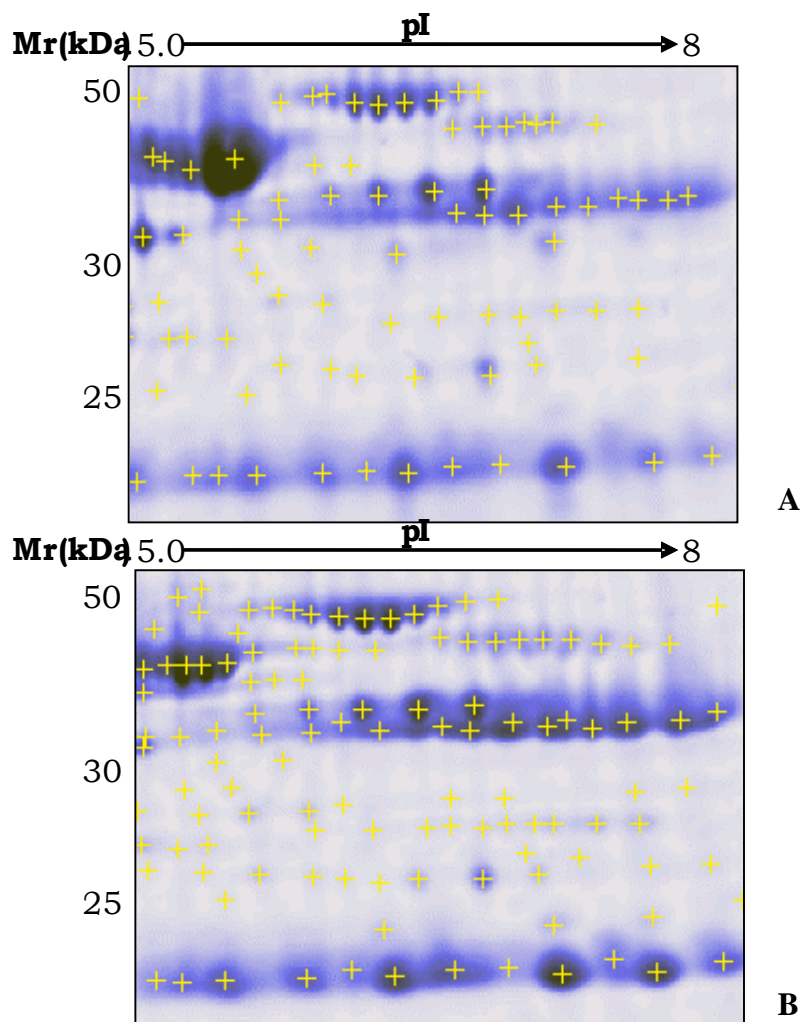


Figure 35\_ Figure shows a specific area with pI [5.0-8.0] and Mr [50-25 kDa] in control gel (A) and treated gel (B). Yellow crosses are the spots detected through PDQuest software.

Concluding these preliminary results, in these regions it was demonstrated that applying the MIP membrane is possible increase spots resolution in region, which is hard to analyse by traditional methods. It was moreover demonstrated that the removal of HSA

doesn't remove the other proteins but allows identifying new spots, often stretched in samples not treated.

Membranes show, then, a particularly selectivity in order to recognize HSA in a complex sample.

Up to the present, human serum was analysed through strips 7 cm 3-10 NL, where a pH gradient of seven units is distributed in 7 cm of length. Therefore, the best approach to increase the resolution on the 2D gels is to run multiple gels that cover narrow pH ranges (e.g. covering one or more pH units). Using these gel systems, it is possible to resolve the proteins.

#### **5.3.6.5. 2D analysis with strips 7 cm [4.0-7.0], gel 10-20% T and [5.0-8.0], gel 10-20% T.**

In a last set of experiments, human serum treated and not treated with PAA membranes is analysed with strips 7 cm but with two different pH ranges, closed to isoelectric point of HSA: 4-7 or 5-8.

800 µg of human serum was treated with PAA membranes. Samples recovered in Ch-II and Ch-III were analysed through 2D gels with strips 7 cm [4.0-7.0] and [5.0-8.0] and stained with Sypro Ruby are showed in Figure 36 and Figure 37 respectively. Through pDQuest analysis the density of HSA spot was evaluated. A decrease of intensity is about 45%±7 in the range [4-7] (Figure 36), while about 52%±5 in the range [5-8] (Figure 37). The difference of spot intensity respect to the value evaluated in the chapter 5.3.8.2 (it is 60%) is

easy to explain. Probably, the amplification of a narrow pH gradient allows a better distribution of HSA, and several proteins, that previously were associated with HSA, now are separated and could be included in the computation of spots intensity.

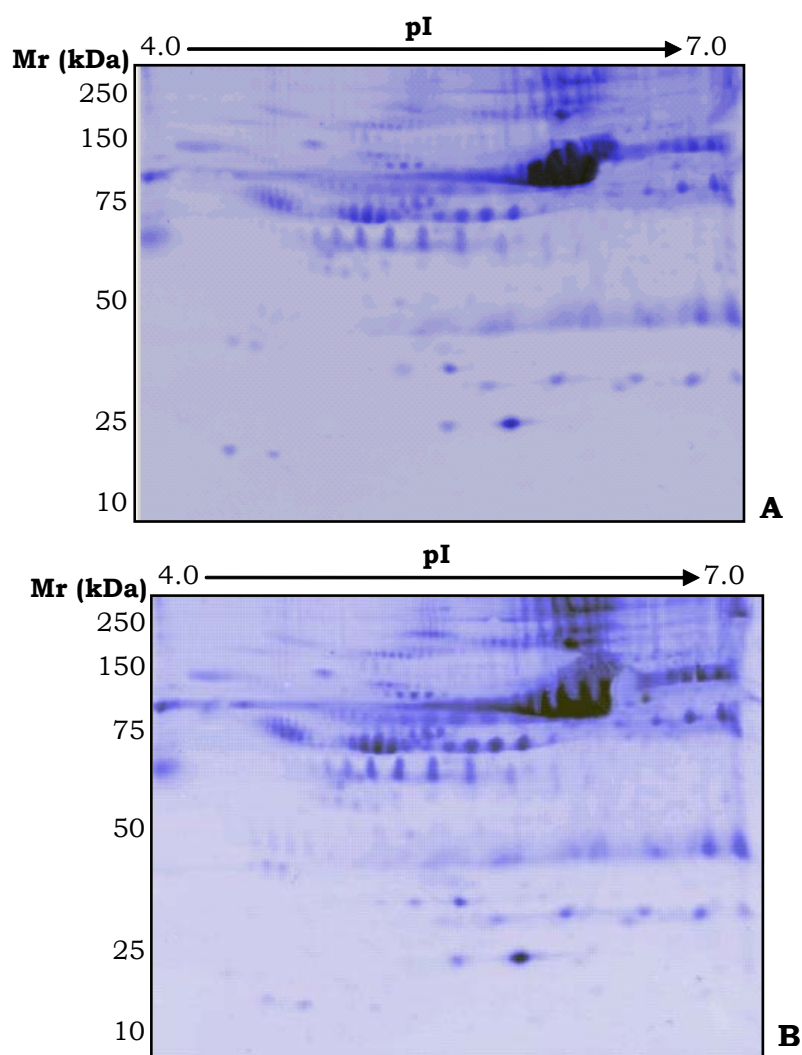


Figure 36\_ Figure shows a specific area with pI [4.0-7.0] and Mr [250-5 kDa] in control gel (A) and treated gel (B).

The number of spots ( $184 \pm 12$ ) is detected in control gel and  $244 \pm 8$  in treated gel for range [4-7] and  $272 \pm 9$  in control gel respect to  $324 \pm 8$  of treated gel in range [5-8].

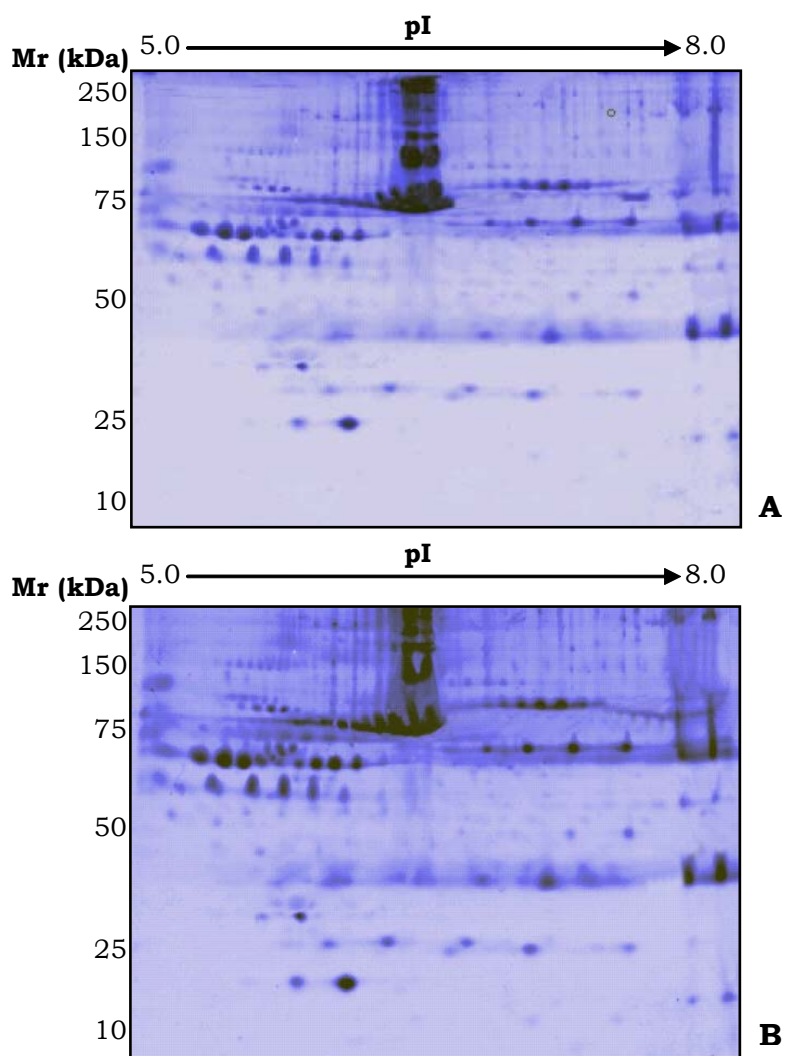


Figure 37\_ Figure shows a specific area with pI [5-8] and Mr [250-10 kDa] in control gel (A) and treated gel (B).

The removal of HSA allows detecting  $60 \pm 10$  and  $52 \pm 9$  new spots respectively, respect to  $28 \pm 5$  and  $34 \pm 5$  spots detected through 3-10

NL as pH range used. Probably, the new distribution of proteins allows higher resolution.

As showed in the master maps showed in Figure 38 A-B, the distribution of new spots is focused mainly close to HSA, even if several proteins are in different areas of the gel. The master map was obtained comparing treated samples to control samples, shown clearly the spot distribution. Green circles are spots present in both kinds of samples while red circles are the new spots detected after treatment with PAA membranes. The master map was obtained comparing treated samples and control samples, showing clearly the spot distribution. Green circles are spots present in both kinds of samples while red circles are the new spots detected after treatment with PAA membranes. At the present, the identity of new spots detected with this treatment is unclear. Deeper analysis may be necessary in order to establish if the newly spots are potential biomarkers. Nevertheless, the results obtained enlarging the area of analysis with the narrow range proteome gels are interesting and promising.



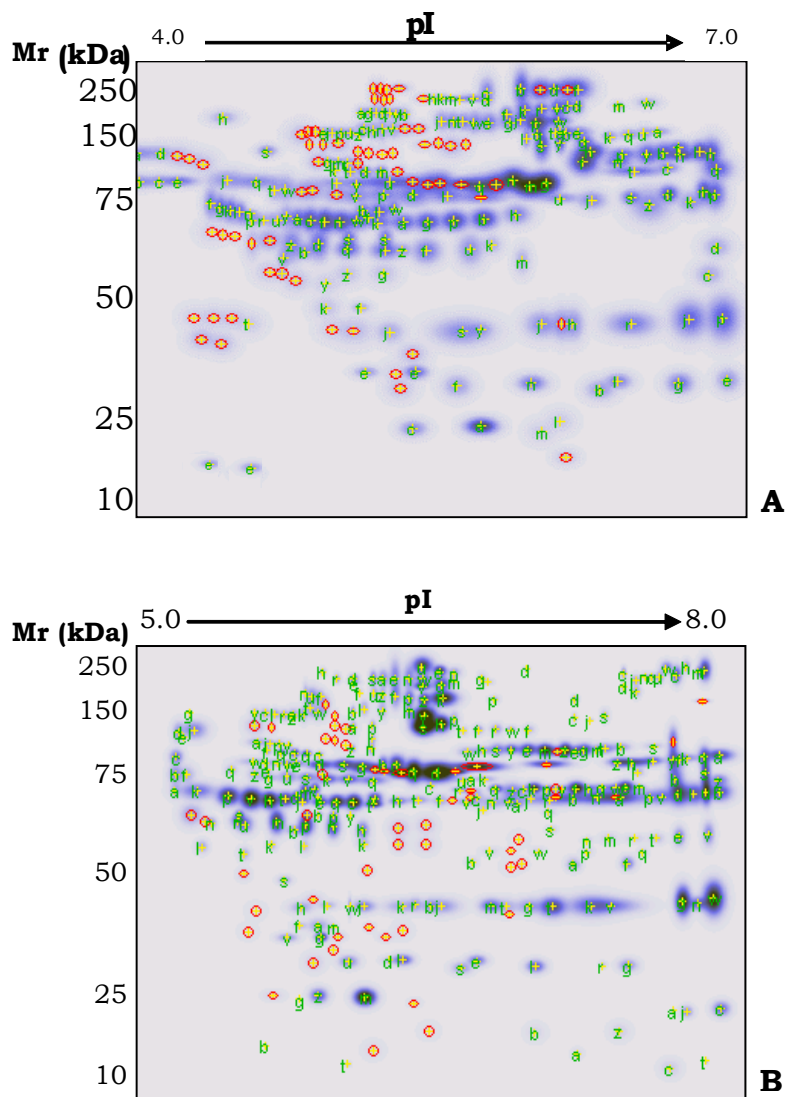


Figure 38\_ Figure shows master map obtained from match between control and treated samples for two different ranges [4-7] (A) and [5-8] (B). Green circle represent common proteins in both samples, while red circle represent the new spot in sample treated with PAA membranes.

#### **5.4. CONCLUSIONS AND FUTURE PERSPECTIVES**

In this chapter a bulk polymerisation approach has been used to prepare MIP membranes based on polyacrylamide. In this case, we direct our attention not to the polymerisation method, but to the polymer quality. The use of PAA presents some advantages as compared to other polymers: it is soft, ductile and very easy to use. Moreover, the polymerisation and the binding experiments are performed in an aqueous environment that is fully compatible with the protein native structure. The system obtained in such a way was applied to the multicompartment electrolyser (MCE), a well known device employed for different examples of proteins purifications (Righetti *et al.*, 1996, 2003). The advantage of purification through MCE is that the proteins are collected in chambers with a minimal volume of buffer, very easy to be recovered for next analysis.

The innovation and peculiarity of the present system consist in combining the favourable features of PAA and the MIP recognition properties with the MCE versatility for a simple (HSA solution) or complex sample (human serum).

With this method, protein removal takes place in a few minutes. In general, the electrophoretic transport through imprinted membranes is faster than in non-imprinted ones. The 'gate effect' depended on the protein sizes, and it is probably related to the altered pores size distribution of PAA as a result of the templating process. Proteins

much smaller than the template appeared to be subjected to a different electro-transport regime.

The optimal conditions for the experiments were set up at the beginning with a model system where the protein template is BSA and after set up with HSA. The experiments were composed of a panel of different proteins, and then human serum was used as sample, in order to selectively remove the serum albumin. The results indicate that the use of imprinted PAA membranes could represent a suitable tool for pre-fractionating biological samples prior to proteome analysis. In fact the treatment of sample with MIP membranes imprinted with HSA allowed for a removal of about 60% of the initial HSA. Moreover the most interesting aspect is the improvement achieved in the total quality of the 2D-maps. In fact, after the prefractionation step, the resolution observed in the 2D maps was considerably higher, particularly near to two specific regions in the 2D maps (pI 5.5-7.5 and Mr 250-65 kDa and pI 5-10 and Mr 50-25 kDa), as showed previously in Figure 35-36. Good results were obtained also with human serum treated with PAA membranes. In fact, in this case, a considerably higher amount of spots could be revealed after sample treatment in two pI and Mr ranges, as clearly displayed in Figure 39. Software-based graphical analysis revealed that about 26% and 28% more spots could be revealed, respectively, in the pI/Mr ranges 5.5-7.5/65-250 kDa and 5.0-10.0/25-50 kDa. The increase of number of spots in this pH range was confirmed

through analysis of 2D maps where a specific range was enlarged and the resolution is higher.

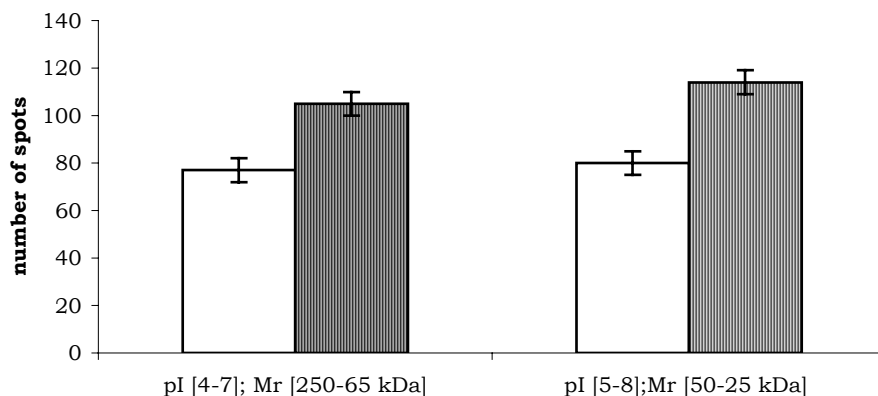


Figure 39\_ Two bar-graphs show the gain in total spot number after sample treatment (human serum) with PAA membranes. The experiments were performed in triplicate. White columns: untreated samples; striped columns: samples treated with PAA-membranes.

60±10 and 52±9 new spots are detected in different range [4-7] and [5-8] respectively indicating higher resolution. Spots could be potentially biomarkers.

Today, biomarkers discovery is a complex process because it correlates with a disease and, because biomarkers are proteins that changed their concentration (down-regulated or up-regulated) depending on the disease.

Our data obtained and compared to literature are encouraging considering what literature showed up to this point.

For example, recently it was reported a new method for identify potential biomarkers based on antibody and micro-arrays (Borrebaeck & Wingren, 2007).

Antibody-based micro arrays have been versatile, rapid and highly multiplexed and high throughput proteomic tools. In several studies, protein expression profiling has been performed in order to identify disease- specific protein signatures (Borrebaeck & Wingren, 2007). The goal of the work here was to identify biomarkers signature that can be used in diagnostic field. An important range of applications has been established within in onco-proteomic and probably the applications will increase in the future. Therefore, the main issue in this case is to create a large polyclonal, monoclonal or recombinant antibody library linked to a specific rigid support, (Borrebaeck & Wingren, 2007).

A different technology was described from Righetti and co-workers that obtained recently important results applying equaliser beads in order to detect the “hidden” proteome (Boschetti *et al.*, 2007). Equaliser beads, the technology described in Chapter III, was applied in different biological fluids (urine, serum, blood) demonstrating the possibility of detecting low abundance proteins often not detected with traditional methods. This study demonstrates that peptide ligand beads are able to capture a highly complex mixture of proteins. The captured fraction of the serum proteome had reduced dynamic range and could thus give a substantially larger amount of

information at the same analytical effort. Combining this technology with 2D analysis and mass spectrometry opens the possibility to discover low abundance proteins differentially expressed as a result of an internal or external stimulus.

Among other possible applications (e.g., follow-up of new drug development, toxicity markers, allergens, stress markers, detection and identification of impurity traces from injectables biopharmaceuticals, etc.), this could be a way to discover new low-abundance biomarkers of disease. For example from serum analysis with 2D methods coupled with MS, very low abundance proteins are detected, such as vitronectin and its fragment C4  $\alpha$ -anaphylatoxin and transthyretin that in general are not visible in untreated serum (Boschetti *et al.*, 2007). These examples show the good potential of the “equaliser beads” approach that couples good capture efficiency with an extremely simple sample handling protocol.

These are only two methods described in literature, but they are an important tool in proteome analysis. Both however are associated with high price.

The method here proposed and based on PAA membranes allowed obtaining interesting results using a rapid, easy and especially cheap technology.

Moreover, it has to underline other important aspect of PAA imprinted membranes strategy. Often, commercial products are made for a set of proteins (albumin, ferritin, antibody). Equaliser beads, for

example, don't discriminate a specific protein but bind the proteins in relation to their quantities; micro arrays for example were made for a set of protein. Instead, with PAA membrane technology presented here it is possible creating in a short time and at low cost, a specific and selective polymer for recognition of whichever proteins, within reason.

Missing aspect in the characterisation of this system is the combination of PAA membranes and 2D analysis with mass spectrometry in order to identify new spots detected. In fact, at the present many methods described in literature (Righetti *et al.*, 2007; Wu *et al.*, 2007) need MS as tool indispensable for a specific and deep analysis.

This aspect must be further investigated in the future, in order to definitely demonstrate the high potency of the present approach in the proteomic field.

In the future, on other perspective could be to made a scale-up of the experiments, using a bigger instrument (for example an prototype), where the volume in each chambers is major. In this case, a greater quantity of sample could be loaded in order to obtain more proteins to analyse. Thus, the next analysis will not limited from sample quantity and 2D maps and MS analysis could be easier.

Moreover, in all these cases, the wide-ranging use of this technology in the different fields of research would be favoured by the possibility of rapidly manufacturing a MIP directed toward whatever polypeptide,

while antibody production or the other methodologies are much more tangled and time consuming. The possibility to rend protein samples less complex in a fast and simple step would allow for the study of the low abundance protein fraction, which is believed to represent the most interesting part of each proteome.



## **CHAPTER VI**

### **GENERAL CONCLUSIONS**

#### **6.1 FINAL CONCLUSIONS**

In the field of diagnostics, the capability of analysing quickly and accurately a specific sample represents an important goal. Often, however, the sample complexity creates manifold problems. For the human serum, for example, the major problem is that the protein concentration range spans some ten orders of magnitude, thus rendering the detection of the “rare” proteome highly problematic. High-abundance proteins are troublesome in 2D maps, as they obliterate the signals of the rare ones, which are often buried under the very large spots (and smears) of the abundant species. During the last 30 years, the removal of high abundance proteins has been accomplished through different approaches (chromatography, electrophoresis, immuno-subtraction, etc) that have been described in the previous chapters. The aim of the present PhD thesis consisted in developing and applying a new technology for selective protein removal that had already been exploited in diagnostic field but that had never been used in the field of proteomic.

The Molecularly Imprinted Technology can be defined as the process of template-induced formation of specific recognition sites (binding or catalytic) in a material, where the template directs the positioning

and the orientation of the material's structural components by a self-assembling mechanism.

In literature one can find two main different approaches concerning the best way to manufacture MIPs: covalent or no-covalent approach (Zhang *et al.*, 2006). Wulff's group pioneered the first one in which functional monomers forms complexes with template molecules via reversible covalent bonds prior the polymerisation; the subsequent rebinding of the analytes to imprinted polymers taking place through the formation of covalent bonds between them (Wulff, 1995).

No-covalent approach utilises only no-covalent interactions between monomers and template molecule (hydrogen bonds, ionic or hydrophobic interactions). It is much more flexible in terms of preparation, because of the absence of complicated synthetic chemistry and the availability of a broad selection of functional monomers and possible target molecules. For these reasons MIPs are being more frequently used in protein research with different kinds of templates (Zhang *et al.*, 2006). In addition, imprinted polymers prepared by the no-covalent imprinting approach show much faster rebinding kinetics than those prepared by the covalent approach, making them particularly suitable for applications involving their use as stationary phases in HPLC system and as sensors. On the other side, the covalent approach usually produces a more homogeneous population of binding sites than the no-covalent approach does, because of the greater stability of the covalent bonds and the high

selectivity of recognition, as also reported by Shimizu and co-workers (Umpleby *et al.*, 2001).

In this work, no covalent approach was chosen and applied in two different ways: no-covalent approach (PAAs membranes, where the template and the polymer are polymerised in bulk) and no-covalent approach with protein template immobilised on the silica surface before the polymer deposition. Both of the methods have been taken into consideration in order to create two different kinds of polymers that have been applied to proteome analysis.

The choice to try both of the methods was determined by the complicated nature of the template molecule and by drawing of different strategies described in literature, immobilised template on a specific surface (Shiomi *et al.*, 2005) or polymerisation in bulk (Hjerten, *et al.*, 1997). In fact, in this case, no short molecule or peptide or drug but a whole protein was used. HSA is quite a large molecule (66 kDa) it has a complex three-dimensional structure and is hardly soluble in organic solvents, due to its hydrophilic nature. For this last reason, in fact, the polymerisation was carried out in aqueous solution with both of the techniques. The advantage of polymerising in aqueous solution is linked to the fact that the protein preserves its native structure, and the site of recognition is able to recognise the specific protein in a biological fluid, *i.e.* in not denaturing conditions.

In the first part of the work, the polymerisation is prepared exploiting the binding between the lysines present on the protein surface and the aldehydic groups of the derivatised beads surface. This approach has some advantages such as, for example, the distribution of binding sites probably is more homogenous. After an extensive quantitative and qualitative characterisation of the beads, the analysis of human serum treated with MIPs revealed a specific removal of HSA without apparently affecting other proteins. The decrease of 58% of HSA in treated samples is a very encouraging result; nevertheless the time required for the polymerisation of beads is fairly long and for this reason such an approach, maybe, will not be applicable to diagnostic field. Therefore, the other approaches based on immobilisation protein had more good results (as described in the previous chapters) and this technology can't be and shouldn't be excluded from scientific landscape.

In order to try to overcome some difficulties previously described (especially the time consuming), a new approach was adopted, that is to say the no-covalent polymerisation method, reported to be much quicker by various authors (Hjerten *et al.*, 1997; Zhang *et al.*, 2006).

MIPs are prepared by free radical copolymerisation of functional monomers and cross-linker in the presence of a protein template in aqueous solvent on a specific support made of glass fibre. Non-functional charged monomers were added because the polymer was used for applications in an electric field. After the characterisation of

MIP membranes and after having chosen the best experimental conditions, the MIPs were applied to human serum. The results obtained are very promising. Similarly, to what observed with the previous method, a consistent decrease of HSA occurred with a consequent increase in the map resolution. In turn, this led to an increase in the number of the spots automatically detected by the software PDQuest in the region adjacent to HSA. Although it was not considered a necessary step in this work, the continuation of the present project should absolutely take into consideration an extensive MS-based analysis of the new spots detected after HSA removal, in order to obtain the protein identities and definitely demonstrate the MIP potentialities. The final aim would be to capture the "hidden proteome", i.e. the low and very low-abundance proteins constituting the vast majority of species in any proteome, a cell or tissue lysate or a biological fluid such as the human serum, urine or cerebrospinal fluid (Boschetti *et al.*, 2007). The importance of low abundance protein was described extensively in literature (Righetti & Boschetti, 2007; Boschetti *et al.*, 2007) and they demonstrated as in the future, probably, the detection of proteins involved in specific diseases will associate to analytical and very specific methods.

Concluding, our experiments have evidenced good and promising results, especially in the second approach where the polymerisation was performed in bulk without template immobilisation. In both cases, probably, the experiments performed are not final. In the

## General conclusions

---

future new tests will be performed in order to improve the methodologies and to obtain new results and new applications in diagnostic and medical field.

## **REFERENCES**

**Aebersold, R. & Mann, M. (2003).** Mass spectrometry-based proteomics. *Nature* **422**, 198-207.

**Anderson, N.L. & Anderson, N.G. (1977).** High resolution two-dimensional electrophoresis of human plasma proteins. *Proceeding of the National Academy of Sciences* **74**, 5421-5425.

**Andersson, L.I., Muller, R., Vlatakis, G. & Mosbach, K. (1995).** Mimics of the binding sites of opioid receptors obtained by molecular imprinting of enkephalin and morphine. *Proceedings of the National Academy of Sciences of the United States of America* **11**, 4788-4792.

**Andersson, N.G., Matheson, A. & Anderson, N.L. (2001).** Back to the future: The human protein index (HPI) and the agenda for post-proteomic biology. *Proteomics* **1**, 3-12.

**Anderson, N.L. & Anderson N.G. (2002).** The human plasma proteome: history, character, and diagnostic prospects *Molecular Cells Proteomics* **1**, 845-867.

**Antonietti, M., Caruso, R.A., Göltner, C.G. & Weissenberger, M.C. (1999).** Morphology variation of porous polymer gels by polymerisation in lyotropic surfactant phases. *Macromolecules* **32**,1383-1389.

**Asnaghi, D., Giglio, M., Bossi, A. & Righetti, P.G. (1995).** Large-scale micro-segregation in polyacrylamide gels (spinodal gels). *The Journal of Chemical Physics* **102**, 9763-9769.

**Assender, H., Bliznyuk, V. & Porfyrakis, K. (2002).** How surface topography relates to materials properties. *Science* **297**, 973-976.

**Bae, S.H., Harris, A.G., Hains, P.G., Chen, H., Garfin, D.E., Hazell, S.L., Paik, Y.K., Walsh, B. & Cordwell, S.J. (2003).** Strategies for the enrichment and identification of basic proteins in proteome projects. *Proteomics* **3**, 569-579.

**Baggiani, C., Anfossi, L. & Giovandoli, C. (2007).** Solid phase extraction of food contaminants using molecular imprinted polymers. *Analytical Chimica Acta* **591**, 29-39.

**Bairoch, A., Boeckmann, B., Ferro, S. & Gasteiger, E. (2004).** Juggling between evolution and stability. *Briefings in Bioinformatics* **5**, 39-55.



**Baltus, R.E., Carmon, K.S. & Luck, L.A. (2007).** Quartz Crystal Microbalance (QCM) with immobilised protein receptors: comparison of response to ligand binding for direct protein immobilisation and protein attachment via disulfide linker. *Langmuir* **23**, 3880-3883.

**Birch, R.M., O'Byrne, C., Booth, I.R. & Cash, P. (2003).** Enrichment of *Escherichia coli* proteins by column chromatography on reactive dye columns. *Proteomics* **3**, 764-776.

**Bjellqvist, B., Ek, K., Righetti, P.G., Gianazza, E., Gorg, A., Westermeier, R. & Postel, W. (1982).** Isoelectric focusing in immobilised pH gradients: principle, methodology and some applications. *Journal Biochemical Biophysical Methods* **6**, 317-339.

**Bolisay, L.D., Culver, J.N. & Kofinas, P. (2006).** Molecularly imprinted polymers for tobacco mosaic virus recognition. *Biomaterials* **27**, 4165-4168.

**Borrebaeck, C.A.K & Wingren, C. (2007).** High throughput proteomic using antibody microarray: an update. *Expert Review of Molecular Diagnostics* **7**, 683-676.

**Boschetti, E., Lomas, L., Citterio, A. & Righetti, P.G. (2007).**

Romancing: the hidden proteome, anno domini two zero zero seven. *Journal of Chromatography A* **1153**, 277-290.

**Bossi, A., Piletsky, S.A., Piletska, E.V., Righetti, P.G. & Turner,**

**A.P.F. (2001).** Surface-grafted molecularly imprinted polymers for protein recognition. *Analytical Chemistry* **73**, 5281-5286.

**Bossi, A., Castelletti, L., Piletsky, S.A., Turner, A.P.F. & Righetti,**

**P.G. (2004).** Properties of poly-aminophenylboronate coatings in capillary electrophoresis for the selective separation of diastereoisomers and glycoproteins. *Journal of Chromatography A* **16**, 297-303.

**Breton, F., Rouillon, R., Piletska, E.V., Karim, K., Guerriero, A.,**

**Chianella, I. & Piletsky, S.A. (2007).** Virtual imprinting as a tool to design efficient MIPs for photosynthesis-inhibiting herbicides. *Biosensors & Bioelectronics* **22**, 1948-1954.

**Burow, M. & Minoura, N. (1996).** Molecular imprinting: synthesis of

polymer particles with antibody-like binding characteristics for glucose oxidase. *Biochemical and Biophysical Research Communications* **227**, 419-422.

**Buter, R., Tan, Y.Y. & Challa, G. (1972).** Radical polymerisation of methyl methacrylate in the presence of isotactic poly(methyl methacrylate). *Journal of Polymer Science: Part A, General papers* **10**, 1031-1049.

**Campostrini, N., Areces, L.B., Rappsilber, J., Pietrogrande, M.C., Dondi, F., Pastorino, F., Ponzoni, M. & Righetti, P.G. (2005).** Spot overlapping in two-dimensional maps: a serious problem ignored for much too long. *Proteomics* **5**, 2385-2395.

**Candiano, G., Musante, L., Bruschi, M., Ghiggeri, G.M., Herbert, B., Antonucci, F. & Righetti, P.G. (2002).** Two-dimensional maps in soft immobilised pH gradient gels: a new approach to the proteome of the Third Millennium. *Electrophoresis* **23**, 292-297.

**Casassa, E.F. (1976).** Comments on exclusion of polymer chains from small pores and its relation to gel permeation chromatography. *Macromolecules* **9**, 182-185.

**Castagna, A., Cecconi, D., Sennels, L., Rappsilber, J., Guerrier, L., Fortis, F., Boschetti, E., Lomas, L. & Righetti, P.G. (2005).** Exploring the hidden human urinary proteome via ligand library beads. *Journal of Proteome Research* **4**, 1917-1930.

**Chailapakul, O. & Crooks, R.M. (1993).** Synthesis and characterisation of simple self-assembling, nanoporous monolayer assemblies: a new strategy for molecular recognition. *Langmuir* **9**, 884-888.

**Chertov, O., Simpson, J.T., Biragyn, A., Conrads, T.P., Veenstra, T.D. & Fisher, R.J. (2005).** Enrichment of low-molecular-weight proteins from biofluids for biomarker discovery. *Expert Review of Proteomics* **2**, 139-145.

**Chianella, I., Piletsky, S.A. & Tothill, I.E. (2003).** Combination of solid phase extraction cartridge and MIP-based sensor for detection of microcystin-LR. *Biosensors & Bioelectronics* **18**, 119-127.

**Chou, P.C., Rick, J. & Chou, T.C. (2005).** Creative protein thin-film molecularly imprinted polymers formed using a micro-contact approach. *Analytica chimica acta* **542**, 20-25.

**Davidsson, P., Paulson, L., Hesse, C., Blennow, K. & Nilsson, C.L. (2001).** Proteome studies of human cerebrospinal fluid and brain tissue using a preparative two-dimensional electrophoresis approach prior to mass spectrometry. *Proteomics* **1**, 444-452.

**De Duve, C., Pressman, B.C., Gianetto, R., Wattiaux, R. & Appelmans, F. (1955).** Intracellular distribution patterns of enzymes in rat-liver tissue. *The Biochemical Journal* **60**, 604–612.

**De Hooge, C.L. & Mann, M. (2004).** Proteomics. *Annual Review of Genomics and Human Genetics* **5**, 267–293.

**Dickert, F.L., Lieberzeit, P., Hayden, O. (2003).** Sensor strategies for microorganism detection--from physical principles to imprinting procedures. *Analytical and Bioanalytical Chemistry* **377**, 540-549.

**Dickert, F.L., Lieberzeit, P. & Hayden, O. (2006).** Molecularly imprinted polymers for mass sensitive sensors- from cells to viruses and enzymes. In Piletsky, Turner, editors. *Molecular imprinting* Georgetown TX USA Landes Biosciences p. 50-63.

**Faupel, M., Barzaghi, B., Gelfi, C. & Righetti, P.G. (1987).** Isoelectric protein purification by orthogonal coupled hydraulic and electric transports in a segmented immobilized pH gradient. *Journal of Biochemical and Biophysical Methods* **15**, 147-161.

**a. Fortis, F., Girot, P., Brieau, O., Castagna, A., Righetti, P.G. & Boschetti, E. (2005).** Isoelectric beads for proteome pre-

fractionation. II: experimental evaluation in a multi-compartment electrolyser. *Proteomics* **5**, 629-638.

**b. Fortis, F., Girot, P., Brieu, O., Boschetti, E., Castagna, A. & Righetti, P.G. (2005).** Amphoteric, buffering chromatographic beads for proteome prefractionation I: theoretical model. *Proteomics* **3**, 620-628.

**Fountoulakis, M., Langen, H., Evers, S., Gray, C. & Takacs, B. (1997).** Two-dimensional map of *Haemophilus influenzae* following protein enrichment by heparin chromatography. *Electrophoresis* **18**, 1193-1202.

**Fountoulakis, M., Langen, H., Gray, C. & Takacs, B. (1998).** Enrichment and purification of proteins of *Haemophilus influenzae* by chromatofocusing. *Journal of Chromatography A* **806**, 279-291.

**Fountoulakis, M., Takacs, M.F. & Takacs, B. (1999).** Enrichment of low-copy-number gene products by hydrophobic interaction chromatography. *Journal of Chromatography A* **833**, 157-168.

**Gianazza, E. & Arnaud, P. (1982).** A general method for fractionation of plasma proteins: Dye-ligand affinity chromatography

on immobilised Cibacron Blue F3-GA. *Journal of Biochemistry* **201**, 129–136.

**Glad, T., Glad, M., Norrlöw, S., Sellergren, B., Siegbahn, N. & Mosbach, K. (1985).** Use of silane monomers for molecular imprinting and enzyme entrapment in polysiloxane-coated porous silica. *Journal of Chromatography* **347**, 11-23.

**Görg, A., Weiss, W. & Dunn, M.J. (2004).** Current two-dimensional electrophoresis technology for proteomics. *Proteomics* **4**, 3665–3685.

**Govorukhina, N.I., Reijmers, T.H., Nyangoma, S.O., van der Zee, A.G., Jansen, R.C. & Bischoff, R. (2006).** Analysis of human serum by liquid chromatography-mass spectrometry: improved sample preparation and data analysis. *Journal of Chromatography A* **1120**, 142-150.

**Graveley, B.R. (2001).** Alternative splicing: increasing diversity in the proteomic world. *Trends Genetics* **17**, 100–107.

**Guerrier, L., Thulasiraman, V., Castagna, A., Fortis, F., Lin, S., Lomas, L., Righetti, P.G. & Boschetti, E. (2006).** Reducing protein concentration range of biological samples using solid-phase ligand

libraries. *Journal of chromatography. B, Analytical technologies in the biomedical and life sciences* **833**, 33-40.

**Guo, T.Y, Xia, Y.Q., Hao, G.J., Song, M.D. & Zhang, B.H. (2004).** Adsorptive separation of haemoglobin by molecularly imprinted chitosan beads. *Biomaterials* **25**, 5905-5912.

**Haupt, K. & Mosbach, K. (1998).** Plastic antibodies: developments and applications. *Trends in Biotechnology* **16**, 468-75.

**Hawkins, D.M., Stevenson, D. & Reddy, S.M. (2005).** Investigation of protein imprinting in hydrogel-based molecularly imprinted polymers (HydroMIPs). *Analytica Chimica Acta* **542**, 61-65.

**Hjerten, S. (1962).** Molecular sieve chromatography on polyacrylamide gels, prepared according to a simplified method. *Archives of Biochemistry and Biophysics*. **1**, 147-151.

**Hjerten, S. & Mosbach, R. (1962).** Molecular-sieve chromatography of proteins on columns of cross-linked polyacrylamide. *Analytical Biochemistry* **3**, 109-119.

**Hjerten, S. (1967).** Free zone electrophoresis. *Chromatographic Reviews* **9**, 122-219.



**Hjerten, S., Liao, J.L., Nakazato, K., Wang, Y., Zamaratskaia, G. & Zhang, H.X. (1997).** Gels mimicking antibodies in their selective recognition of proteins. *Chromatographia* **44**, 227-235.

**Hulvatt, J.F., & Stupp, S.I. (2003).** Liquid-crystal templating of conducting polymers. *Angewandte Chemie International Edition* **42**, 778-781.

**Hyde, S., Andersson, S., Larsson, K., Blum, Z., Landh, T., Lidin, S., & Ninham, B.W. (1997).** *The Language of Shape. The Role of Curvature in Condensed Matter: Physics, Chemistry.* Elsevier, The Netherlands.

**Jacobs, J.M., Adkins, J.N., Qian, W.J., Liu, T., Shen, Y., Camp, D.G. & Smith, R.D. (2005).** "Utilising human blood plasma for proteomic biomarker discovery". *Journal of Proteome Research* **4**, 1073-1085.

**Katz, A. & Davis, M.E. (2000).** Molecular imprinting of bulk, microporous silica. *Nature* **403**, 286-289.

**Kempe, M. & Mosbach, K. (1995).** Separation of amino acids, peptides and proteins on molecularly imprinted stationary phases. *Journal of Chromatography A* **691**, 317-323.

**Kempe, M., Glad, M. & Mosbach, K. (1995).** An approach towards surface imprinting using the enzyme ribonuclease A. *Journal of Molecular Recognition* **8**, 35-39.

**Kohli, M., Siegel, E., Bhattacharya, S., Khan, M.A., Shah, R. & Suva, L.J. (2006).** Surface-enhanced laser desorption/ionisation time-of-flight mass spectrometry (SELDI-TOF MS) for determining prognosis in advanced stage hormone relapsing prostate cancer. *Cancer Biomarkers* **2**, 249-258.

**Krause, S. (1972).** Polymer compatibility. *Journal Macromolecules* **7**, 251 -314.

**Kreider, B.L. (2001).** Post-translational modifications in proteins. *Annual Reports in Medicinal Chemistry* **36**, 227-235.

**Kumar, A., Biebuyck, H.A., & Whitesides, G.M. (1994).** Patterning SAMs: Applications in Materials Science. *Langmuir* **10**, 1498-1511.

**Lanza, F. & Sellergren, B. (1999).** Method for synthesis and screening of large groups of molecularly imprinted polymers. *Analytical Chemistry* **71**, 2092-2096.

**Lau, A.T.Y., Qing-Yu, H.E. & Chiu, J.F. (2003).** Proteomic technology and its biomedical applications. *Acta Biochimica Biophysica Sinica* **35**, 965-975.

**Leatherbarrow, R.J. & Dean, P.D. (1980).** Studies on the mechanism of binding of serum albumins to immobilised cibacron blue F3GA. *Journal of Biochemistry* **189**, 27-34.

**Liao, J.L., Wang, Y. & Hjerten, S. (1997).** A novel support with artificially created recognition for the selective removal of proteins and for affinity chromatography. *Chromatographia* **42**, 259-262.

**Lin, H.Y., Hsu, C.Y., Thomas, J.L., Wang, S.E., Chen, H.C., Chou, T.C. (2006).** The micro-contact imprinting of proteins: the effect of cross-linking monomers for lysozyme, ribonuclease A and myoglobin. *Biosensors & Bioelectronics* **15**, 534-543.

**Lin, H.Y., Rick, J. & Chou, T.C. (2007).** Optimising the formulation of a myoglobin molecularly imprinted thin-film polymer-formed using

a micro-contact imprinting method. *Biosensors & Bioelectronics* **22**, 3293-3301.

**Linke, T., Doraiswamy, S. & Harrison, E.H. (2006).** Rat plasma proteomics: Effects of abundant protein depletion on proteomic analysis. *Journal of Chromatography. B, Analytical technologies in the biomedical and life sciences* **849**, 273-280.

**Liu, L., Li, F., Fang, Y. & Guo, S. (2006).** Regioselective grafting of poly (ethylene glycol) onto chitosan and the properties of the resulting copolymers. *Macromolecules Bioscience* **6**, 855-861.

**Lopez, M.F. (2000).** Better approaches to finding the needle in a haystack: optimising proteome analysis through automation. *Electrophoresis* **21**, 1082-1093.

**a. Mallik, S., Jhonson, R.D. & Arnold, F.H. (1994).** Synthetic bis-metal ion receptors for bis-imidazole protein analogs. *Journal of The American Chemical Society* **116**, 8902-8911.

**b. Mallik, S., Plunkett, S.D., Dhal, P.K., Johnson, R.D., Pack, D., Shnek, D. & Arnold, F.H. (1994).** Towards materials for the specific recognition and separation of proteins. *New Journal Of Chemistry* **18**, 299-304.

**Martosella, J., Zolotarjova, N., Liu, N., Nicol, G., Barry, E. & Boyes, A. (2005).** Reversed-Phase High-Performance Liquid Chromatographic Prefractionation of Immuno-depleted Human Serum Proteins to Enhance Mass Spectrometry Identification of Lower-Abundant Proteins *Journal of Proteome Research* **4**, 1522-1537.

**Marx, K.A. (2003).** Quartz crystal microbalance: a useful tool for studying thin polymer films and complex bio-molecular systems at the solution-surface interface. *Biomacromolecules* **4**, 1099-1120.

**Mastro, R. & Hall, M. (1999).** Protein de-lipidation and precipitation by tri-n-butylphosphate, acetone, and methanol treatment for isoelectric focusing and two-dimensional gel electrophoresis. *Analytical Biochemistry* **273**, 313-315.

**Mattoso, L.H.C., Manohar, S.K., MacDiamid, A.G. & Epstein, A.J. (1995).** Studies on the chemical synthesis and on the characteristics of polyaniline derivatives. *Journal of Polymer Science. Part A-1, Polymer chemistry* **33**, 1227-1130.

**Mehta, A.I., Ross, S., Lowenthal, M.S., Fusaro, V., Fishman, D.A., Petricoin, E.F. 3<sup>rd</sup> & Liotta, L.A. (2003).** Biomarker amplification by serum carrier protein binding. *Disease Markers* **19**, 1-10.

**Miklos, G.L.G., & Maleszka, R. (2001).** Protein functions and biological contexts. *Proteomics* **1**, 169–178.

**Minoura, N. & Rachkov, A. (2000).** Recognition of oxytocin and oxytocin-related peptides in aqueous media using a molecularly imprinted polymer synthesised by the epitope approach. *Journal of Chromatography A* **889**, 111-118.

**Mirsky, V.M., Hirsch, T., Piletsky, S.A. & Wolfbeis, O.S. (1999).** Spreader-bar approach to molecular architecture: formation of artificial chemo-receptors. *Angewandte Chemie (International ed. in English) Links* **38**, 1108-1110.

**Mosbach, K. (1994).** Molecular Imprinting. *Trends in Biochemical Science* **19**, 9-14.

**Nesterenko, V., Tylley, M. & Upton, S. (1994).** A simple modification of Blum's silver stain method allows for 30 minutes detection of proteins in polyacrylamide gels. *Journal of Biochemical and Biophysical Methods* **28**, 239-242.

**Neuhoff, V., Arold, N., Taube, D. & Ehrhardt, W. (1988).** Improved staining of proteins in polyacrylamide gels including isoelectric

focusing gels with clear background at nanogram sensitivity using Coomassie Brilliant Blue G-250 and R-250. *Electrophoresis* **9**, 255–262.

**Nishino, H., Huang, C.S. & Shea, K. (2006).** Selective protein capture by epitope imprinting. *Angew Chemie Int. Ed. Eng.* **118**, 2452–2456.

**Ogston, A.G. & Sherman, T.F. (1958).** Electrophoretic removal of protein from hyaluronic acid. *Nature* **181**, 482-483.

**O'Farrell, P.H. (1975).** High-resolution two-dimensional electrophoresis of proteins. *Journal of Biochemical and Biophysical Methods* **250**, 4007–4021.

**Ou, S.H., Wu, M.C., Chou, T.C. & Liu, C. (2004).** Polyacrylamide gels with electrostatic functional groups for the molecular imprinting of lysozyme. *Analytica Chimica Acta* **504**, 163-166.

**Pampi, P. & Kofinas, P. (2004).** Biomimetic glucose recognition using molecularly imprinted polymer hydrogels. *Biomaterials* **25**, 1969-1973.

**Pieranski, P., Sittler, L., Sotta, P. & Imperor-Clerc M. (1986).** Growth and shapes of a cubic lyotropic liquid crystal. *The European physical journal. E, Soft matter* **5**, 317-328.

**Piletsky, S.A., Parhometz, Y.P., Panasyuk, T.L. & El'skaya, A.V. (1994).** Sensors for low-weight organic molecules based on molecular imprinting technique. *Sensors and Actuators B* **8**, 629-631.

**Piletsky, S.A., Piletskaya, E.V., Elskaya, A.V., Levi, R., Yano, K. & Karube, I. (1997).** Optical detection system for triazine based on molecularly-imprinted polymers. *Analytical Letters* **30**, 445-455.

**Piletsky, S.A., Piletska, E.V., Chen, B.N., Karim, D., Weston, D., Barrett, G., Lowe, P. & Turner, A.P.F. (2000).** Chemical grafting of molecularly imprinted homopolymers to the surface of microplates. Application of artificial adrenergic receptor in enzyme-linked assay for beta-agonists determination. *Analytical Chemistry* **72**, 4381-4385.

**Piletsky, S.A., Piletska, E.V., Bossi, A., Karim, K., Lowe, P. & Turner, A.P.F. (2001).** Substitution of antibodies and receptors with molecularly imprinted polymers in enzyme-linked and fluorescent assays. *Biosensors & Bioelectronics* **16**, 701-707.



**Rabilloud, T. (1998).** Use of thiourea to increase the solubility of membrane proteins in two-dimensional electrophoresis. *Electrophoresis* **19**, 758-760.

**Rachkov, A. & Minoura, N. (2000).** Recognition of oxytocin and oxytocin-related peptides in aqueous media using a molecularly imprinted polymer synthesised by the epitope approach. *Journal of Chromatography A* **889**, 111-118.

**Rachkov, A. & Minoura, N. (2001).** Towards molecularly imprinted polymers selective to peptides and proteins. The epitope approach. *Biochimica and Biophysica Acta. Protein Structure and Molecular Enzimology* **1544**, 255-266.

**Rachkov, A., Hu, M.J. & Bulgarevich, E. (2004).** Molecularly imprinted polymers prepared in aqueous solution selective for [Sar(1),Ala(8)]angiotensin II. *Analytica Chimica Acta* **504**, 191-197.

**Rick, J. & Chou, T.C. (2005).** Imprinting unique motifs formed from protein-protein associations. *Analytica Chimica Acta* **542**, 26-31.

**Righetti, P.G. & Caravaggio, T. (1976).** Isoelectric points and molecular weights of proteins. *Journal of Chromatography* **127**, 1-28.

**Righetti, P.G. (1983).** Isoelectrofocusing. Theory, methodology and applications. Elsevier. Amsterdam.

**Righetti, P.G., Brost, B.C.W. & Snyder, R. (1981).** On the limiting pore size of hydrophilic gels for electrophoresis and isoelectric focusing. *Journal of Biochemical and Biophysical Methods* **4**, 347-363.

**Righetti, P.G., Wensch, E. & Faupel, M. (1989).** Preparative protein purification in a multi-compartment electrolyser with immobilized membranes. *Journal of Chromatography A* **475**, 293-309.

**Righetti, P.G., Caglio, S., Saracchi, M. & Quadroni, S. (1992).** Laterally aggregated polyacrylamide gels for electrophoresis. *Electrophoresis* **13**, 587-595.

**Righetti, P.G., Bossi, A., Wensch, E. & Orsini, G. (1996).** Protein purification in multicompartiment electrolysers with isoelectric membranes. *Journal of Chromatography B* **699**, 105-115.

**Righetti, P.G., Castagna, A. & Herbert, B. (2001).** Prefractionation techniques in proteome analysis. *Analytical Chemistry* **73**, 320-326.

**Righetti, P.G., Castagna, A., Herbert, B., Reymond, F. & Rossier, J.S. (2003).** Prefractionation techniques in proteome analysis. *Proteomics* **3**, 1397-1407.

**Righetti, P.G., Castagna, A., Antonucci, F., Piubelli, C., Cecconi, D., Campostrini, N., Antonioli, P., Aster, H. & Hamdan, M. (2004).** Critical survey of quantitative proteomics in two-dimensional electrophoretic approaches. *Journal of Chromatography A* **8**, 3-17.

**Righetti, P.G., Castagna, A., Antonioli, P. & Boschetti, E. (2005).** Prefractionation techniques in proteome analysis: The mining tools of the third millennium. *Electrophoresis* **26**, 297-319.

**Righetti, P.G. & Boschetti, E. (2007).** Sherlock Holmes and the proteome - a detective story. *FEBS Journal* **274**, 897-905.

**Rill, R.L., Locke, B.R., Liu, Y., Dharia, J. & Van Winkle, D. (1996).** Protein electrophoresis in polyacrylamide gels with templated pores. *Electrophoresis* **17**, 1304-12.

**Schulze, W.X. & Mann, M. (2004).** A novel proteomic screen for peptide-protein interactions. *Journal of Biological Chemistry* **279**, 10756-10764.

**Sergeyeva, T.A., Brovko, O.O., Piletskam E.V., Piletsky, S.A., Goncharova, L.A., Karabanova, L.V., Sergeyeva, L.M. & El'skaya, A.V. (2006).** Porous molecularly imprinted polymer membranes and polymeric particles. *Analitica Chimica Acta* **582**, 311-319.

**Shaaya, E. (1976).** Polymerisation kinetics of polyacrylamide gels I. Effect of different cross-linkers. *Analytical Biochemistry* **75**, 325-328.

**Sheffield, L.G. & Gavinski, J.J. (2003).** Proteomics methods for probing molecular mechanisms in signal transduction. *Journal of Animal Science* **3**, 48-57.

**Shevchenko, A., Wilm, M., Vorm, O. & Mann M. (1996).** Mass spectrometric sequencing of proteins silver-stained polyacrylamide gels. *Analytical Biochemistry* **68**, 850-858.

**Shi, H.Q., Tsa, W.B.I., Garrison, M.D., Ferrari, S. & Ratner, B.D. (1999).** Template imprinted nano-structured surface for protein recognition. *Nature* **398**, 593-597.

**Shiomi, T., Matsui, M., Mizukami, F. & Sakaguchi, K. (2005).** A method for the molecular imprinting of haemoglobin on silica surfaces using silanes. *Biomaterials* **27**, 5564-5571.

**Slinchenko, O., Rachkov, A., Miyachi, H., Ogiso, M., Minoura, N. (2004).** Imprinted polymer layer for recognising double-stranded DNA. *Biosensors & Bioelectronics* **20**, 1091-1097.

**Smith, F.M., Gallagher, W.M., Fox, E., Stephens, R.B., Rexhepaj, E., Petricoin, E.F. 3rd, Liotta, L., Kennedy, M.J. & Reynolds, J.V. (2007).** Combination of SELDI-TOF-MS and data mining provides early-stage response prediction for rectal tumours undergoing multi-modal neo-adjuvant therapy. *Annals of Surgery*. **245**, 259-266.

**Southan, C. (2004).** Has the yo-yo stopped? An assessment of human protein-coding gene number. *Proteomics* **4**, 1712-1726.

**Spvbek, J. & Schneider, R. (1987).** Aggregation of stereoregular poly(methyl methacrylates). *Advances in Colloid and Interface Science* **27**, 81-150.

**Steinberg, T.H., Chernokalskaya, E., Berggren, K., Lopez, M.F., Diwu, Z., Haugland, R.P. & Patton, W.F. (2000).** Ultra-sensitive fluorescence protein detection in isoelectric focusing gels using a ruthenium metal chelate stain. *Electrophoresis* **21**, 486-496.

**Steel, L.F, Trotter, M.G., Nakajima, P.B., Mattu, T.S., Gonye, G. & Block, T. (2003).** Efficient and specific removal of albumin from human serum samples. *Molecular & Cellular Proteomics* **2**, 262-270.

**Sugio, S., Kashima, A., Mochizuki, A., Noda, M., Kobayashi, K. (1999).** Crystal structure of human serum albumin at 2.5Å resolution. *Protein Engineering* **12**, 439-446.

**Sylvester, A. (2004).** The development of a novel native prothrombin assay for the more efficient management of oral anticoagulation therapy. *Ph.D. thesis*. Cranfield.

**Takatsy, A., Kilar, A., Kilar, F. & Hjerten, S. (2006).** Universal method for synthesis of artificial gel antibodies by the imprinting approach combined with a unique electrophoresis technique for detection of minute structural differences of proteins, viruses, and cells (bacteria): Ia. gel antibodies against proteins (transferrins). *Journal of Separation Science* **29**, 2802-2809.

**Tam, S. (2006).** Electrophoretic prefractionation: new commercial tools from an old concept. *Expert Review in Proteomics* **3**, 379-381.

**Thorsell, A., Portelius, E., Blennow, K. & Westman-Brinkmalm, A. (2007).** Evaluation of sample fractionation using micro-scale liquid-

phase isoelectric focusing on mass spectrometric identification and quantitation of proteins in a SILAC experiment. *Rapid Communications in Mass Spectrometry: RCM*. **21**, 771-778.

**Travis, J. & Pannell, R. (1973)**. Selective removal of albumin from plasma by affinity chromatography. *Clinical Chimica Acta* **49**, 49-52.

**Turck, N., Richert, S., Gendry, P., Stutzmann, J., Kedinger, M., Leize, E., Simon-Assmann, P., Van Dorsselaer, A. & Launay, J.F. (2004)**. Proteomic analysis of nuclear proteins from proliferative and differentiated human colonic intestinal epithelial cells. *Proteomics* **4**, 93-105.

**Turner, N.W., Piletska, E.V., Karim, K., Whitcombe, M., Malecha, M., Magan, N., Baggiani, C. & Piletsky, S.A. (2004)**. Effect of the solvent on recognition properties of molecularly imprinted polymer specific for ochratoxin A. *Biosensors & Bioelectronics* **20**, 1060-1067.

**Turner, N.W., Liu, X., Piletsky, S., Hlady, V. & Britt, D. (2007)**. Recognition of conformational changes in  $\alpha$ -lactoglobulin by molecularly imprinted thin films. *Biomacromolecules* **8**, 2781-2787.

**Ulbrich, M. (2004).** Membrane separations using molecularly imprinted polymers. *Journal of Chromatography B* **803**, 113-125.

**Umpleby, R.J., Baxter, S.C., Chen, Y., Shah, R.N. & Shimizu, K.D. (2001).** Characterisation of molecularly imprinted polymers with the Langmuir-Freundlich isotherm. *Analytical Chemistry* **73**, 4584-4591.

**van Reis, R. & Zydney, A. (2001).** Membrane separation in biotechnology. *Current opinion in biotechnology* **12**, 208-211.

**a. Venton, D.L. & Gudipati, E. (1995).** Entrapment of enzymes using organo-functionalised polysiloxane copolymers. *Biochimica et Biophysica Acta* **1250**, 117-125.

**b. Venton, D.L. & Gudipati, E. (1995).** Influence of protein on polysiloxane polymer formation: Evidence for induction of complementary protein-polymer interactions. *Biochimica et biophysica acta. Protein Structure And Molecular Enzymology* **1250**, 126-136.

**Vetri, L., Librizzi, F., Leone, M. & Militello, V. (2007).** Thermal aggregation of bovine serum albumin at different pH: comparison with human serum albumin. *European Biophysics Journal* **36**, 717-725.



**Vlatakis, G., Andersson, L.I., Muller, R. & Mosbach, K. (1993).** Drug assay using antibody mimics made by molecular imprinting. *Nature* **361**, 645-647.

**Yuan, X. & Desiderio, D.M. (2003).** Proteomics analysis of phosphotyrosyl-proteins in human lumbar cerebrospinal fluid. *Journal of Proteome Research* **2**, 476-487.

**Wall, D.B., Kachman, M.T., Gong, S., Hinderer, R., Parus, S., Misek, D.E., Hanash, S.M. & Lubman, D.M. (2000).** Isoelectric focusing nonporous RP HPLC: a two-dimensional liquid-phase separation method for mapping of cellular proteins with identification using MALDI-TOF mass spectrometry *Analytica Chemistry* **72**, 1099-1111.

**Wang, H., Kachman, M.T., Schwartz, D.R., Cho, K.R. & Lubman, D.M. (2002).** A protein molecular weight map of ES2 clear cell ovarian carcinoma cells using a two-dimensional liquid separations/mass mapping technique. *Electrophoresis* **23**, 3168-3181.

**Watts, A.D., Hunt, N.H., Hambly, B.D. & Chaudhri, G. (1997).** Separation of tumor necrosis factor alpha isoforms by two-dimensional polyacrylamide gel electrophoresis. *Electrophoresis* **18**, 1086-1091.

**Wilkins, M. (1995).** Government backs proteome proposal. *Nature* **22**, 378-653.

**Wittmann-Liebold, B., Graack, H.R. & Pohl, T. (2006).** Two-dimensional gel electrophoresis as tool for proteomics studies in combination with protein identification by mass spectrometry. *Proteomics* **6**, 4688-4703.

**Wu, J., Shakey, Q., Liu, W., Schuller, A. & Follettie, M.T. (2007).** Global profiling of phosphopeptides by titania affinity enrichment. *Journal of Proteome Research* **12** [Epub ahead print].

**Wulff, G. (1995).** Molecular imprinting in cross-linked materials with the aid of molecular templates - a way toward artificial antibody. *Angewandte Chemie (International ed. in English)* **34**, 1812-1832.

**Yilmaz, E., Haupt, K. & Mosbach, K. (2000).** The use of immobilised templates. A new approach in Molecular Imprinting. *Angewandte Chemie (International ed. in English)* **39**, 2115-2118.

**Zhang, H., Ye, L. & Mosbach K. (2006).** Non-covalent molecular imprinting with emphasis on its application in separation and drug development. *Journal of Molecular Recognition* **19**, 248-259.

**Zhu, K., Yan, F., O'Neil, K.A., Hamler, R., Lin, L., Barder, T.J., Lubman, D.M. (2003).** Proteomics using 2D liquid separations of intact proteins from whole cell lysates. *Current Protocol in Protein Science* **23**, 2-28.



# Surface imprinted beads for the recognition of human serum albumin

Francesca Bonini<sup>a</sup>, Sergey Piletsky<sup>b</sup>, Anthony P.F. Turner<sup>b</sup>,  
Adolfo Speghini<sup>a</sup>, Alessandra Bossi<sup>a,\*</sup>

<sup>a</sup> *Department of Science and Technology, University of Verona, Strada le Grazie 15, 37134 Verona, Italy*

<sup>b</sup> *Cranfield Health, Cranfield University, Silsoe, Bedfordshire MK45 4DT, UK*

Received 3 May 2006; received in revised form 21 December 2006; accepted 21 December 2006

Available online 17 January 2007

## Abstract

The synthesis of poly-aminophenylboronic acid (ABPA) imprinted beads for the recognition of the protein human serum albumin (HSA) is reported. In order to create homogeneous recognition sites, covalent immobilisation of the template HSA was exploited. The resulting imprinted beads were selective for HSA. The indirect imprinting factor (IF) calculated from supernatant was 1.6 and the direct IF, evaluated from the protein recovered from the beads, was 1.9. The binding capacity was 1.4 mg/g, which is comparable to commercially available affinity materials. The specificity of the HSA recognition was evaluated with competitive experiments, indicating a molar ratio 4.5/1 of competitor was necessary to displace half of the bound HSA. The recognition and binding of the imprinted beads was also tested with a complex sample, human serum and targeted removal of HSA without a loss of the other protein components was demonstrated. The easy preparation protocol of derivatised beads and a good protein recognition properties make the approach an attractive solution to analytical and bio-analytical problems in the field of biotechnology. © 2007 Elsevier B.V. All rights reserved.

**Keywords:** Molecularly imprinted polymers; Human serum albumin; 3-Aminophenylboronic acid; Serum depletion; Proteome

## 1. Introduction

Molecularly imprinted polymers (MIPs) are polymers prepared in presence of a template that serves as a mould for the formation of template-complementary binding sites (Mosbach, 1994; Sellergren, 2001a,b). Thus, MIPs can be created to recognise a large variety of target molecules often with affinity and selectivity comparable to those exhibited by poly- or monoclonal antibodies. MIPs are less expensive and quicker to prepare than biological receptors. Additionally, they are capable of withstanding much harsher conditions than antibodies, such as high temperature, pressure, extreme pH, and organic solvents. These properties have made them extremely attractive for solving problems in the fields of preparative chemical separations (Sellergren, 2001a,b), solid phase extraction (Lanza and Sellergren, 2001; Andersson and Schweitz, 2003) and sensing (Chianella et al., 2003; Haupt and Mosbach, 2000), or for the removal of specific molecular targets from food (Whitcombe et al., 1997; Ramstrom et al., 2001).

MIPs have been prepared using polypeptides (Kempe et al., 1995; Andersson et al., 1995; Minoura and Rachkov, 2000), bacteria (Dickert and Hayden, 2002), low molecular mass compounds (Katz and Davis, 2000; Chianella et al., 2003) and proteins (Burow and Minoura, 1996; Bossi et al., 2001; Guo et al., 2004) as templates. In the case of proteins, however, only modest success has been obtained due to the specific properties of these templates. First, all proteins are water-soluble compounds that are not always compatible with mainstream MIP technologies, which relies on the use of organic solvents for the polymer preparation. Second, proteins have a large amount of functional groups available for the interaction with functional monomers. Third, proteins have a flexible structure and conformation, which can be easily affected by changes in temperature or the nature of the solvent. Thus, from a thermodynamic and practical standpoint, it is difficult to develop successful imprints for such molecules.

In the last 10 years, some new approaches have been proposed, which use both covalent and non-covalent methods (Wulff, 1993; Mosbach and Ramstrom, 1996). The immobilisation of the protein template on a supporting surface (Shi et al., 1999; Yilmaz et al., 2000; Shiomi et al., 2005) provides a number of advantages, i.e. it allows the imprinting of templates

\* Corresponding author. Fax: +39 045 8027929.

E-mail address: [alessandra.bossi@univr.it](mailto:alessandra.bossi@univr.it) (A. Bossi).

independently of their solubility in the polymerisation mix, it minimises protein aggregation and it creates more homogeneous binding sites.

In the present contribution, we report the preparation of imprinted beads for the recognition of human serum albumin (HSA). The protein template is immobilised at the surface of the beads, with an approach modified from [Shiomi et al. \(2005\)](#) in which covalent immobilisation was achieved by derivatising silica beads with aldehyde groups, these were then exploited to form imine bonds with the amino groups of lysine in the HSA. The polymer was made of 3-aminophenyl boronic acid (APBA) ([Piletsky et al., 2001](#); [Bossi et al., 2001](#); [Pribyl and Skladal, 2006](#)) using a polymerisation process described earlier by our group ([Bossi et al., 2001](#)). The beads thus obtained were characterised in order to evaluate the percentage of polymer derivatised, the binding capacity for HSA, the binding kinetics, the specificity of the HSA binding and the recovery of bound protein.

Finally, the imprinted beads were applied to a real biological fluid, human serum, in which HSA is the most abundant protein (ca. 60% of the total proteins) ([Andersson and Anderson, 2002](#); [Tirumalai et al., 2003](#)). The high quantity of HSA in serum is considered as a drawback, since it seriously hampers the detection of low abundant proteins, which are often marker of diseases. It has been demonstrated that if serum is selectively depleted of albumin, it would facilitate the analysis of such low-abundant proteins. Albumin removal has been achieved through adsorption to immobilized dyes ([Ahmed et al., 2003](#)), immuno-affinity extraction ([Wang et al., 2003](#)) or affinity capture by immobilized phage-derived peptides ([Sato et al., 2002](#)), but to date there have been no reports concerning the use of molecularly imprinted polymers. In the present case, we attempt the use of a synthetic receptor, the imprinted beads, for the specific removal of HSA from serum.

## 2. Materials and methods

### 2.1. Materials and reagents

Acetic acid, aminopropyl silica (particle size 15–40  $\mu\text{m}$ , mean pore size 60  $\text{\AA}$ ), 3-amino propyl trimethoxysilane (APTMS), ammonium persulfate (APS), Bradford assay, [(3-cholamidopropyl)dimethylammonio]-1-propanesulfonate (CHAPS), ethanol, glycine, glutaraldehyde, human serum albumin (HSA) (Mr 66 kDa), methilic acid, 2N-morpholine ethane sulfonic acid (MES), oxalic acid, propyl triethoxy silane, sodium chloride (NaCl), SDS, Sypro Ruby, thiourea, trizma, urea, were obtained from Sigma–Aldrich Chemie GmbH (Steinheim, Germany). Acrylamide, *N,N*-methylenebisacrylamide, *N,N,N,N*-tetramethyl-ethylenediamine (TEMED), dithiothreitol (DTT), linear Immobiline dry strips pH gradient 3–10 (7 cm) were obtained from Bio-Rad (Hercules, CA, USA).

### 2.2. Preparation of human serum albumin (HSA)-imprinted silica using immobilized templates

Silica beads (1 g) were derivatised with 10% (w/v) APTMS in methanol in order to introduce  $\text{NH}_2$  functional groups. The

beads were washed three times with ethanol and three times with deionised water and then dried at 50 °C for 24 h. They were then incubated with 10 mM 2N-morpholine ethane sulfonic acid (MES) buffer, pH 5.5 containing 1% glutaraldehyde for 12 h at room temperature, in order to introduce aldehyde groups. The product was washed repeatedly with deionised water. Finally, 1 ml of a 10 mM 3N-morpholino propane sulfonic acid (MOPS) solution (pH 7.0) containing 2.0 mg/ml human serum albumin (HSA) and 0.1 M NaCl was admixed as the template for 3 h at 4 °C, in order to covalently bind the protein on the aldehyde groups. The beads were then incubated with 1 M Tris for 30 min in order to block the un-reacted aldehyde groups. Washes with deionised water followed and finally 1 ml of 50 mM ABPA water solution was added to the beads. After 45 min incubation, 1 ml of 25 mM ammonium persulfate (APS) water solution was added in order to start the polymerisation reaction. The polymerisation was carried out at room temperature for 1 h, after which the beads were washed again with deionised water for five times. Finally, 1 ml of 1 M oxalic acid was added in order to remove the template. This step was carried out at room temperature for 12 h. The derivatisation protocol was checked at each step by FT-IR spectroscopy with a Magna FT-IR 760 Spectrophotometer (Nicolet, Offenbach Germany), samples were prepared mixing 10 mg of beads with 200 mg KBr, sample reading was 32 $\times$ . The beads were finally conditioned with 10 mM phosphate buffer, pH 8.0, in order to increase the pH and remove the free HSA in solution produced by the treatment with 1 M oxalic acid.

### 2.3. Evaluation of the percentage of derivatisation

In order to evaluate the percentage of silica beads derivatised, 0.500 g of beads were derivatised (with APTMS, glutaraldehyde, APBA, as previously described). After each step, the beads were dried overnight at 87 °C and they were weighed. The degree of derivatisation was calculated as follows:

$$\text{DG (\%)} = \frac{(\text{mg of "polymer" bound})}{(\text{g beads})} \times 100.$$

### 2.4. Calculation of the binding capacity

In order to evaluate the binding capacity, 0.500 g of beads were conditioned with 10 mM phosphate buffer, pH 8.0 and incubated with 300  $\mu\text{l}$  of HSA solution at different concentrations (0.036, 0.058, 0.073, 0.18, 0.3, 1.0, 2.6, 2.74 and 4.08  $\mu\text{g}/\mu\text{l}$ ) for different times (3, 5, 20, 60 min). The beads were centrifuged at 4000  $\times g$  for 3 min at room temperature, then the supernatant was transferred in new tubes and it was quantified by Bradford assay at 595 nm. The protein bound was expressed as the difference between the total micrograms of HSA loaded and micrograms of HSA in solution after the binding.

### 2.5. Binding kinetics

In order to evaluate the binding kinetics, a 0.500 g of control or MIP beads, conditioned with 10 mM phosphate buffer pH 8.0, were incubated with 300  $\mu\text{l}$  of HSA solution at different

concentrations (0.036, 0.058, 0.073, 0.18, 0.3, 1.0, 2.6, 2.74 and 4.08  $\mu\text{g}/\mu\text{l}$ ) for different times (3, 5, 20, 60 min). The quantity of bound protein was evaluated as described in the previous paragraph.

### 2.6. Protocol for HSA elution from the beads

In order to evaluate the quantity of protein bound from beads, a 15 mg of control or MIP beads, conditioned with 10 mM phosphate buffer pH 8.0, were incubated with 300  $\mu\text{l}$  of 0.1  $\mu\text{g}/\mu\text{l}$  HSA solution for 5 min. The beads were washed once with 10 mM phosphate buffer pH 8.0. The supernatant was discarded and the beads were incubated with a solution of 7% acetic acid and 0.1% Tween-20. After 10 min the beads were centrifuged and the supernatant was recovered. The proteins were precipitated with 8 volumes of cold acetone and analysed through SDS-PAGE.

### 2.7. Binding experiment with human serum

In order to evaluate the binding of HSA from a real complex sample, 0.300 g of MIP beads, conditioned with 10 mM phosphate buffer pH 8.0, were incubated with 300  $\mu\text{l}$  of 0.1  $\mu\text{g}/\mu\text{l}$  human serum solution for 5 min. The beads were washed as previously described. The supernatant was recovered and the proteins were precipitated and analysed through 2D PAGE.

### 2.8. SDS-PAGE and 2D PAGE

Electrophoresis of proteins was performed using regular SDS PAGE with 12% polyacrylamide gel, with a Tris-glycine cathode buffer (192 mM glycine, 0.1% SDS and 40 mM Tris to pH 8.3). The run was performed by applying 15 mA/gel for 20 min followed by 25 mA/gel until the dye front reached the bottom of the gel.

For 2D-maps, the desired volume of each sample was subjected to protein precipitation in a cold mixture of acetone and methanol (v/v ratio 8:1) for 2 h at  $-20^\circ\text{C}$ , in order to remove lipids and salts and to regulate the concentration of protein; the solution was then centrifuged at  $10,000 \times g$  for 20 min. The pellet was solubilised in the 2D sample buffer (7 M urea, 2 M thiourea, 3% 3-[(3-cholamidopropyl)dimethylammonio]-1-propanesulfonate, 40 mM TRIS, 5 mM tributylphosphine and 10 mM acrylamide) and allowed to be alkylated at room temperature for 90 min. Dithiothreitol (10 mM) was used to block the alkylation reaction, and then trace amounts of 0.5% ampholine and bromophenol blue were added to the solution. An aliquot (150 ml) of protein solution was subsequently used for rehydrating 7 cm long non-linear immobilized pH gradient (IPG) strips (Bio-Rad), pH 3 to 10, for 4 h. Isoelectric focusing (IEF) was performed with a Protean IEF Cell (Bio-Rad) at low initial voltage, followed by a voltage gradient up to 5000 V; the total product time voltage applied was 25,000 V h for each strip. For the second dimension, the IPGs strips were equilibrated for 26 min in a solution containing 6 mM urea, 2% SDS, 20% glycerol, and 375 mM Tris-HCl, pH 8.8, under gentle shaking. The IPG strips were then laid on an 8–18% T-gradient SDS-gel slab

and cemented *in situ* with 0.5% agarose in the cathode buffer (192 mM glycine, 0.1% SDS, and Tris to pH 8.3). The electrophoretic run was performed by setting a current of 5 mA/gel for 1 h, followed by 10 mA/gel for 1 h and 20 mA/gel until run completion.

Finally, for SDS-PAGE and 2D-maps, gels were incubated in a fixing solution containing 40% ethanol and 10% acetic acid for 1 h, followed by overnight staining in a ready-to-use Sypro Ruby solution. Destaining was performed in 10% methanol and 7% acetic acid, followed by a rinse of at least 3 h in pure water. The gels were scanned with a Versa Doc Imaging System (Bio-Rad, Hercules, CA) and analysed with the software PDQuest Version 7.1 (Bio-Rad, Hercules, CA). A match set was created from the protein patterns of three replicate gels for each independent sample. A standard gel was generated out of the image with the highest spot number. Spot quantities of all gels were normalized to remove non expression-related variations in spot intensity. The results were evaluated in terms of spot OD (optical density).

## 3. Results and discussion

### 3.1. Derivatisation of the imprinted beads

Aminophenylboronate based molecularly imprinted polymers were prepared as described in Section 2. The approach includes first exploiting silica beads as supports for the template (HSA) immobilisation, followed by the polymerisation of the homopolymeric material onto the derivatised beads and finally the cleavage of the protein-silica covalent bonds, resulting in leaving the imprinted cavities freely accessible for binding.

The silica beads were derivatised with 10% APTMS in order to introduce  $\text{NH}_2$  groups. Next, a treatment with 1% glutaraldehyde was performed to introduce aldehydic groups. The immobilisation of the protein on the surface of the silica beads happens through a covalent bond between  $\epsilon$  amino groups of lysines of the template and aldehyde groups on the silica beads.

APBA was used as functional monomer. The polymerisation procedure, is straightforward: a 1:1 (v/v) ratio of the ammonium persulfate (50 mM) and APBA (100 mM) solution in water were allowed to react together in the presence of the protein-derivatised beads for 1 h, gently stirred at room temperature (Bossi et al., 2001, 2004). Studies on the polymerisation of monomers of the same family of ABPA (e.g. aniline) showed that the polymer in solution forms relatively short chains (Mattoso et al., 1995), flocculating in aggregates, while on the supporting surface, it deposits in a reasonably thin and ordered film (MacQuade et al., 2000).

After APBA polymerisation, it was necessary remove the HSA immobilised at the surface of the beads to get free binding cavities. Strong acids have to be used in order to break the silica-protein covalent bonds. Thus, incubation in 1 M oxalic acid for 12 h was adopted as removing procedure (Shiomi et al., 2005).

### 3.2. Evaluation of the derivatisation

The quality of the derivatisation process was checked by FT-IR measurements, highlighting modifications in the vibra-



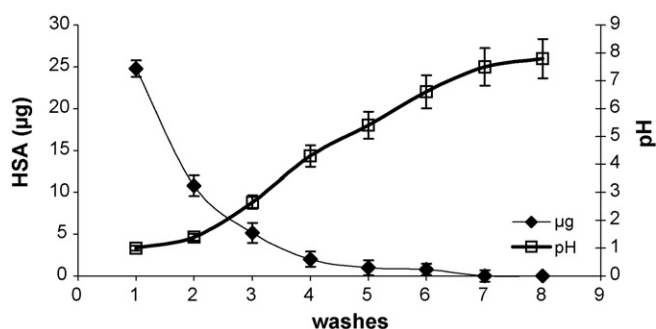


Fig. 1. Influence of the washing protocol on the pH of the beads and on the removal of template.

tional spectrum after each derivatisation step. In particular, the protein covalent immobilisation resulted the detection of signals typical of peptide bonds ( $1650\text{ cm}^{-1}$ ) and carboxy groups ( $1300\text{--}1400\text{ cm}^{-1}$ ). The further polymerisation of APBA was confirmed by the vibration of phenylboronic groups (region  $1100\text{--}1200\text{ cm}^{-1}$ ; a shoulder at  $1250\text{ cm}^{-1}$ ; boronate contribution around  $3200\text{--}3400\text{ cm}^{-1}$ ).

### 3.3. Assessment of a suitable protocol for template removal

Next, washing steps were performed to remove the protein released from the beads and to condition the beads in a buffer suitable for the binding experiments. In order to remove HSA and to increase the pH from 1.2 to 8.0, six washes with 10 mM phosphate buffer were performed. After each washing step, the pH of the solution was measured and the proteins removed were recovered by acetone precipitation and analysed by SDS-PAGE, followed by quantification of the HSA released through densitometry analysis. The data were then plotted as a function of the number of the washing steps, as shown in Fig. 1. No free template was detected in solution after seven washing steps. Moreover, after seven washes, the pH of the solution had risen to 8.0, which was the pH chosen for the binding experiments.

It is probable that a small part of the HSA previously bound to the beads remained embedded in the polymer matrix. The contribution of such remaining template might be negative, occupying the binding sites of the polymer and thus affecting its rebinding properties. Nevertheless there are many documents reporting a positive effect of the non-complete removal of the embedded template. As reported by Hjertén and co-workers, the residual template can improve the mechanical stability of the polymer architecture, conferring rigidity to the binding sites (Hjertén et al., 1997).

### 3.4. Derivatisation extent and reproducibility of the polymer deposition

The quantity of the polymer deposited on the beads was evaluated too on eight preparation. Starting from a known quantity of beads, the weight of the batch of beads was monitored after the derivatisation step, after drying. The quantity of ABPA deposited around the silica beads was  $15.2 \pm 0.5\text{ mg}$  of polymer per gram of beads. It is probable that the treatment with oxalic acid, used

to remove the covalently bound HSA, removes a few superficial layers of APBA MIP-polymer too. A qualitative evaluation of the persistence of the dark brown colour of the APBA-beads suggests that, in any case, part of the ABPA layers are resistant to the strong acidic treatment.

### 3.5. Binding experiments

Binding experiments were performed in order to evaluate the binding capacity for HSA of both control and imprinted APBA beads. Control and MIP beads (0.500 g), conditioned with 10 mM phosphate buffer pH 8.0, were incubated with increasing quantities of HSA. The quantity of bound protein was evaluated by difference, measuring the residual free protein in the supernatant. The micrograms bound were plotted as a function of the quantity of HSA used, as shown in Fig. 2. No difference in the amount of bound protein was observed between control and MIP beads when the quantity of protein used was below  $780\text{ }\mu\text{g}$ , while a difference was observed when the quantity of protein used was above  $780\text{ }\mu\text{g}$  (Fig. 2). The difference between MIP and control beads correlated with the quantity of available binding sites. When the protein quantity was not enough to saturate the unspecific binding, there was no difference between control and MIP beads, but when HSA was saturating ( $>780\text{ }\mu\text{g}$ ), the presence of specific binding cavities on the MIP became evident. The indirect binding capacities, calculated from the quantity of HSA left unbound in the supernatant, was  $1.4\text{ mg/g}$  for MIP beads and  $0.9\text{ mg/g}$  for control. These values are in accordance to binding capacities reported for commercial affinity materials.

Kinetic experiments were performed to evaluate the optimum binding time within the range 0.5–60 min. The binding kinetic was evaluated for concentrations of HSA ranging from  $0.073$  to  $4.1\text{ }\mu\text{g}/\mu\text{l}$ . As shown in Fig. 3, the best incubation time was 5 min, irrespective of the HSA concentration used. This result is confirmed by the profile of the time course of the imprinting factor (IF,  $\mu\text{g}$  bound by MIP/ $\mu\text{g}$  bound by ctrl) plotted in Fig. 4, showing a maximum IF of  $1.6 \pm 0.08$  for high HSA concentration at 5 min and a maximum IF of  $1.2 \pm 0.05$  for low, non-saturating, concentrations. The binding profile (Figs. 3(b) and 4) for non saturating HSA concentrations indicates that for short incubation times ( $<5\text{ min}$ ) the HSA molecules approach the surface and sticks randomly to it (IF is only slightly in favour of

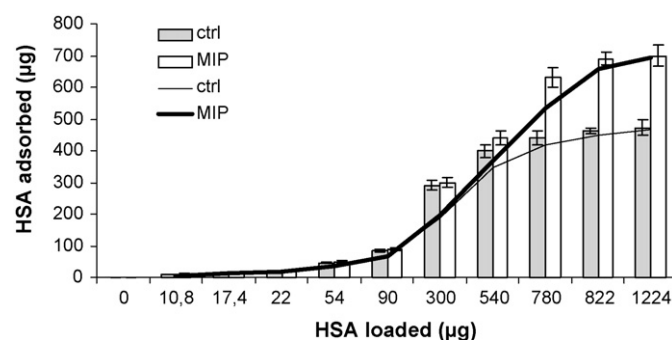


Fig. 2. Evaluation of the binding capacity for control (open) and MIP beads (solid). The amount in micrograms bound from beads is plotted as function of amount in micrograms used for binding.



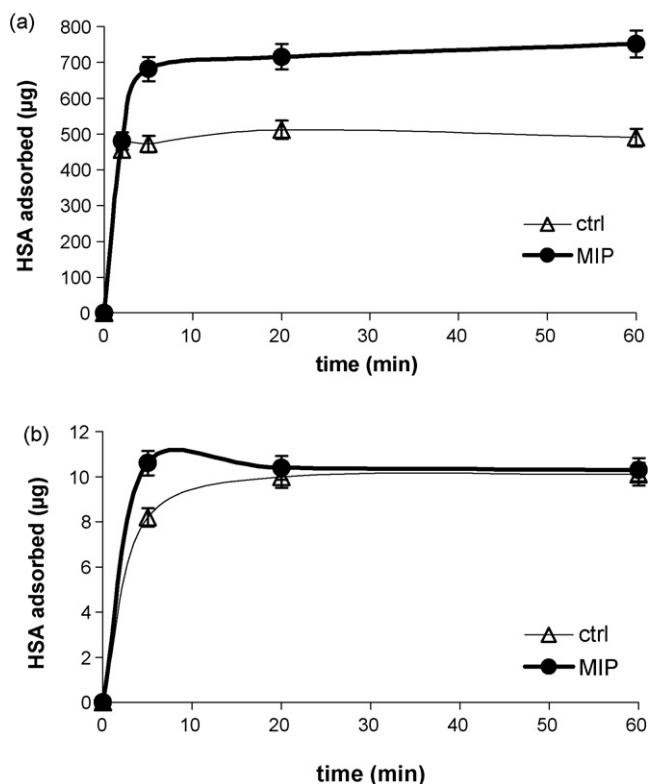


Fig. 3. Binding kinetics. The amount in micrograms of HSA bound are plotted as function of the time, under saturated conditions (a) and non-saturated conditions (b).

MIPs). When the incubation time rises to 5 min, the binding to specific cavities is appreciable and maximised (IF reaches its maximum). Since the total quantity of protein bound did not change significantly with respect to 3 min incubation, this suggests a thermodynamically driven rearrangement of the bound proteins took place and proteins on the MIP moved to the specific cavities. The course of the binding kinetic might be explained by several different interaction being established during the binding of the protein to the surface, thus weak forces, hydrogen bonding and hydrophobic interactions have to take place (Thulasiraman

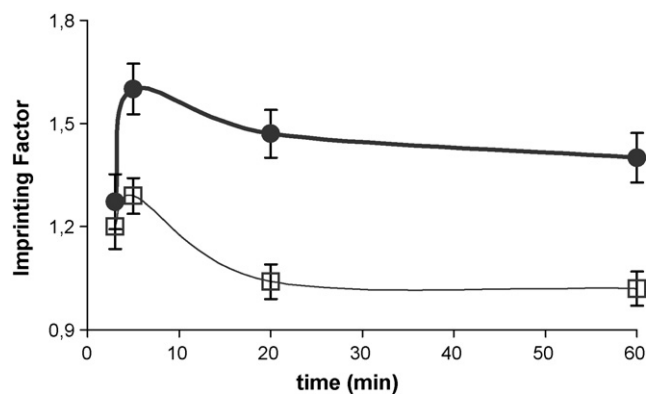


Fig. 4. The IF calculated as micrograms of HSA bound by MIP/micrograms of HSA bound by the control is plotted as function of the time, both for saturated conditions and non-saturated conditions.

et al., 2005). The nature of APBA polymer is both hydrophobic and hydrophilic, allowing to establish multiple interactions with the protein. The protein binding mechanism to MIP p-APBA beads is supposed to include spatial recognition between the protein and the imprinted cavities and several binding contributions that derives from the interaction of several aminoacid lateral chains (i.e. hydroxyl of serine, threonine, tyrosine) with boronate groups (Bossi et al., 2001). Plus, hydrophobic interactions occur between the aromatic structure of the polymer and both the aromatic side chains and the backbone of the protein (Bossi et al., 2004).

Longer incubation times (20–60 min) did result in a loss of specific binding, most likely due to a co-aggregation of proteins from the solution to the bound proteins, as reported for other protein-MIPs (Turner et al., 2006).

### 3.6. Recovery of bound protein

The recovery of the bound protein onto the beads was evaluated. A protocol for protein elution was optimised. In particular, after binding, five different conditions for elution of HSA from beads were tried in order to select the most effective washing procedure. The first protocol was 7 M urea, 2.2 M thiourea, 3% CHAPS, 40 mM Tris, pH 8.0 (TUC buffer), that is, a strongly denaturant buffer. It is usually applied to treat sample before 2D-gel electrophoresis (Righetti et al., 2004). The second one was TUC buffer, followed by 9 M urea and 5% acetic acid, pH 3.0, which is usually applied for protein elution from affinity capture beads, as described by Fortis et al. (2005a,b). The third was 7% Acetic Acid, 0.1% Tween-20. This solution was reported for washing APBA-MIPs polymers by Bossi et al. (2001). The fourth protocol was an acidic buffer supplemented with salt to increase the ionic strength: 0.1 M glycine, pH 3.0, 0.5 M NaCl and finally the last washing procedure was a high ionic strength solution of 1 M NaCl. The quantity of HSA eluted was evaluated by SDS-PAGE. As reported in Table 1, no protein release was observed for alkaline washing, while washing with acid or high ionic strength allowed the HSA to be recovered. However, among all the protocols applied only the third gave good results, similar to those achieved with the Bradford assay. The other protocols recovered a small quantity of protein, thus in all the following experiments, washing with 7% acetic acid 0.1% Tween-20 was adopted for elution of the protein from beads.

From these results, it was possible to calculate the direct binding capacity for MIP and control (calculated from the quantity of HSA recovered from the beads), which was 0.696 mg/g on

Table 1  
Recovery of HSA from MIP and control beads

Solution used for elution	Control beads ( $\mu\text{g}$ )	MIP beads ( $\mu\text{g}$ )
TUC buffer pH 8.8	$0.3 \pm 0.25$	$0.23 \pm 0.20$
TUC buffer + 9 M urea, pH 3.0	$5.5 \pm 0.52$	$6.0 \pm 0.40$
7% acetic acid + 0.1% Tween-20	$5.8 \pm 1.20$	$9.2 \pm 1.50$
0.1 M glycine + 0.5 M NaCl, pH 3.0	$0.4 \pm 0.12$	$0.24 \pm 0.15$
1 M NaCl	$0.57 \pm 0.15$	$0.85 \pm 0.16$

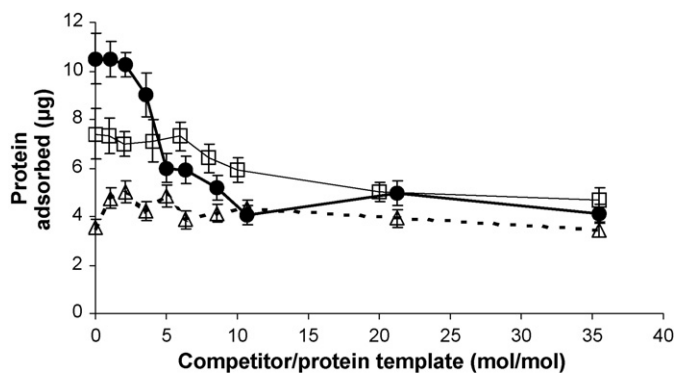


Fig. 5. Competitive experiments. Open triangles indicate the HSA adsorbed onto control beads upon addition of increasing amount of the competitor protein carbonic anhydrase (CA). Filled circles indicate the amount of HSA adsorbed onto MIP-HSA beads when challenged with CA competitor. Open squares indicate the amount of CA adsorbed onto MIP-CA beads when challenged with HSA competitor.

MIP beads and 0.363 mg/g on the control. The advantage of a direct calculation of binding capacity is the elimination of part of the unspecific contributions. The consequence is fairly low values of binding capacities with respect to those calculated indirectly, whereas a significant increase in the IF 1.91 was observed, thus indicating the binding cavities on the imprinted beads are specific for HSA recognition.

### 3.7. Competitive experiments to evaluate specific binding

In order to evaluate the specificity of binding, a competitive experiment was performed (Fig. 5). The beads were assayed for the rebinding with a mixture made of a fixed concentration of the template and an increasing concentration of a competing protein. The quantity of the protein bound to the beads was evaluated after elution by SDS-PAGE. The competitor first chosen was carbonic anhydrase (CA), which has approximately the same isoelectric point as HSA but a smaller molecular mass (31 kDa) (Righetti and Caravaggio, 1976). The shape effect on the binding was evaluated. In control beads, the HSA binding (Fig. 5, open squares) did not change significantly by the presence of CA, the HSA bound ( $3.5 \pm 0.5 \mu\text{g}$ ) was considered as non-specific adsorption. In the MIP, the HSA bound was  $10.3 \mu\text{g}$  (Fig. 5, solid circles); the displacement of HSA from the CA competitor was appreciable only upon an addition of CA of 4.5/1 mol/mol respect to HSA. In the case half of the HSA was displaced. When CA/HSA ratio was above 8/1 mol/mol a complete displacement of the bound HSA was observed. These results indicate that the HSA binding is displaced only for relative high concentrations of competitor.

In a second set of experiments CA was used as template and HSA as competitor, as shown in Fig. 5 (open squares). The amount of CA bound to the MIP is  $8 \mu\text{g}$ . The addition of HSA does not displace CA significantly. The results indicate that the binding to the polymer is very much dimension-dependent, thus HSA being far bigger than CA, a scarce competition effect was evident. The shape of the protein is therefore crucial for the binding. This might limit the selectivity properties of the MIP-beads, thus efforts should be addressed to further tailor the selection.

### 3.8. The specific removal of a protein exploited for proteome analysis: depletion of human serum albumin

Despite the selectivity of the MIP beads was not extremely tuned, an interesting application was still envisaged, as we focus the interest on samples like human serum, which contains a large predominance of albumin (the 60–80%, w/w). In the case, the problems of competition for the imprinted binding sites might be negligible. For these reasons, the last part of our work was devoted to the evaluation of the binding performance of imprinted beads on real biological fluid, human serum. Serum samples are composed of thousands of proteins and peptides, released from various organs and travelling through the body through the vasculature, accounting for the high complexity of such fluid. Despite the fact that albumin and immunoglobulins constitute the vast majority of the proteic fraction of serum (ca. 90%), interest is focused on proteins that form the minor fraction, as their presence or their quantitative variations are often correlated to pathological states. Therefore, methods for efficient removal of HSA are highly welcomed, as they permit tracing and analysis of low abundance proteins, usually masked by serum HSA. In the present research we attempted the use of the imprinted beads for albumin removal. Serum samples were incubated with imprinted beads, the supernatants recovered and their proteins precipitated with TCA. Recovered proteins were subjected to bi-dimensional (2D) electrophoresis analysis. The 2D maps of untreated serum and serum depleted of albumin with imprinted beads were analysed with the software PDquest (Biorad, Hercules, CA) and are shown in Fig. 6. The total number of protein spots counted for serum was 124 and 116 for MIP-treated serum, indicating again that the imprinted beads targeted HSA and did not randomly remove other serum components. By analysing the optical density of the albumin spot, a decrease was reported for serum depleted with imprinted beads, in fact the spot intensity decreased a factor  $1.7 \pm 0.3$  upon treatment (i.e. the 58% HSA was removed). The quantity of albumin removed with the beads was of  $183 \mu\text{g}$ , starting from  $311 \mu\text{g}$  of HSA. It can be concluded that the imprinted beads also removed the protein target in a complex fluid, leaving the other proteins nearly unchanged. The removal process was easy and straight-

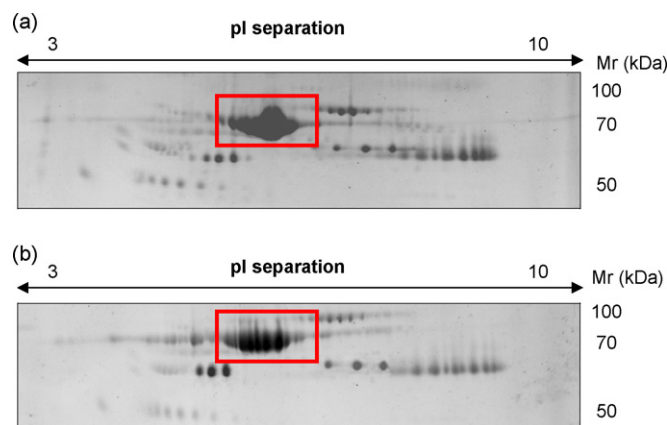


Fig. 6. 2D-maps of human serum: (a) untreated serum sample, (b) serum treated with imprinted beads, for the depletion of HSA.

forward with an optimal incubation time of 5 min. Naturally, the preliminary experiments with a complex fluid need further investigation where the quantity of imprinted beads would be optimised to obtain an almost complete depletion of HSA from serum.

#### 4. Conclusions

The results presented here are a further achievement in the area of protein imprinting. The p-APBA derivatised beads shows the possibility to create specific recognition sites directed towards the binding of a protein. To obtain more homogeneous population of binding sites, the protein template was immobilised to the silica scaffold, followed by the polymerisation of APBA. The MIP beads show a recognition mainly due to shape interactions. Results demonstrate the binding ability of the imprinted beads both in simple and complex samples, i.e. biological fluids. The MIP beads were used for the first time as a tool for the pre-fractionation of the sample prior to proteome analysis (removal of the 58% of albumin in serum), thus opening the route for a new area of application of MIP recognition materials.

#### References

- Ahmed, N., Barker, G., Oliva, K., Garfin, D., Rice, G., 2003. *Proteomics* 3, 1980–1987.
- Andersson, L.I., Muller, R., Vlatakis, G., Mosbach, K., 1995. *Proc. Natl. Acad. Sci. USA* 92, 4788–4792.
- Andersson, L.I., Schweitz, L., 2003. *Handb. Anal.* 4, 45–71.
- Andersson, N.L., Anderson, N.G., 2002. *Mol. Cell. Proteomics* 1, 845–867.
- Bossi, A., Piletsky, S.A., Piletska, E.V., Righetti, P.G., Turner, A.P.F., 2001. *Anal. Chem.* 73, 5281–5286.
- Bossi, A., Castelletti, L., Piletsky, S.A., Turner, A.P.F., Righetti, P.G., 2004. *J. Chromatogr. A* 1023, 297–303.
- Burow, M., Minoura, N., 1996. *Biochem. Biophys. Res. Commun.* 227, 419–422.
- Chianella, I., Piletsky, S.A., Tothill, I.E., Chen, B., Turner, A.P.F., 2003. *Biosens. Bioelectron.* 18, 119–127.
- Dickert, F.L., Hayden, O., 2002. *Anal. Chem.* 74, 1302–1306.
- Fortis, F., Girot, P., Brieau, O., Castagna, A., Righetti, P.G., Boschetti, E., 2005a. *Proteomics* 5, 629–638.
- Fortis, F., Girot, P., Brieau, O., Castagna, A., Boschetti, E., Righetti, P.G., 2005b. *Proteomics* 5, 620–628.
- Guo, T.Y., Xia, Y.Q., Hao, G.J., Song, M.D., Zhang, B.H., 2004. *Biomaterials* 25, 5905–5912.
- Haupt, K., Mosbach, K., 2000. *Chem. Rev.* 100, 2495–2504.
- Hjertén, S., Liao, J.L., Nakazato, K., Wang, Y., Zamaratskaia, G., Zhang, H.X., 1997. *Chromatographia* 44, 227–234.
- Katz, A., Davis, M.E., 2000. *Nature* 403, 286–289.
- Kempe, M., Glad, M., Mosbach, K., 1995. *J. Mol. Recognit.* 8, 35–39.
- Lanza, F., Sellergren, B., 2001. *Adv. Chromatogr.* 3, 41137–41173.
- MacQuade, D.T., Pullen, A.F., Swager, T.M., 2000. *Chem. Rev.* 14, 2537–2574.
- Mattoso, L.H.C., Manohar, S.K., MacDiamid, A.G., Epstein, A.J., 1995. *Polym. Sci. Polym. Chem.* 33, 1227–1230.
- Minoura, N., Rachkov, A., 2000. *J. Chromatogr. A* 889, 111–118.
- Mosbach, K., 1994. *Trends Biochem. Sci.* 19, 9–14.
- Mosbach, K., Ramstrom, O., 1996. *Biotechnology* 14, 163–170.
- Piletsky, S.A., Piletska, E.V., Bossi, A., Karim, K., Lowe, P., Turner, A.P.F., 2001. *Biosens. Bioelectron.* 16, 701–707.
- Pribyl, J., Skladal, P., 2006. *Biosens. Bioelectron.* 21, 1952–1959.
- Ramstrom, O., Skudar, K., Haines, J., Patel, P., Bruggemann, O., 2001. *J. Agric. Food Chem.* 49, 2105–2114.
- Righetti, P.G., Caravaggio, T., 1976. *J. Chromatogr.* 127, 1–28.
- Righetti, P.G., Castagna, A., Antonucci, F., Piubelli, C., Cecconi, D., Camprostrini, N., Antonoli, P., Astner, H., Hamdan, M., 2004. *J. Chromatogr. A* 8, 3–17.
- Sato, A.K., Sexton, D.J., Morganelli, L.A., Cohen, E.H., Wu, Q.L., Conley, G.P., Streltsova, Z., Lee, S.W., Devlin, M., De Oliveira, D.B., Enright, J., Kent, R.B., Wescott, C.R., Ransohoff, T.C., Ley, A.C., Ladner, R.C., 2002. *Biotechnol. Prog.* 18, 182–192.
- Sellergren, B., 2001a. *Techniques and Instrumentation in Analytical Chemistry*, vol. 23. Elsevier, Amsterdam.
- Sellergren, B., 2001b. In: Subramanian, G. (Ed.), *Chiral Separation Techniques*, 2nd ed. Wiley-VCH, Weinheim, pp. 153–184.
- Shi, H.Q., Tsa, W.B.I., Garrison, M.D., Ferrari, S., Ratner, B.D., 1999. *Nature* 398, 593–597.
- Shiomi, T., Matsui, M., Mizukami, F., Sakaguchi, K., 2005. *Biomaterials* 27, 5564–5571.
- Thulasiraman, V., Lin, S., Gheorghiu, L., Lathrop, J., Lomas, L., Hammond, D., Boschetti, E., 2005. *Electrophoresis* 26, 3561–3571.
- Tirumalai, R.S., Chan, K.C., Da Rue, A.P., Issaq, H.J., 2003. *Mol. Cell. Proteomics* 2, 1096–1103.
- Turner, N., Wright, B.E., Hlady, V., Britt, D., 2006. *J. Coll. Interf. Sci.*, Dec 15; [Epub ahead of print].
- Wang, Y.Y., Cheng, C.P., Chan, D.W., 2003. *Proteomics* 3, 243–248.
- Whitcombe, M.J., Alexander, C., Vulfson, E.N., 1997. *Trends Food Sci. Technol.* 8, 140–145.
- Wulff, G., 1993. *Trends Biotechnol.* 11, 85–87.
- Yilmaz, E., Haupt, K., Mosbach, K., 2000. *Angew. Chem. Int. Ed.* 39, 2115–2118.

# 'Gate effect' in templated polyacrylamide membranes influences the electrotransport of proteins and finds applications in proteome analysis

Alessandra Bossi · Matteo Andreoli · Francesca Bonini · Sergey Piletsky

Received: 30 December 2006 / Revised: 14 February 2007 / Accepted: 9 March 2007 / Published online: 5 April 2007  
© Springer-Verlag 2007

**Abstract** Templating is an effective way for the structural modifications of a material and hence for altering its functional properties. Here protein imprinting was exploited to alter polymeric polyacrylamide (PAA) membranes. The sieving properties and selection abilities of the material formed were evaluated by studying the electrically driven transport of various proteins across templated PAA membranes. The sieving properties correlated with the templating process and depended on the quantity of template used during the polymerisation. For 1 mg/mL protein-templated membranes a 'gate effect' was shown, which induced a preferential migration of the template and of similar-size proteins. Such template preferential electrotransport was exploited for the selective removal of certain proteins in biological fluids prior to proteome analysis (depletion of albumin from human serum); the efficiency of the removal was demonstrated by analysing the serum proteome by two-dimensional electrophoresis experiments.

**Keywords** Molecularly imprinted polymers · Polyacrylamide membranes · Electrotransport · Human serum albumin depletion · Proteome

## Introduction

Manipulation at a molecular level of the structure of a material is an effective way to alter its mechanical, optical and functional properties [1–3]. Polymer design is of particular interest in bioanalytical separations and sensing. In particular, hydrophilic polyacrylamide (PAA) is a typical constructing block that has a notable impact on bioanalysis. Variations in the PAA structure, such as large pores, were applied for the separation of large biological entities or DNA fragments [4]. However, the use of a low cross-linking level led to the creation of mechanically very weak or soft gels, which changed easily their degree of swelling. Instead, PAA recipes based on a high level of cross-linking produced highly porous materials with high mechanical stability [5]. These gels showed a sponge-type structure with large cavities, as indicated by scanning electron microscopy analysis [6].

Meso-structured PAA gels were synthesised by exploiting the principles of microsegregation and partitioning typically observed for polymer blends [7, 8]. Upon addition of poly(ethylene glycol) the dynamics of the gelation process was drastically influenced, inducing a lateral chain aggregation and the formation of thicker and thicker bundles of PAA, as confirmed by measurements of low-angle static light scattering [9].

The spatial distribution and the three-dimensional organisation of polymeric chains could be controlled through a templating approach, in which the presence of the template, with a defined molecular mass and geometry in the polymerisation mixture, causes modification of the growing polymer networks [10–12]. Mesoscale PAA architectures were reported upon the polymerisation of acrylamides in the presence of lyotropic surfactants, which could assemble

A. Bossi (✉) · M. Andreoli · F. Bonini  
Department of Science and Technology, University of Verona,  
Strada le Grazie 15,  
37134 Verona, Italy  
e-mail: alessandra.bossi@univr.it

S. Piletsky  
Cranfield Health, Cranfield University,  
Silsoe,  
Bedfordshire MK45 4DT, UK

in ordered hexagonal, bicontinuous cubic, or lamellar fashion [13, 14]. The surfactant assemblies formed voids, as they displaced the polymer. Nanometre-sized to micron-sized pores, separated by highly cross-linked polymer regions that provide mechanical stability, were reported [15]. Channels or spheroidal pores were embedded in PAAs by Rill et al. [16], demonstrating a geometry transfer in the templating process: semirigid rodlike polyelectrolytes (short fragments of DNA or xanthan) or spherical micelles of sodium dodecyl sulfate (SDS) were used as templates, inducing the distinct formation of channels and pores, respectively, which were used for the electrophoretic separation of biological macromolecules.

The high degree of transferred spatial order achievable through a template approach was fully demonstrated by the work of Hjerten et al. [17]. In this case, PAA gels were synthesised in the presence of a protein template, following a noncovalent molecular imprinting method [18]. The templated cavities were selective for the template protein (horse myoglobin) but not for its homologous form (whale myoglobin), accounting for a significant conservation of the template geometry in the pores formed and representing an important achievement in the area of recognition materials [19, 20].

Here we imprinted hydrophilic PAA membranes with proteins to induce template selection. The structural properties and recognition abilities of the materials formed were evaluated by studying the electrically driven transport through such PAA membranes of various proteins. It was anticipated that the PAA pore size and distribution would correlate with the quantity and type of template used for the polymerisation and would be reflected in varying electric transport properties.

A very interesting application for such membranes, explored here for the first time, would be their use in proteome research for removal of a specific protein from a complex sample [21–23]. It would be particularly important in a two-dimensional analysis of biological fluids where the predominant presence of certain proteins, e.g. albumin, masks the resolution of a vast population of low-expressed proteins. The membranes templated with human serum albumin (HSA) were employed in this work for the selective removal of albumin from serum.

## Materials and methods

### Reagents

Tris(hydroxymethyl)aminomethane (Tris), acetic acid, glutamic acid, bovine serum albumin (BSA), HSA, whale skeletal myoglobin, and catalase were purchased from Sigma (St. Louis, MO, USA). Ammonium persulfate, *N,N,N',N'*-tetramethylethylene diamine (TEMED), acrylamide, *N,N'*-

methylene bisacrylamide were purchased from Bio-Rad (Hercules, CA, USA). Immobiline chemicals were from Pharmacia Amersham (UK). All other reagents, purchased from commercial sources, were of analytical grade. Support for membranes was provided by Whatmann GF/D glass fibre membranes, 2 cm in diameter.

### Electrophoresis on templated gel slabs

The PAA stock solution was prepared with 28.8 g acrylamide and 1.2 g bisacrylamide to a final volume of 100 mL in water. It was defined as 30% T, according to its content being 30% of the total monomer and cross-linker content, and 4% C, with the cross-linker being 4% of the total monomer content (1.2 g bisacrylamide cross-linker in 30 g total monomers).

Thin gels, of 0.5-mm thickness, polymerised onto a Gel-Bond-PAG supporting film (Pharmacia-GE, Sweden), were prepared by diluting the stock solution to 6, 10, and 15% T, keeping the bisacrylamide at 4% C. The polymerisation was done with 1  $\mu\text{L}/\text{mL}$  of 40% (w/w) ammonium persulfate, and 0.5  $\mu\text{L}/\text{mL}$  TEMED for 2 h at ambient temperature. To obtain templated PAAs, the template, BSA, was added at concentrations of 0.5, 1, 3, and 10 mg/mL to the monomer mixture. The template removal was achieved through water washing steps (three steps of 1 h each) under mild agitation, followed by 2,000-Vh electroelution. The gels were then dehydrated. Prior to use, the gels were rehydrated for 2 h with the 298 mM Tris–HCl running buffer solution, pH 8.8.

After protein loading, the gels were run for 3 hours at 150 V and then stained with Coomassie blue R-250. The relative electrophoretic migration ( $R_e$ ) was measured as the migration distance of the protein with respect the migration of the front, i.e. of a small dye not interacting with the pores. The imprinting factor (IF) for each template/control pair was calculated as the ratio between  $R_e$  of templated PAA and  $R_e$  of a control PAA.

### Protein transport through templated PAA membranes in a free-flow electrophoresis system

The equipment used for analysis of electrophoretic properties of PAA membranes was from Talent (Trieste, Italy) [28, 29]. The electrolyser was assembled with four chambers of 4-mL volume: at the extremes an anodic and a cathodic chamber, in the middle a loading chamber (Ch-II) and a collecting chamber (Ch-III). The chambers were delimited by three 10% T, 4% C membranes: anodic pI 3.0, templated PAA or control PAA and cathodic pI 9.0. The anodic chamber contained 100 mM acetic acid, whereas the cathodic reservoir was filled with 1 M Tris. Ch-II and Ch-III were filled with 20 mM glutamic acid. Anodic and cathodic compartments were introduced to avoid direct contact between electrodes and proteins, thus preventing electrooxidation of the protein.



Before starting the experiments, the instrument was subjected to a 2-h process of electrical conditioning at 4 mA, in order to remove nonreacted monomers and to swell the membranes in the solution with chosen pH. When the electrolyser was equipped with templated membranes, the electrical conditioning served also for the removal of the template protein from the membrane pores. During such a process, the solutions in Ch-II and Ch-III were repeatedly exchanged. To monitor the removal process the solutions in Ch-II and Ch-III were checked for their protein content with a Bradford assay. After 1 h the process of removal was complete, but the electrical conditioning was protracted for up to 2 h.

The proteins (4 mg per protein, or an equal quantity in moles) were loaded in Ch-II, delimited by the templated membrane or by the control membrane, and collected in Ch-III. The electromigration conditions chosen were 75 V and 4 mA for 120 min. The transport progress was monitored by Bradford protein reagent assay (Sigma, St. Louis, MO, USA) from aliquots harvested in Ch-II and Ch-III. Quantification of protein contents was done by comparing absorbance units obtained from the Bradford assay with a calibration curve made for each protein.

Quantification of the protein transport was also made by analysing fractions withdrawn from Ch-II and Ch-III (10  $\mu$ L sample mixed with 10  $\mu$ L loading buffer and boiled for 5 min) by electrophoresis using regular SDS PAA gel electrophoresis (PAGE) with 14% T PAA gel, with a Tris–glycine cathode buffer (192 mM glycine, 0.1% SDS, and 40 mM Tris to pH 8.3). The run was performed by applying 15 mA per gel for 20 min followed by 25 mA per gel until the dye front reached the bottom of the gel. Gels were stained with Coomassie blue (0.5g in 10% acetic acid, 30% methanol) followed by overnight destaining in 10% acetic acid, 30% methanol. The gels were scanned with a Versa Doc Imaging System (Bio-Rad, Hercules, CA, USA) and analysed with the software GQuest version 7.1 (Bio-Rad, Hercules, CA, USA). Protein quantitation was evaluated in terms of optical density and compared with densitometric calibration curves.

#### Removal of HSA from human serum through templated PAA membranes

Aliquots of about 800  $\mu$ g of human serum (70 mg/mL stock solution) were diluted to 0.2 mg/mL and a final volume of 4 mL in 20 mM glutamic acid. The protein content after dilution was quantified by Bradford assay. The serum solution was loaded in Ch-II and an electrophoresis run was performed at 75 V, 4 mA, 1 W. The run time was 12 min, then the contents of Ch-II and Ch-III were recovered and quantified by Bradford assay.

The effectiveness of the albumin removal was evaluated by mapping the proteome with a two-dimensional analysis

of treated and untreated human serum, loading 500  $\mu$ g of total proteins on each two-dimensional map.

#### Two-dimensional electrophoresis

Samples (Ch-II and Ch-III contents) for two-dimensional electrophoresis were precipitated with 15% trichloroacetic acid. The pellet was washed three times with cold acetone, then solubilised, reduced, and alkylated in the sample solution for isoelectric focusing (IEF) containing 7 M urea, 2 M thiourea, 3% 3-[(3-cholamidopropyl)dimethylammonio]-1-propanesulfonate, 5 mM tri-*n*-butyl phosphate, 10 mM acrylamide, 10 mM DTT, 40 mM Tris, and 1% carrier ampholytes [36].

Two-dimensional PAGE was performed using a Protean  $\sim$ IEF cell on commercial 7-cm immobilised pH gradient strips (Bio-Rad, Hercules, CA, USA) pH 3–10. The run was stopped at 25,000 V h. The second dimension was performed with 8–18% Tris–glycine, 0.1% SDS gels. The SDS-PAGE was performed at 5 mA per gel for 1 h, followed by 10 mA per gel for 1 h and 20 mA per gel until run completion. Gels were stained in Coomassie blue G 250 and destained with 5% acetic acid. The images of the gels were digitalised with a Versa Doc Imaging System (Bio-Rad, Hercules, CA, USA) and analysed with the software PDQuest version 7.1 (Bio-Rad, Hercules, CA, USA). A match set was created of the protein patterns of three replicate gels for each independent sample. The results were evaluated in terms of spot optical density and spot number.

#### Result and discussion

The sieving properties of a polymer correlate to the fraction of gel volume accessible to particles of different dimensions, according to the work of Ogston and Sherman [24]. In other terms, for a certain molecule, the fraction of gel volume accessible depends on the mean radius of the pores and on the pore size distribution around the mean pore-size. PAAs have been demonstrated to have a wide variety of pore distributions depending on their composition: a precious characteristic that makes them highly versatile supports in separation techniques.

In the present work, we focus attention on the study of the alterations of the PAA functional electrotransport properties induced by a protein-templating process, relating these changes to modifications occurring in the PAA structure.

Templated PAA gel slabs were prepared with a bulk imprinting strategy, in which the template, BSA, and the monomers were solvated together in an aqueous solution. The total monomer and cross-linker contents were 6, 10, and 15% T. The gels were chemically polymerised for 2 h

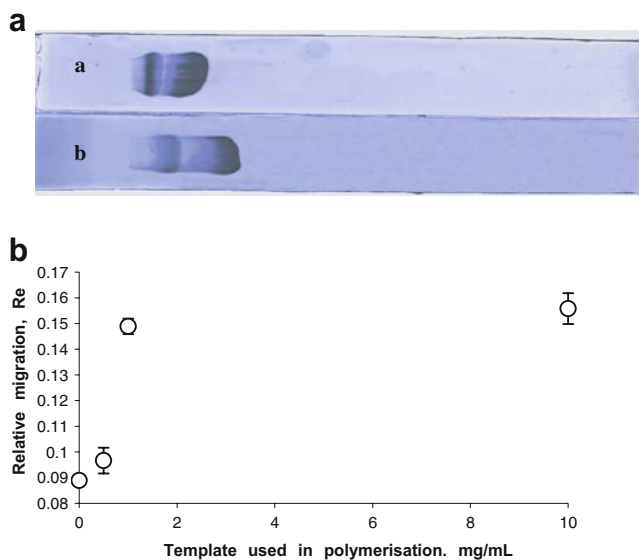


**Fig. 1** **a** The electrophoretic migration of BSA in standard running conditions (100 V, 3 h) on control (*a*) and templated (*b*) polyacrylamide (PAA) gel slabs. **b** The effect of the template quantity on the gel structure. The bovine serum albumin (BSA) concentration was varied between 0.5 and 10 mg/mL in the prepolymerisation mixture

at ambient temperature, then washed extensively and electroconditioned to ensure effective removal of the template. The electrophoretic migration of proteins on control and templated PAA gels was calculated as the relative electrophoretic migration ( $R_e$ ), as shown in Fig. 1a. The IF calculated from Fig. 1 was  $1.35 \pm 0.05$ , indicating that BSA migrates faster in templated gels. Low-cross-linked materials demonstrated a lower IF (6% gels had an IF of 1.05). Gels with 15% T were mechanically fragile and cracked after drying.

The effect of the template quantity on the gel structure was investigated (Fig. 1b) by varying the BSA concentration in the prepolymerisation mixture and by monitoring the electromigration of BSA. The use of 0.5 mg/mL BSA did not result in an appreciable variation of the migration in the

templated gels compared with the control. BSA at 1 mg/mL affected the  $R_e$  of BSA significantly. The use of 10 mg/mL BSA implies in practice great protein consumption and washings steps prolonged for days, thus it was considered of scarce interest for further practical developments. In general, the migration trends observed for protein-templated PAAs gel slabs were in agreement with the results described for other templating processes [16]. Insufficient washing always resulted in a marked retention of BSA during the migration; thus, the apparent IF fell below 1.0. Whenever the template removal was successfully accomplished, it led to significant reduction of about 30% of the electromigration time of the template protein. The preferential electrotransport of the template through templated gels can be described as a form of facilitated permeation [25] coupled with an alteration of the sieving properties via swelling, as reported for other imprinted structures [26].

As the gel slab format proved to be excessively labour-intensive, experiments towards a more detailed analysis of the templating effect on PAA, by the investigation of the permeation properties, were performed in the free-flow electrophoresis system equipped with PAA membranes (templated or control). The free electrophoresis format permitted us to overcome gel-slab limitations, allowing a fast and highly reproducible collection of results. The scheme of the electrolyser used [28] is reported in Fig. 2. An anodic and a cathodic chamber were introduced in the setup, to prevent the protein from contacting the electrode, which causes protein oxidation and breaking [29]. Proteins were loaded in Ch-II and collected in Ch-III, and the electromigration process was monitored by quantifying the protein content in the two chambers over a time course of 60 min. Comparison of the migration curves through control and BSA-templated membranes of three proteins is reported in Fig. 3. An overall reduction in the migration times characterised the transport through templated membranes. A hyperbolic saturation course is evident for the smallest protein tested,

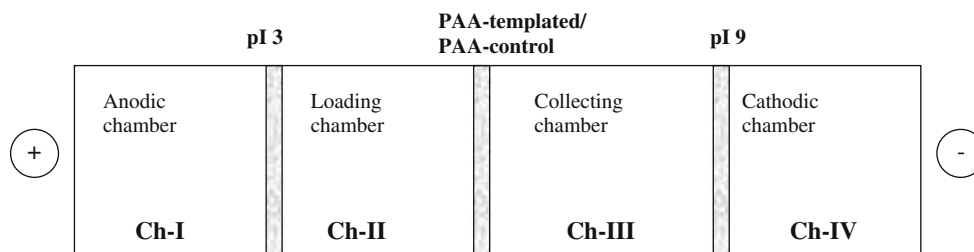


**Fig. 2** The free-flow electrophoresis system. The instrument was equipped with four chambers, delimited by three PAA membranes. Chamber I (*Ch-I*), anodic, and chamber IV (*Ch-IV*), cathodic, were delimited by isoelectric membranes at pI 3.0 and 9.0, respectively, which created pI-selective barriers, preventing protein loss at the extremes. Chamber I was filled with 0.1 M acetic acid solution, chamber II (*Ch-II*) and chamber III (*Ch-III*) were filled with 20 mM

glutamic acid, and chamber IV was filled with 1 M Tris. The concentration of the solutions was adjusted in order to minimise the differences in conductivity between the chambers. The templated or control membranes were placed between chambers II and III. Proteins were loaded in chamber II and collected in chamber III, the electromigration process was monitored by quantifying the protein content in these two chambers over a time course of 60 min

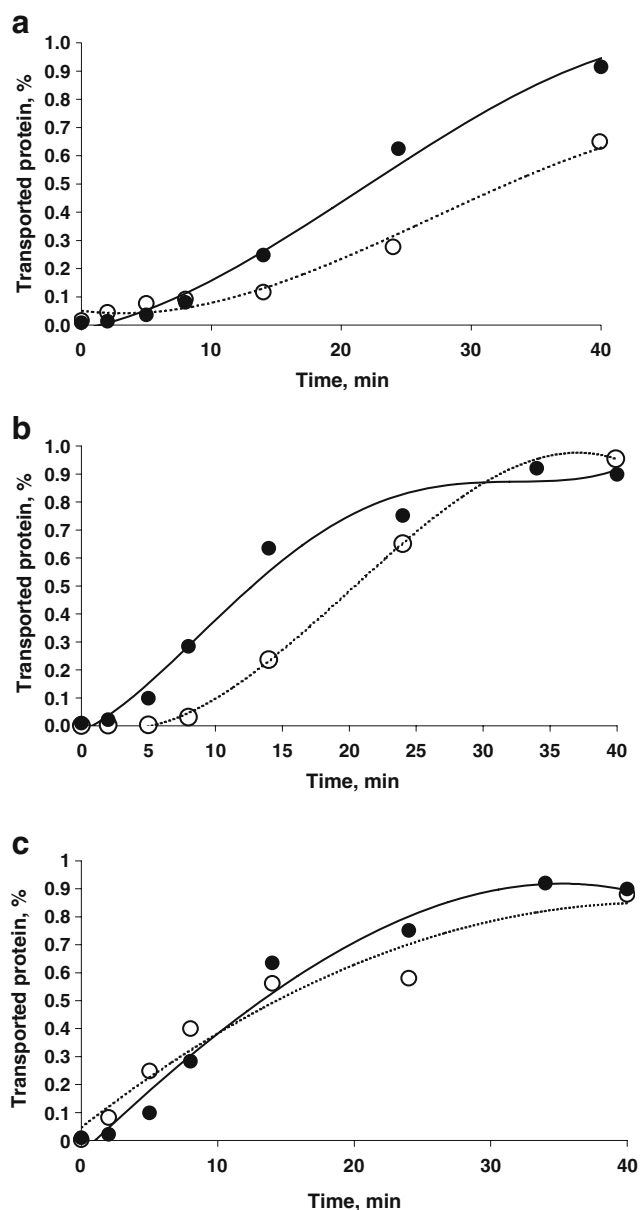


**Fig. 3** Time course of the electric transport of proteins through control PAA membranes (*dotted line*) and PAA membranes templated with BSA (*solid line*). **a** Catalase, **b** BSA, **c** myoglobin

myoglobin, while the profiles become sigmoidal upon increase of protein dimensions, accounting for a sieving effect of PAA for large molecules. As shown by the data reported in Table 1, the templating process had no impact on the transport of myoglobin, the smallest protein tested, while significantly faster transport was evident in templated PAA for proteins of higher dimensions, i.e.  $Tr_{50\%}$  was 39% faster for BSA and 32% faster for catalase.

The electric transport through the templated PAA was tested for a variety of proteins, differing in molecular masses and pIs (Table 2). To standardise the measurement conditions by fully protonating the proteins tested, acidic

**Table 1** Comparison of protein transport times in templated and control polyacrylamide (PAA) membranes

Protein	Molecular mass (g/mol)	pI	$Tr_{50\%}$ templated PAA (min)	$Tr_{50\%}$ control PAA (min)
Bovine serum albumin	66,400	6.8	12.7	20.7
Myoglobin	17,000	6.8	11.2	12.5
Catalase	220,000	5.4	21.5	32.0

pH 3.2 was chosen. The molar transport ( $1.5 \times 10^{-2} \mu\text{mol}$ ) was plotted as function of time (Fig. 4).

The transport of proteins through templated PAA membranes depended significantly on the templating conditions applied. Experiments showed that the transport times of 11–77-kDa proteins across the membrane templated with 0.5 mg/mL BSA (Fig. 4a, solid circles) and a control PAA membrane (Fig. 4a, open circles) were superimposable. The transport times were distributed in the range 3–25 min. A linear dependence of the logarithm of the molecular masses versus transit times was calculated ( $R^2=0.94$ ), in accordance with the permeation theory for PAAs [37]. As 0.5 mg/mL templated membranes display the sieving properties expected for nontemplated PAA (Fig. 4a, open circles), it could be concluded that 0.5 mg/mL is too low a template concentration to induce significant numbers of template–monomer interactions capable of altering the polymerisation rate and to finally induce extended pore size modifications [27]. In case of PAAs templated with 10 mg/mL (Fig. 4c), however, all the proteins tested, in the range of masses between 11 and 77 kDa, migrated through the membrane barrier within an 8-min range (11 kDa in 4 min and 77 kDa in 12 min). A scarce sieving effect was evident, but there was a significant alteration in the permeability.

**Table 2** Molecular mass and charge characteristics of the protein tested

Protein	Molecular mass (kDa)	pI <sup>a</sup>
Bovine serum albumin	66.4	6.2
Human serum albumin	65.6	5.9
Hemoglobin	Tetramer, 64.0	7.1
Myoglobin	17.0	7.4
Horseradish peroxidase	39.0	Isoforms, 4.7–9.13
Trypsin	23.9	4.9
Conalbumin	75.8	6.7
Glucose oxidase	Dimer, 160	4.2
$\beta$ -Lactoglobulin b	Dimer, 36.4	4.8
Cytochrome <i>c</i>	11.0	10.2
Carbonic anhydrase	29.0	6.4

<sup>a</sup> Isoelectric points and molecular masses of proteins according to [35] and Swiss-Prot, ExpASY



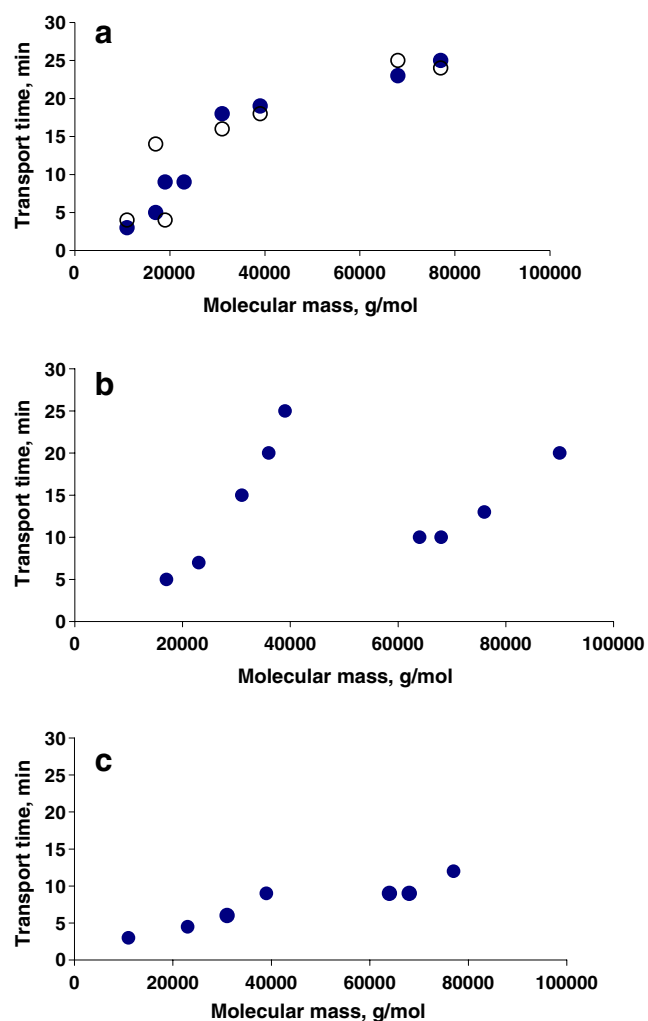


**Fig. 4** Protein molar transport versus time (templated PAA membranes). **a** The transport across the membrane templated with 0.5 mg/mL (solid circles) shows a sieving course comparable with that of nontemplated PAA (open circles). **b** PAA templated with 1 mg/mL showed two different electrotransport behaviours, depending on the size of proteins. A fast transport of the template and similar-dimension proteins is evident. **c** The transport across a 10 mg/mL templated PAA membrane is characterised by quite fast transport times for all the proteins tested, thus accounting for a scarce sieving effect

The most interesting results were observed for the transport through the 1.0 mg/mL templated PAA (Fig. 4b), in which the membrane shows a double sieving behaviour, seemingly molecular mass dependent. In this case, proteins with size up to 45 kDa had migration times distributed between 5 and 25 min. The transport follows a ‘slow’ exponential kinetics behaviour, with the equation  $y = 28.96x - 311.25$ ;  $R^2 = 0.91$  plotted on a semilog scale. The template and similar-mass-range proteins (64–67 kDa) migrate faster (10–12 min) than is expected from the above equation (transport time for the template being comparable to that of a 27-kDa protein with slow kinetics). Proteins with molecular masses above 67 kDa followed ‘fast’ exponential kinetics, with migration times varying from

11 to 20 min, described through a semilog plot by the equation  $y = 22.83x - 219.53$ ;  $R^2 = 0.91$ .

Apparently, it could be hypothesised that there are different structural moduli in the 1 mg/mL templated membranes that can be roughly classified into (1) sieving pores that are able to fit proteins smaller than 45 kDa, (2) sieving pores of template dimension, and (3) sieving pores of higher dimensions. The generation of different pore classes during the polymerisation is a phenomenon expected from the conventional ‘bulk’ molecularly imprinted materials technology, in which there is a simultaneous generation of randomly oriented imprinted sites together with the formation of the polymer matrix, including its own pore structures [30]. As a consequence, there is a random distribution of uneven sieving pores in the volume of the templated PAA membrane together with the specialised templated pores. The templating process resulted in a significant modification of the sieving properties of PAA, more than a high selection. Templating, rather than forming a specific barrier, resulted in both the preferential template selection together with the transfer of several different proteins. Figure 4b shows that the migration time for the template protein coincides with the migration time of proteins below 26 kDa. There is, however, a marked preferential electro-transport of the template that had striking resemblance to the ‘gate effect’, a phenomenon reported for the electrotransport of the substrate molecule through substrate-selective membranes, defined broadly as alteration of the permeability/conductivity of the material upon template binding/interaction [31–33].

The preferential transport of the template is attributed to the effect of the templating process which leads to the formation of template size-specific homogeneous pores, regularly distributed in the three-dimensional space; moreover, an adaptation of the templated structures when they interact with the template is supposed. As a consequence, the protein template and molecules of about 65 kDa find preferential electromigration pathways, fitting perfectly within the channels (Fig. 5, pathway A). A minority of the pores have the typical dimensions of nontemplated PAAs, with a range of distribution up to  $9 \pm 2$  nm: small proteins could distribute during the electromigration process both in templated channels and in randomly distributed pores, thus migrating through a twisty path, with the consequence of an increase in transport times (Fig. 5, pathway B). The mechanism hypothesised resembles a size-exclusion chromatography process, where large proteins have a shorter path to reach the column’s end, and vice versa for small molecules, fully explaining the observed preferential electromigration of the template.

Membranes with novel selective abilities are required especially in the area of bioseparation [34], where many very specialised fractionations are needed, often as a key step for complex and multistep analytical tasks, like in

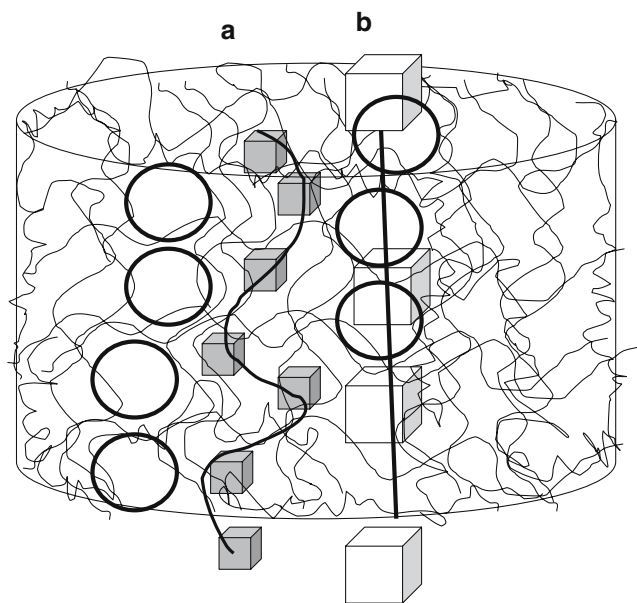


**Fig. 5** The hypothesised mechanism for the electric transport of the template (fast kinetics, **b**) and nontemplate small proteins (slow kinetics, **a**), which resembles with the elution mechanism of size-exclusion chromatographic processes

genome and proteome analysis [30]. The sieving properties of the templated PAA membranes match the needs of proteome analysis performed with two-dimensional electrophoresis, as the analysis focuses mainly on a protein population with size of more than 25 kDa. In our case, the permeation properties of the templated PAA membranes were further exploited for the selective removal (prefractionation) of a predominant protein from a complex biological fluid—which is an important task in proteome analysis.

PAA membranes templated with HSA have been used for the treatment of human serum, in order to prefractionate the sample and remove albumin, whose high abundance (50–70% of the total proteins in serum) poses serious problems in the detection of low-expressed proteins [22]. The removal of albumin prior to proteome analysis of serum is essential for increasing the resolution of the proteome analysis [23]. In our experiments 800  $\mu\text{g}$  serum was loaded in Ch-II and the albumin electrodepletion was performed for 12 min. About  $231 \pm 10 \mu\text{g}$  protein was detected in Ch-III after the process, and  $525 \pm 5 \mu\text{g}$  protein was measured in Ch-II. In order to evaluate the efficiency of the removal, aliquots of 500  $\mu\text{g}$  of nontreated and electrodepleted serum were analysed by two-dimensional electrophoresis. Images of the two-dimensional maps, shown in Fig. 6, were compared using the software PDquest (Bio-Rad, Hercules, CA, USA). The efficiency of the templated-PAA method for albumin removal was evaluated densitometrically, and indicated a reduction of the albumin spot intensity of 60%. In order to evaluate the specificity of the removal, the total number of protein spots was counted both on electrodepleted

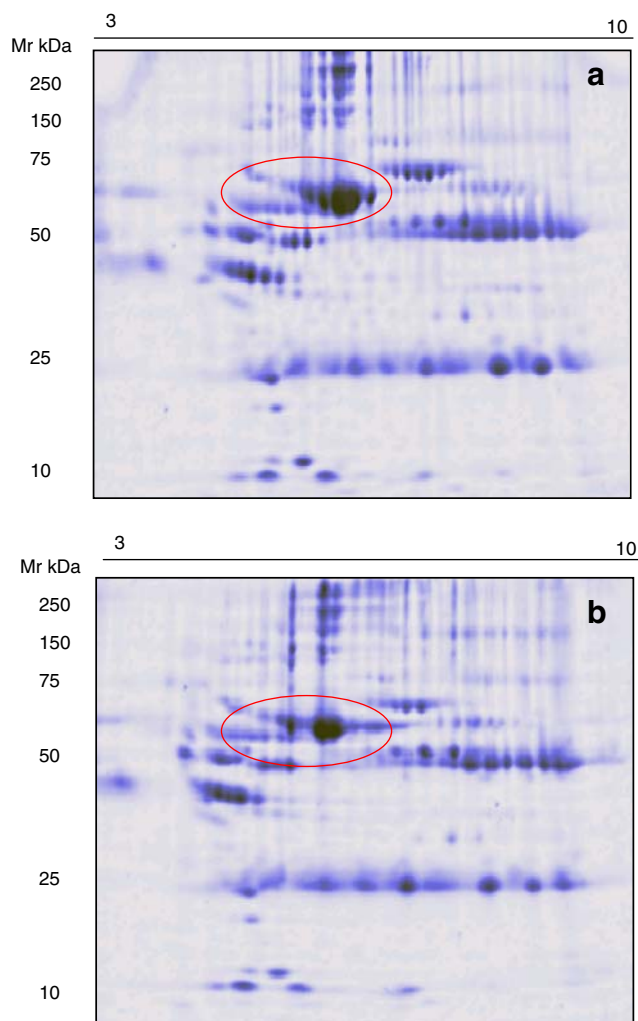


**Fig. 6** The effectiveness of the templated PAA for removal of the high-abundance protein human serum albumin from serum samples was demonstrated by the two-dimensional electrophoresis of serum subjected to electrodepletion of albumin (**b**) and control serum (**a**). The two-dimensional maps of depleted serum (**b**) show a significant reduction of the albumin spot upon PAA membrane treatment of the sample

and on control two-dimensional maps. The number of spots counted was 207 (considering the preliminary character of these experiments, serum was run on a minigel, thus accounting for the limited resolving power). The same number of proteins was retrieved on control and depleted sample maps, accounting for the selective removal of albumin, without apparent variation of the other protein components.

The results indicate that templated PAA membranes are promising materials for the pretreatment of proteome samples.

## Conclusions

The protein-templated PAA membranes demonstrated a different electrotransport performance from that of the

nontemplated membranes. The fractionation of proteins was performed in an aqueous environment, well compatible with the protein structure. Rapid (on the order of minutes) operational time was required. In general, the transport in templated membranes is faster than in nontemplated ones. The template and proteins with structural properties similar to those of the template are always transported through the template membrane faster than other proteins. Such a ‘gate effect’ is dependent on the size of the proteins and has to be ascribed to an altered pore size distribution of PAA as a result of templating process. Proteins with dimensions well below those of the template were subjected to a different electrotransport regime. The selective electrotransport properties of templated PAA might be exploited for novel separation systems. In one such example, the templated PAA was used for the selective removal of serum albumin from human serum. The results indicate the use of templated PAA membranes might be a suitable tool for prefractionating biological samples prior to proteome analysis. The application of such membranes to the free-flow electrophoretic system could be hypothesised and further developed by the addition of several membranes with different permeabilities in series, thus to obtain a multiple fractionation in one step.

## References

- Assender H, Bliznyuk V, Porfyrakis K (2002) *Science* 297:973
- Chailapakul O, Crooks RM (1993) *Langmuir* 9:884–888
- Kumar A, Biebuyck HA, Whitesides GM (1994) *Langmuir* 10:1498
- Shaaya E (1976) *Anal Biochem* 75:325–328
- Righetti PG, Brost BCW, Snyder R (1981) *J Biochem Biophys Methods* 4:347–363
- Righetti PG, Caglio S, Saracchi M, Quaroni S (1992) *Electrophoresis* 13:587–592
- Krause S (1972) *J Macromol Sci Rev Macromol Chem C* 7:251
- De Gennes P-G (1979) *J Phys* 40:L69
- Asnaghi D, Giglio M, Bossi A, Righetti PG (1995) *J Chem Phys* 102:9763–9769
- Buter R, Tan YY, Challa G (1972) *J Polym Sci A* 10:1031–1049
- Spvbek J, Schneider R (1987) *Adv Colloid Interface Sci* 27:81–150
- Hulvat JF, Stupp SI (2003) *Angew Chem Int Ed Engl* 42:778–781
- Pieranski P, Sittler L, Sotta P, Imperor-Clerc M (1986) *Eur Phys J E* 5:317–328
- Hyde S, Andersson S, Larsson K, Blum Z, Landh T, Lidin S, Ninham BW (1997) (eds) *The language of shape. The role of curvature in condensed matter: physics, chemistry*. Elsevier, Amsterdam
- Antonietti M, Caruso RA, Göltner CG, Weissenberger MC (1999) *Macromolecules* 32:1383–1389
- Rill RL, Locke BR, Liu Y, Dharia J, Van Winkle D (1996) *Electrophoresis* 17:1304–1312
- Hjerten S, Liao JL, Nakazato K (1997) *Chromatographia* 44:227–234
- Mosbach K (1994) *Trends Biochem Sci* 19:9–14
- Vlatakis G, Andersson LI, Muller R, Mosbach K (1993) *Nature* 361:645–647
- Haupt K, Mosbach K (1998) *Trends Biotechnol* 16:468–475
- Righetti PG, Castagna A, Herbert B (2003) *Proteomics* 3:1397–1407
- Chertov O, Simpson JT, Biragyn A, Conrads TP, Veenstra TD, Fisher RJ (2005) *Expert Rev Proteomics* 2:139–145
- Steel LF, Trotter MG, Nakajima PB, Mattu TS, Gonye G, Block T (2003) *Mol Cell Proteomics* 2:262–270
- Ogston AG, Sherman TF (1958) *Nature* 181:482–483
- Noble RD (1992) *J Membr Sci* 75:121–129
- Yan M, Ramstrom K (eds) *Molecularly imprinted materials, science and technology*. Dekker, New York (in press)
- Oral E, Peppas NA (2004) *Polymer* 45:6163–6173
- Righetti PG, Wenisch E, Faupel M (1989) *J Chromatogr* 475:293–309
- Righetti PG, Bossi A, Wenisch E, Orsini G (1996) *J Chromatogr B* 699:105–115
- Ulbrich M (2004) *J Chromatogr B* 804:113–125
- Piletsky SA, Dubey IY, Fedoryak DM, Kukhar VP (1990) *Biopolym Kletka* 6:55–58
- Piletsky SA, Butovich IA, Kukhar VP (1992) *Zh Anal Khim* 47:1681–1684
- Piletsky SA, Parhometz YP, Panasyuk TL, El’skaya AV (1994) *Sens Actuators B* 8/19:629–631
- van Reis R, Zydney A (2001) *Curr Opin Biotechnol* 12:208–211
- Righetti PG, Caravaggio T (1976) *J Chromatogr* 127:1–28
- Molloy MP, Herbert BR, Williams KL, Gooley AA (1999) *Electrophoresis* 20:701–704
- Casassa EF (1976) *Macromolecules* 9:182–185

Review

# Molecularly imprinted polymers for the recognition of proteins: The state of the art

A. Bossi<sup>a,\*</sup>, F. Bonini<sup>a</sup>, A.P.F. Turner<sup>b</sup>, S.A. Piletsky<sup>b</sup>

<sup>a</sup> Department of Science and Technology, University of Verona, Strada le Grazie 14, 37134 Verona, Italy

<sup>b</sup> Cranfield Health, Cranfield University, Silsoe, Bedfordshire MK45 4DT, United Kingdom

Received 15 February 2006; received in revised form 22 May 2006; accepted 20 June 2006

Available online 7 August 2006

## Abstract

Molecular imprinting has proved to be an effective technique for the creation of recognition sites on a polymer scaffold. Protein imprinting has been a focus for many chemists working in the area of molecular recognition, since the creation of synthetic polymers that can specifically recognise proteins is a very challenging but potentially extremely rewarding objective. It is expected that molecularly imprinted polymers (MIPs) with specificity for proteins will find application in medicine, diagnostics, proteomics, environmental analysis, sensors and drug delivery. In this review, the authors provide an overview of the progress achieved in the decade between 1994 and 2005, with respect to the challenging area of MIPs for protein recognition. The discussion furnishes a comparative analysis of different approaches developed, underlining their relative advantages and disadvantages and highlighting trends and possible future directions.

© 2006 Elsevier B.V. All rights reserved.

**Keywords:** Protein; Molecular imprinting; Molecular recognition; Review

## Contents

0. Introduction	1131
1. Recognition through the placement of few constrains on the polymer	1132
2. Shape recognition with polyacrylamide gels	1133
3. Epitope approach: exploiting a small structural element of the protein for its whole recognition	1134
4. Molecularly imprinted polymers grafted on surfaces	1135
5. Immobilising the template on a surface	1135
6. Silica-based materials imprinted for protein recognition	1136
7. Conclusions and future perspectives	1137
References	1137

## 0. Introduction

Molecular imprinting allows the creation of artificial recognition sites in synthetic polymers (Wulff, 1993; Mosbach, 1994). These sites are tailor-made *in situ* by co-polymerisation of functional monomers and cross-linkers around the template molecules. The print molecules are subsequently extracted from

the polymer, leaving accessible complementary binding sites in the polymeric network (Fig. 1).

Molecularly imprinted polymers (MIPs) have considerable potential for applications in the areas of clinical analysis, medical diagnostics, environmental monitoring and drug delivery. Molecular imprinting technology allows the creation of synthetic receptors with binding constants comparable to natural receptors, but capable of withstanding much harsher conditions such as high temperature, pressure, extreme pH, and organic solvents compared to proteins and nucleic acids. These materials are also less expensive to synthesise and can be manufactured in

\* Corresponding author. Tel.: +39 045 8027946; fax: +39 045 8027929.  
E-mail address: [alessandra.bossi@univr.it](mailto:alessandra.bossi@univr.it) (A. Bossi).



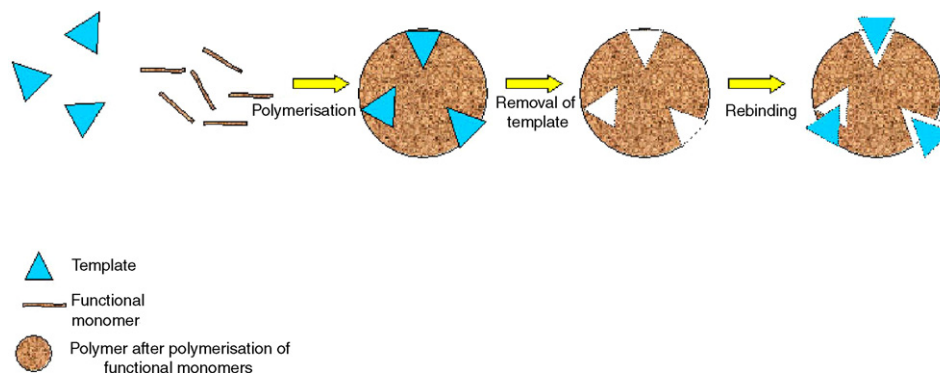


Fig. 1. Schematic representation of protein imprinting.

large quantities with good reproducibility. Nevertheless, molecular imprinting technology still needs to overcome some weakness, such as template leakage, poor accessibility of the binding sites, low binding capacity and non-specific binding.

From the 1990s, MIP technology has been extensively exploited to create recognition sites for a range of different templates. Some examples are: polypeptides (Kempe and Mosbach, 1995; Andersson et al., 1995; Minoura and Rachkov, 2000), bacteria (Dickert and Hayden, 2002), low molecular mass compounds (Katz and Davis, 2000; Pampi and Kofinas, 2004; Yilmaz et al., 2000) and proteins (Burow and Minoura, 1996; Bossi et al., 2001; Guo et al., 2004).

Of all the examples listed above, imprinting of proteins represents one of the most challenging tasks. The first report on protein imprinting was proposed in 1985 (Glad et al., 1985), no longer followed by other contributions in the following years. The reason for this could be found in several factors related to the properties of the protein templates. First of all, proteins are water-soluble compounds that are not always compatible with mainstream MIP technology, which relies on using organic solvents for the polymer preparation. Secondly, proteins have a flexible structure and conformation, which can be easily affected by changes in temperature or in the environment. Thermodynamically and practically it is difficult to develop successful imprints for such molecules, according to the calculation proposed by Nicholls (1995). Thirdly, proteins have large number of functional groups available for the interaction with functional monomers. There is always a trade-off involved in the selection of imprinting protocols which rely in some cases on using strong/dissociable (e.g. methacrylic acid) or in others on weak/neutral binding monomers (e.g. acrylamide) for the template recognition. The present review furnishes a comparative analysis of different approaches developed, underling the advantages and disadvantages, highlighting the trends and hypothesising on future possibilities.

### 1. Recognition through the placement of few constrains on the polymer

In general, approaches to protein imprinting can be divided into two major groups: either the imprinted polymer is targeted to recognise the sequence of the protein, or a part of it, or to

recognise the shape of a protein. The first attempt to imprint protein by using a sequence-recognition approach was proposed in 1995, by Kempe and co-workers.

The concept of synthetic receptors composed of scaffolds of variable length carrying metal ions coordinating groups, to selectively bind protein functional groups (i.e. the exposed histidine) on a protein's surface was demonstrated by Mallik et al. (1994a,b). Taking advantages of these results, Kempe and co-workers, exploited metal co-ordination for the polymer–protein interactions. The MIP polymer was capable of partial discrimination of the spatial orientation of the protein, as shown in Fig. 1 (Kempe and Mosbach, 1995; Kempe et al., 1995). Silica surfaces were derivatised with 3-(trimethoxysilyl)-propyl-methacrylate, thus introducing double bonds, which were then used as anchorage points for the imprinted polymer. The template protein, ribonuclease A, was mixed with metal ions and with the functional monomer *N*-(4-vinyl-benzyl)-iminodiacetic acid (VBIDA). Imidazole groups (Im) of the histidines exposed on the surface of the protein formed complexes with the metal chelating functional monomers, creating complementary cavities with 'anchoring points' for the recognition of the protein (Fig. 2).

The imprinted silica particles were packed into chromatography columns, and tested for their separation selectivity. Binding capacity was evaluated by using the capacity factor  $k' = (t - t_0)/t_0$ , where  $t$  is the elution volume of the protein and  $t_0$  the void volume. Results indicated that the stationary phase imprinted with ribonuclease A (RNase) in presence of metal ions, had a capacity factor ( $k'$ ) of 5.79 versus 2.46 measured for a competitor protein, lysozyme. Furthermore, the silica particles were compared with reference particles, prepared in the presence of bovine serum albumin (BSA). In this latter case,  $k'$  was 2.68 for RNase and 1.63 for lysozyme, indicating that the imprinting strategy was effective in producing a surface selective for the template molecule. The RNase/lysozyme separation factor ( $\alpha$ ) achieved was 2.35 for imprinted adsorbent versus 1.64 for reference adsorbent. Despite encouraging results, the metal chelating approach was not further exploited. The main reason for this could be the limitation of such an approach solely to protein targets that have exposed histidines residues on their surface. Additionally, metal chelating groups provide strong anchoring points for non-specific interactions, which in real samples might seriously impede specific recognition.

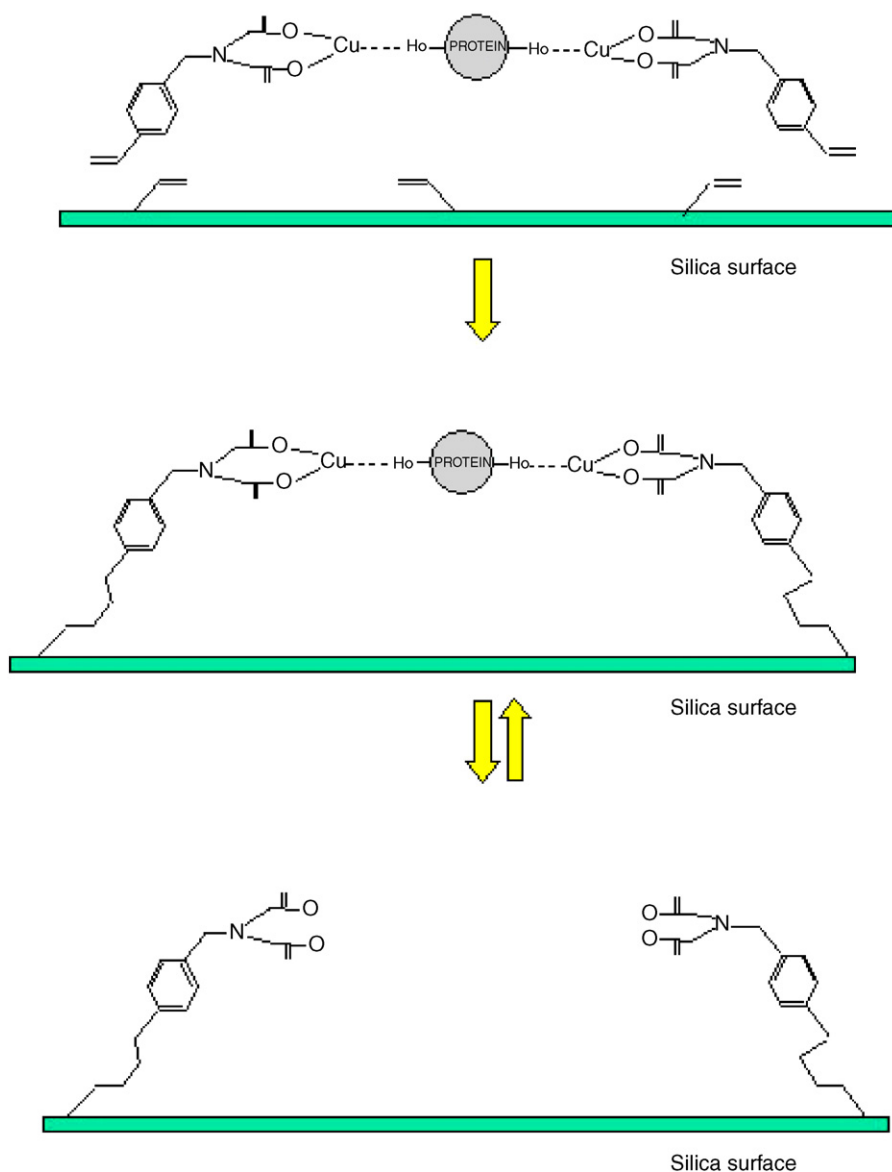


Fig. 2. Schematic representation of the metal-chelate approach (modified from Kempe and Mosbach, 1995; Kempe et al., 1995).

## 2. Shape recognition with polyacrylamide gels

Contemporaneous to the work of Kempe, in the mid-1990s, Hjertèn and co-workers were engaged in the development of a different approach to create molecularly imprinted polymers for the recognition of proteins. They chose to use a “soft” polyacrylamide (PAA) gel as matrix (Hjerten et al., 1997; Liao et al., 1996). This choice was motivated by the inert nature of PAA, its biocompatibility and its neutrality, thus non-specific interactions with proteins were expected to be minimised (Hjerten, 1962; Hjerten and Mosbach, 1962). The PAA gels, made of acrylamide and *N,N'*-methylene-bisacrylamide, mixed at different ratios, were imprinted with the following proteins: ribonuclease (RNase), haemoglobin, lysozyme, myoglobin and human growth factor (HGF) peptide. PAA imprinted gels were then pressed through a 100-mesh net to produce granules, which were packed into chromatographic columns. Each imprinted PAA

polymer was tested for its binding affinity. The results showed that polymers had high recognition abilities (evaluated by measuring the differences in protein retention times on imprinted and non-imprinted columns). For example, the column prepared with RNase as template, was able to adsorb only RNase and not the competitor (haemoglobin). Of particular interest was the demonstration of the ability of the PAA-imprinted polymers to discriminate between two homologous proteins that differ only in 20 residues of a total sequence of 153 residues. In this case, a column prepared using myoglobin from horse as template was proven to recognise, i.e. adsorb, this template but not myoglobin from whale.

The PAA-soft-gel imprinting approach demonstrated a higher specificity and a broader applicability as compared with the metal-chelate approach. Moreover, the PAA-templating approach has been later modified by the incorporation of chargeable functional monomers in the polymeric backbone. The use

of acrylic acid together with acrylamide and *N,N*-dimethylaminopropyl-acrylamide was described in the preparation of a material for the recognition of lysozyme (Hirayama et al., 2001). Silica beads covered with a lysozyme-imprinted polymer layer were demonstrated to selectively adsorb the template, respect other proteins, i.e. haemoglobin. Such imprinted polymer was then exploited with success for the fabrication of a quartz crystal microbalance sensor targeted for lysozyme recognition (Hirayama et al., 2001).

In another paper, both methacrylic acid and 2-(dimethylamino)-ethyl-methacrylate were used for the preparation of a recognition polymer targeted for lysozyme binding (Ou et al., 2004). The imprinting factor, calculated as a binding ratio between MIP and control polymers, for lysozyme was 1.83. Binding was demonstrated to be dependent on ionic strength, cross-linking degree and amount of template removal. The lysozyme-imprinted polymer was also tested for the binding of cytochrome *c*, which has a molecular weight and isoelectric point (*pI*) similar to lysozyme, and for the binding of albumin, which differs greatly in dimensions and charge. In contrast to the results obtained by Hjerten, the results indicated that the imprinted polymer could not discriminate efficiently between different proteins.

Despite some promising results, soft-gel imprinting with proteins still suffer from limitations, in particular with the difficulties of template removal. In this respect a recent paper (Hawkins et al., 2005) investigates on the efficiency of the washing methods, for template-protein removal. In the case, the template removal strategy exploits the combination of a strong cationic surfactant, sodium dodecyl sulfate (SDS), in combination with acetic acid and compare the efficiency of already in-use protocol, based on trypsin digestion, showing a superior removal efficiency for the employment of surfactant.

To our judgement, a main limitation of PAA gels is the softness and the limited mechanical strength of such material. Strategies to overcome such issue are highly welcomed. Guo and co-workers proposed a possible answer. They developed a new method for derivatising beads made of PAA gel. In order to improve the mechanical strength of PAA gel, macroporous chitosan beads were used as matrix. Chitosan is a natural polysaccharide, a biopolymer comprising *D*-glucosamine and *D*-acetyl-glucosamine, which is non-toxic and bio-adsorbable. The soft polyacrylamide gel is entrapped in the chitosan beads and so the polymer beads obtained possess good mechanical

strength and chemical stability, as well as hydrophilicity (Guo et al., 2004). The selectivity test for chitosan–PAA MIPs was carried out using bovine serum albumin (BSA) as reference protein and haemoglobin (Hb) as template, evaluating the amount of each protein adsorbed to the MIP under equilibrium conditions. The distribution coefficient,  $K_D$  is defined as:  $K_D = 1/4 C_p \times C_s$  (where  $C_p$  is the concentration of protein on the MIP beads (mg/g) and  $C_s$  is the concentration of protein in the solution (mg/ml)). Generally, beads show a high specificity degree versus template molecule with respect to the protein reference ( $K_D$  for Hb is average 40 versus  $K_D = 1.7$  for BSA). Thus, the chitosan–PAA MIPs represent a fine and relatively easy strategy for reinforcing PAA porous gels, while maintaining a good degree of selectivity. Selectivity was demonstrated to be strongly related to the shape of the protein template. Hb and BSA are both globular proteins, but Hb is a tetrameric protein composed of pairs of two different polypeptide chains and has biconcave shape. BSA consists of one polypeptide and has an ellipsoidal shape. Results showed that the cavities formed in the MIP recognised preferentially Hb, indicating that cavities matched the size of Hb better than BSA.

### 3. Epitope approach: exploiting a small structural element of the protein for its whole recognition

In nature, antibody–antigen interactions depend on the recognition between the antibody and an antigenic site of the protein, the epitope. The epitope is a short amino-acid sequence complementary to binding site of antibody. In the field of molecular imprinting, Rachkov and co-workers applied this observation to develop a new concept for the synthesis of protein recognition polymers (Rachkov and Minoura, 2000, 2001). Instead of the whole proteins, a short peptide sequence, often exposed at the protein surface, was used as a template for MIP preparation. Once the matrix has been polymerised the resultant imprinted material should be able to recognize and bind the whole protein. The concept was proven using as a template a short sequence (3–4 residues) of a bioactive peptide (Fig. 3).

In their studies, Rachkov and co-workers created an imprinted polymer specific for the nona-peptide oxytocin, a neurohypophyseal hormone (Cys-Tyr-Ile-Gln-Asn-Cys-Pro-Leu-Gly-NH<sub>2</sub>). A small oxytocin sequence of three amino acids proved to be enough for recognition of the whole sequence by the MIP. The polymer was made of methacrylic acid (MAA) and ethyl-

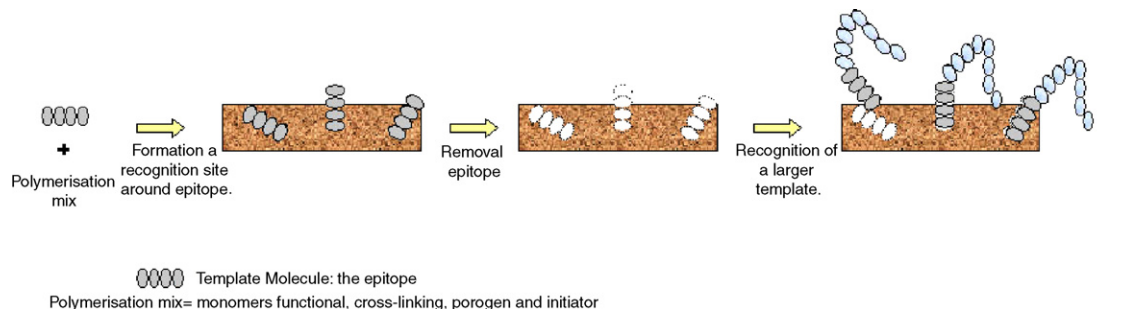


Fig. 3. Schematic representation of the epitope approach (modified from Rachkov and Minoura, 2001).

lene glycol di-methacrylate (EGDMA). HPLC columns packed with epitope-imprinted polymers were used to define the optimal pH and ionic strength conditions for the oxytocin–MIP recognition. Ionic strength was varied in the range 0.5–20 mM, showing that the increase in the salt concentration decreased the template retention time. Thus, ionic interactions gave an essential contribution to the recognition and binding process. The pH for the recognition was carefully chosen since the mobile phase pH played a crucial role in the binding. Another factor affecting the recognition process was the template to functional monomer ratio. The optimum template-peptide/MAA ratio was found to be between 1:10 and 1:20. An accurate tuning of all these parameters allowed the optimal binding conditions for the polymers to be found. To evaluate the selectivity of the MIP, a polymer made of template-peptide/MAA 1:10 was tested for its binding capacity toward the template itself and oxytocin-related peptides. The mobile phase consisted of 10% water/90% acetonitrile, with different concentrations of acetic acid. The values of the separation factor  $\alpha$  (ratio between  $k'$  for tetrapeptide and  $k'$  for oxytocin) depended on the concentration of acetic acid and pH. The best  $\alpha$  value, 3.64, was obtained at pH 6.0 (2.5 mM acetic acid), while at pH 5.0  $\alpha$  value dropped to 1.68.

Subsequently, the epitope-approach was applied for the recognition of the octa-peptide hormone angiotensin II (Rachkov et al., 2004). Moreover, the epitope approach was extended to silica-based materials using double strand DNA as a template (Slinchenko et al., 2004). It is outside of the scope of this review to describe approaches that includes templates different from proteins, but it accounts for a quite broad success and for the versatility of the epitope approach. However, concerning protein recognition, it is difficult to evaluate the true efficiency of the epitope approach, since in all experiments reported by far, the epitope exploited were up to few amino acid long and the template they were intended to mimic were just small peptides, 8–10 amino acid long, thus non-three-dimensionally structured. Concerning the exploitation of the epitope approach for the recognition a protein (sequences above 200 amino acids), attention should be paid to three-dimensional structure of the selected epitopes, as it would play a significant role in recognition.

#### 4. Molecularly imprinted polymers grafted on surfaces

All the approaches described so far make use of polymeric networks extended in 3D-space. It is believed, however, that two-dimensional imprints could have improved binding kinetics by reducing the protracted time needed to attain diffusion-controlled equilibrium in the interior of three-dimensional polymeric matrices (Mirsky et al., 1999). Earlier, Piletsky and co-workers had described a technique for coating polystyrene microplates with a thin polymer made of 3-amino-phenylboronic acid (ABPA). This technique was applied for small molecules, such as atrazine or epinephrine (Piletsky et al., 2001) and for proteins (Piletsky et al., 2000; Bossi et al., 2001). In the case of protein imprinting, after optimisation of washing and re-binding conditions, MIP plates were tested for their binding selectivity. The authors used lactoperoxidase, haemoglobin, horseradish peroxidase, cytochrome *c* and microperoxidase as

templates, which differed in size and isoelectric points. Rebinding experiments demonstrated that size and charge affected the binding capacity. The results indicate that small proteins have dissociation constants,  $K_d$ , in the  $\mu\text{M}$  range, while large proteins, such as lactoperoxidase, haemoglobin or horseradish peroxidase, have  $K_d$ 's a 1000 times smaller. The significant potential of the surface imprinting approach was demonstrated by the ability of the polymer to discriminate between haemoglobin (Hb) and its glycosylated isoforms (Hb-A1), with  $K_d$  values differing by more than three-fold.

Subsequently, the same approach was exploited by Rick and co-worker for the development of a protein sensor (Rick and Chou, 2005). In this case, poly-APBA was deposited onto a quartz microbalance crystal (QCM), using lysozyme or cytochrome *c* as templates. The authors demonstrated a good selectivity for the template proteins, both on a lysozyme-templated polymer and on a polymer templated with cytochrome *c*. Negligible rebinding was observed for other protein competitors such as albumin or myoglobin. A remarkable achievement of the experiment was the demonstration of the ability of imprinted polymer to recognise two proteins, lysozyme and cytochrome *c* when used simultaneously as templates.

The extent of this idea, i.e. the creation of specific cavities for a structure more complex than a single protein, was developed by Chou et al. (2005). The novelty of their approach consists in exploiting a micro-contact imprinting for transferring defined protein recognition sites to the MIP prepared onto a glass support. The micro-contact imprinting approach is a chemical structuring method that involves the conformal stamping of self-assembling mono-layers in a specific pattern on a surface, so that it is possible to form recognition sites for templates were formed in a solvent free system. They prepared a single layer on the surface of a microscope cover glass, together with the functional monomer (*O*-4-nitrophenylphosphorylcholine, 4NPPC), the cross-linker (polyethylene glycol 400 di-methacrylate, PEG400MAA) and the template, which was C-reactive protein (CRP), a protein composed of five identical non-glycosylated sub-units of 206 amino acids each, associated into a pentameric structure. Binding experiments demonstrated a good binding capacity for the polymer imprinted with the template protein, equal to  $1 \mu\text{g}/\text{cm}^2$  of CRP bound versus approximately 0.3 and  $0.1 \mu\text{g}/\text{cm}^2$  of human serum albumin and lysozyme, respectively. Under competitive binding conditions, it was demonstrated that the polymer imprinted with CRP is able to bind  $3.78 \text{ ng}/\text{cm}^2$  of CRP protein versus  $0.08 \text{ ng}/\text{cm}^2$  of the competitor protein (in this case human serum albumin). The results indicate that the micro-contact imprinting approach is able to generate MIPs having both good binding capacity and selectivity for the template molecule. It is not clear, however, if MIP imprinted with protein complexes is capable of distinguishing between template of similar size and properties.

#### 5. Immobilising the template on a surface

Another imprinting method is based on the oriented immobilisation of the template molecule on solid sacrificial supports. The growing MIP is polymerised in close contact with the template-



carrying surface. After polymerisation, the support is dissolved by harsh chemical treatment. There are a number of advantages in using a molecule bound onto the surface as template. For example, a template, which is insoluble in the polymerisation mix, can be easily used. Moreover, template immobilisation minimises protein aggregation and the binding surface could be homogenous.

In a paper by Shi et al. (1999), template was deposited over a support surface such as mica, which is hydrophilic and negatively charged. This is important to prevent the denaturation of the adsorbed proteins. The protein template was deposited onto mica. The protein-surface was coated with a disaccharide layer, and next with a thin film (10–30 nm) of hexafluoropropylene. The resulting film was fixed onto a glass cover by using epoxy resin, which was finally cured in an oven. Harsh washes were used to detach the mica support from the imprinted film, leaving cavities complementary to the template and free for a new binding. The selectivity of an imprint for its template protein was proven by competitive binding experiments, estimating the amount of competitor required to cause a 50% reduction in the maximum adsorption ( $R_{50}$ ). To investigate the shape specificity, two proteins which were very similar in physical chemical properties and isoelectric point were used, namely lysozyme and ribonuclease A (RNAase). In the case of RNAase adsorption from a mixture of lysozyme and RNAase, there was a 20-fold increase in selectivity for RNAase for the RNAase imprint. This demonstrates the high specificity of template recognition achieved in the case and accounted for the far superior homogeneity of binding sites achievable through template immobilisation.

## 6. Silica-based materials imprinted for protein recognition

The first attempt of protein imprinting reported in literature made use of silica materials (Glad et al., 1985), these results surely indicated that silane imprints could discern differences in tertiary structure of proteins. As consequence, the

imprinting of proteins onto silicates and polysiloxanes was explored by quite a number of groups in the following years. Particularly, Venton and Gudipati (1995a,b), demonstrated that organo-functional side chains of silica-based monomers tended to associate complementary with residues on the protein surface, during the polymerisation process, this leading to the formation of complementary binding pockets in the polysiloxane, capable of protein recognition. The polymer made of 3-aminopropyltriethoxysilane and tetraethylorthosilicate (1:3 molar ratio) in the presence a specific protein (urease or bovine serum albumin (BSA)) was able to recognize the protein, previously used for imprinting. The preferential binding suggested the protein surface chemistry was inducing a complementary order in the polymer during the polymerisation process. Further, in order to investigate deeper the process of monomer's assembling around the template during the polymerisation, two closely related protein were studied (radio-labeled haemoglobin  $^{125}\text{I}$ -Hb and radio-labeled myoglobin  $^{125}\text{I}$ -Mb). It was demonstrated that once the template protein rebind the recognition sites onto the polymer, it does not equilibrate with the labelled protein in solution, indicating a very tight association with the polymer surface (although no dissociation constant were calculated in the paper). Results accounted silica materials as very promising for protein imprinting. Moreover, a major advantage of silica is the stability of the imprints, on the contrary to soft-gels, which are subjected to swelling.

Silica-based monomers were exploited from to create imprinted polymer for the recognition of Ricin, a glycoprotein consisting of two polypeptide chains A and B, which are joined by a disulphide bond (Lulka et al., 2000). The imprinted polymer was made of 2-hydroxy-ethyl-aminopropyltriethoxysilane and tetraethoxysilane (3:1) prepared according to a recipe already proposed (Glad et al., 1985). The template binding monitored exploiting intrinsic fluorescence of Ricin. The results demonstrated that molecular imprint exhibited high affinity for both Ricin chain A and chain B and for Ricin. The  $K_d$  calculated, in according to Scatchard analysis shows that the value is 107 nM for chain A and 100.5 nM for chain B. These data accounts for

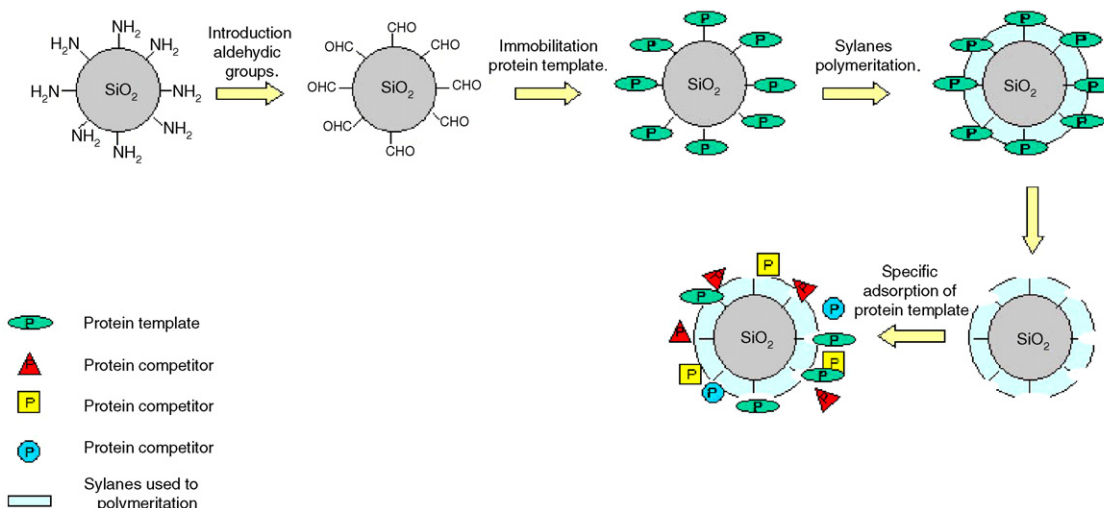


Fig. 4. Schematic representation of the protein imprinting using immobilised template on silica beads (modified from Shiomi et al., 2005).

the usefulness of intrinsic fluorescence as detection method in combination with molecular imprints (Fig. 4).

The versatility of organo-silanes for creation of imprinted polymer was fully proven. A recent paper, published in 2005 (Shiomi et al., 2005), exploits another approach based on the use of the silanes monomers, conjugating the silica material to the concept of template immobilisation. In the case, the protein template is not free in the polymerisation mixture but it is covalently anchored to supporting silica beads. The protein (haemoglobin) is at first covalently immobilised on the derivatised silica surface, then the polymerisation took place. A comparison between such imprinted materials and imprinted silica beads obtained with conventional non-immobilised haemoglobin template is performed, showing the immobilised template give rise to a slightly higher binding capacity for the template, but to a far better performance in competitive binding experiments: MIPs were able to bind the template specifically, while other proteins such as transferrin and chymotrypsinogen A, were practically non-absorbed. Results indicate the formation of more homogeneous binding cavities achieved through the immobilisation of the template. However, proteins with charge status similar to the template protein, such as myoglobin, with a *pI* almost the same as haemoglobin, appear to be slowly sequestered by MIPs from solution for pro-longed incubation times. Nevertheless, imprinting with immobilised template is to be considered as very promising way to create biomaterials for separation and sensing. In addition, immobilised template could be used for repetitive re-creation of imprinted layers, thus being promising for a mass production of recognition layers, which could be exploited, e.g. in sensors fabrication (Shiomi et al., 2005).

## 7. Conclusions and future perspectives

Molecular imprinting technology has gained considerable momentum in its development since 1990. Important results have been achieved and discussed elsewhere with imprinting experiments using small molecules, such as peptides or amino acids. As regarding proteins, MIP development has been considerably slower, because it is quite difficult to create polymer cavities specific for complex molecules such as proteins. The problems associated with imprinting of relatively unstable three-dimensional conformations, possible rearrangement processes and poor solubility of the template in organic solvents are usually the main reasons why the imprinting of proteins remains difficult. Different approaches have been developed to overcome these problems, the most important of which have been briefly discussed in this review. It is clear that more work is needed in order to make protein imprinting a truly practical approach for molecular recognition in diagnostics, separations, drug delivery and other applications demanding accurate discrimination of these critical components of living systems.

## References

- Andersson, L.I., Muller, R., Vlatakis, G., Mosbach, K., 1995. *Proc. Natl. Acad. Sci. U.S.A.* 92 (11), 4788–4792.
- Bossi, A., Piletsky, S.A., Piletska, E.V., Righetti, P.G., Turner, A.P.F., 2001. *Anal. Chem.* 73 (21), 5281–5286.
- Burow, M., Minoura, N., 1996. *Biochem. Biophys. Res. Commun.* 227 (2), 419–422.
- Chou, P.C., Rick, J., Chou, T.C., 2005. *Anal. Chim. Acta* 542 (1), 20–25.
- Dickert, F.L., Hayden, O., 2002. *Anal. Chem.* 74 (6), 1302–1306.
- Glad, T., Glad, M., Norrlöw, S., Sellergren, B., Siegbahn, N., Mosbach, K., 1985. *J. Chromatogr.* 347 (2), 11–23.
- Guo, T.Y., Xia, Y.Q., Hao, G.J., Song, M.D., Zhang, B.H., 2004. *Biomaterials* 25 (27), 5905–5912.
- Hawkins, D.M., Stevenson, D., Reddy, S.M., 2005. *Anal. Chim. Acta* 542 (1), 61–65.
- Hirayama, K., Sakai, Y., Kameoka, K., 2001. *J. Appl. Polym. Sci.* 81 (14), 3378–3387.
- Hjerten, S., 1962. *Arch. Biochem. Biophys. Suppl.* 1, 147–151.
- Hjerten, S., Mosbach, R., 1962. *Anal. Biochem.* 3, 109–119.
- Hjerten, S., Liao, J.L., Nakazato, K., Wang, Y., Zamaratskaia, G., Zhang, H.X., 1997. *Chromatographia* 44 (6), 227–235.
- Katz, A., Davis, M.E., 2000. *Nature* 403 (6767), 286–289.
- Kempe, M., Glad, M., Mosbach, K., 1995. *J. Mol. Recognit.* 8 (1/2), 35–39.
- Kempe, M., Mosbach, K., 1995. *J. Chromatogr. A* 691 (1/2), 317–323.
- Liao, J.L., Wang, Y., Hjerten, S., 1996. *Chromatographia* 42 (5/6), 259–262.
- Lulka, M.F., Iqbal, S.S., Chambers, J.P., Valdes, E.R., Thompson, R.J., Goode, M.T., Valdes, J.J., 2000. *Mater. Sci. Eng. C* 11 (2), 101–105.
- Mallik, S., Jhonson, R.D., Arnold, F.H., 1994a. *J. Am. Chem. Soc.* 116 (20), 8902–8911.
- Mallik, S., Plunkett, S.D., Dhal, P.K., Johnson, R.D., Pack, D., Shnek, D., Arnold, F.H., 1994b. *New J. Chem.* 18 (3), 299–304.
- Minoura, N., Rachkov, A., 2000. *J. Chromatogr. A* 889 (1/2), 111–118.
- Mirsky, V.M., Hirsch, T., Piletsky, S.A., Wolfbeis, O.S., 1999. *Angew. Chem. Int. Ed.* 38 (8), 1108–1110.
- Mosbach, K., 1994. *Trends Biochem. Sci.* 19 (1), 9–14.
- Nicholls, I.A., 1995. *Chem. Lett.* 11, 1035–1036.
- Ou, S.H., Wu, M.C., Chou, T.C., Liu, C., 2004. *Anal. Chim. Acta* 504 (1), 163–166.
- Pampi, P., Kofinas, P., 2004. *Biomaterials* 25 (10), 1969–1973.
- Piletsky, S.A., Piletska, E.V., Chen, B., Karim, K., Weston, D., Barret, G., Lowe, P., Turner, A.P.F., 2000. *Anal. Chem.* 72 (18), 4381–4385.
- Piletsky, S.A., Piletska, E.V., Bossi, A., Karim, K., Lowe, P., Turner, A.P.F., 2001. *Biosens. Bioelectron.* 16 (9–12), 701–707.
- Rachkov, A., Minoura, N., 2000. *J. Chromatogr. A* 889 (1/2), 111–118.
- Rachkov, A., Minoura, N., 2001. *Biochim. Biophys. Acta* 1544 (1/2), 255–266.
- Rachkov, A., Hu, M.J., Bulgarevich, E., 2004. *Anal. Chim. Acta* 504 (1), 191–197.
- Rick, J., Chou, T.C., 2005. *Anal. Chim. Acta* 542 (1), 26–31.
- Shi, H.Q., Tsai, W.B.I., Garrison, M.D., Ferrari, S., Ratner, B.D., 1999. *Nature* 398 (6728), 593–597.
- Shiomi, T., Matsui, M., Mizukami, F., Sakaguchi, K., 2005. *Biomaterials* 26 (27), 5564–5571.
- Slinchenko, O., Rachkov, A., Miyachi, H., Ogiso, M., Minoura, N., 2004. *Biosens. Bioelectron.* 20 (6), 1091–1097.
- Venton, D.L., Gudipati, E., 1995a. *Biochim. Biophys. Acta* 1250 (2), 117–125.
- Venton, D.L., Gudipati, E., 1995b. *Biochim. Biophys. Acta* 1250 (2), 126–136.
- Wulff, G., 1993. *Trends Biotechnol.* 11 (3), 85–87.
- Yilmaz, E., Haupt, K., Mosbach, K., 2000. *Angew. Chem. Int. Ed.* 39 (12), 2115–2118.

# N-Terminal Deletion Affects Catalytic Activity of Saporin Toxin

Francesca Bonini,<sup>1</sup> Roberta Traini,<sup>1</sup> Fabrizio Comper,<sup>1</sup> Giulio Fracasso,<sup>1</sup> Rossella Tomazzoli,<sup>2</sup> Mauro Dalla Serra,<sup>2</sup> and Marco Colombatti<sup>1\*</sup>

<sup>1</sup>Department of Pathology, Section of Immunology, University of Verona, Italy

<sup>2</sup>ITC & CNR, Institute of Biophysics, Section of Trento, Povo (Trento), Italy

**Abstract** Single-chain ribosome inactivating proteins (RIPs) are cytotoxic components of macromolecular pharmaceuticals for immunotherapy of cancer and other human diseases. Saporin belongs to a family of single-chain RIPs sharing sequence and structure homology. In a preliminary attempt to define an active saporin polypeptide of minimum size we have generated proteins with deletions at the N-terminus and at the C-terminus. An N-terminal (sapΔ1–20) deletion mutant of saporin displayed defective catalytic activity, drastically reduced cytotoxicity but increased ability to interact with liposomes inducing their permeabilization at low pH. A C-terminal (sapΔ239–253) deletion mutant showed instead a moderate reduction in cytotoxic activity. A substantial alteration of secondary structure was evidenced by Fourier transformed infrared spectroscopy (FTIR) in the sapΔ1–20 mutant. It can be hypothesized that the defective functions of sapΔ1–20 are due to alterations of its spatial configuration. *J. Cell. Biochem.* 98: 1130–1139, 2006.

© 2006 Wiley-Liss, Inc.

**Key words:** saporin; catalytic activity; secondary structure; ribosome inactivating proteins

Ribosome inactivating proteins (RIPs) from plants are toxic translation inhibitors that inactivate ribosomes by catalyzing the hydrolysis of a specific N-glycosidic bond of large rRNA [Barbieri et al., 1993]. RIPs have been classified into two types; type I RIPs, for example, saporin, trichosanthin, and pokeweed antiviral protein (PAP), are single-chain proteins lacking a second cell-binding domain unlike their type II

counterparts that include ricin and abrin. Because of the absence of a binding domain, the single-chain type I RIPs lack the non-specific cytotoxicity shown by the type II RIPs and are, therefore, toxins of choice for the construction of immunotoxins. Thus, they are useful for treating cancer and autoimmune diseases and also against HIV infection [McGrath et al., 1989]. By virtue of their antiviral properties, type I RIPs might also be used to improve defence mechanisms of transgenic plants of interest [Lodge et al., 1993; Taylor et al., 1994].

Structure comparisons between saporin and other RIPs revealed that the catalytic site and the general 3-D organization are very similar [Savino et al., 2000]. Several isoforms of saporin with different chromatographic properties have been described [Barbieri et al., 1993] and some of them have been obtained in recombinant form [Barthelemy et al., 1993]. The isoform SO6 conjugated with vehicle molecules has been successfully applied to eradicate target cells in vitro and in vivo [Barthelemy et al., 1993]. SO6 is made up of two domains, the N-terminal domain which is predominantly  $\beta$ -stranded, and the C-terminal domain which is predominantly  $\alpha$ -helical. The N-terminal domain is very similar to that of other RIPs [Savino et al., 2000]. The

Abbreviations used: RIPs, ribosome inactivating proteins; SO6, major isoform of saporin extracted from seeds; RTA, ricin toxin A-chain; APRT, adenine phosphoribosyl transferase; LUVs, large unilamellar vesicles; FTIR, Fourier transformed infrared spectroscopy; PC, phosphatidylcholine; PA, phosphatidic acid.

Francesca Bonini and Roberta Traini contributed equally to this work.

Grant sponsor: MIUR; Grant number: PRIN 2003; Grant sponsor: Fondazione Cassa di Risparmio di Verona, Vicenza, Belluno e Ancona.

\*Correspondence to: Marco Colombatti, MD, Sezione di Immunologia, Dipartimento di Patologia, Università di Verona, c/o Policlinico "G.B.Rossi", L.go L.A.Scuro 10, I-37134 Verona, Italy. E-mail: marco.colombatti@univr.it

Received 3 October 2005; Accepted 12 January 2006

DOI 10.1002/jcb.20845

© 2006 Wiley-Liss, Inc.

C-terminal domain contains eight  $\alpha$ -helices with canonical geometry. The active site residues Glu176, Arg179, and Trp208 of saporin are completely superimposable with those of other RIPs and in the C-terminal region three lysyl residues (220, 226, and 234) have been identified which map a structural motif highly conserved in all RIPs and possibly involved in the enzyme-substrate molecular recognition mechanism [Savino et al., 2000]. Structure-based alignments show that positively charged or polar residues are located in the corresponding positions of the RIPs PAP, momordin (MOM), and ricin toxin A-chain (RTA). RTA is the most studied representative of a number of RIPs that are under investigation for application in human diseases. Thus, substantial efforts have been made to relate the structure of RTA to its mechanism of action. Using deletion mutants it was initially demonstrated that in RTA the sum of all aminoacids that can be removed from various constructs without loss of activity amounts to 83%, indicating that a large number of the residues is neither absolutely essential for folding into an effective conformation nor for catalysis [Morris and Wool, 1992]. However, deleting the first nine residues from the N-terminus of RTA did not affect toxicity whereas deleting further three residues inactivated the polypeptide [May et al., 1989]. Bagga et al. [2003a] have demonstrated that point mutation of Tyr 16 of saporin drastically affects its catalytic activity. Mutated saporin retained, however, a substantial cytotoxicity against cell cultures, indicating that other functions besides its N-glycosylase activity could be responsible for saporin effects or that other N-terminal residues may be involved in saporin functions and/or its structural stabilization. These studies reinforce the conviction that deletion analysis is a valuable procedure for defining the overall role of discrete protein domains in saporin function and the minimal cohort of aminoacids necessary for substrate recognition and for catalysis. Considering the structural similarities between RTA and saporin, we have set out to initiate a systematic study of structure-function relationships in saporin based on a deletion approach. In the present study, we have investigated the role of discrete saporin domains using one N-terminal and one C-terminal deletion mutants. The results obtained support the notion that the N-terminal 20 aminoacids are crucial for enzymatic activity and for folding.

## MATERIALS AND METHODS

### Cloning, Expression, and Purification of Saporin Isoforms

Plasmid isolation, preparation of competent cells and transformation, and DNA manipulations were carried out according to published procedures [Sambrook et al., 1989].

To obtain saporin deletion mutants we used the genomic clone 4 (G4) [Barthelemy et al., 1993] cloned in pET-11d (Novagen). The construct used was pET-11d-SAP3 in which a *SacII-EcoRI* fragment from sequence three DNA [Barthelemy et al., 1993] was ligated to pET-11d-DNA digested with *EcoRI* and *NcoI* in the presence of a linker-adapter containing *NcoI-SacII* sites. The construct pET-11d-SAP3 [Fabbrini et al., 1997] was kindly supplied by Dr. S. Fabbrini (Department of Biological and Technological Research—Dibit, San Raffaele Scientific Institute, Milan, Italy). pET-11d-SAP3 was PCR-mutated to create two different mutants deleted of 20 aminoacids at the N-terminus (sap $\Delta$ 1–20), and of 15 aminoacids at the C-terminus (sap $\Delta$ 239–253), respectively.

**Synthetic oligonucleotides.** The primers used to obtain the mutant sap $\Delta$ 1–20 were: (1) *Oligo-“sense”* 5'-GAGATATACCATGGTCACATCAATC-3' (in which an *adapter* CCATGG corresponding to an *NcoI* restriction site was inserted for ease of cloning), (2) *oligo-“anti-sense”* CCGGAATTCTACACCTGCCTCAC-TT-TTCC (containing an *EcoRI* restriction site). The primers used to obtain the mutant sap $\Delta$ 239–253 were: (1) *Oligo-“sense”* GCGCCATGGATAAAATCCGAAAC and (2) *oligo-“anti-sense”* TCTTGAAGAATTCGCCTC-GTT (which contains an *adapter* introducing the stop codon (TAG) and an *EcoRI* restriction site).

**Polymerase chain reaction.** Reactions were carried out with 0.5  $\mu$ g of pET-11d-SAP3 in 50  $\mu$ l, 10 mM Tris-HCl (pH 8.3), 50 mM KCl, 1.5 mM MgCl<sub>2</sub>, 0.2 mM deoxynucleotide triphosphates, and 0.15 mM of each primer. One unit of DNA Polymerase AmpliTaqGold™ (Invitrogen, Carlsbad, CA) was then added and incubations carried out in a GeneAmp PCR System 2400 (Perkin-Elmer, Wellesley, MA). Amplification cycles consisted of a denaturation step (94°C for 1 min), an annealing step (55°C for 1 min), and an elongation step (72°C for 1 min). After 25 cycles an aliquot of each reaction was loaded onto a 0.8% agarose gel.

**Transformation.** The *Escherichia coli* strain BL21(DE3)pLysS (Novagen, Milan, Italy) was transformed with the different constructs of saporin according to the manufacturer's instructions.

**Expression of saporin isoforms.** Hundred milliliter of LB-medium, complemented with 100 µg/ml ampicillin and 35 µg/ml chloramphenicol, was inoculated with one transformed colony of *E. coli* strain BL21(DE3)pLysS and incubated overnight at 37°C, with stirring. Total volume was then brought to 1 L with LB-medium additioned with 100 µg/ml ampicillin and 50 µg/ml chloramphenicol, and the cells were incubated at 37°C. Expression of heterologous proteins was induced by adding 1 mM isopropyl-β-thiogalactopyranoside (IPTG) and subsequent incubation for 3 h at 30°C. Bacteria were then pelleted (5000 rpm, 15 min at 4°C) and lysed with 50 mM Tris, 2 mM EDTA, pH 8.0, complemented with 1× complete protease inhibitor (Roche, Basel, Switzerland). After lysis the cells were sonicated on ice in 3 × 45 s bursts using a Labsonic-U ultrasonic disintegrator (B. Braun Biotech International, Melsungen, Germany). Lysates were then centrifuged (20 min, 22,000 rpm at 4°C) and the supernatant dialyzed overnight against 5 mM Na<sub>2</sub>HPO<sub>4</sub>, 5 mM NaH<sub>2</sub>PO<sub>4</sub> buffer pH 6.5 at 4°C.

**Purification.** The supernatant was filtered with a 0.5 µm Millipore filter to eliminate debris and subjected to FPLC chromatography with a High-S cartridge column (Bio-Rad, Richmond, CA) equilibrated in 5 mM phosphate buffer, pH 6.5, wild type (wt) saporin or its mutants were eluted with a 0–300 mM NaCl gradient. Saporin isoforms were then further purified by gel filtration chromatography with a Superdex 75 (Hi Load 16/60, Pharmacia, Uppsala, Sweden) column equilibrated in PBS and run at 1 ml/min.

**Western blotting.** The purity of the purified proteins was then checked by SDS-PAGE and Western blotting using an antisaporin antibody from rabbit (kindly supplied by Dr. Fabbrini). Analysis by SDS-PAGE was as described in [Sambrook et al., 1989] using 12.5% (w/v) acrylamide separating gels. For Western blot analysis, proteins transferred onto nitrocellulose were probed with a rabbit antirabbit-horseradish peroxidase-conjugate antiserum (Sigma, St. Louis, MO). The major isoform of saporin isolated from seeds (SO6) was used in our investigation [Barbieri et al., 1993]. SO6 was kindly supplied by Dr. S. Fabbrini.

### Determination of Enzymatic Activity

The enzymatic activity of saporin isoforms was determined as described in [Heisler et al., 2002] by measuring adenine release from a substrate in a colorimetric assay. Briefly, samples of saporin isoforms were separately incubated with denatured herring sperm DNA (Gibco BRL, Gaithersburg, MD) at different concentrations (0.5–50 pmol) for 2 h at 30°C. Ethanol (100 µl, –20°C) was then added and the precipitate was pelleted by centrifugation (13,000 rpm for 30' at 4°C). The supernatant was vacuum-dried, resuspended in 50 µl water and transferred to modular 96-well microplates (Nunc, Wiesbaden, Germany). To each sample 100 µl of cold "basic master mix" (8 µl adenine phosphoribosyl transferase (APRT) (0.3 µg/µl), 2 µl purine nucleoside phosphorylase (PNP) (100 U/ml) (Molecular Probes, Eugene, OR), 3 µl 5-phospho-D-ribose-1-α-pyrophosphate (PRPP) (10 mM) (Sigma), 50 µl 2-amino-6-mercapto-7-methylpurine ribonucleoside (MESG) (1 mM) (Molecular Probes), 17.5 µl reaction buffer (400 mM Tris, 20 mM magnesium chloride, 2 mM sodium azide) and 50 µl of cold "starter mix" (10 µl inorganic phosphatase (1 U/ml) (Sigma), 5 µl 5'-nucleotidase (5 U/ml) (Sigma), 2.5 µl reaction buffer (see above) were added to start inorganic phosphate release and thus the colorimetric reaction. The kinetics of adenine release was monitored every 5 min with a microplate reader (VERSA max, Molecular Device, Sunnyvale, CA). The adsorbance measured at 360 nm was converted into a turnover rate by using a standard curve of adenine concentration.

### Cytotoxicity

The cytotoxic activity of saporin isoforms was compared in protein-synthesis-inhibition assays. Cells (Jurkat, human leukaemia, and DU145, human prostate carcinoma) were from the American Tissue Culture Collection (Rockville, MD). Protein synthesis was measured by dispensing 5 × 10<sup>4</sup> cells in leucine-free RPMI-1640 medium (complemented with FBS 10% and glutamine 5%) in 96-well flat-bottomed microtitration plates. Saporin isoforms (ten-fold dilutions of toxins in 10 µl of PBS/BSA 0.2%) were then added (final volume, 100 µl) and samples tested in triplicates. Microcultures were incubated for 24 h, followed by a 4 h pulse with 1 µCi of [<sup>14</sup>C]-leucine. At the end of the

assay, the cells were washed with water and harvested onto glass-fiber filters (Dynatech, Chantilly, VA). Radioactivity incorporated by the cells was then measured in a beta-spectrometer (Wallac 2406). Mock-treated controls supplied the incorporation values corresponding to 100% protein synthesis.

#### Interaction With Large Unilamellar Vesicles

The interaction of saporin and saporin mutants with model membranes was investigated using a membrane permeabilization assay of large unilamellar vesicles (LUVs) prepared by extrusion technique [MacDonald et al., 1991].

**Preparation of vesicles.** LUVs were made by phosphatidylcholine (PC), phosphatidic acid (PA) (Avanti Polar Lipids, Alabaster, AL) or PA and PC at a 1:1 molar ratio. Lipid films were formed by removing chloroform from a lipid solution in a rounded flask with rotary evaporation and final vacuum drying (1 h). Multilamellar liposomes (at a total lipid concentration of 5 mg/ml) were suspended in a solution containing 80 mM calcein and subjected to six cycles of freezing and thawing. Using a two-syringe extruder (liposofast Basic unit; Avestin, Ottawa, Canada) they were repeatedly (31 passages) passed through two-stacked polycarbonate filters bearing holes of 100-nm diameter (Millipore, Billerica, MA). To remove untrapped calcein, the vesicles were spun through minicolumns (Phenomenex, Torrance, CA) loaded with Sephadex G-50 (medium, Sigma) pre-equilibrated with 140 mM NaCl, 20 mM HEPES and 1 mM EDTA, pH 7.0. Dimension and homogeneity of the vesicles were routinely estimated by dynamic light scattering using a Malvern Zeta-Sizer three apparatus (Malvern Instruments, Malvern, UK).

**Permeabilization assay.** Permeabilization was determined by measuring the fluorescence of calcein released from the vesicles [Kayalar and Duzgunes, 1986], using a fluorescence microplate reader (Fluostar Galaxy, Offenburg, Germany). Fluorescence was induced by excitation at 480 nm through a narrow-band interference filter, and was detected after a second interference filter centered at 540 nm.

Each well of a white microtitration plate (Greiner Bio-One, Kremsmuenster, Austria) was pre-incubated with prionex 0.1 mg/ml (Pentapharm, Basel, Switzerland) and filled

with 100  $\mu$ l of buffer (140 mM NaCl, 20 mM HEPES, 1 mM EDTA for pH 7.0 and 140 mM NaCl, 20 mM MES, 1 mM EDTA for pH 4.0, 5.0, and 6.0) plus 100  $\mu$ l of LUVs in the same solution. The final toxin concentrations were variable, and are reported in the text. After mixing vesicles and toxins, the release of calcein from the vesicles produced an increase in the fluorescence value  $F$  (due to dequenching of the dye into the external medium) which was resolved in time. The values reported are consecutive readings of the same well (taken every 16 s for 45 min). Spontaneous leakage of calcein was usually negligible; when present, it accounted for less than 10% release and it was subtracted on the basis of the spontaneous release observed in control experiments. In some cases fluorescence was measured in a spectrofluorometer (FluoroMax, Longjumeau, France). In these experiments, excitation was set at 494 nm and emission at 520 nm. In both cases, Maximum release was obtained by adding 1 mM Triton X-100 (Merck) (final concentration) and provided the fluorescence value  $F_{\max}$ . The percentage of release,  $R_{\%}$ , was calculated as follows:

$$R_{\%} = (F_{\text{fin}} - F_{\text{in}}) / (F_{\text{max}} - F_{\text{in}}) \times 100$$

where  $F_{\text{in}}$  and  $F_{\text{fin}}$  represent the initial and the final (steady-state) value of fluorescence before and after toxin addition. The experiments were carried out at room temperature.

#### Secondary Structure of Saporin Isoforms

**Fourier transformed infrared spectroscopy.** Fourier transformed infrared spectroscopy (FTIR) spectra were collected in the attenuated total reflection (ATR) configuration, as described in [Menestrina et al., 1999], on a Bio-Rad FTS 185 FTIR spectrometer equipped with a mercury-cadmium-tellurium detector and a KBr beamsplitter. Three samples were analyzed: SO6 and saporin mutants  $\Delta 1-20$  and  $\Delta 239-253$ . For each experiment, 100  $\mu$ g of protein were deposited in a thin layer on one side of a 10-reflection germanium crystal (45° cut), flushed with D<sub>2</sub>O-saturated nitrogen and housed in a vertical ATR attachment (provided by Specac). A number of interferograms (64) were recorded, Fourier transformed and averaged. Absorption spectra in the region between 4000 and 500  $\text{cm}^{-1}$  were obtained using a clean ATR crystal as the background, at a resolution of one point every 0.5  $\text{cm}^{-1}$ . These spectra were

analyzed with the Bio-Rad WIN-IR software package based on GRAMS platform: They were at first corrected by subtracting the absorbance of residual H<sub>2</sub>O and then processed to evaluate secondary structure content. Briefly, the amide I' band, between 1700 and 1600 cm<sup>-1</sup>, was deconvoluted into a set of Lorentzians whose frequencies were assigned to a particular secondary structure in the standard way. The original spectrum was then curve-fitted with this set of Lorentzian components and the relative content of secondary structure elements was eventually estimated by dividing the areas of the individual peaks by the area of the whole amide I' band.

## RESULTS AND DISCUSSION

The purification of saporin (SO6 and recombinant from *E. coli* cultures) and of the deletion mutants yielded preparations of >95% pure intact protein with negligible amounts of contaminants (<5%), as evaluated by SDS-PAGE and by immunoblotting (not shown). Protein samples were used in the assays described below.

### Enzymatic Properties of SapΔ1–20 and SapΔ239–253 Mutants

To assess the enzymatic properties of the various proteins under study we used a test based on the release of adenine, which is in turn proportional to the N-glycosidase activity of the toxin preparations [Heisler et al., 2002]. A standard calibration curve was first established using known adenine concentrations and the enzymatic activity of the different forms of saporin was then titrated and compared on the standard curve. Results are summarized in Table I.

Reduced efficacy of sapΔ1–20 was further confirmed by kinetic assays (Fig. 1). Adenine release reaches a plateau at a much lower level

as compared to wt isoforms of saporin or of sapΔ239–253, indicating that adenine amounts released by the enzymatic reaction are greatly affected. Moreover, calculated initial rate of adenine release values (V<sub>0</sub>) (0.630 nmol/min) are also inferior to those of wt saporins or to sapΔ239–253, which range between 0.79 and 0.812 nmol/min (Table I).

### Interaction of SapΔ1–20 and SapΔ239–253 Mutants With Artificial Membranes

The internalization and intracellular trafficking of a toxin are strongly dependent upon its ability to interact with the membranes of the intoxicated cell. Artificial membrane models mimicking the composition and behavior of cell membranes may, therefore, supply important information as regards internalization and routing mechanisms and possible perturbing factors influencing the cell intoxicating potential of different types of toxins. We have thus investigated the ability of the different saporin isoforms to induce the release of calcein entrapped in LUVs made with phosphatidic acid (PA), phosphatidylcholine (PC), or with an equimolar amount of PA and PC (PAPC). The net superficial charge is one electronic charge for PA and zero for PC phospholipids. Because the intracellular routing of internalized toxins involves compartmentalization within subcellular organelles at low pH, we have measured calcein release at pH values of 4.0, 5.0, and 6.0. Results are expressed as percent maximal release obtained by treating LUVs with the detergent Triton X-100. From summary Table II the following results can be evinced: (1) All forms of saporin interact only weakly with PC LUVs; (2) SO6 has an optimal effect of calcein release at pH 4.0 with PAPC LUVs (>90% release), at pH 5.0 with PA LUVs (>90%) and shows lower efficacy at pH 6.0 with PA LUVs (10–30%); (3) wt recombinant saporin shows a remarkable interaction with PAPC LUVs at

**TABLE I. Comparison of Enzymatic Efficacy of Saporin and its Deletion Mutants**

Toxin	Pmol adenin/pmol toxin/h	% Activity <sup>a</sup>	V <sub>0</sub> (nmol/min)
SO6	492 ± 1	98.4	0.79
Saporin <sub>wt</sub> (recombinant)	500 ± 1	100	0.81
SapΔ1–20	74 ± 1	14.8	0.63
SapΔ239–253	500 ± 0.5	100	0.80

<sup>a</sup>The enzymatic activity of full-length saporin<sub>wt</sub> (recombinant) is taken as 100%.



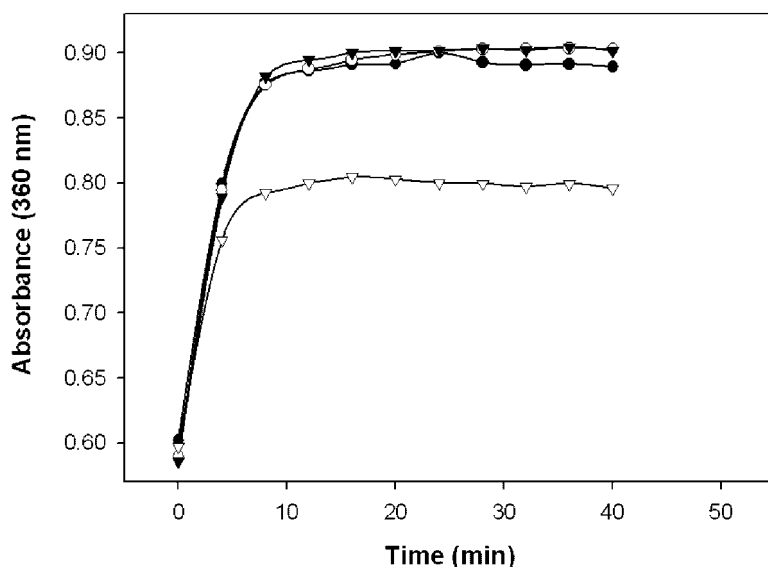


**Fig. 1.** The enzymatic activity of saporin isoforms was determined by measuring adenine release from the substrate denatured herring sperm DNA in a colorimetric assay. The kinetics of adenine release was monitored every 5 min with a microplate reader and the adsorbance measured at 360 nm. Symbols are as follows: Filled circles, SO6; empty circles, wt saporin, recombinant; filled triangles, sap $\Delta$ 239–253; empty triangles, sap $\Delta$ 1–20.

pH 4.0 (60–90% calcein release) but a modest effect on PAPC LUVs at pH 5.0 and on PALUVs at pH 6.0 (10–30% and <10% calcein release, respectively). It appears, therefore, that SO6 and the wt isoform of recombinant origin may differ substantially as regards their ability to effect the release of calcein from LUVs of different composition (from this viewpoint calcein release from PA LUVs at pH 5.0 is particularly significant, Table II). In the deduced structure of SO6 alternative residues in positions 48 and 91 can be present [Savino et al., 2000], therefore, SO6 may exist in at least four different variants. Moreover, in our recombinant form of saporin a Phe is present in position 223 instead of the Val found in SO6 [Barthelemy et al., 1993]. Thus, although these

variations are not likely to induce gross structural or behavioral differences we cannot rule out that at least some of the differences observed between our recombinant form of saporin and SO6 could be ascribed to them. In fact, the heterogenous composition of the sample obtained from seeds could explain the greater calcein release from LUVs treated with SO6 in some instances. Whether this be due to differences in the exposure of hydrophobic patches or to differences in the spatial orientation of protein microdomains remains to be investigated; (4) sap $\Delta$ 239–253 behaves in a manner similar to wt recombinant saporin, that is, strong interaction with PAPC LUVs at pH 4.0 (60–90% calcein release), intermediate and modest interaction with PAPC LUVs at pH 5.0

**TABLE II. Release of Calcein From LUVs of Different Composition**

Toxin (15 $\mu$ g/ml)	PA			PAPC			PC		
	pH 4.0	pH 5.0	pH 6.0	pH 4.0	pH 5.0	pH 6.0	pH 4.0	pH 5.0	pH 6.0
SO6	+++ <sup>a</sup>	+++	±	+++	+	±	–	–	–
Saporin <sub>wt</sub> (recombinant)	±	–	–	++	±	–	±	–	–
Sap $\Delta$ 1–20	++	+	–	+++	++	±	–	–	–
Sap $\Delta$ 239–253	±	±	–	++	+	–	–	–	–

<sup>a</sup>Values represent percentage of calcein release with respect to maximal release induced by treatment with Triton X-100; +++, R > 90%; ++, 60% < R < 90%; +, 30% < R < 60%; ±, 10% < R < 30%; –, R < 10%.



and with PA LUVs at pH 6.0 (30–60% and <10% calcein release respectively); (5) *sap*Δ1–20 displays efficient interaction with PAPC LUVs at pH 4.0 (>90% calcein release) and a considerable effect at pH 5.0 (60–90%). If the two deletion mutants are compared taking the calcein release effect of the wt recombinant form of saporin as 100% under the different conditions, it appears that although their interaction with PC LUVs is negligibly different from that of wt, *sap*Δ1–20 shows a considerable increase (144.7–329.7%) in the ability to effect calcein release from PA and PAPC LUVs. With respect to wt recombinant saporin the deletion mutant *sap*Δ239–253 displays instead similar effects on PA and PAPC LUVs (range of calcein release as a percent of wt recombinant saporin between 17.8 and +114%).

#### Cytotoxicity of *Sap*Δ1–20 and *Sap*Δ239–253 Mutants

To evaluate the effects of deletions on the cell intoxication potential of saporin we measured the cytotoxicity of the different saporin forms in a protein synthesis inhibition assay. The overall cytotoxicity in this case will be dependent upon several complex mechanisms, including binding to the cell surface, internalization kinetics, routing through subcellular compartments, interaction with intracellular membranes, and with molecular chaperones. Cytotoxicity was assayed in two cell lines of different histotype (Jurkat, a human leukemia, and DU145, prostate carcinoma). To rule out intrinsic resistance to ribosome inactivating mechanisms mediated by toxins and to compare the effects of various forms of saporin in cell lines of different histotype, the cytotoxic effects of whole heterodimeric ricin and of its catalytic subunit ricin A-chain were also studied in parallel. The results obtained in cytotoxicity assays are illustrated in Figure 2 and can be summarized as follows: (1) The cytotoxic effects of the wt isoforms of saporin are comparable in the same cell line, although DU145 cells show a greater resistance to intoxication by saporin. This however appears to be due to a general resistance to the effect of toxins, inasmuch as DU145 are less sensitive also to the effects of whole ricin ( $IC_{50}$  of  $6.77 \times 10^{-13}$  M in DU145 cells and of  $1.96 \times 10^{-13}$  M in Jurkat cells; results not shown) and in particular of its catalytic subunit ricin A-chain which, similar to saporin, lacks the ability to bind cell surface structures (Fig. 2); (2) both deletion mutants

display a lower cytotoxicity in Jurkat and DU145 cells although, similar to the effect of wt saporin, the decrease is greater in Jurkat cells. In particular, however, *sap*Δ1–20 shows the greatest loss in cytotoxic activity, as compared to *sap*Δ239–253. Whereas the reduced cytotoxicity of *sap*Δ1–20 could be attributed mostly to a deficiency in catalytic activity, the diminished cell intoxicating effect of *sap*Δ239–253 might be due to more complex phenomena involving interaction with subcellular structures and membranes participating in intracellular routing and cytosol entry processes. In addition, our results with *sap*Δ1–20 allow to conclude that removal of a sizable domain at the N-terminus does not abolish saporin cytotoxicity confirming and extending results by Bagga et al. [2003a] who demonstrated that N-terminally point mutated saporin retained substantial cytotoxicity.

Saporin extracted from seeds of *S. officinalis* has been shown to bind to  $\alpha_2$ -macroglobulin receptor, also called as low-density lipoprotein receptor-related protein (LRP) [Cavallaro et al., 1995]. It was recently found, however, that saporin toxicity is independent of the LRP expression in different cell lines, inasmuch as LRP-negative and LRP-defective cell lines showed the same sensitivity to saporin as LRP-positive cell lines [Bagga et al., 2003b]. Moreover, differences in cytotoxicity between LRP-positive and LRP-negative cell lines of different saporin isoforms were attributed solely to differences in catalytic activity [Bagga et al., 2003b]. It is, therefore, likely that also in our case the main differences could be attributed to mechanisms other than binding to specific cell surface receptors. Indeed, association of saporin to the cell line that we found least sensitive to saporin (i.e., DU145) was superior to the binding observed in a LRP-positive highly sensitive reference cell line (i.e., U937), as evaluated by indirect immunofluorescence and flow cytometry (not shown).

#### Secondary Structure of *Sap*Δ1–20 and *Sap*Δ239–253 Mutants

To investigate if the altered properties displayed by the deletion mutants of saporin could be due to substantial modifications of the protein structural organization, we evaluated secondary structures by means of infrared spectroscopy. To compare our observations with crystallographic data on SO6 [Savino et al.,

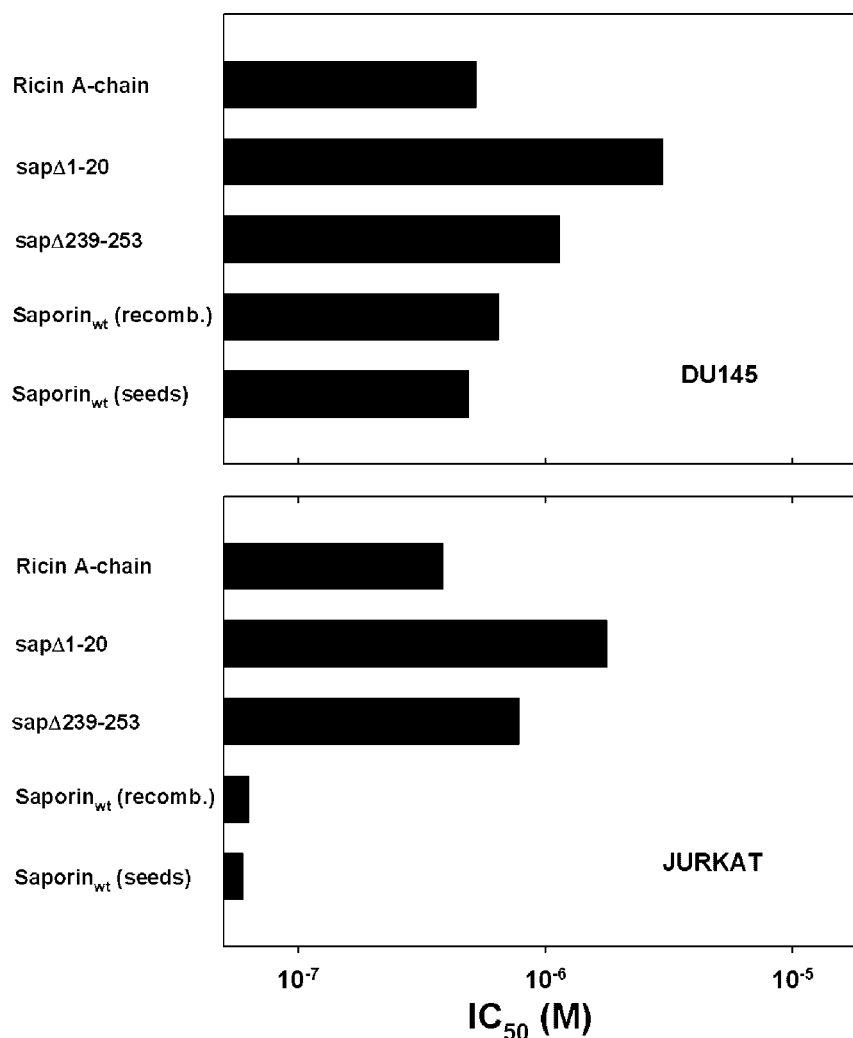


**Fig. 2.** The cytotoxicity of saporin forms was evaluated in a protein synthesis inhibition assay. The dose (mol/L) inhibiting 50% [<sup>14</sup>C]-leucine incorporation (IC<sub>50</sub>) is reported for the two cell lines (Jurkat and DU145) used in the assay. Standard deviation between replicates was <5% and is not reported in the Figure.

2000], we examined SO6 with the recombinant forms of saporin. The secondary structure composition of the different proteins was estimated by deconvolution and curve fitting with a sum of Lorentzians, which were assigned to different structural elements. According to

[Susi and Byler, 1986] the following assignments were used: Band at  $1675 \pm 4 \text{ cm}^{-1}$  or in the region  $1640\text{--}1628 \text{ cm}^{-1}$ ,  $\beta$  sheet structure; band at  $1654 \pm 3 \text{ cm}^{-1}$ ,  $\alpha$  helix. Data are reported in Table III. Based on [Savino et al., 2000] we predicted the distribution of different

**TABLE III. Secondary Structure of Saporin Forms**

Toxin	$\beta$ -Sheet		$\alpha$ -Helix		Other	
	Expected <sup>a</sup>	Observed	Expected	Observed	Expected	Observed
SO6	17.79	20.73 <sup>b</sup>	33.99	30.36	48.22	48.91
Saporin <sub>wt</sub> (recombinant)	17.79	27.93	33.99	25.88	48.22	46.19
SapΔ239–253	18.90	21.05	34.80	31.73	46.20	47.22
SapΔ1–20	16.73	48.68	31.75	14.29	51.50	37.03

<sup>a</sup>Estimated structure is according to Savino et al. [2000].

<sup>b</sup>Figures represent percent of total.

secondary structures and then compared our observations with the expected results. It can be noticed that, compared to all other saporin forms, the N-terminal deletion sap $\Delta$ 1–20 mutant shows a sizeable increase in  $\beta$ -sheet structures with a drastic decrease in  $\alpha$ -helices, considerably differing from predictions. It could be hypothesized that the deletion of the N-terminal fragment induces a profound rearrangement of saporin structure leading to an enhanced ability to interact with artificial membranes and also affecting the catalytic site. That the mutant sap $\Delta$ 1–20 indeed displays a substantial alteration of secondary structure is also confirmed by tryptophan fluorescence analysis (not shown). Our results, therefore, indicate that diminished catalytic activity resulting from N-terminal deletions could depend on both the lack of the crucial Tyr 16 but also on considerable alterations of saporin structure. Likewise, an effect of N-terminal deletions on catalytic activity was observed in the case of ricin A-chain [May et al., 1989]. In this case, however, no data are available on possible structure rearrangements. Pittaluga et al. [2005] examined the effects of a 19 aminoacid deletion at the C-terminus of saporin and found that in such a deletion mutant the toxicity to bacterial cells is abolished and the enzymatic activity of saporin on polynucleotide substrates (RNA or DNA) is severely impaired. In our case, we examined the effects of a deletion of only the last 15 C-terminal residues and we observed only a variable reduction of the cytotoxic properties of the molecule with negligible effects on its enzymatic properties in cell-free systems and on its overall structure. Moreover no major alteration of saporin secondary structure appears evident from our FTIR analysis after deletion of the 15 C-terminal aminoacids (Table III), although some variations were indeed observed with respect to full-length recombinant saporin. It is, therefore, possible that the further four aminoacids deleted by Pittaluga et al. [2005] are responsible for the effects that they observe, in particular the missing aminoacids could be important to stabilize saporin domains involved in the catalytic activity or in other functions necessary to enhance cytotoxicity in whole cells. As shown in Table III the observed structure of whole recombinant saporin differs somewhat from that of SO6. This aspect needs to be further elucidated. However, part of the considerations

reported above to explain the different behavior of SO6 and recombinant saporin as regards their interaction with LUVs hold also in this case. In particular, the greater homogeneity of recombinant saporin may result in a secondary structure slightly different from what expected based on the data obtained with the more heterogeneous SO6.

Thus, collectively our data point to the fact that the N-terminal portion heavily influences both catalytic activity and interaction with lipid bilayers and can hardly be removed without profoundly affecting saporin functions. The C-terminal domain affects instead intracellular trafficking. It remains to be investigated whether further deletions in the C-terminal domain might allow to obtain a smaller saporin molecule retaining catalytic activity and cell intoxicating properties when delivered by cell-selective reagents. Additionally, new non-terminal deletions could be explored to evaluate whether size of saporin can be reduced while maintaining cytotoxic functions.

#### ACKNOWLEDGMENTS

This work was partially supported by MIUR (PRIN 2003) and by Fondazione Cassa di Risparmio di Verona, Vicenza, Belluno e Ancona (Bando 2004, "Integrazione tra Tecnologia e Sviluppo di Settore"). Dr. S. Fabbrini (Department of Biological and Technological Research—Dibit, San Raffaele Scientific Institute, Milan, Italy) is gratefully acknowledged for the gift of reagents. We are also indebted to Dr. R. Ippoliti (Università de L'Aquila, Italy) for his advice and critical reading of the manuscript. Dr. H. Fuchs and Dr. I. Hersler (Charité, Berlin) are thanked for their help with APRT assay.

#### REFERENCES

- Bagga S, Seth D, Batra JK. 2003a. The cytotoxic activity of ribosome-inactivating protein saporin-6 is attributed to its rRNA N-glycosidase and internucleosomal DNA fragmentation activities. *J Biol Chem* 278:4813–4820.
- Bagga S, Hosur MV, Batra JK. 2003b. Cytotoxicity of ribosome-inactivating protein saporin is not mediated through alpha2-macroglobulin receptor. *FEBS Lett* 541: 16–20.
- Barbieri L, Battelli MG, Stirpe F. 1993. Ribosome-inactivating proteins from plants. *Biochim Biophys Acta* 1154: 237–282.
- Barthelemy I, Martineau D, Ong M, Matsunami R, Ling N, Benatti L, Cavallaro U, Soria M, Lappi DA. 1993. The

- expression of saporin, a ribosome-inactivating protein from the plant *Saponaria officinalis*, in *Escherichia coli*. *J Biol Chem* 268:6541–6548.
- Cavallaro U, Nykjaer A, Nielsen M, Soria MR. 1995. Alpha 2-macroglobulin receptor mediates binding and cytotoxicity of plant ribosome-inactivating proteins. *Eur J Biochem* 232:165–171.
- Fabbrini MS, Rappocciolo E, Carpani D, Solinas M, Valsasina B, Breme U, Cavallaro U, Nykjaer A, Rovida E, Legname G, Soria MR. 1997. Characterization of a saporin isoform with lower ribosome-inhibiting activity. *Biochem J* 322(Pt 3):719–727.
- Heisler I, Keller J, Tauber R, Sutherland M, Fuchs H. 2002. A colorimetric assay for the quantitation of free adenine applied to determine the enzymatic activity of ribosome-inactivating proteins. *Anal Biochem* 302:114–122.
- Kayalar C, Duzgunes N. 1986. Membrane action of colicin E1: Detection by the release of carboxyfluorescein and calcein from liposomes. *Biochim Biophys Acta* 860:51–56.
- Lodge JK, Kaniewski WK, Tumer NE. 1993. Broad-spectrum virus resistance in transgenic plants expressing pokeweed antiviral protein. *Proc Natl Acad Sci USA* 90:7089–7093.
- MacDonald RC, MacDonald RI, Menco BP, Takeshita K, Subbarao NK, Hu LR. 1991. Small-volume extrusion apparatus for preparation of large, unilamellar vesicles. *Biochim Biophys Acta* 1061:297–303.
- May MJ, Hartley MR, Roberts LM, Krieg PA, Osborn RW, Lord JM. 1989. Ribosome inactivation by ricin A chain: A sensitive method to assess the activity of wild-type and mutant polypeptides. *EMBO J* 8:301–308.
- McGrath MS, Hwang KM, Caldwell SE, Gaston I, Luk KC, Wu P, Ng VL, Crowe S, Daniels J, Marsh J. 1989. GLQ223: An inhibitor of human immunodeficiency virus replication in acutely and chronically infected cells of lymphocyte and mononuclear phagocyte lineage. *Proc Natl Acad Sci USA* 86:2844–2848.
- Menestrina G, Cabiaux V, Tejuca M. 1999. Secondary structure of sea anemone cytolytins in soluble and membrane bound form by infrared spectroscopy. *Biochem Biophys Res Commun* 254:174–180.
- Morris KN, Wool IG. 1992. Determination by systematic deletion of the amino acids essential for catalysis by ricin A chain. *Proc Natl Acad Sci USA* 89:4869–4873.
- Pittaluga E, Poma A, Tucci A, Spano L. 2005. Expression and characterisation in *E. coli* of mutant forms of saporin. *J Biotechnol* 117:263–266.
- Sambrook J, Fritsch EF, Maniatis T. 1989. Molecular cloning. A laboratory manual. New York: Cold Spring Harbor Laboratory Press.
- Savino C, Federici L, Ippoliti R, Lendaro E, Tsernoglou D. 2000. The crystal structure of saporin SO6 from *Saponaria officinalis* and its interaction with the ribosome. *FEBS Lett* 470:239–243.
- Susi H, Byler DM. 1986. Resolution-enhanced Fourier transform infrared spectroscopy of enzymes. *Methods Enzymol* 130:290–311.
- Taylor S, Massiah A, Lomonossoff G, Roberts LM, Lord JM, Hartley M. 1994. Correlation between the activities of five ribosome-inactivating proteins in depurination of tobacco ribosomes and inhibition of tobacco mosaic virus infection. *Plant J* 5:827–835.